EVALUATION OF A METAL SHEAR WEB
SELECTIVELY REINFORCED
WITH FILAMENTARY COMPOSITES
FOR SPACE SHUTTLE APPLICATION

PHASE III SUMMARY REPORT
SHEAR WEB COMPONENT TESTING AND ANALYSIS

By

J. H. Laakso & J. W. Straayer

THE ***BOEING*** COMPANY

August 1973

Prepared for

NATIONAL AERONAUTICS AND SPACE ADMINISTRATION

Langley Research Center

Hampton, Virginia

EVALUATION OF A METAL SHEAR WEB

SELECTIVELY REINFORCED WITH FILAMENTARY

COMPOSITES FOR SPACE SHUTTLE APPLICATION

PHASE III SUMMARY REPORT - SHEAR WEB COMPONENT TESTING AND ANALYSIS

By

J. H. Laakso and J. W. Straayer

Prepared by the

Research and Engineering Division

Boeing Aerospace Company

Seattle, Washington

For

Langley Research Center

National Aeronautics and Space Administration

August 1973
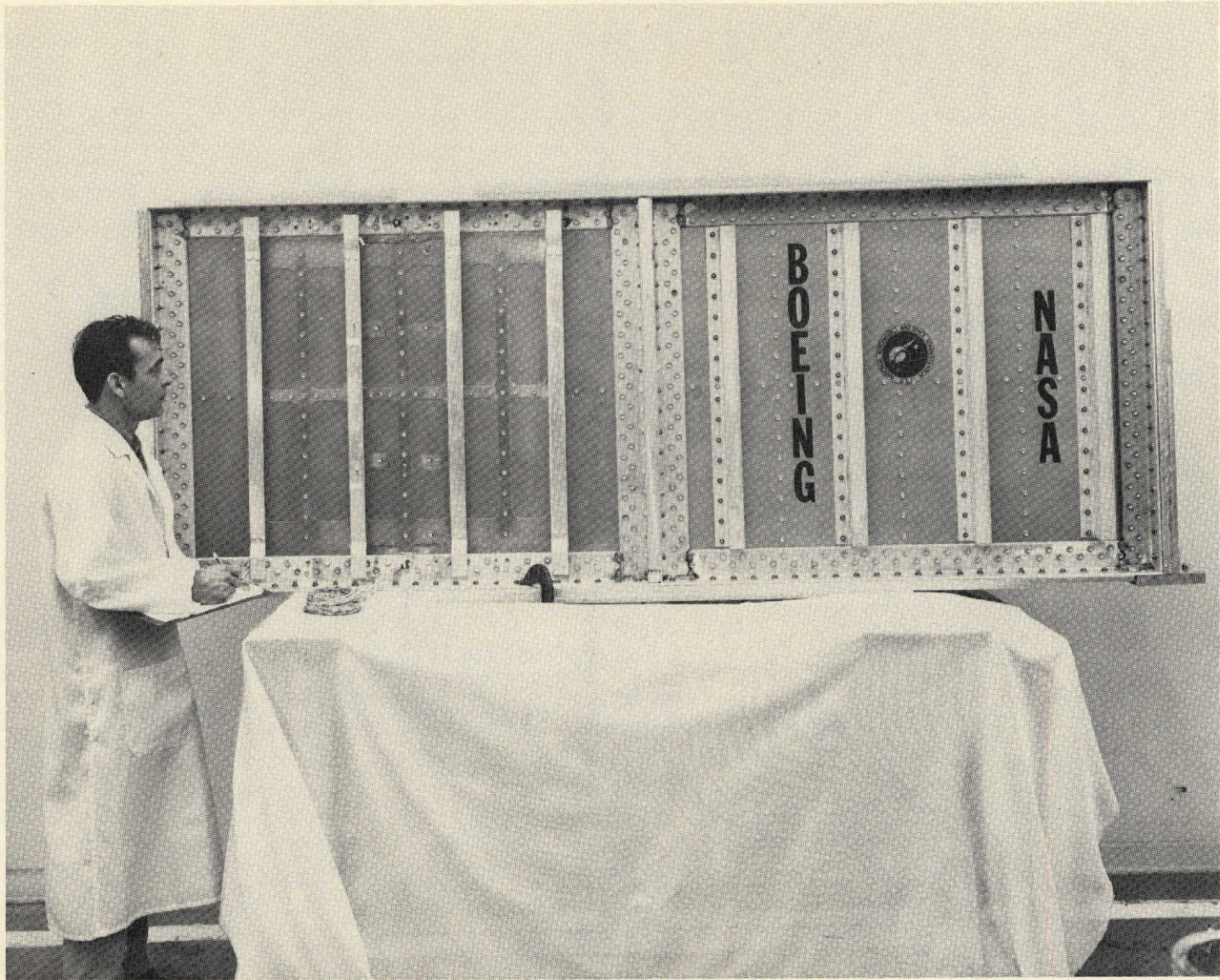
Figure 1: THIRD SHEAR WEB COMPONENT TEST ASSEMBLY

ABSTRACT

Testing and Analysis activities are summarized which were conducted under Phase III of NASA/Langley Research Contract NAS 1-10860, *Evaluation of a Metal Shear Web Selectivity Reinforced with Filamentary Composites for Space Shuttle Application.* Three large scale advanced composite shear web components were tested and analyzed to evaluate application of the design concept developed in Phase I to a Space Shuttle Orbiter thrust structure. The shear web design concept consisted of a titanium-clad $\pm45°$ boron/epoxy web laminate stiffened with vertical boron/epoxy reinforced aluminum stiffeners. The design concept was evaluated to be efficient and practical for the application that was studied. Because of the effects of buckling deflections, a requirement is identified for shear buckling resistant design to maximize the efficiency of highly-loaded advanced composite shear webs. An approximate analysis of pre-buckling deflections is presented and computer-aided design results, which consider prebuckling deformations, indicate that the design concept offers a theoretical weight saving of 31 percent relative to all metal construction. Recommendations are made for design concept options and analytical methods that are appropriate for production hardware.

FOREWORD

This report was prepared by the Research and Engineering Division, Boeing Aerospace Company, under NASA Contract NAS 1-10860, *Evaluation of a Metal Shear Web Selectively Reinforced with Filamentary Composites For Space Shuttle Application.* The program is being sponsored by the Design Technology Branch of the Langley Research Center under the direction of the contracting officer's representative, Mr. James P. Peterson.

The technical performance reported summarizes Phase III contract activities during the period of March 1972 to May 1973.

Performance of the contract is under the management of Mssrs. D. K. Zimmerman and J. W. Straayer, Advanced Structures Development Group; Mr. John H. Laakso is the Technical Leader.

The authors wish to acknowledge the contributions of the following program participants:

TABLE OF CONTENTS

LIST OF FIGURES

1.0 INTRODUCTION

This report presents the results of the third and final phase of a program for the development of a practical advanced composite shear web concept which is a candidate for near-term application to primary flight vehicle structure. The program consists of three phases:

Phase I   Shear Web Design Development

Phase II   Shear Web Component Fabrication

Phase III   Shear Web Component Structure Testing and Analysis

In Phase I [1], the Space Shuttle orbiter main engine thrust beam structure was selected for the shear web application study area because of the high shear loading occurring in this area. The center-loaded thrust beam was selected for study from an early orbiter configuration and has basic dimensions of 40 in. deep by 200 in. span (1 m x 5.1 m). Design development was then performed which involved computer-aided design and analysis, detailed design evaluation, testing of unique and critical details, and structural test planning. Particular emphasis was placed on computer-aided design to screen candidate concepts. Various web design concepts having both boron/epoxy reinforced and all-metal construction were synthesized by a computer-aided adaptive random search procedure.

A practical shear web was identified by the design concept evaluation study in Phase I. This concept had a titanium-clad $\pm 45°$ boron/epoxy web plate with vertical boron/epoxy reinforced aluminum stiffeners.

1

Detailed thrust beam drawings using the B;E reinforced design concept
and an all-titanium construction were prepared in Phase I. Weight trades
showed a 24% savings with the selected concept relative to an all-metal
construction. Cost per pound of weight savings was estimated to be less
than $250 (551 $ US/kg). Critical details and reliability considerations
for the B/E reinforced design were identified and structural element tests
were made to substantiate the design details. Cyclic load and tempera-
ture design environments were simulated in some of the element tests. A
significant outcome of the element test program was the determination of
titanium cladding reinforcement required to preclude failure at joints
and fastener holes. Two small scale shear web elements 18 in. by 25 in.
(45.7 cm x 63.5 cm) were tested to demonstrate the performance of the
basic web laminate details.

Phase II [2] activities were oriented primarily toward the fabrication
of three large scale B/E reinforced shear web test components. The test
webs were 36 in. high by 47 in. long (0.9 m x 1.2 m). Test fixtures
for the shear web test elements and the large scale web components were
also fabricated during Phase II. The center-loaded beam test fixture
was configured so that the test web components could be installed in
one half of the beam for each test. The test fixtures were fabricated
from available standard extruded aluminum sections and plates.

Phase III was concerned with structural analysis and testing of the
three B/E reinforced shear web components. The first web design was
established from the baseline B/E reinforced shear web design developed
in Phase I. Slight changes were made in web depth and stiffener details

2

to simplify fabrication of the test web. Based on the static test results of the first test web, improvements in analysis and fabrication procedures were made to enhance shear buckling resistance.

The second test web was tested to demonstrate fatigue resistance; 400 loadings to a simulated limit load level were applied with no apparent fatigue damage resulting in spite of high prebuckling deformations. After post-test analysis, the second test web was delivered to the Langley Research Center.

The third test web, shown in Figure 1 (frontispiece), was redesigned using an improved computer-aided design procedure. Provision for longi-tudinal stiffening and buckling analyses based on discrete stiffening were added to the OPTRAN code used in Phase I; weight trades conducted with the code indicated that longitudinal stiffening would be beneficial. The static strength test results for the third web indicated that per-formance of the design concept was significantly improved by the addi-tional stiffening and was strongly dependent on shear buckling resistance qualities.

Because of the importance of prebuckling deformations to load carrying performance, an approximate prebuckling analysis procedure was studied and incorporated in the Boeing OPTRAN code for the B/E reinforced web concept. Weight trades were then conducted using OPTRAN code to establish correlation with the third test web and final weight compari-sons between the B/E reinforced concept and all-metal construction.

2.0 SUMMARY

The titanium/clad B/E shear web concept is evaluated to be practical and efficient for the Space Shuttle thrust structure application that was studied. This assessment is based on the test and analysis of three 36 in. high by 47 in. long (0.9m x 1.2m) shear web components having titanium-clad $\pm45°$ B/E web plates stiffened with vertical B/E reinforced aluminum stiffeners and, in the case of the third web, a longitudinal aluminum stiffener. The results of the shear web component tests, summarized below, indicate shear web efficiency is improved by shear buckling resistant design:

TEST WEB	MAXIMUM LOAD LB (MN)	RESULTS
1	540,000 (2.4)	o Failed by composite panel fracture in post-buckling condition.
2	530,000 (2.36)	o No failure at maximum load after loaded 400 times to 400,000 lb (1.78 MN).
		o Web had large prebuckle strains during fatigue loading.
		o Web was in post-buckled condition in final loading.
3	575,000 (2.56)	o Stiffening optimized by computer-aided design.
		o Failed by composite panel fracture in a panel that was in a prebuckled condition.

A computer-aided design methodology, employing the OPTRAN code, was found to be partially effective in establishing the final test component design; the design ultimate load was 600,000 lb. (2.67 MN). A suitable (quick execution) prebuckling analysis method was developed for incorporation in the shear web OPTRAN code to treat the design constraints of composite and metal cladding strain in prebuckled panels. Based on a correlation with the third web test and other design optimization cases, the ultimate allowable composite strain in prebuckled panels will generally govern the strength of highly loaded stiffened composite shear web configurations of the type studied in this program. Because of the importance of pre-buckling deformations and related hazards of low post-buckling strength, the composite reinforced design concept will require more sophisticated structural analysis than in the case of conventional metal webs for a production hardware application. The nominal weight savings (without weight penalties for edge joints, etc.) predicted using the final version of the shear web OPTRAN code is 31% for a titanium-clad $\pm45°$ B/E web with B/E reinforced aluminum stiffening relative to a titanium web with aluminum stiffeners. Replacing the B/E reinforced stiffeners with inex-pensive all-aluminum stiffeners reduced the weight savings slightly to 28%. The all-metal stiffeners are recommended for first generation hardware because of their expected lower fabrication cost and inherent straightness (absence of residual thermal strains) after fabrication which simplifies shear web assembly.

3.0 TEST WEB COMPONENTS

3.1 DESIGN

The three test web components were designed to simulate the design
features and internal loads associated with the thrust structure appli-
cation shown in Figure 2. An objective in selecting the test web con-
figuration was to have large size and realistic design details so that
evaluation of the design concept could be made without scaling problems.
The test components were sized 36 in. high by 47 in. long (0.9 m by
1.2 m) and had the general stiffener and web laminate details illustrated
in Figures 3 and 4. The test components were installed in one-half of
a center-loaded beam fixture for testing; the assembled test beam assembly
is shown in Figure 1 (frontispiece). Design criteria for the test and
webs are given in the Phase I [1] Report; a basic design requirement was
that the webs be buckling resistant. Detailed design drawings for the
test hardware may be found in the Phase II [2] Report and in Appendix D
(test web 3).
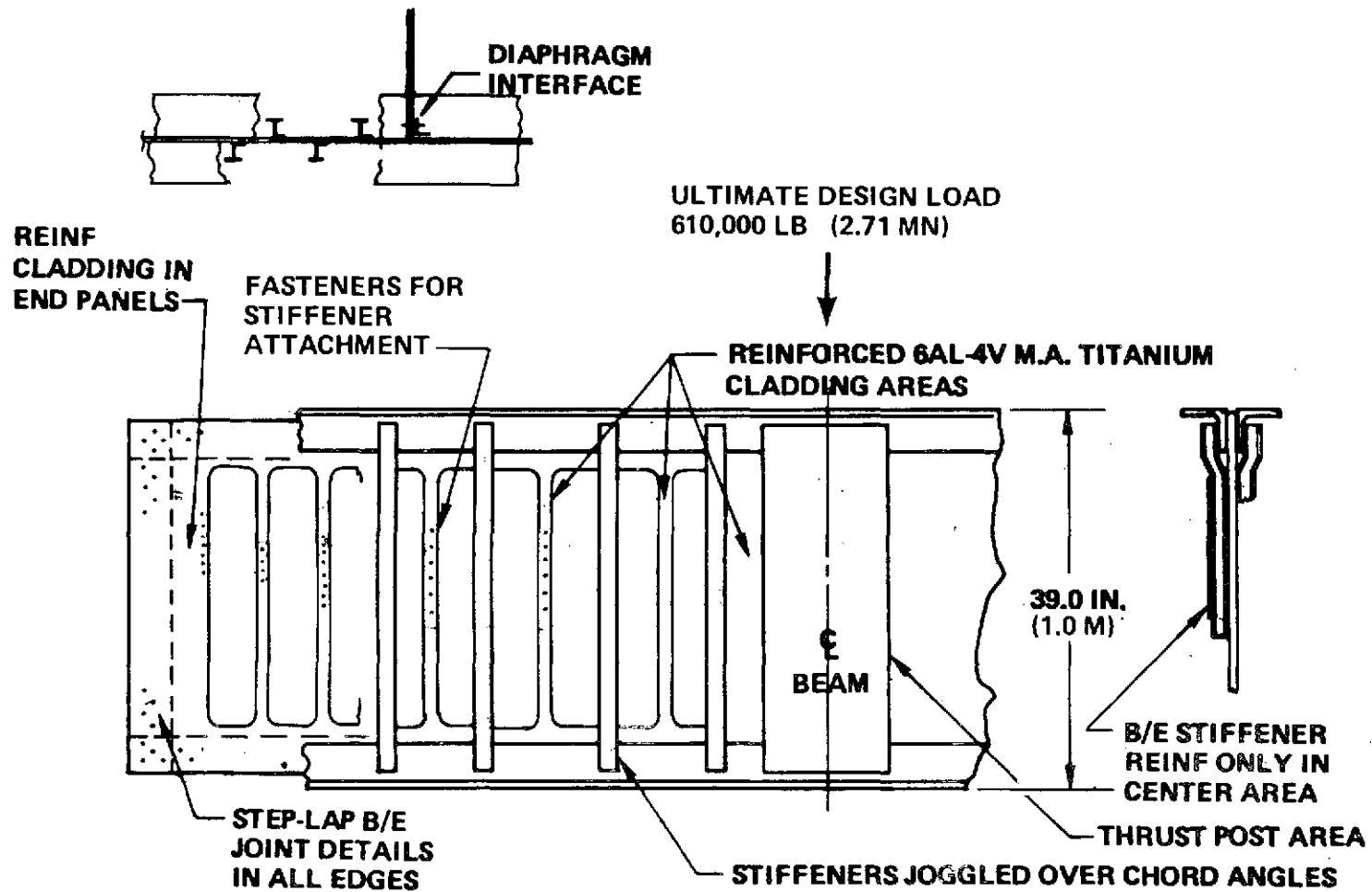
Figure 2: B/E REINFORCED SHEAR WEB DESIGN CONCEPT

REINF
CLADDING

NOMINAL TI
CLADDING (6AL–4V
MILL ANNEALED)

WEB LAMINATE AT STIFFENERS

B/E LAY-UP
ADH/+45, –45, +45 –45/ADH/
–45, +45, –45 +45/ADH/+45 . . . .

₵
SYMM

DOUBLE STEP
LAP DETAILS
(0.5 STEP LENGTH)

WEB LAMINATE AT EDGES
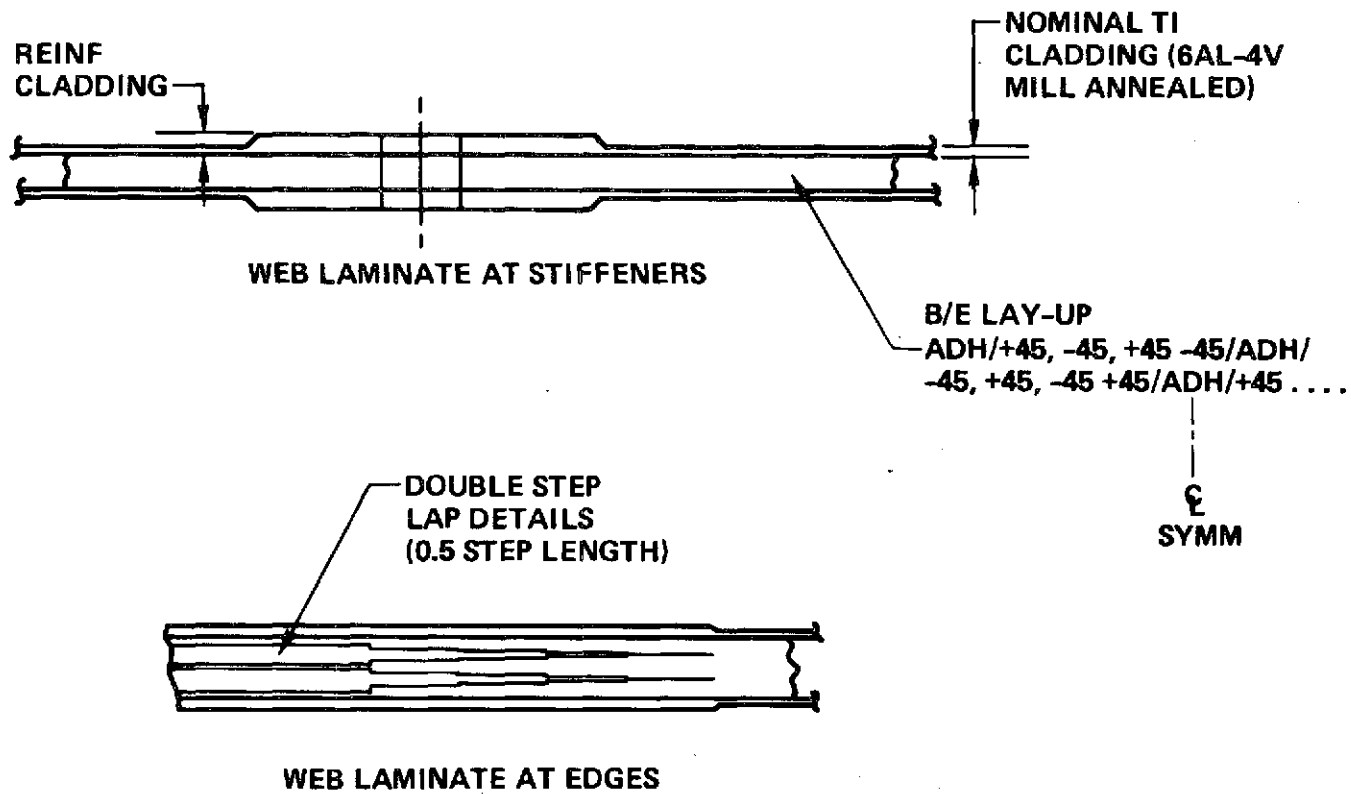
Figure 3: B/E REINFORCED SHEAR WEB DESIGN DETAILS

SPLICE IN NEAR SIDE STEP-LAP DETAIL

ALUMINUM

SPLICE IN FAR SIDE
STEP-LAP DETAIL

WEB LAMINATE
AT CORNERS

STIFFENERS
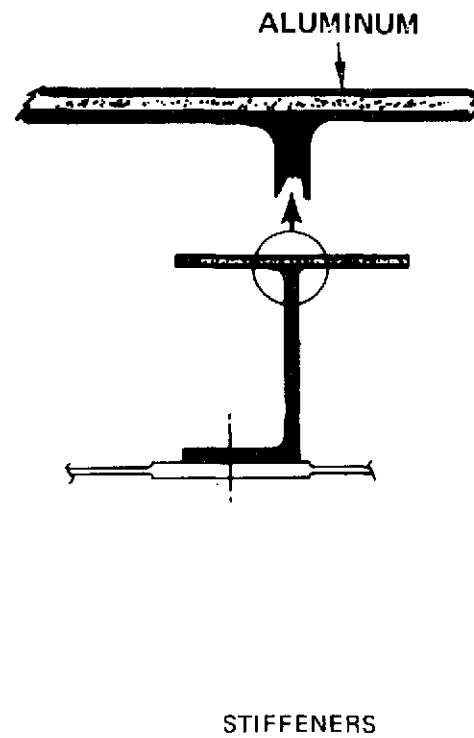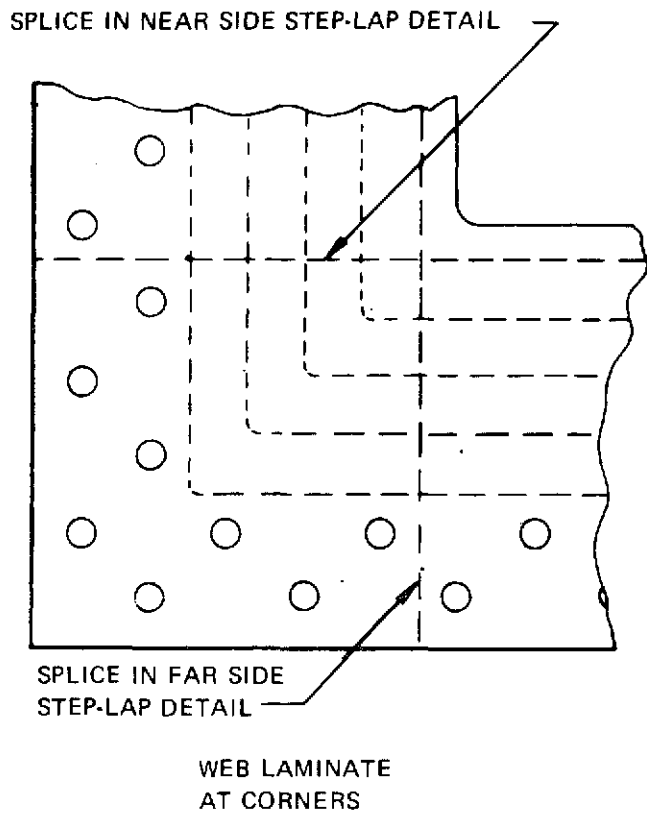
Figure 4: B/E REINFORCED SHEAR WEB DESIGN DETAILS

Figure 5 summarizes the design approaches taken for each test web. In each test the goal was to exceed 600,000 lb (2.67 MN) and the results would then be used to predict the performance of a production web which would be designed for a higher beam chord strain than achieved in the test fixture.

Test web 1 was configured with details from the baseline B/E reinforced web design developed in Phase I [1]. The analysis methods, which were used in Phase I as part of the shear web OPTRAN code, indicated a failure load of 640,000 lb (2.85 MN) whereas the actual failure load was 540,000 lb (2.4 MN). While the analysis methods were simple with respect to allowing early incorporation with a computer-aided design procedure, they were incomplete since they did not treat coupled plate/discrete stiffener buckling. The assumption made of smeared stiffening in computing general instability and the neglect of discrete stiffening requirements resulted in intermediate web buckling and failure by composite fracture due to high membrane and bending panel strains in the post-buckling condition. The results from the first web test clearly indicated the requirement for shear buckling resistant design for maximum composite shear web efficiency.

Test web 2 was designed to have higher buckling resistance than test web 1; the web laminate thickness was increased by addition of an additional adhesive filler ply at the mid-plane and stiffener bending stiffness was increased by additional flange material. This test web was tested under repeated loading to the effective design limit shear

TEST WEB	MAX TEST LOAD LB (MN)	INITIAL BIFURCATION BUCKLING LOAD	PREDICTED SHEAR RESISTANT FAILURE LOAD	SHEAR RESISTANT DESIGN ANALYSIS APPROACHES
1	FAILURE AT 540,000 (2.4)	370,000 (1.65)	640,000 (2.85)	DESIGN SIMILAR TO FULL SCALE DESIGN (PHASE I REPORT) EXCEPT FOR REDUCED SIZE AND STIFFENER. DESIGN GOAL WAS TO DEVELOP MEMBRANE STRAIN OF 4710 $\mu\epsilon$ IN NOMINAL LAMINATE B/E. SMEARED ECCENTRIC STIFFENING ASSUMED. ORTHOTROPIC PLATE GENERAL INSTABILITY ANALYSIS. LOCAL PANEL BUCKLING ANALYSIS BASED ON SIMPLY SUPPORTED PANELS WITH HEIGHT SAME AS NOMINAL LAMINATE. PREBUCKLING EFFECTS NEGLECTED.
2	NO FAILURE AT 525,000 (2.34) AFTER 400 CYCLES TO 400,000 (1.78)	425,000 (1.89)	715,000 (3.18)	SAME AS ABOVE EXCEPT PANEL HEIGHT ASSUMED SAME AS WEB CLEAR HEIGHT (INCLUDES REINFORCED WEB EDGES) RESULTING IN INCREASES IN STIFFENER AND WEB LAMINATE STIFFNESSES REQUIREMENTS.
3	FAILURE AT 575,000 (2.56)	580,000 (2.58)	600,000 (2.67)	DESIGN ESTABLISHED BY COMPUTER–AIDED DESIGN APPROACH (OPTRAN CODE). DISCRETE, NONECCENTRIC STIFFENING ASSUMED. CLADDING LANDS ADDED TO STIFFENER EI. COUPLED PANEL/STIFFENER GENERAL INSTABILITY. EFFECTIVE SIMPLY SUPPORTED PANEL HEIGHT ASSUMED SAME AS NOMINAL PANEL HEIGHT. PREBUCKLING EFFECTS NEGLECTED.

Figure 5: TEST WEB DESIGN/ANALYSIS APPROACHES

load (Nxy) level. Except for a different assumption of effective web panel height, the second web was analyzed similar to test web 1. Significant prebuckling deformation developed at the limit load level such that the fatigue test conditions are categorized as "worst" case.

Test web 3 was designed to be buckle resistant at an ultimate design load of 600,000 lb (2.67 MN). An improved version of the shear web OPTRAN code was used to establish the design. An analysis was included in the OPTRAN code for coupled plate/stiffener buckling considering discrete transverse and longitudinal stiffening. Discussion of this analysis and related assumptions is given in the Design Analysis Methods Section (Section 9.0). The test failure load of 575,000 lb (2.56 MN) was less than the design load; however, the web was in a prebuckled condition (shear resistant) at the time of failure. The reduced prebuckling deflections and improved performance of this test web verifies that the general design requirement for buckling resistance is necessary for efficient highly loaded composite shear webs. This test also demonstrated the need to treat prebuckling deformations as they are influenced by initial imperfections; this area of analysis is discussed in the Design Analysis Methods Section.

3.2 FABRICATED DETAILS AND DIMENSIONS

Details of the test webs are shown in Figures 6 and 10. The webs have similar details except for the third web which has closer transverse stiffener spacing and a longitudinal central stiffener. Detailed design drawings of the third test web are included in the appendix.

Detail dimensions of the test webs are given in Figures 11 to 13. These dimensions were determined from measurements of the fabricated hardware. The values shown for laminate part thicknesses are average values; small variations occurred due to chem-mill tolerances, resin flow and stock material tolerances. Since the variations were small, the structural analysis results reported herein are based on the dimensions shown.

3.3 TEST BEAM FIXTURE

The center-loaded test beam fixture was designed to provide (1) a convenient means of testing the shear web components, and (2) realistic web-to-chord attachment details. As can be noted in Figure 10, standard 7075-T6 aluminum sections and high strength steel fasteners were used in the fixture. Cover plates with varying lengths were used to provide uniform strain conditions at the web edges. Due to the expected repeated use of the fixture, the chord strain due to beam bending was limited to approximately 1,500 $\mu\varepsilon$ along length of the beam. During the three web tests, the beam fixture functioned in a satisfactory manner.

13
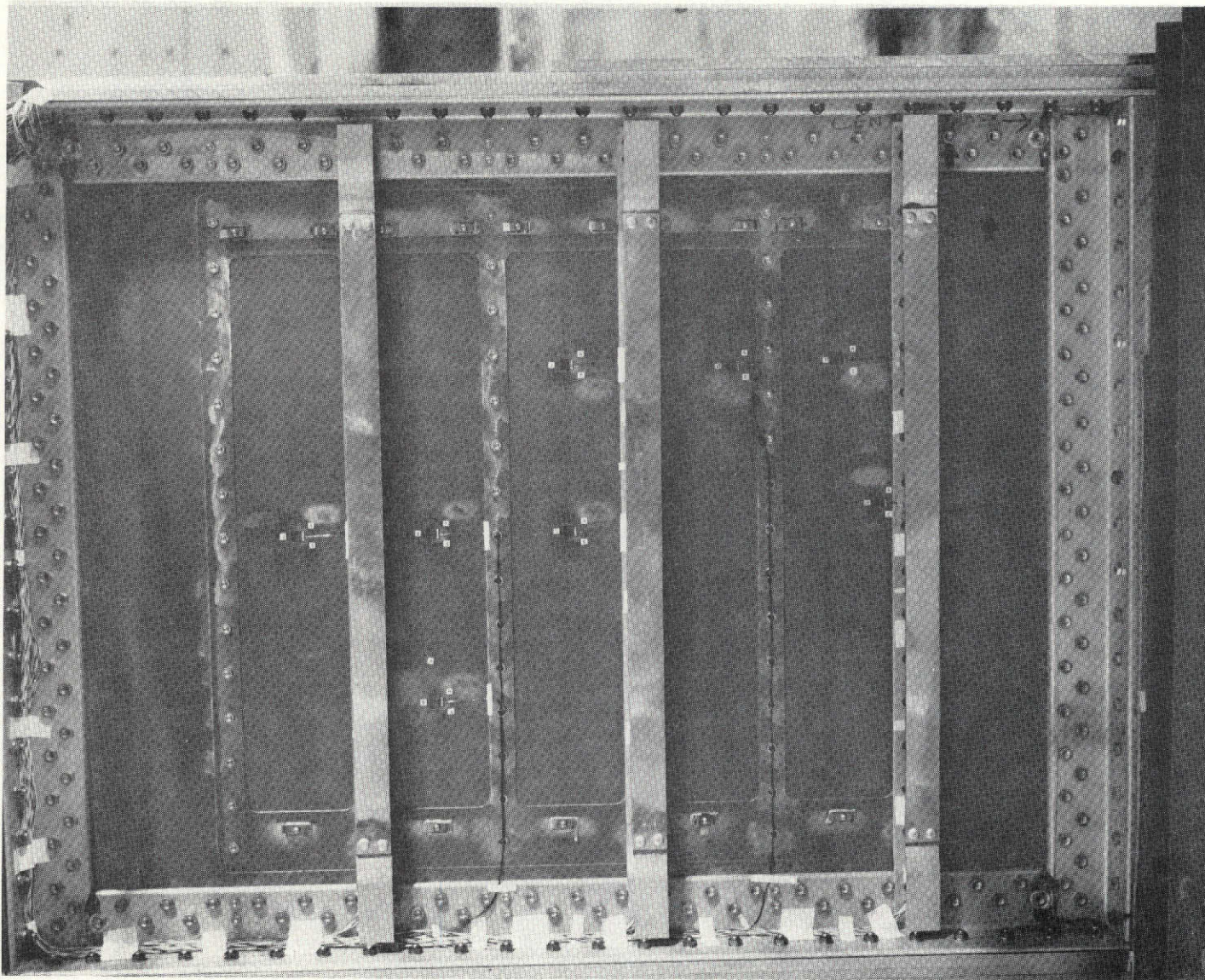
Figure 6: *TEST WEB 1 ASSEMBLY*
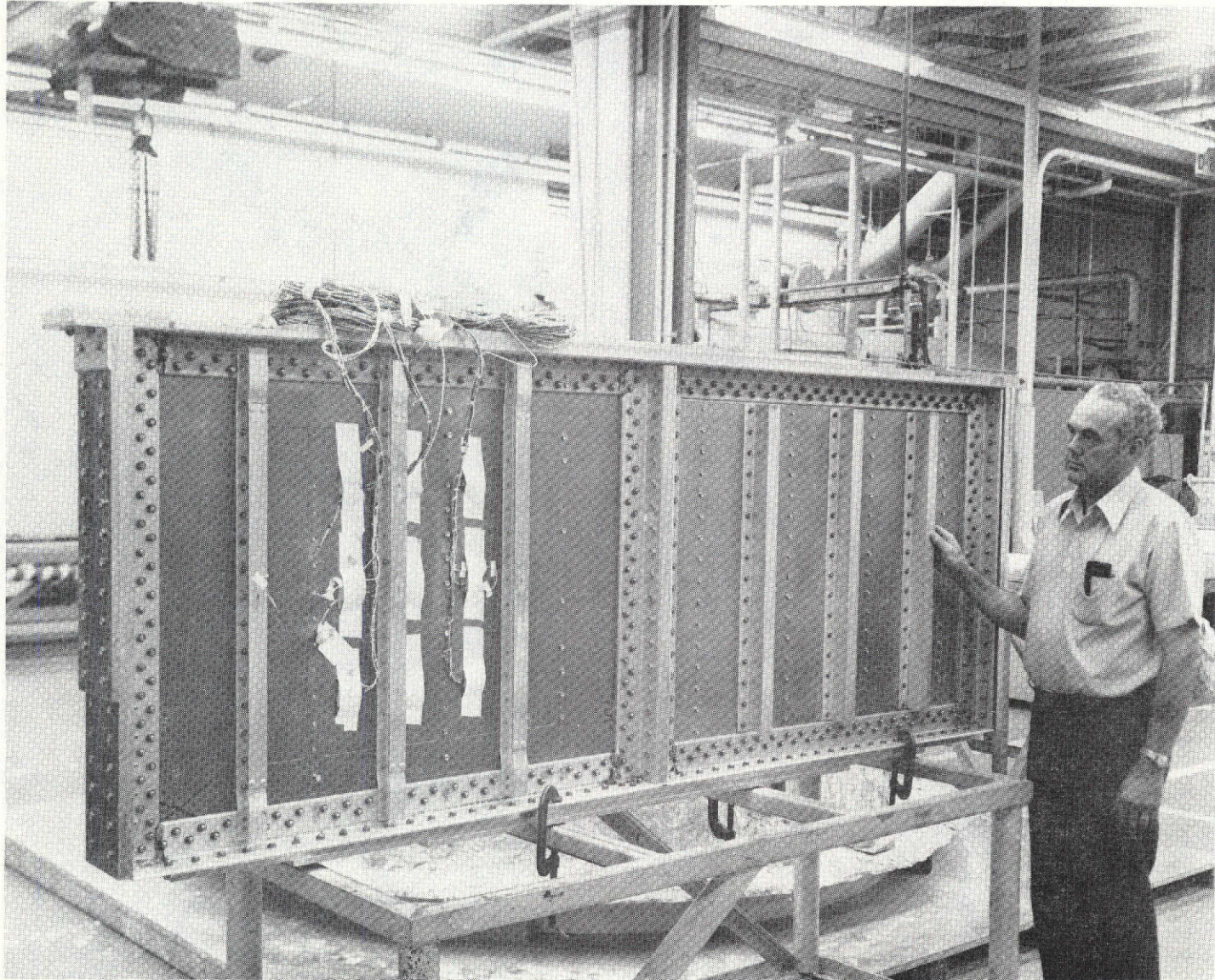
Figure 7: TEST WEB 2 ASSEMBLY
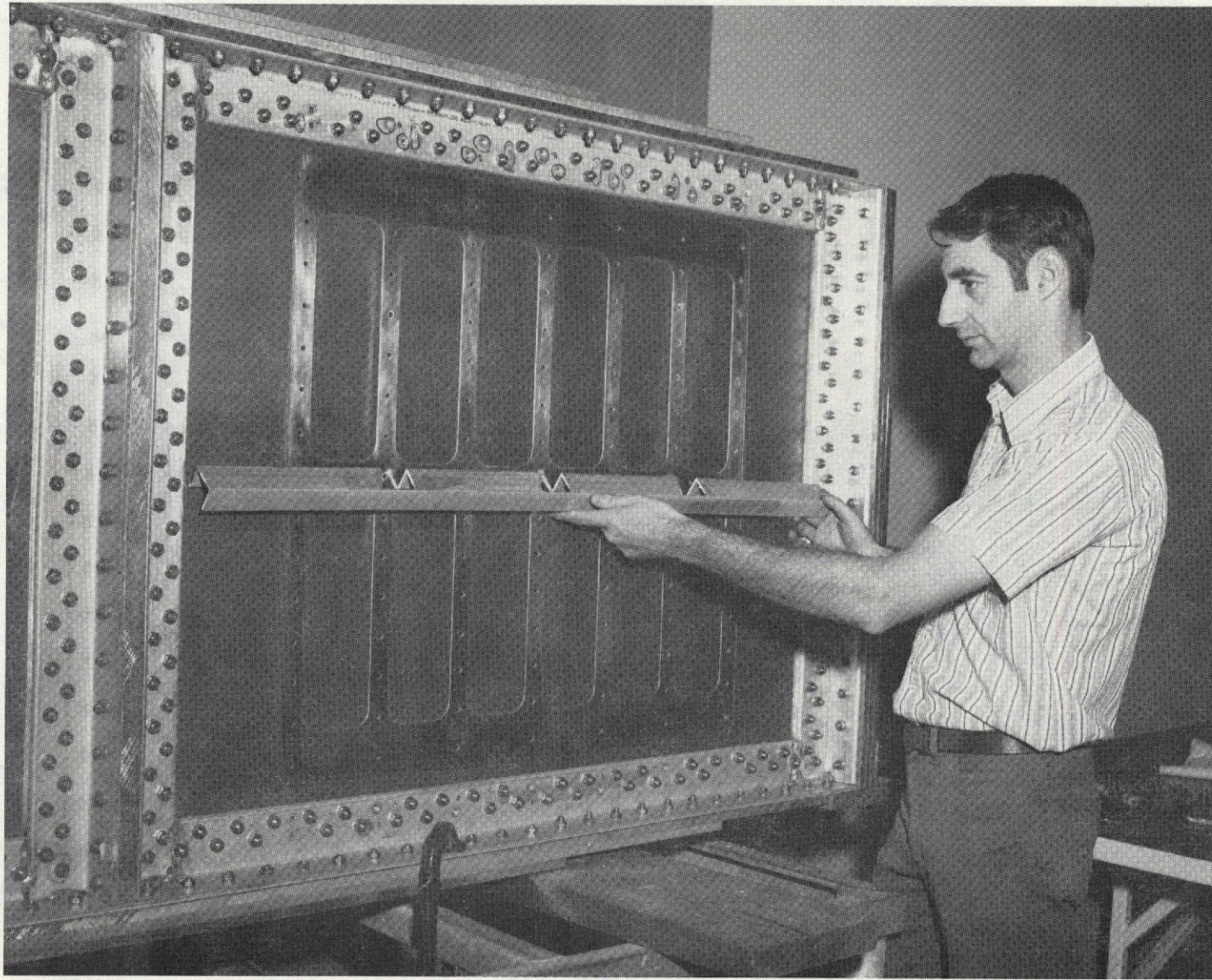
Figure 8: TEST WEB 3 SUBASSEMBLY
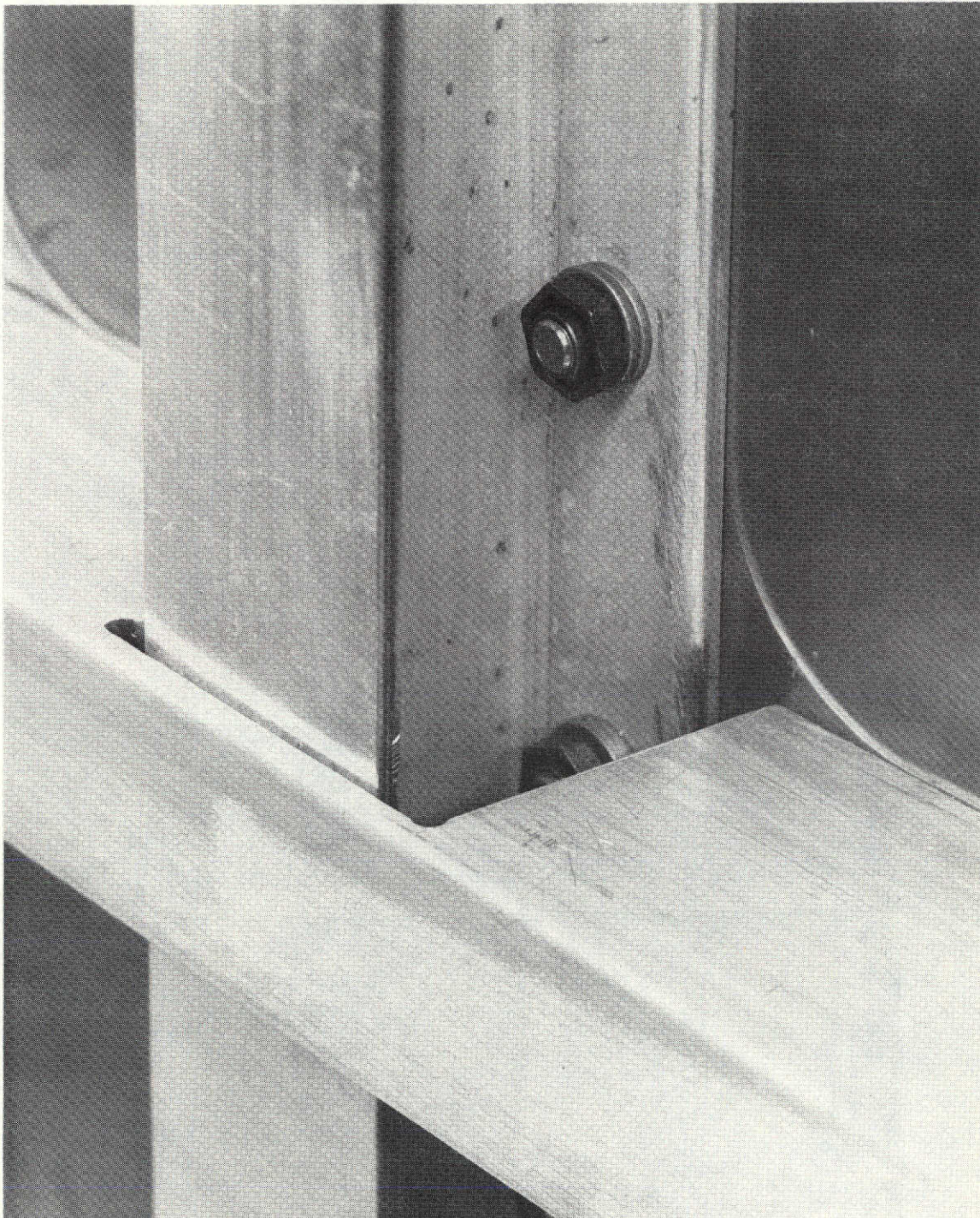
Figure 9: TEST WEB 3 LONGITUDINAL/TRANSVERSE STIFFENER CROSS-OVER DETAILS
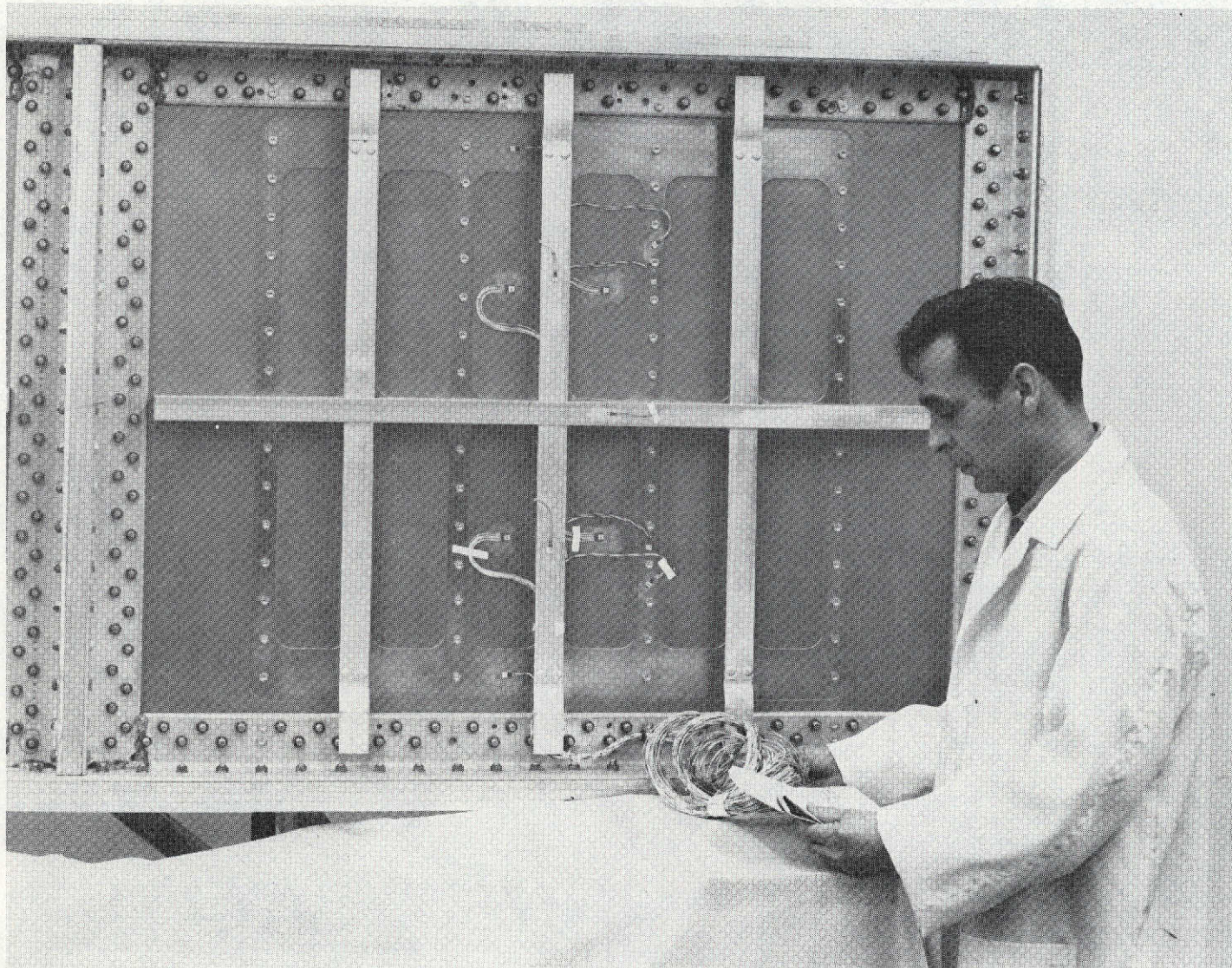
Figure 10: TEST WEB 3 ASSEMBLY

	6AL–4V Ti M.A. CLADDING		TEST WEB COMPONENT	

Label	TW–1	TW–2	TW–3
6AL–4V Ti M.A. CLADDING	0.022 (0.559)	0.022 (0.559)	0.0195 (0.495)
±45° B/E NARMCO 5505/4 16 PLIES @	0.0052 (0.132)	0.0052 (0.132)	0.0051 (0.132)
METLBOND 329 ADHESIVE NO. PLIES ▷2 @ ₵	5	6 ▷	5
PLY THK.	0.011 (0.279)	0.011 (0.279)	0.009 (0.229)
6AL – 4V Ti M.A. CLADDING	0.022 (0.559)	0.022 (0.559)	0.0195 (0.559)
NOMINAL LAMINATE THICKNESS	0.1822 (4.628)	0.1932) (4.907)	0.1656 (4.206)
CLADDING REINFORCEMENT PAD-UP AT STIFFENERS	0.030 (0.762)	0.030 (0.762)	0.030 (0.762)
TRANSVERSE STIFFENER SPACING	6.0(15.24)	6.0(15.24)	5.0(12.7)

1.0 (25.4)

UNITS
IN (mm)

Figure 11: WEB LAMINATE FABRICATED DIMENSIONS USED IN STRUCTURAL ANALYSES

	TEST WEB COMPONENT		
	TW-1	TW-2	TW-3
7075-T6 AL.	0.020 (0.508)	0.020 (0.508)	0.020 (0.508)
BMS 5-51, TYPE 2, GDS EPOXY ADHESIVE 2 PLIES @	0.003 (0.0762)	0.003 (0.0762)	0.003 (0.0762)
UNIDIRECTIONAL B/E NARMCO 5505/4 8 PLIES @	0.0052 (0.132)	0.0052 (0.132)	0.0052 (0.132)
FLANGE THICKNESS	0.020 (0.508)	0.125 (3.175)	0.030 (0.762)
7075-T6 AL. STIFFENER	0.09 (2.286)	0.125 (3.175)	0.125 (3.175)
STIFFENER SPACING	6.0 (15.2)	6.0 (15.2)	5.0 (12.7)

1.5 (38.1)

1.5 (38.1)

T_s

T_s

1.0 (25.4)

UNITS
IN (mm)
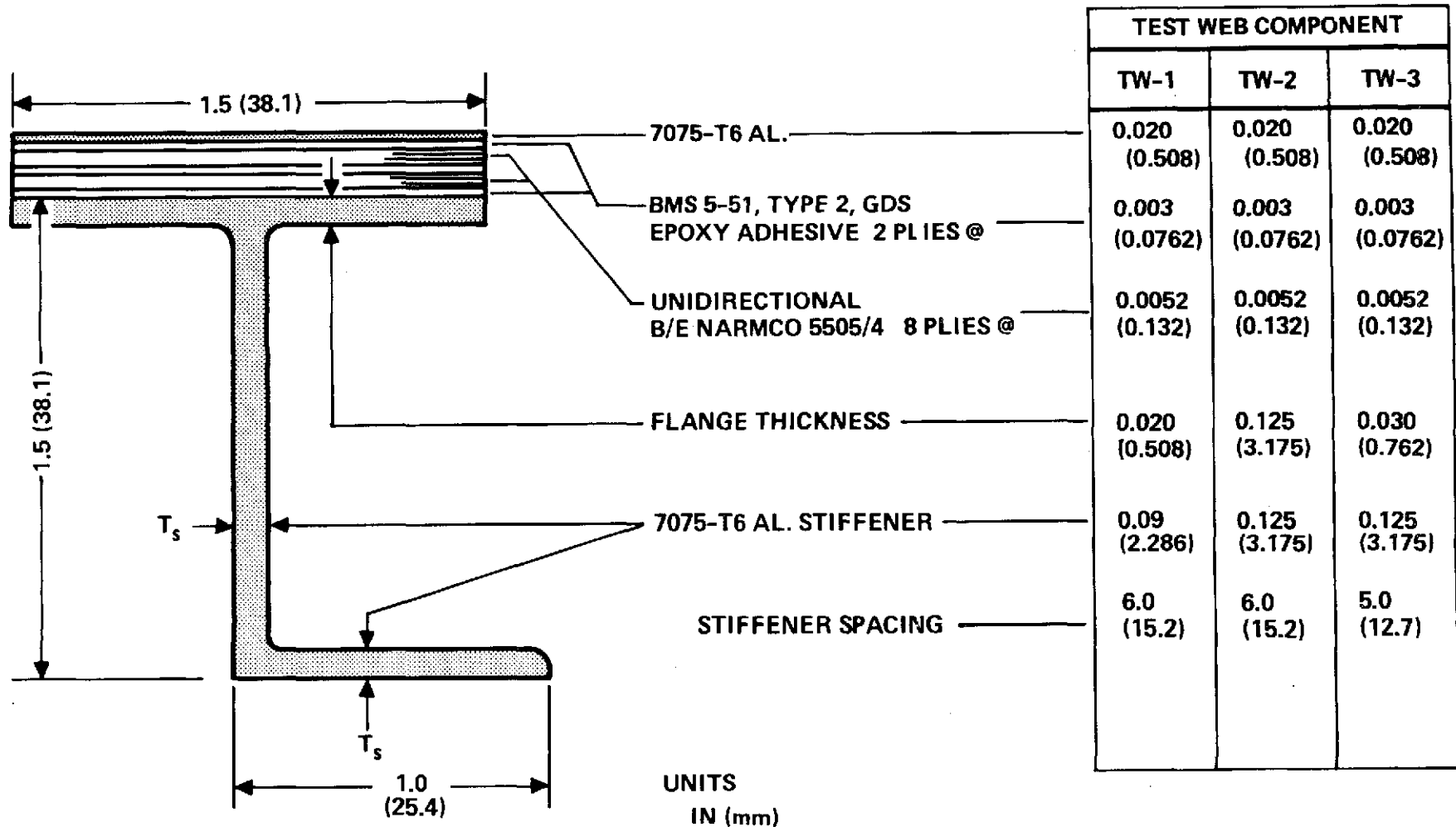
Figure 12: TRANSVERSE STIFFENER FABRICATED DIMENSIONS USED IN STRUCTURAL ANALYSES
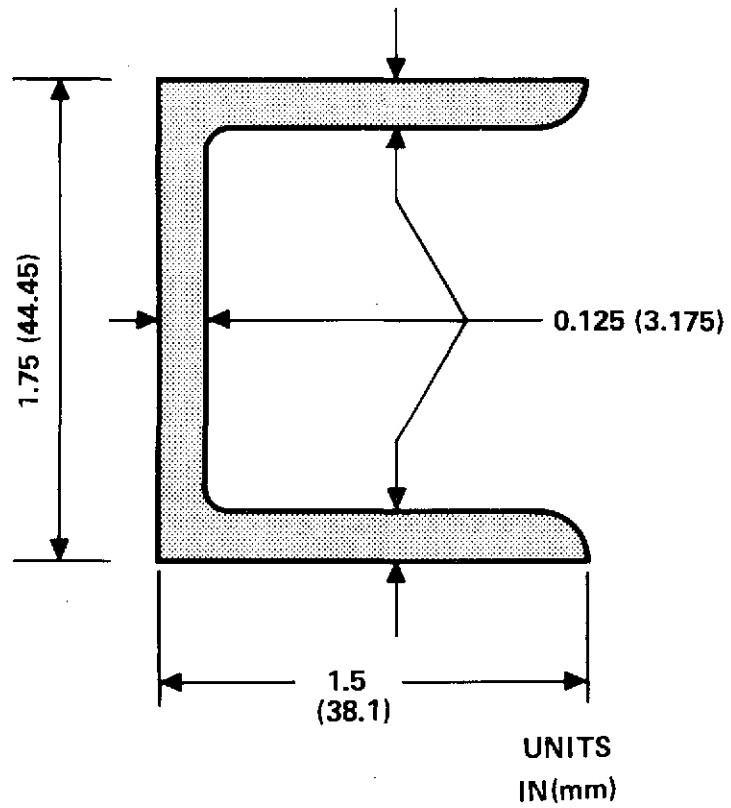
CENTRAL LONGITUDINAL STIFFENER
USED ONLY ON TEST WEB 3

2024-T3511 ALUMINUM
(AND 10137-1606)

0.125 (3.175)

1.75 (44.45)

1.5
(38.1)

UNITS
IN (mm)

Figure 13: LONGITUDINAL STIFFENER DIMENSIONS USED IN STRUCTURAL ANALYSES

4.0 TEST PROCEDURES

Figure 14 lists the test beam loads applied in the three shear web component tests. All testing was done at room temperature. The first and third tests were conducted to failure. The second test was terminated in the 411th loading when strain gage data indicated that proportional limit strain was reached in the titanium cladding of the web laminate. This web was then examined for fatigue damage and later shipped to NASA/Langley.

The test webs were instrumented to record Moire fringes (buckling displacements), strains, vertical and lateral deflections and acoustic emissions. A summary of the test instrumentation used in the first test is given in the test plan contained in the Phase I [1] Report; the instrumentation used in the second and third tests was essentially the same as in the first test.

The general test set-up is shown in Figure 15 and 16. The test beam was laterally supported at the ends and at the center where the loading was applied. Rollers were used to provide simple supports at the beam ends.

The test web responses were monitored by a particularly effective method known as the Moire fringe technique (3). Equipment used to acquire Moire fringe data appears in front of test web side of the beam. A light source (the box with focusing lens) directs a strong light beam to a

TEST WEB 1 STATIC STRENGTH TEST		TEST WEB 2 LOW-CYCLE FATIGUE TEST				TEST WEB 3 STATIC STRENGTH TEST	
1.	250,000 LB (1.11 MN)	1.	200,000 LB (.89 MN)	407.	450,000 (2.00)	1.	200,000 LB (.89 MN)
2. to 102.	100 CYCLES TO 400,000 (1.78)	2.	400,000 (1.78)	408.	425,000 (1.89)	2.	575,000 FAILURE (2.56)
103.	540,000 FAILURE (2.40)	3.	400,000 (1.78)	409.	490,000 (2.18)		
		4. to 404.	400 CYCLES TO 400,000 (1.78)	410.	490,000 (2.18)		
		405.	436,000 (1.94)	411.	530,000 (2.36)		
		406.	449,000 (2.00)		NO FAILURE		

*Figure 14: TEST BEAM LOADINGS*
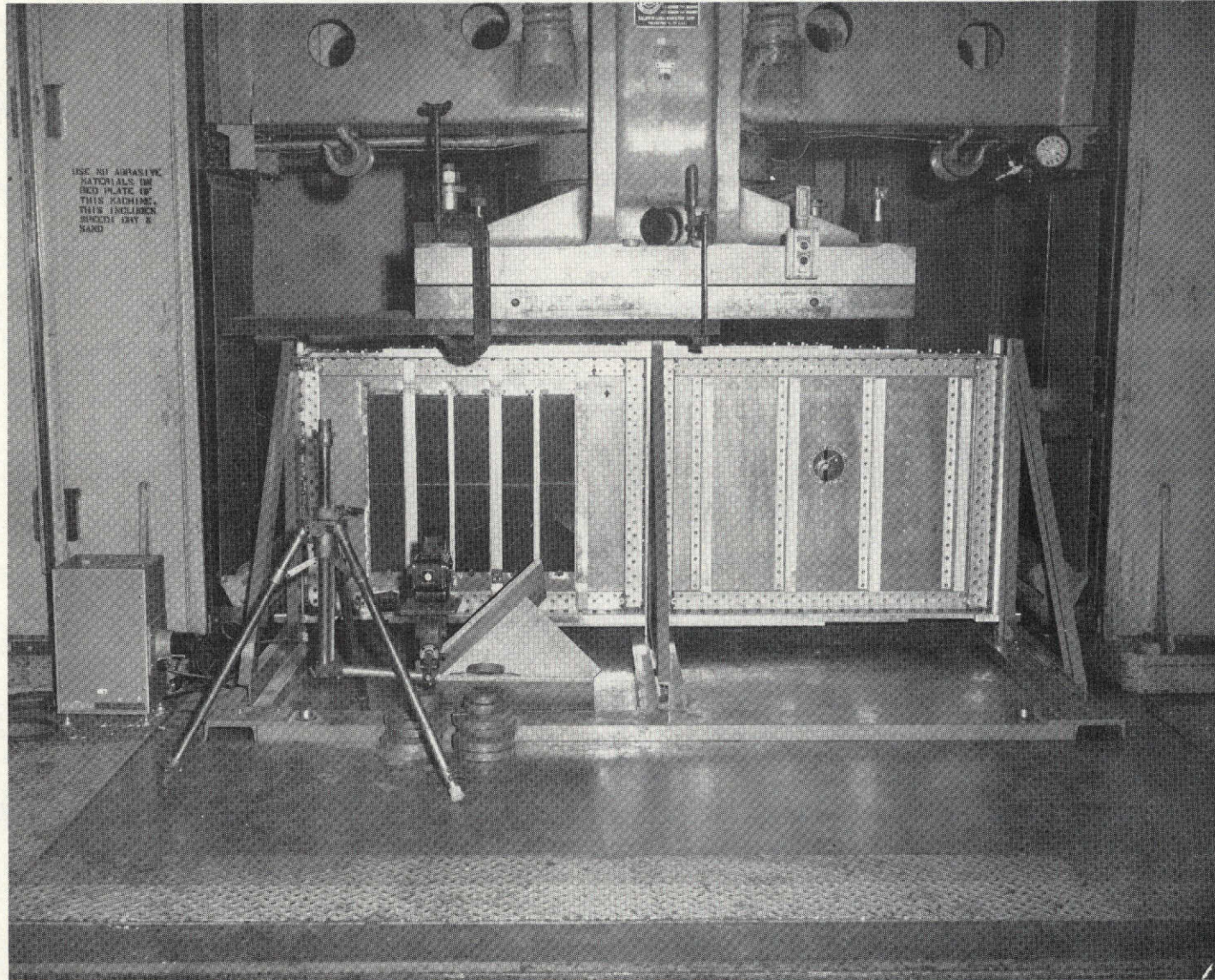
Figure 15: SHEAR WEB COMPONENT TEST SET-UP
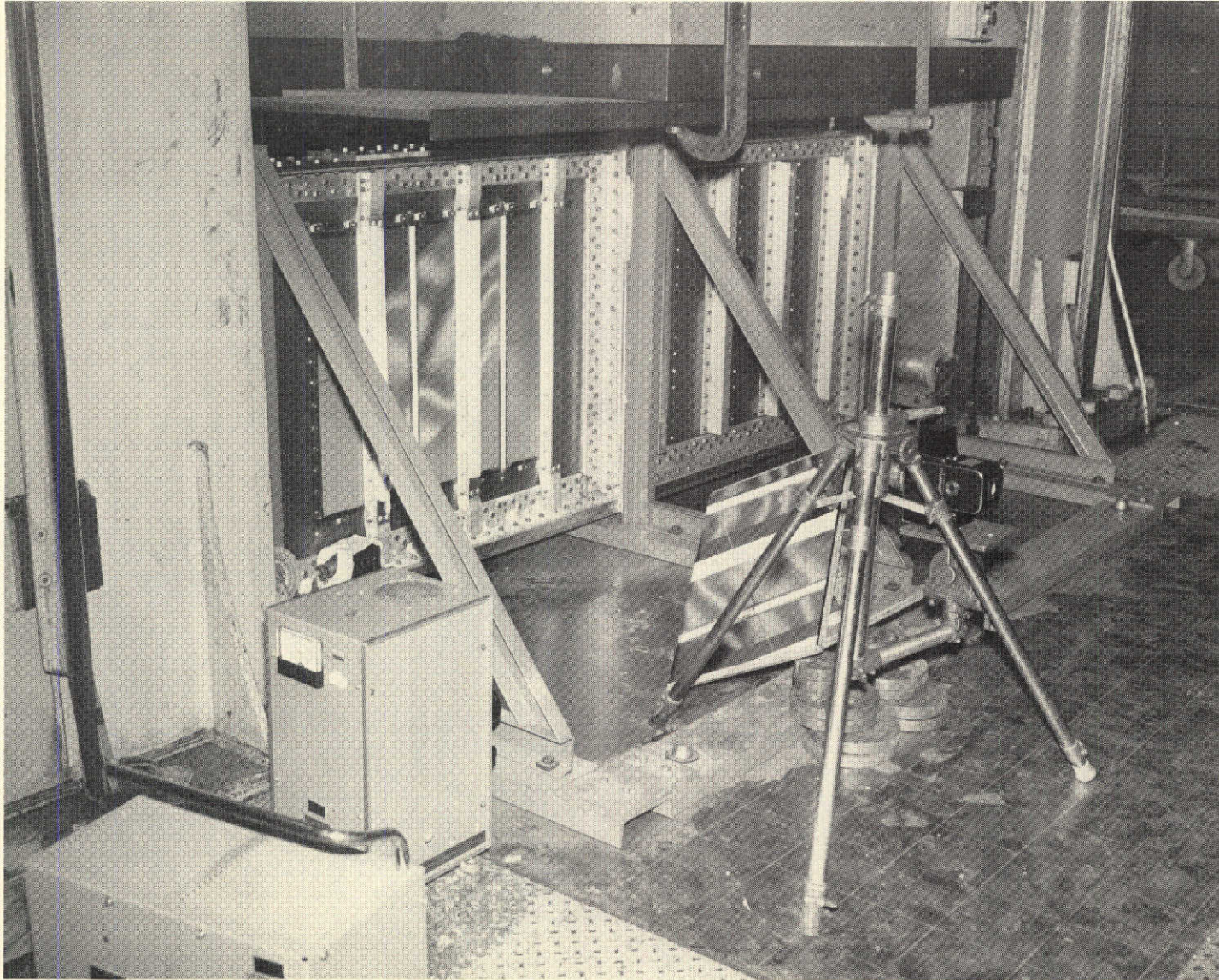
Figure 16: MOIRE FRINGE INSTRUMENTATION SET-UP

mirror located on the floor which reflects the beam to a mirror mounted to the glass Moire grid panes mounted on the test web component. A camera was positioned in front of the web to record the Moire fringe patterns developed during testing.

5.0 TEST DATA SUMMARY

The observed test results are summarized in Figure 17. These results will be analyzed and discussed in detail in the following sections. The results that are unique or important to the evaluation of the composite design concept are:

Lack of post-buckled strength

High low-cycle fatigue resistance

Evidence of time dependent lateral web deflections

5.1 LOAD/DEFLECTION DATA

The load/center deflection responses are given in Figure 18. The non-linear response is due to slippage in the test beam assembly and web buckling deflections. The stepped response of test web 3 is a result of time-dependent lateral web deflections which occurred in load holding periods during the final loading; this response will be discussed in the Time Dependent Response Section (Section 6.4).

TEST WEB	MAXIMUM LOAD	COMMENTS
1	540,000 LB (2.4 MN)	• FAILED BY COMPOSITE FRACTURING IN POST-BUCKLED PANELS AT A 1.5 MAX. LOAD TO BIFURCATION BUCKLING LOAD RATIO
2	530,000 LB (2.36 MN)	• LOADED 400 CYCLES TO 400,000 LB (1.78 MN) WHICH PRODUCED 0.1 IN. (2.54 MN) MAXIMUM PANEL PRE-BUCKLING DEFLECTION • WEB WAS IN POST BUCKLED CONDITION AT MAXIMUM LOAD • NO APPARENT DAMAGE OCCURED
3	575,000 LB (2.56 MN)	• FAILED BY COMPOSITE FRACTURING AT HIGH PRE-BUCKLING PANEL STRAINS • FAILURE OCCURED WHILE HOLDING MAXIMUM LOAD (2.1 MINUTES) • EVIDENCE OF SMALL TIME-DEPENDENT LATERAL WEB DEFLECTION RESPONSE

*Figure 17: SHEAR WEB COMPONENT TEST RESULTS SUMMARY*
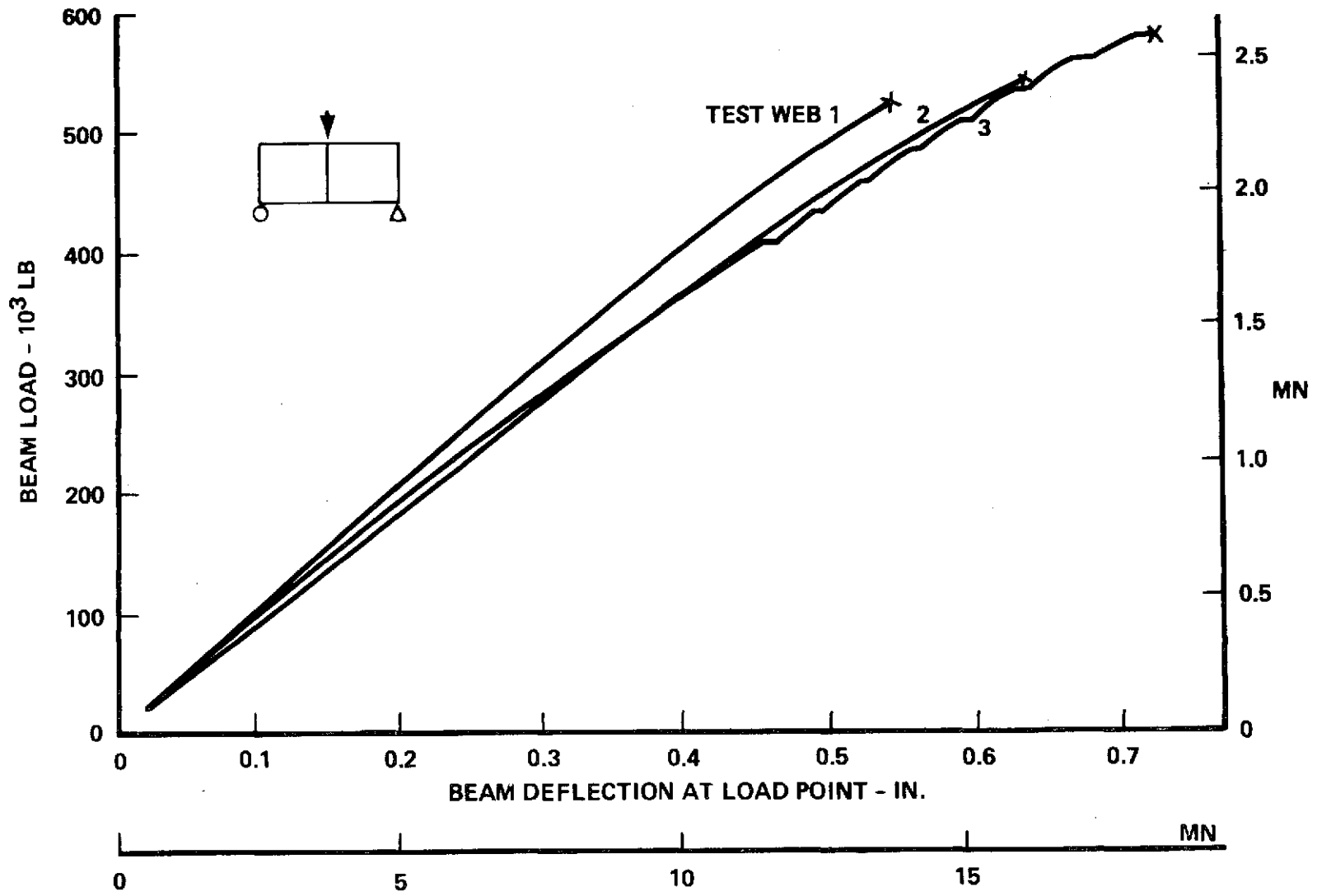
Figure 18: LOAD/DEFLECTION RESPONSES

5.2 STRAIN DATA

Principal strain data from strain gages at or near critical panel deflection areas are shown in Figures 19 to 21. The other strain data that was recorded is presented in Appendix A. The strain data reflects the increase in buckling resistance obtained in going from test web 1 to 3. Web laminate bending (buckling) deformation is indicated in the plots by a deviation of the respective strains from the back-to-back gages. The influence of initial imperfections is apparent in the case test web 1 (which had the highest initial flatness imperfection) where the web bending response initiated at low load. Test web 3 was relatively buckle resistant until near the failure load.

5.3 MOIRE FRINGE PATTERN DATA

The Moire fringe patterns recorded at selected load levels are presented in Figures 21 to 25 for test web 1, Figures 26 to 29 for test web 2 and Figures 30 to 34 for test web 3. Patterns for test web 2 and 3 at other load levels are given in Appendix B.

The instrumentation parameters for each test are listed as follows and are defined in Reference [3]. The grid density was decreased after the first web test to improve pattern resolution at high deflection magnitudes.
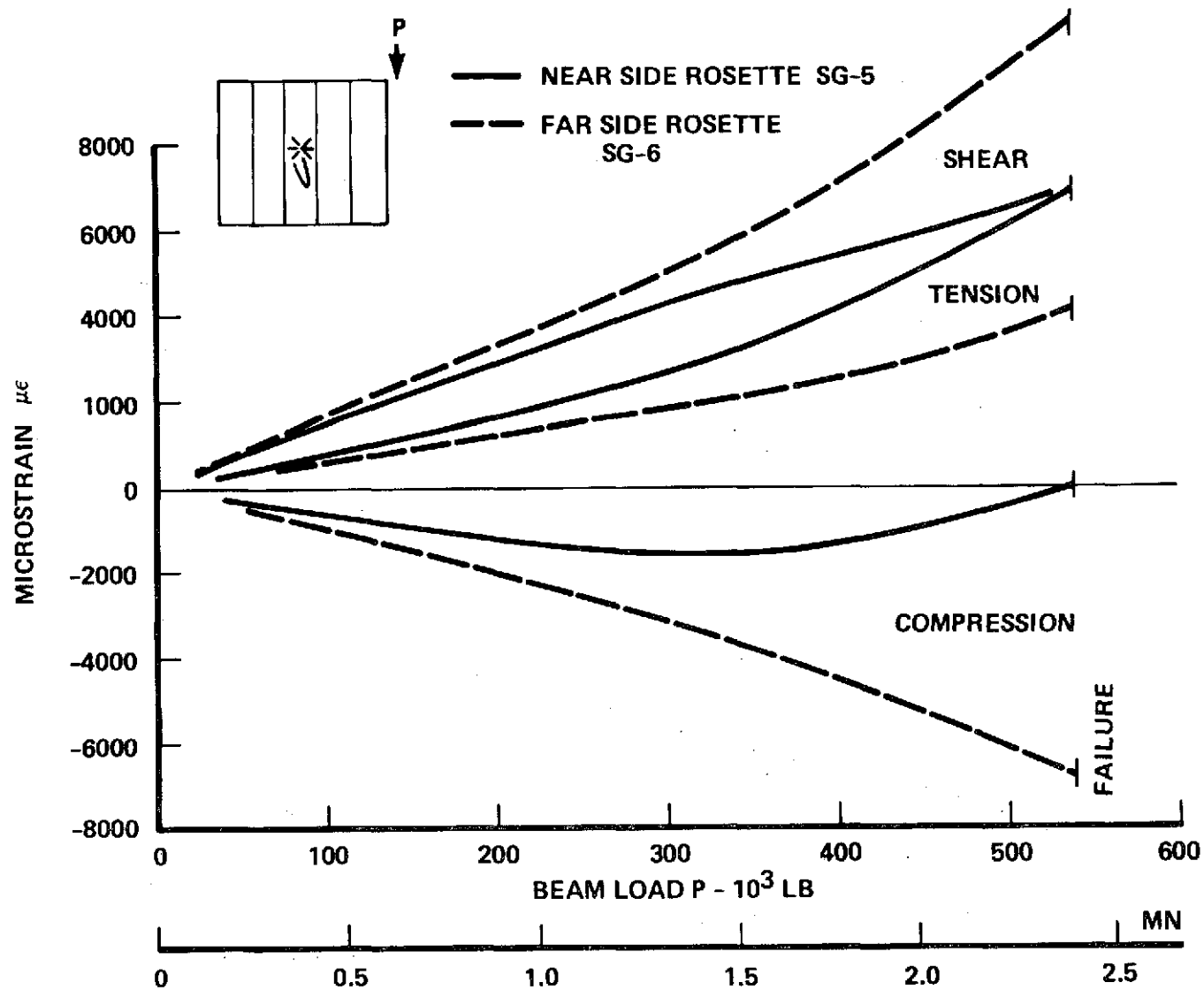
Figure 19: TEST WEB 1 PRINCIPAL SURFACE STRAINS IN CRITICAL BUCKLE AREA

31
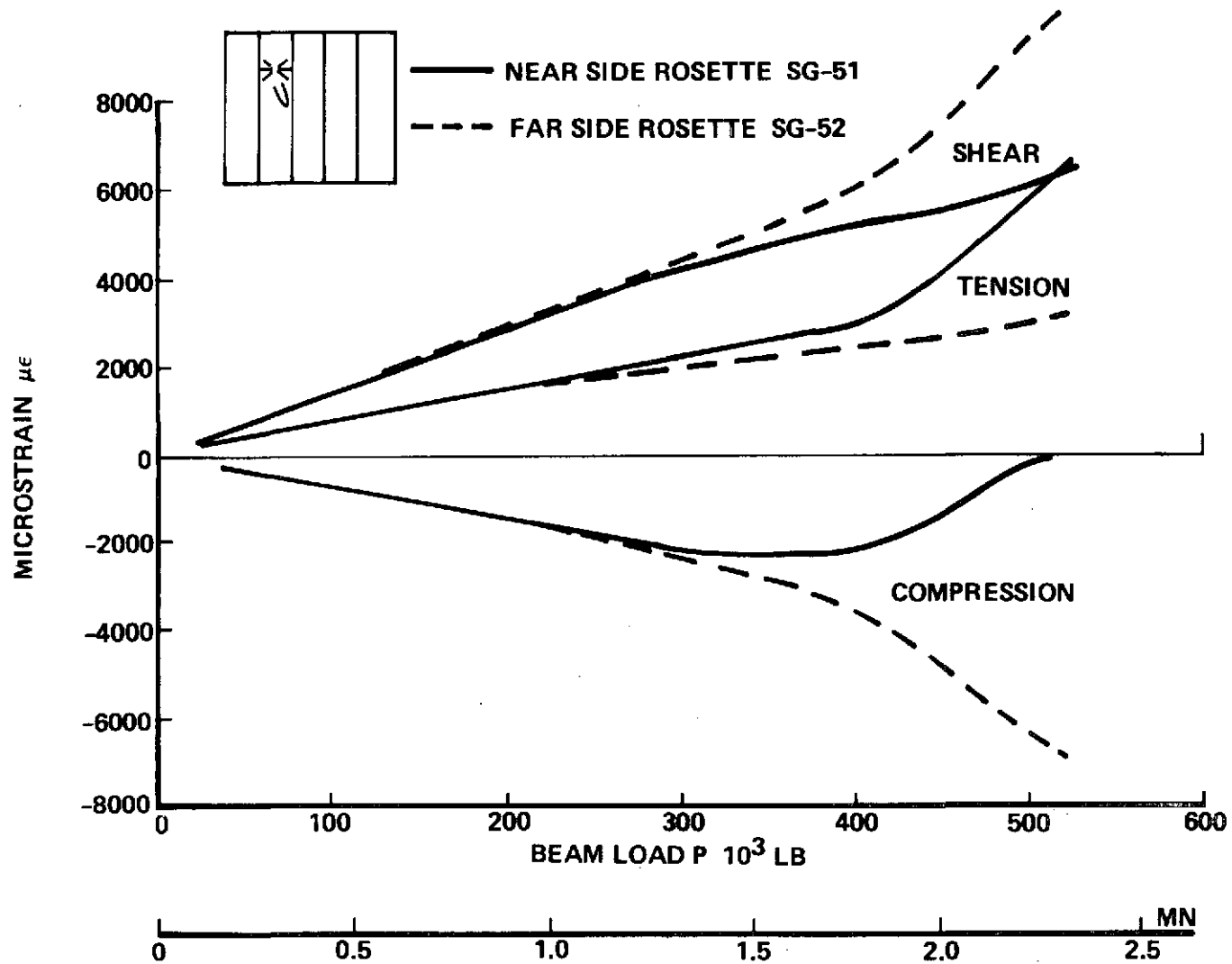
Figure 20: TEST WEB 2 PRINCIPAL SURFACE STRAINS IN CRITICAL BUCKLE AREA
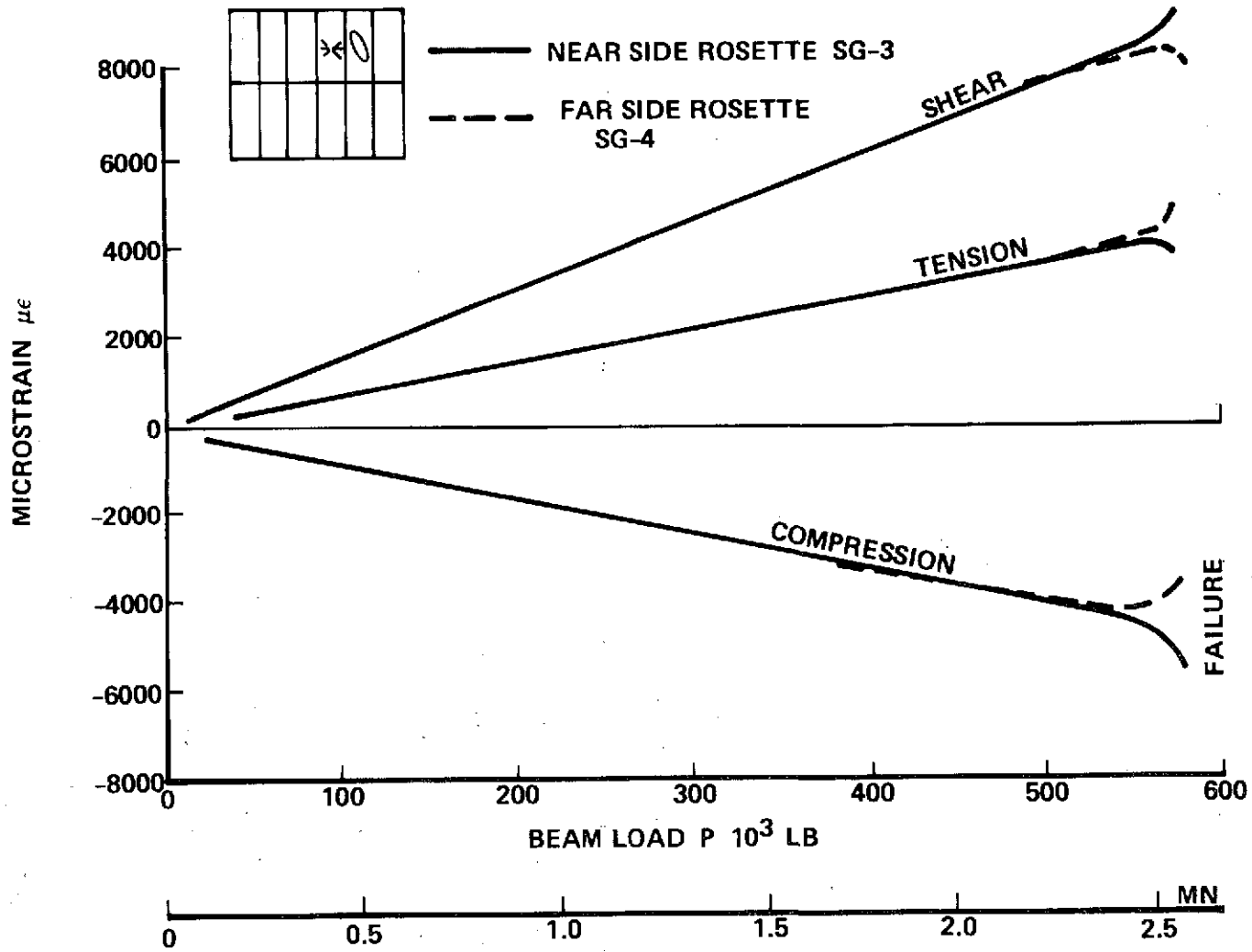
Figure 21: TEST WEB 3 PRINCIPAL SURFACE STRAINS NEAR CRITICAL BUCKLE AREA

33

Test Web	Web/grid separation gap inch (mm)	Grid density lines/inch (lines/mm)	Incidence angle degrees	Lateral deflection sensitivity inches/fringe order (mm/fringe order)
1	0.17 (4.32)	100 (3.94)	61°	0.0055 (0.140)
2	0.75 (19.1)	33-1/3 (1.31)	58°	0.01875 (0.476)
3	0.75 (19.1)	33-1/3 (1.31)	60°	0.01730 (0.439)

The attachment points of the glass grid panes can be seen in the figures; a three point mounting arrangement was used for each pane to isolate the pane from the central web deflections. Glued pane splices were used and they can be seen along the web centerline. The shadows from these splices are indicators of the buckle deflections. In the second test, horizontal tape stripes and short posts bonded to the stiffeners cast shadows which assist in defining the deflection state. The post shadows indicate stiffener rotation in terms of shadow movement from an initial reference mark.

The Moire fringe patterns for the first test web at zero load after 100 load cycles (Figure 22) indicate a level of imperfection on the order of ± 0.016 in (0.406 mm) deviation from a mean flat surface. This imperfection resulted, as described in Reference (2), from unsatisfactory aluminum built-up shim stock placed between the stiffeners and the web laminate (shims used on the second and third webs were molded plastic material). Several perbutations are visable in the pattern where shim

layers ended and the web laminate was distorted by fasteners in areas of partial shim contact.

As the first web was loaded, the resulting Moire fringe patterns indicate severe buckling deflections. Coupled plate/stiffener buckling is evident by the intersecting of panel fringes with stiffeners. The critical buckle area is in the center panel; a set of rosette strain gages is located at the center of this panel close to the buckle peak. Because of high buckle deflections, the glass grid panes came in contact with the web and were fractured at 500,000 lb (2.22 MN). Initially, the panes were spaced 0.17 in (4.32 mm) from the web panels.
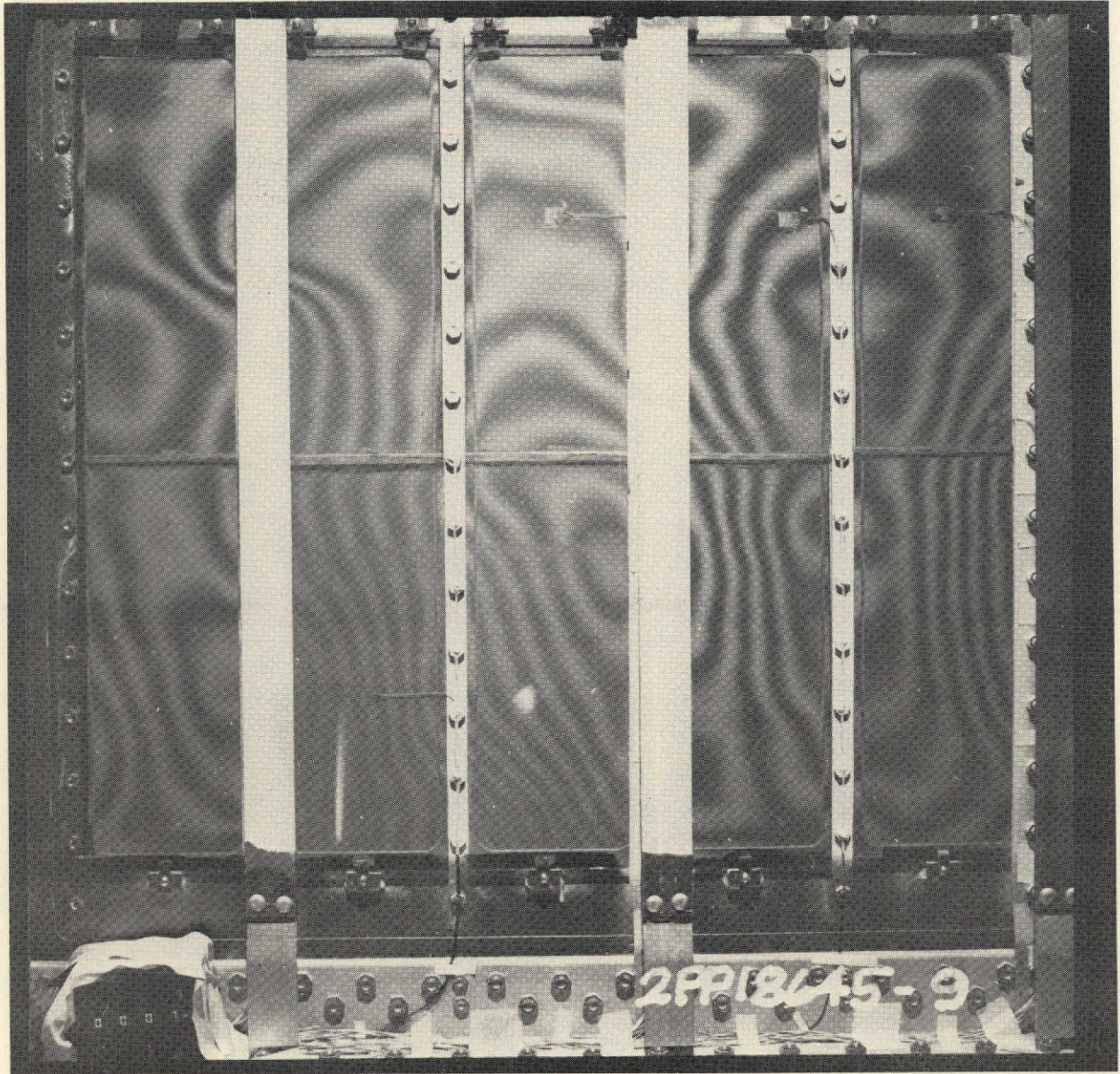
Figure 22: TEST WEB 1 MOIRE FRINGE PATTERN AT ZERO LOAD AFTER 100 LOAD CYCLES
TO 400,000 LB (MN)
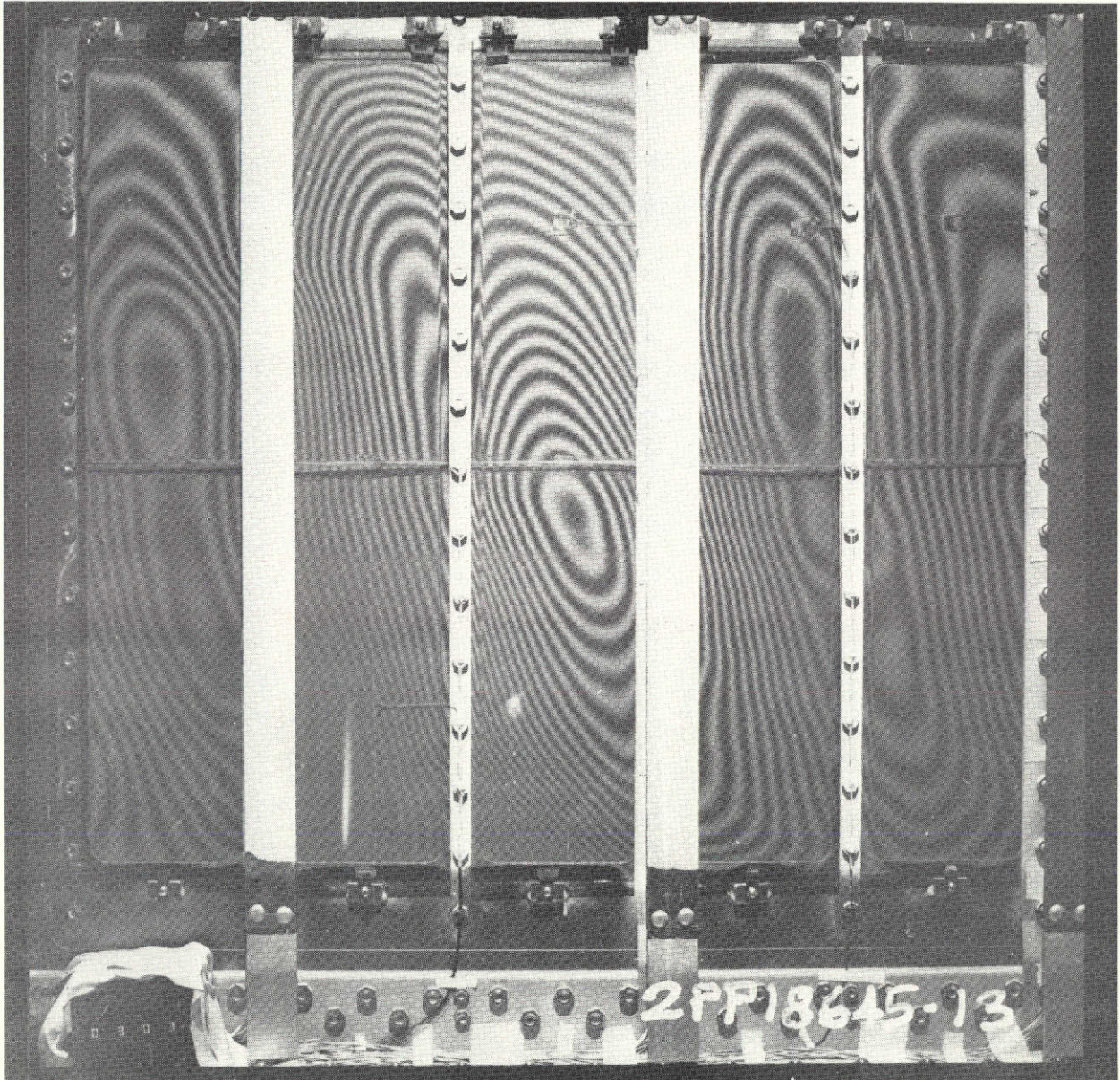
Figure 23: TEST WEB 1 AT 300,000 LB (1.33 MN)
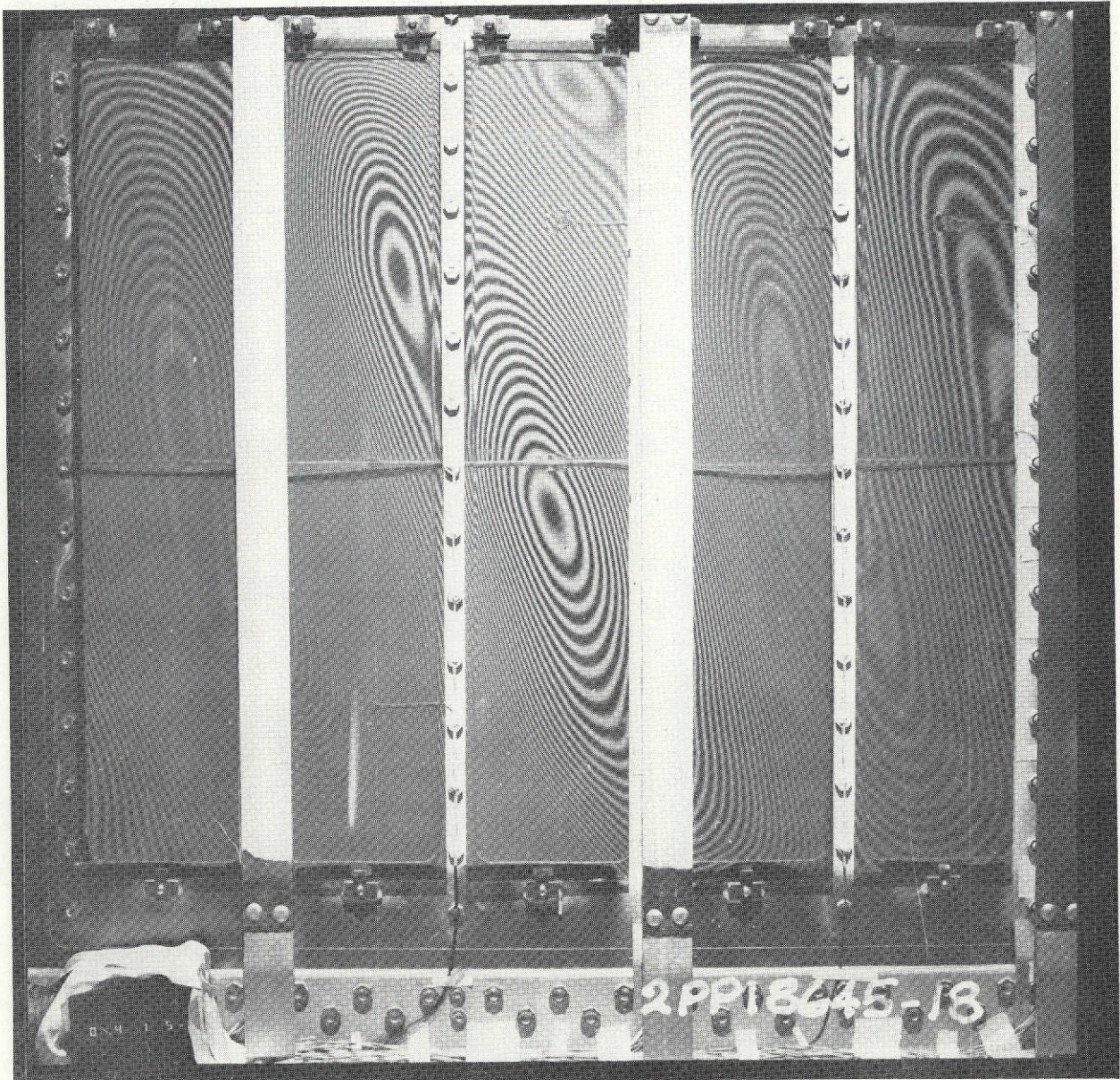
Figure 24: TEST WEB 1 AT 410,000 LB (1.82 MN)
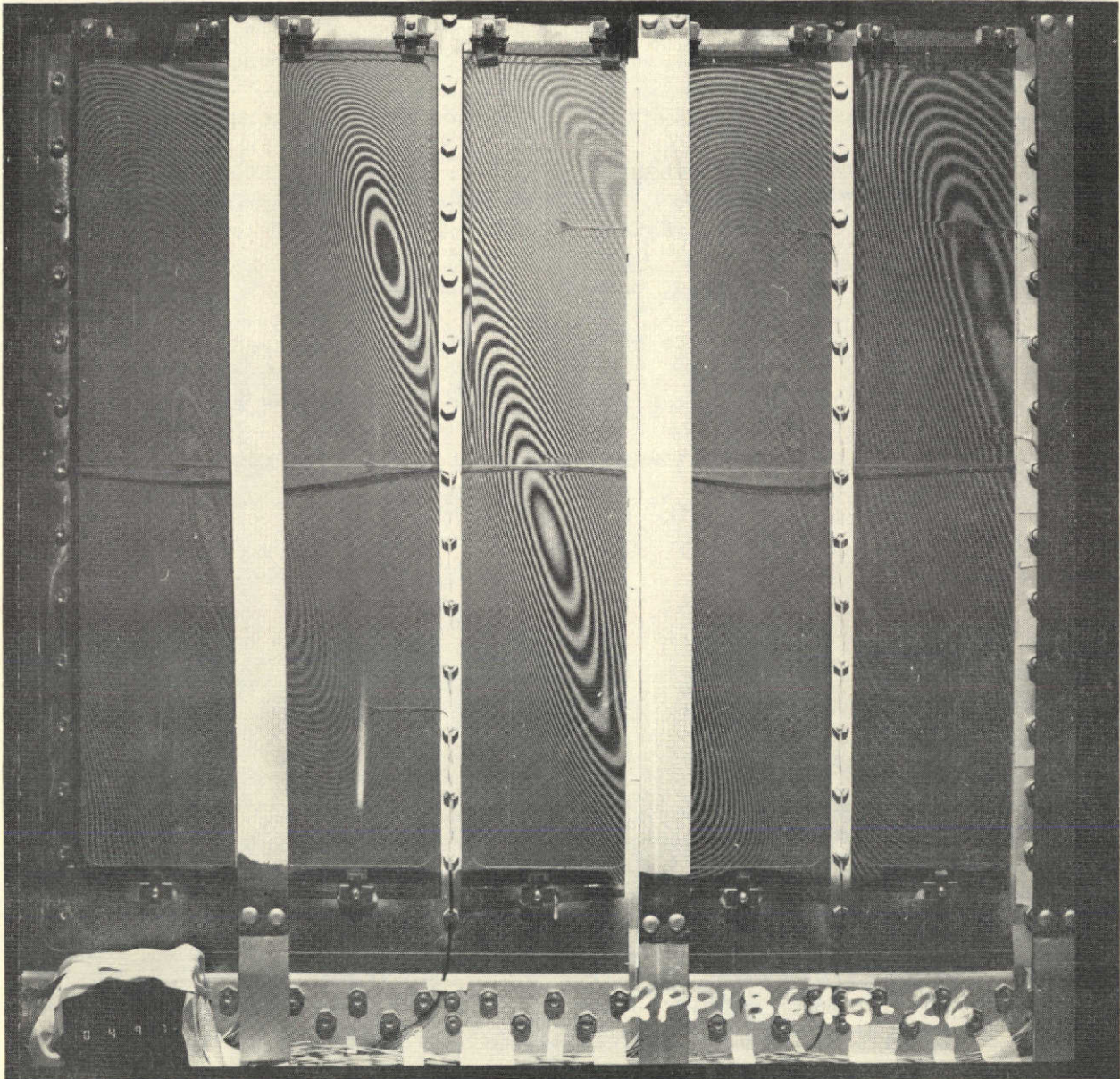
Figure 25: TEST WEB 1 AT 497,000 LB (2.21 MN)

The second test web is shown in Figure 26 at zero load. Initial flatness imperfections were also introduced in this web during final assembly. The imperfections grew slightly during load cycling to about level of +0.014 in (0.356mm) deviation from a mean flat surface. This growth in imperfection is attributed to slippage between the stiffeners and the web laminate (the fasteners were non-hole filling and were torqued to low level to avoid laminate crushing). At the cyclic load level of 400,000 lb (1.78 MN), the maximum prebuckling panel deflection is on the order of +0.1 in (2.54 mm) or about one-half laminate thickness. Coupled plate/stiffener pre- and post-buckling is clearly displayed in Figures 28 and 29, respectively. Significant stiffener rotations are indicated by movement of the post shadows. A set of back-to-back rosette strain gages are located close to the critical buckle in the upper part of the panel second from the left.
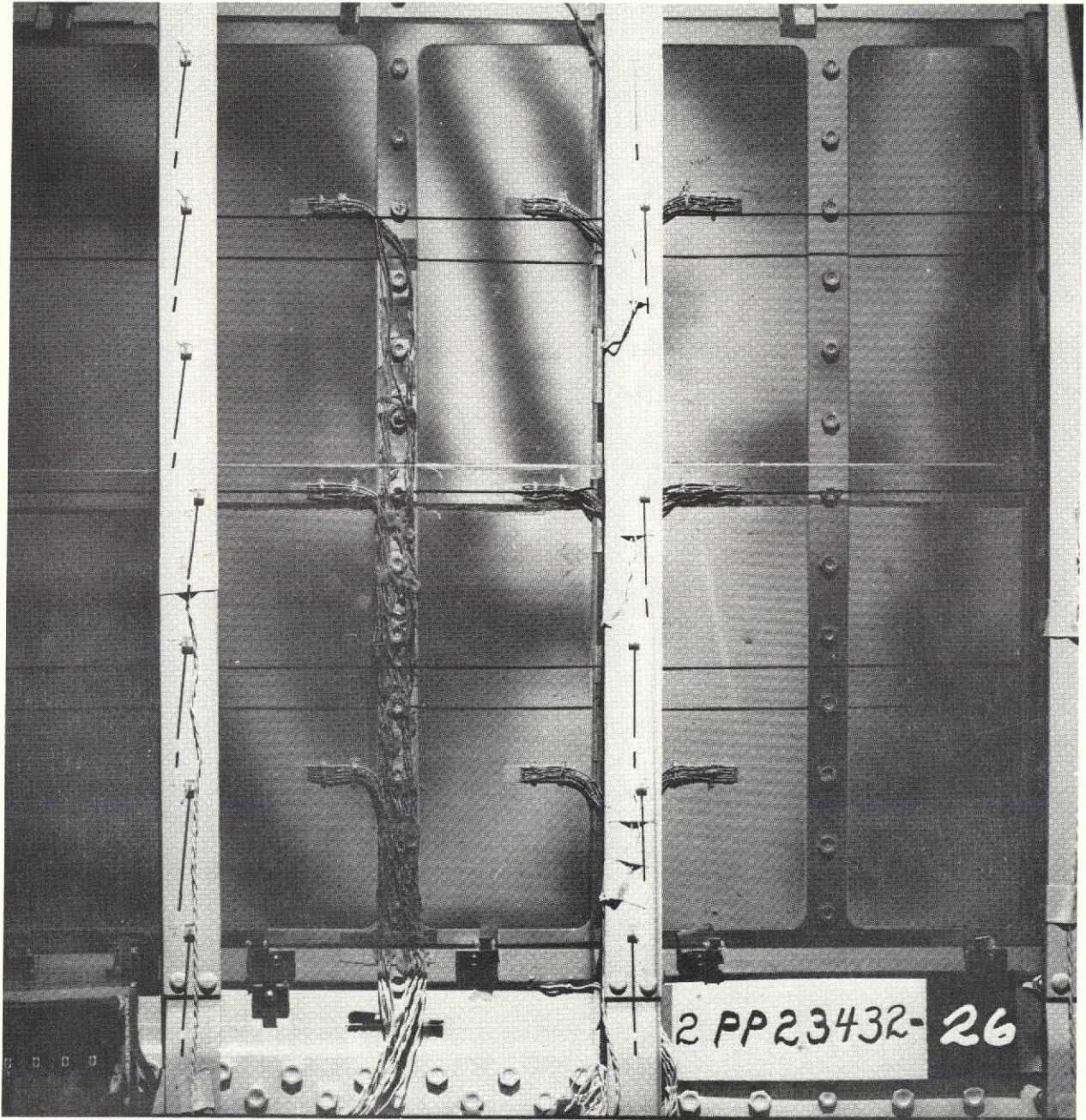
Figure 26: TEST WEB 2 MOIRE FRINGE PATTERN AT ZERO LOAD BEFORE LOAD CYCLING
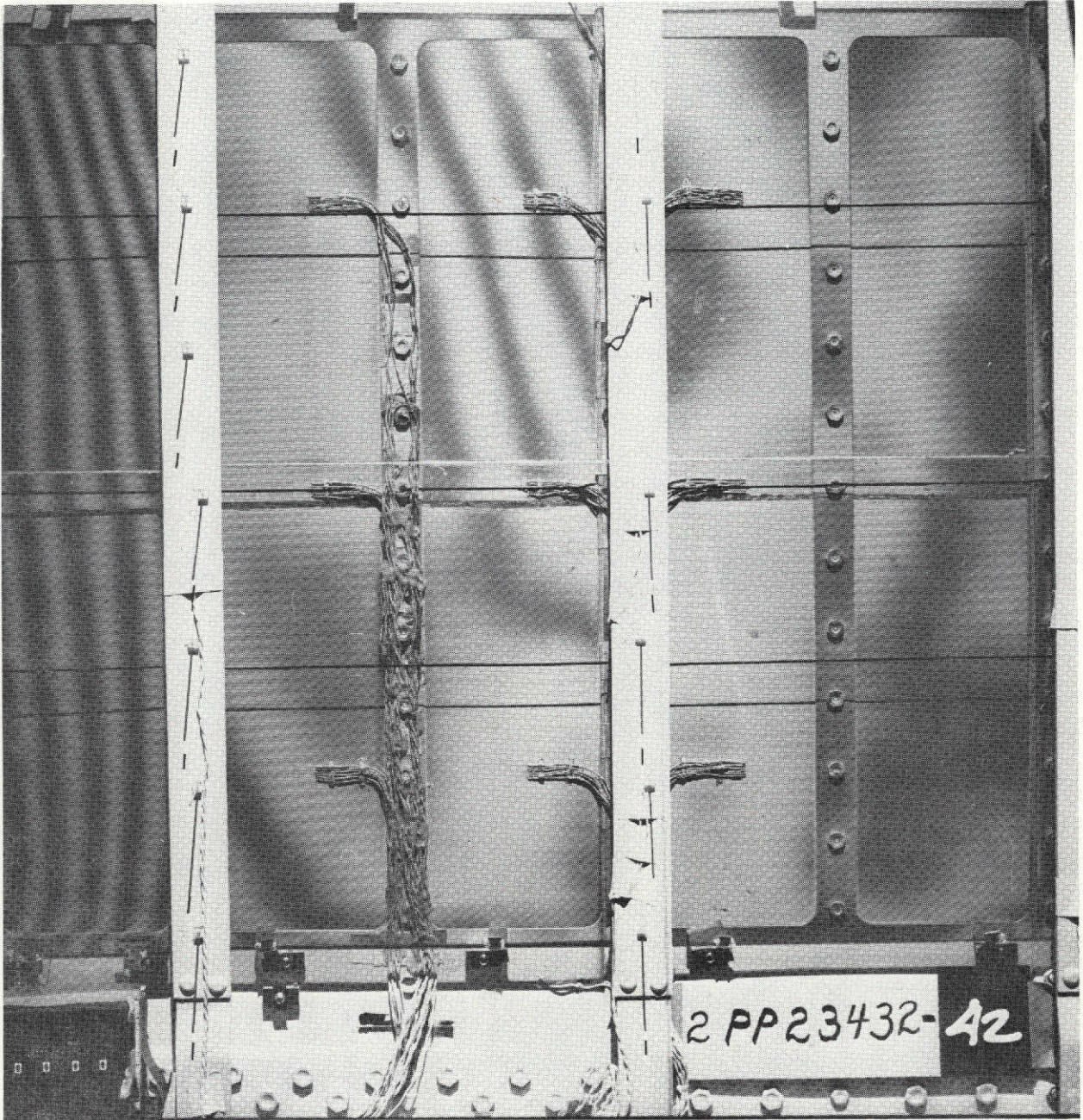
Figure 27: TEST WEB 2 AT ZERO LOAD AFTER LOAD CYCLING
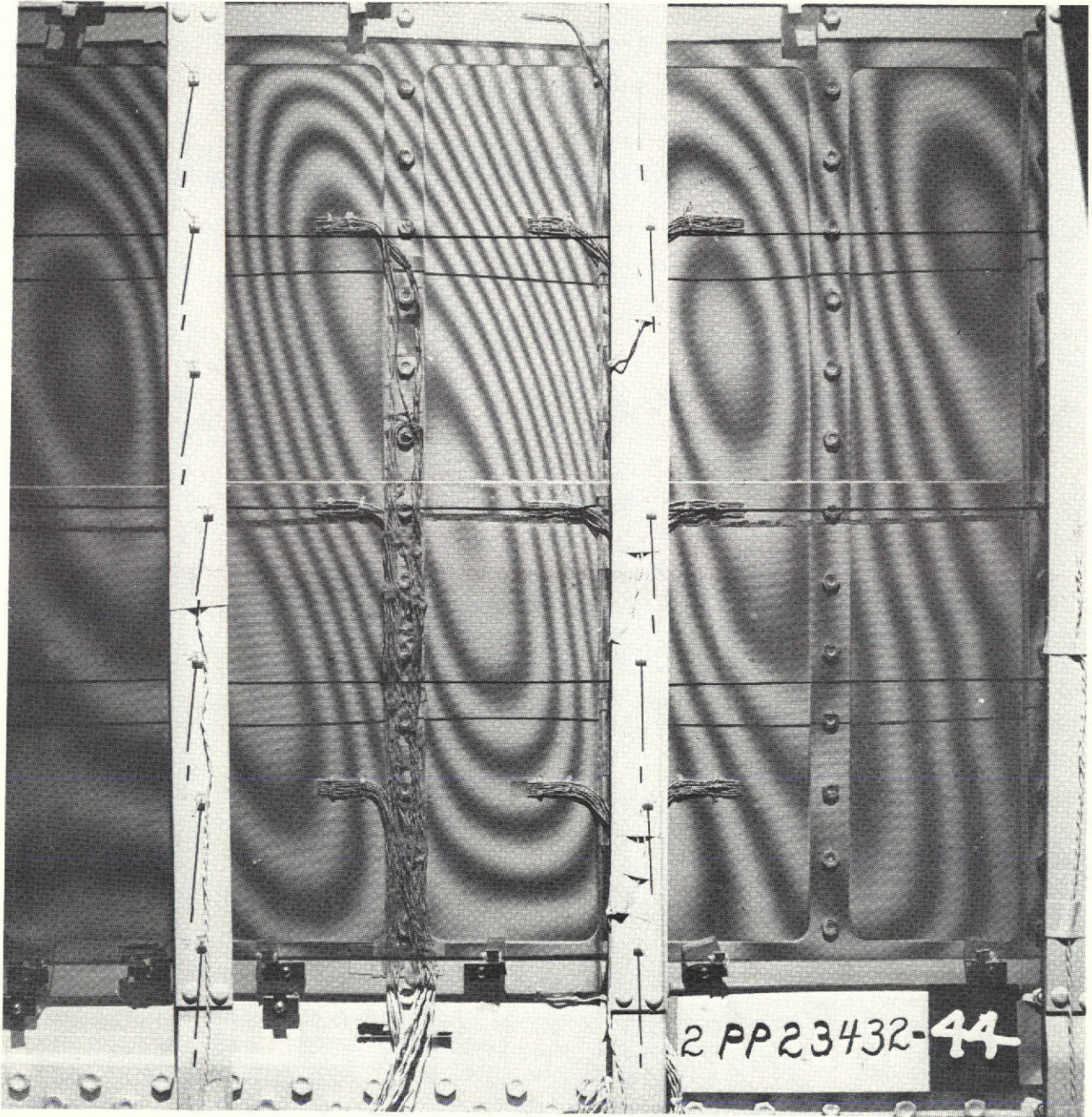
Figure 28: TEST WEB 2 AT 400,000 LB (1.78 MN)
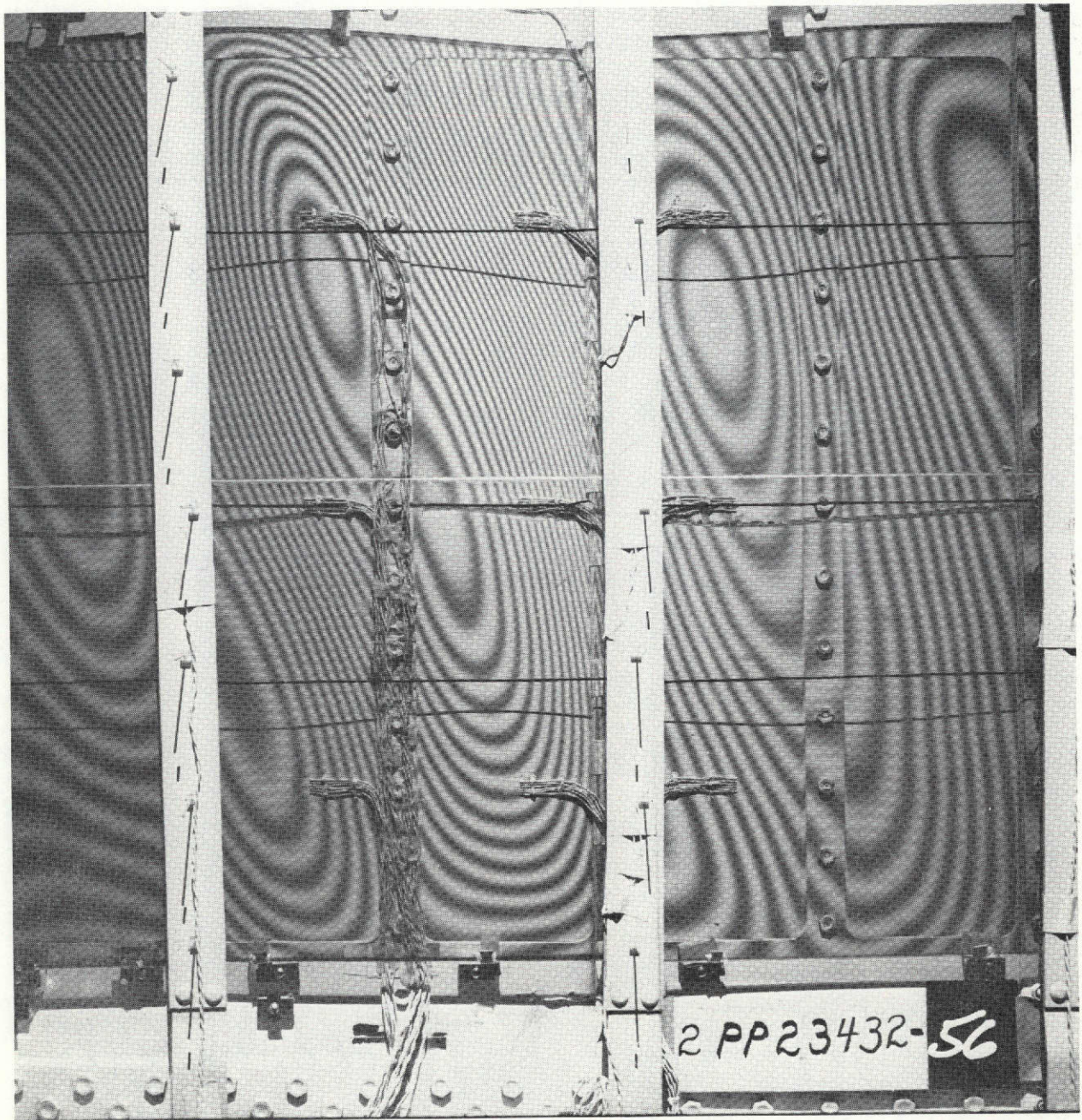
Figure 29: TEST WEB 2 AT 530,000 LB (2.36 MN)

Test web 3 displayed high stability during loading until about 500,000 lb (2.22 MN) when buckle-like deformations initiated in the upper parts of the two right most panels (Figure 32). As loading proceeded to failure, the critical prebuckling deformation developed in the second right panel with evidence of coupled plate/stiffener response. The estimated initial imperfection in this area is ±0.003 in (0.076 mm) based on measurements and the initial Moire fringe data. There was a slight thickness under-run of the web laminate in the critical buckle area (2) and this, along with the proximity to the loading area, is believed to have triggered the buckling response.

Non-linear strains were recorded by a strain gage just above the panel third from the left (on the reinforced laminate area, SG-19 in Appendix A). These strains and the Moire fringe patterns shown in Figure 34 indicate that buckling type deformations were extending into areas near the chord angles; e.g., the effective panel height was greater than the nominal laminate panel height. An assessment of the effective panel height is given in the Buckling Analysis/Test Correlations Section (Section 8.3).
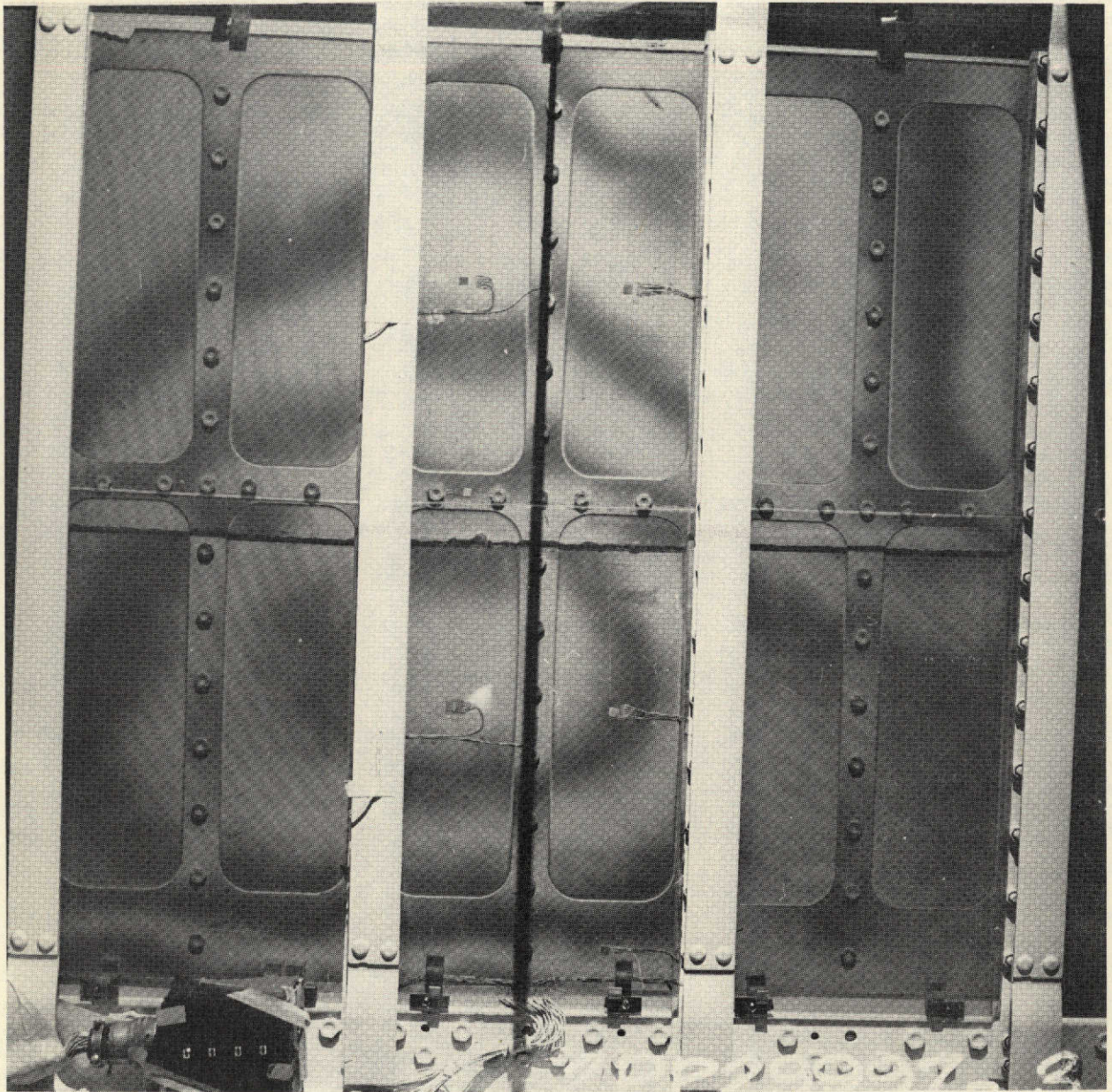
Figure 30: TEST WEB 3 MOIRE FRINGE PATTERN AT ZERO LOAD
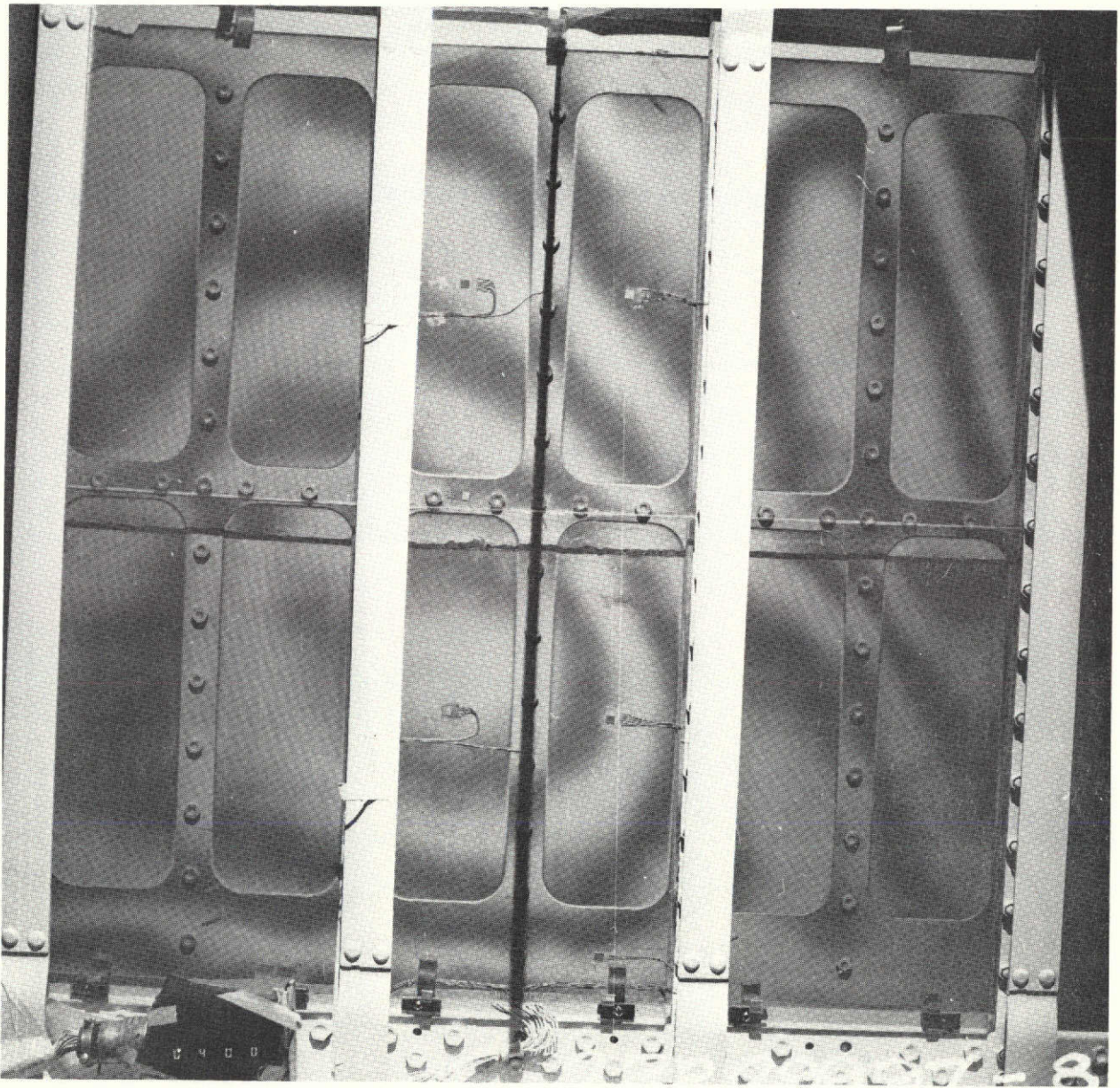
Figure 31: TEST WEB 3 AT 400,000 LB (1.78 MN)
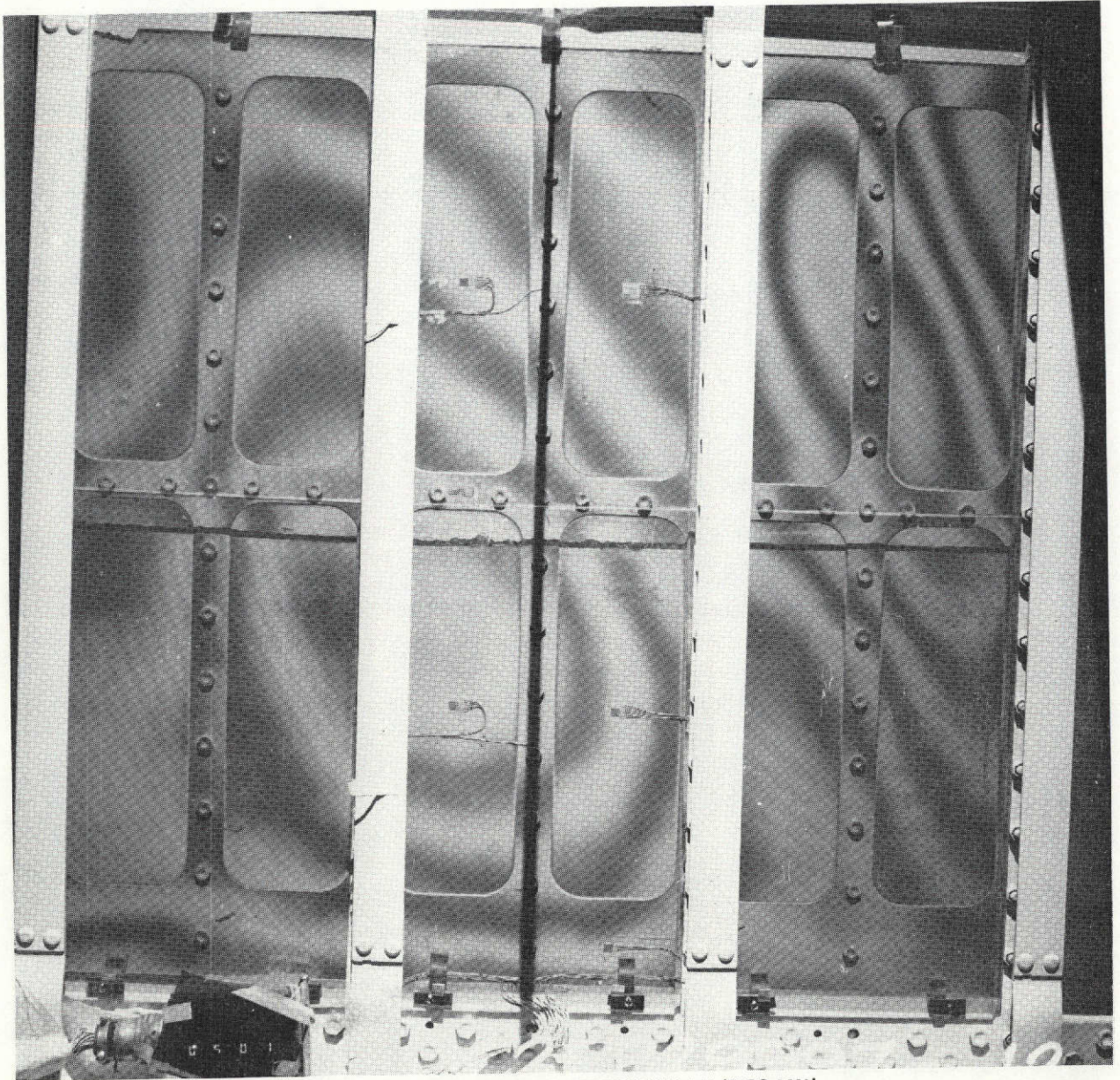
Figure 32: TEST WEB 3 AT 500,000 LB (2.22 MN)

Figure 33: TEST WEB 3 AT 550,000 LB (2.45 MN)
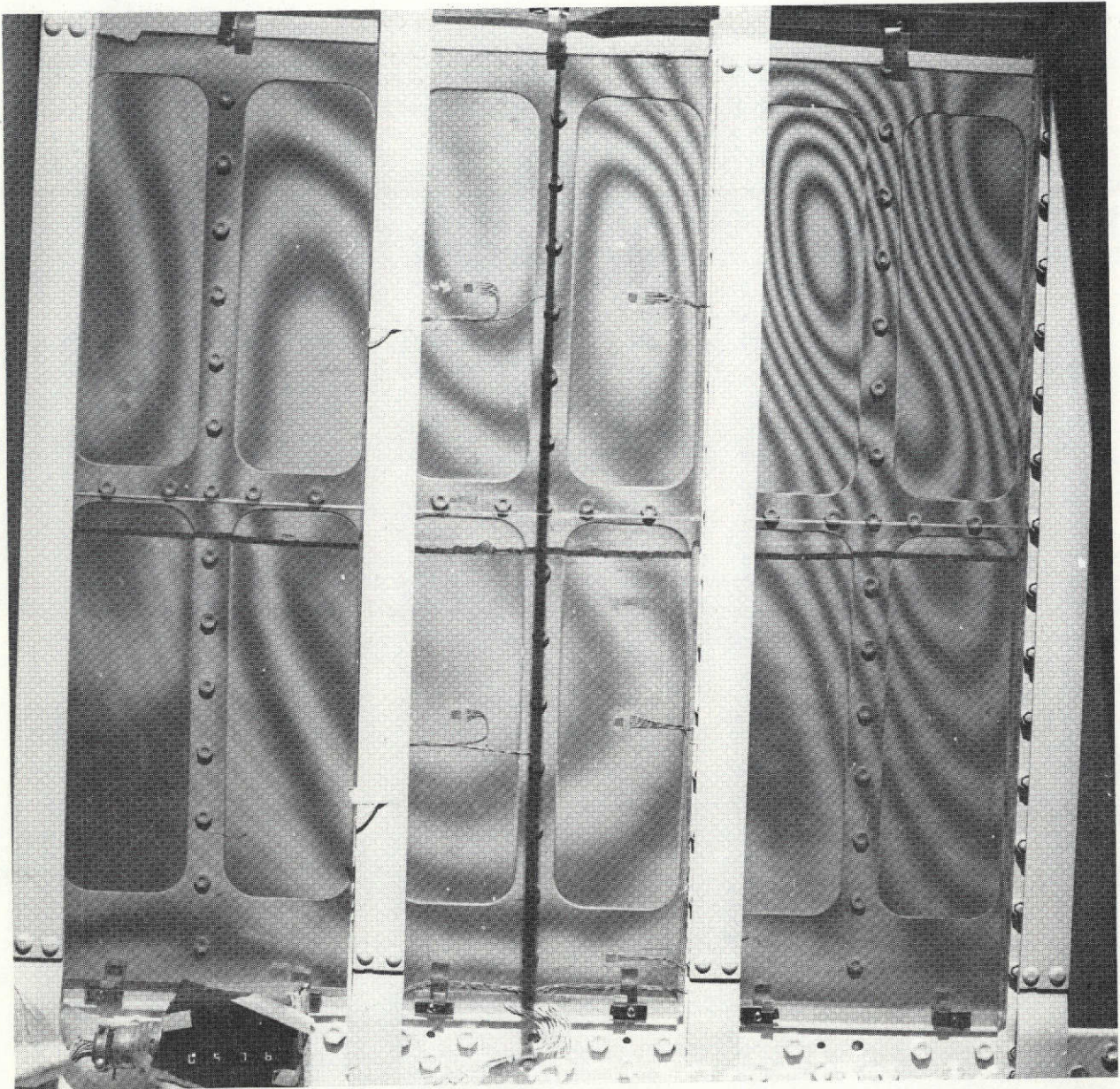
Figure 34: TEST WEB 3 AT 575,000 LB (2.56 MN)

5.4 ACOUSTIC EMISSION DATA

High and low frequency acoustic emissions were recorded during the web
component tests. Unlike the results obtained in tension element testing
in Phase I [1], the web component emission data was difficult to
interpret. Emissions having a signature like composite fracture did
occur momentarily at failure. The test beam assembly was noisy during
loading due to local slippages and the webs responded as microphones to
background laboratory noise. These annoyances made analysis of the
recorded emissions difficult but it is believed that damaging composite
fracturing did not occur in any test except when failure occurred.

5.5 POST TEST INSPECTIONS

Inspections of the web components after testing revealed no areas where
local design detail improvements would be necessary. The joint and
reinforced laminate areas appear to have functioned properly. Figures
35 to 37 show the first and third webs after failure. The "brittle"
nature of failure of this type of construction is apparent in the
figures. Fracturing extends into the edge joint areas although the
failures originated in the buckled panels.

Ultrasonic scans were made of the second test web (fatigue test compo-
nent) before and after testing and the scan recordings are shown in
Figures 38 and 39. There are essentially no differences in the signa-
tures except for those due to a change in sonic scan power level. In
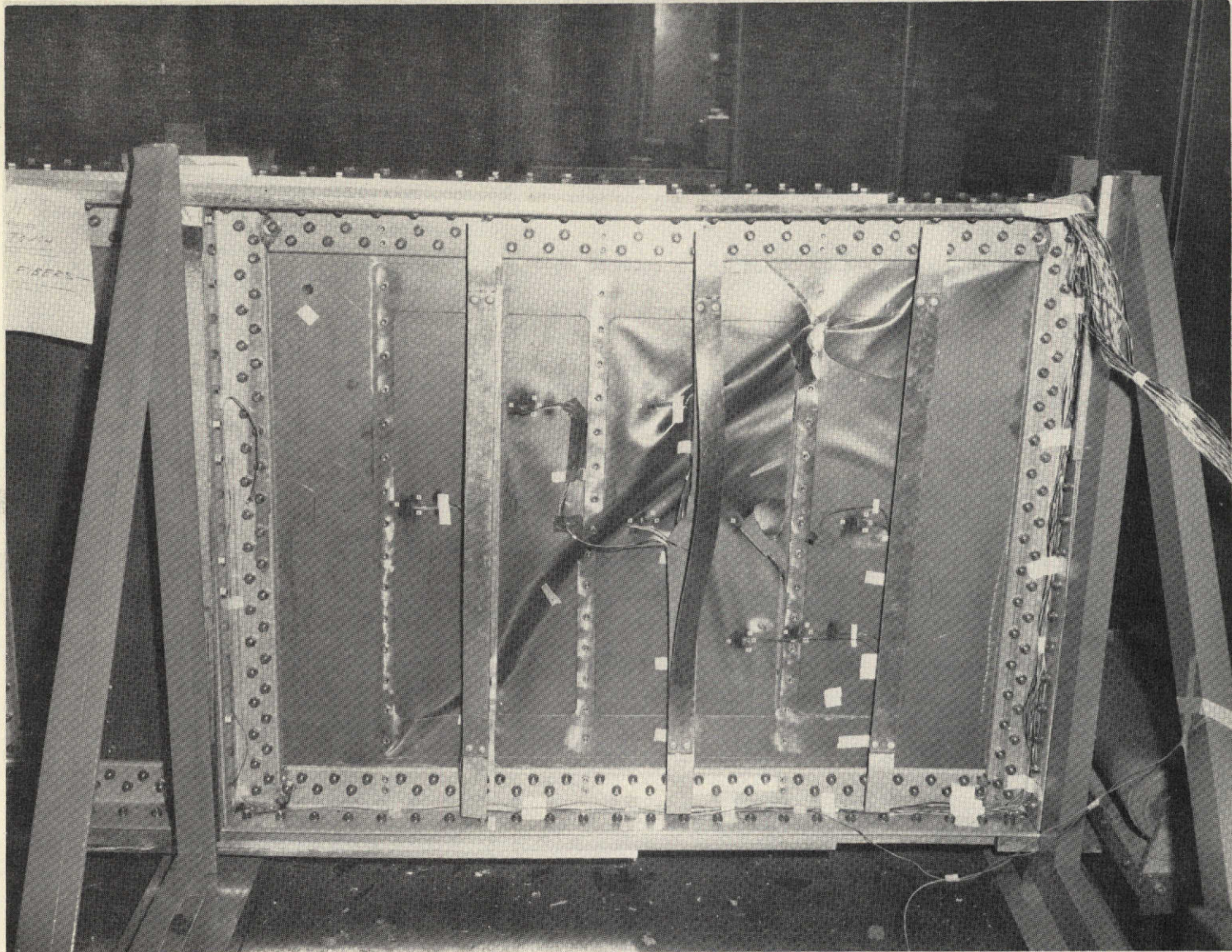
Figure 35: TEST WEB 1 AFTER FAILURE
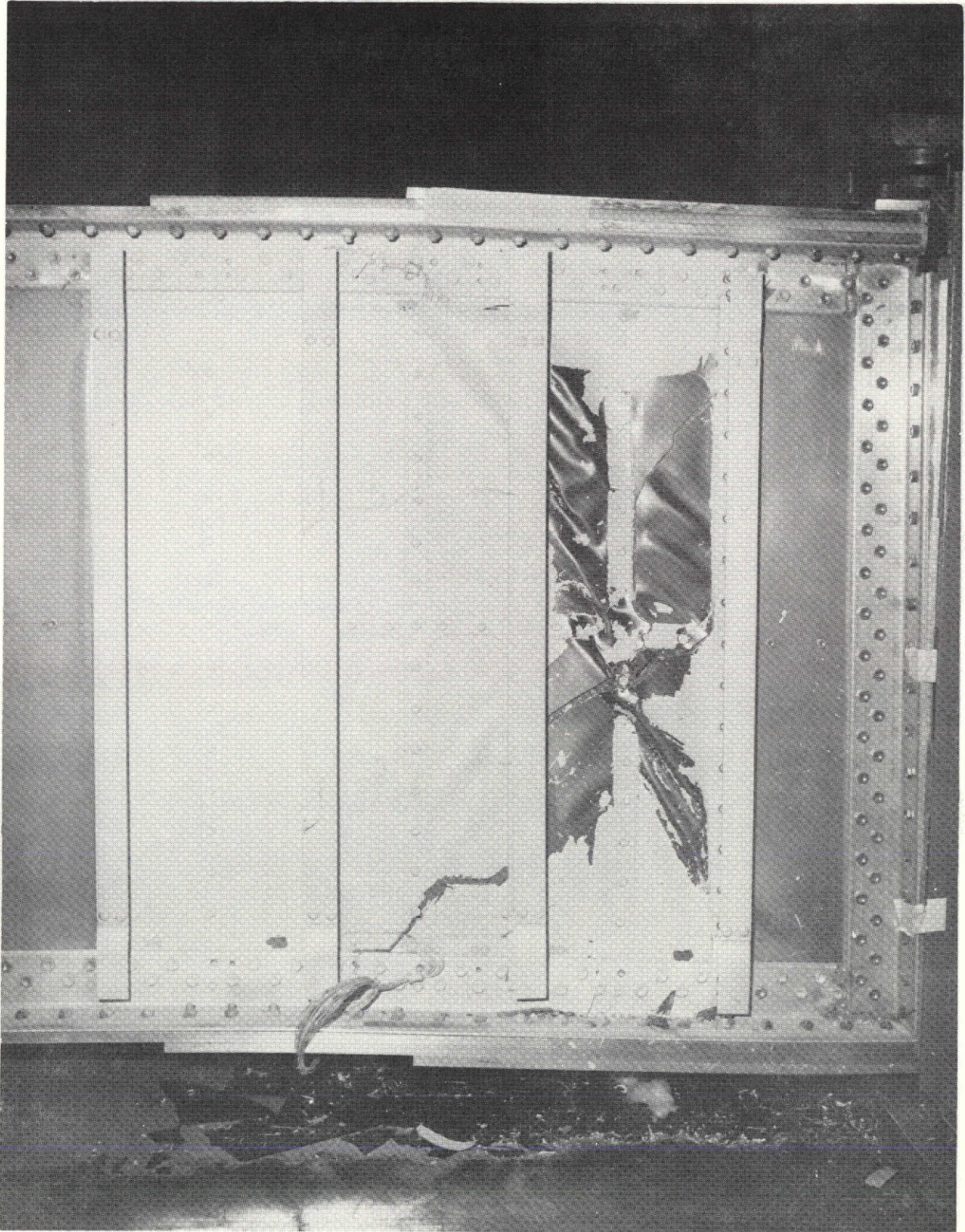
Figure 36: TEST WEB 3 AFTER FAILURE (FRONT SIDE)
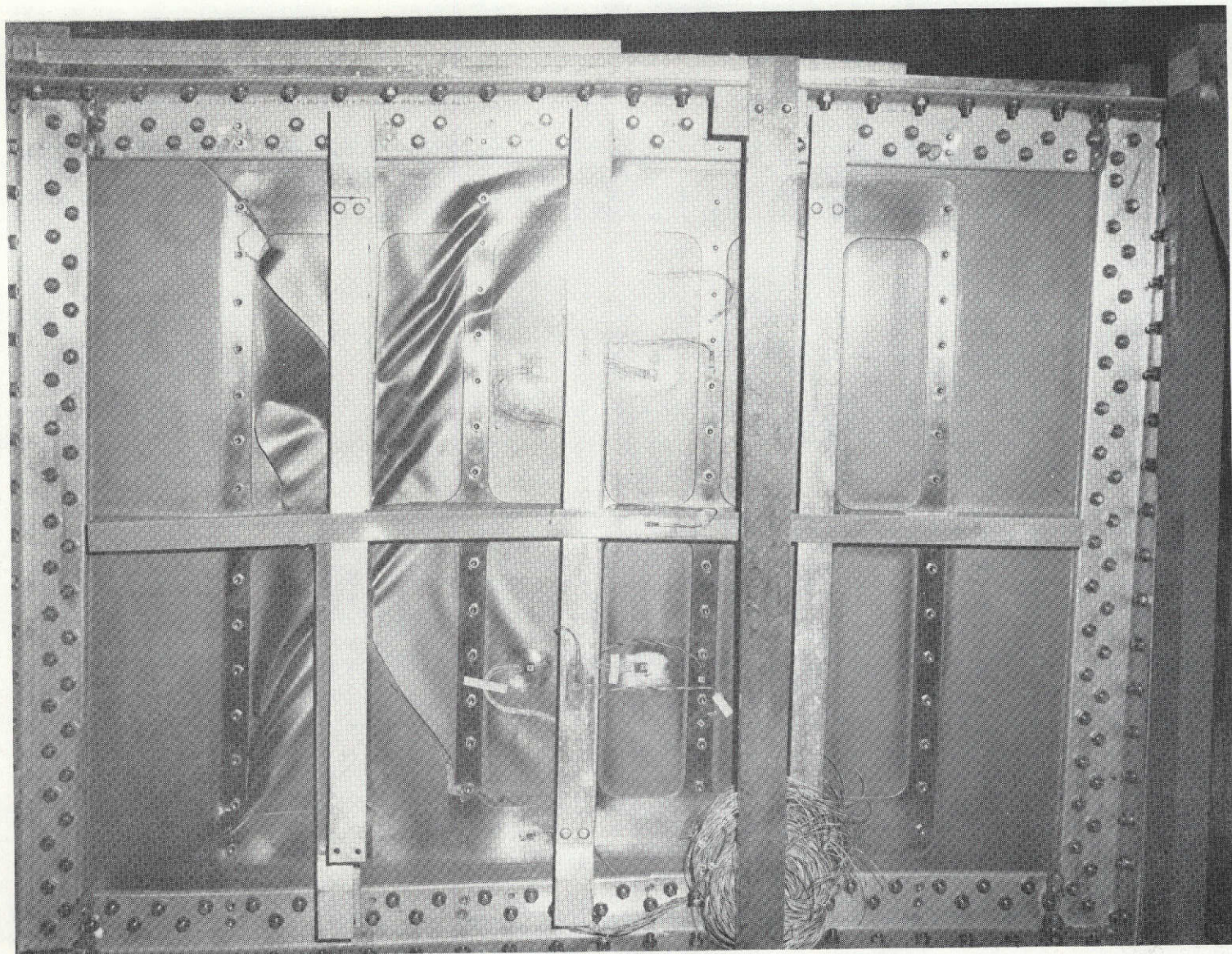
Figure 37: TEST WEB 3 AFTER FAILURE (REAR SIDE)

LOAD AREA

CENTER OF BEAM
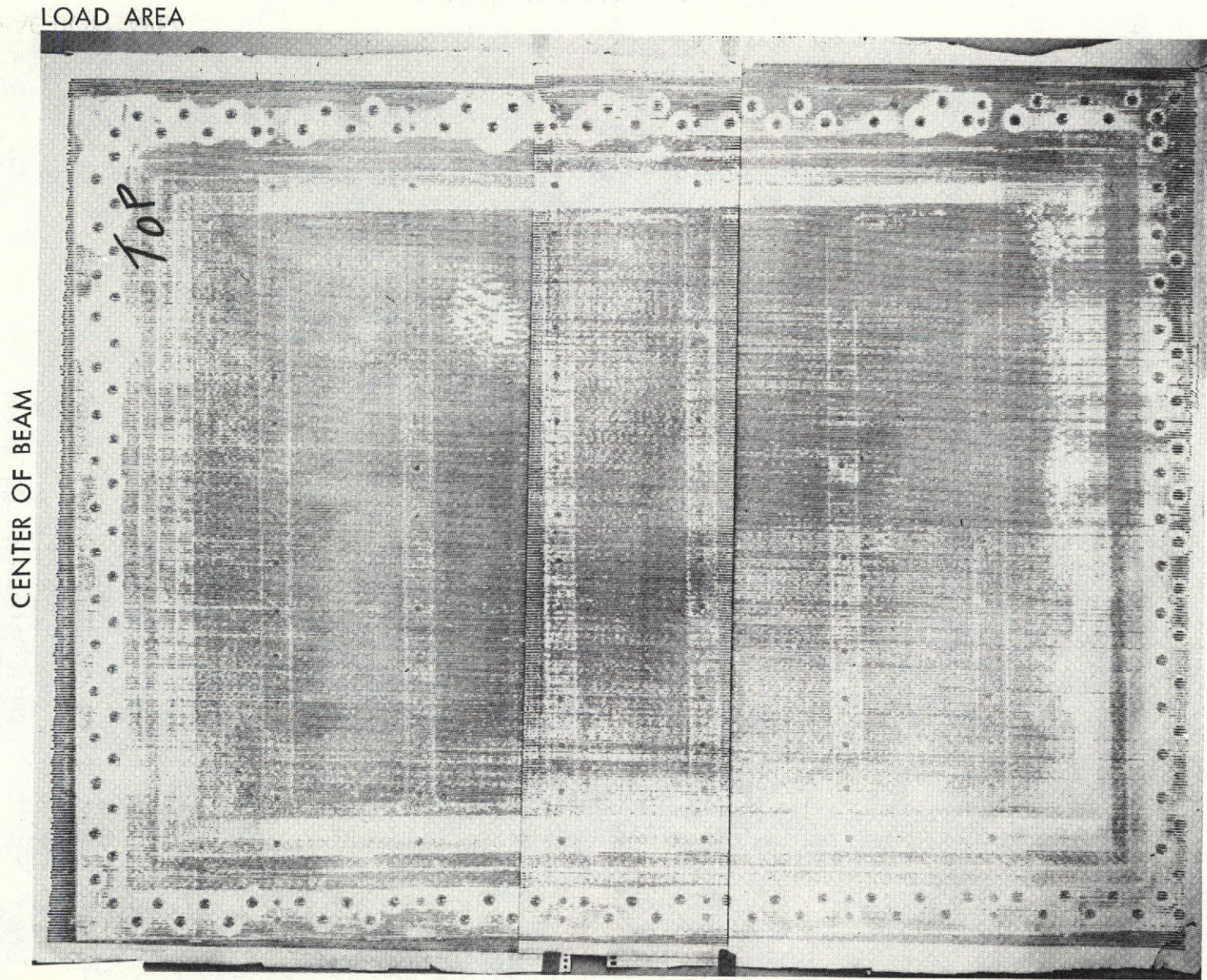
REACTION AREA

Figure 38: TEST WEB 2 ULTRASONIC SCAN BEFORE TESTING

55

LOAD AREA

CENTER OF BEAM

REACTION AREA
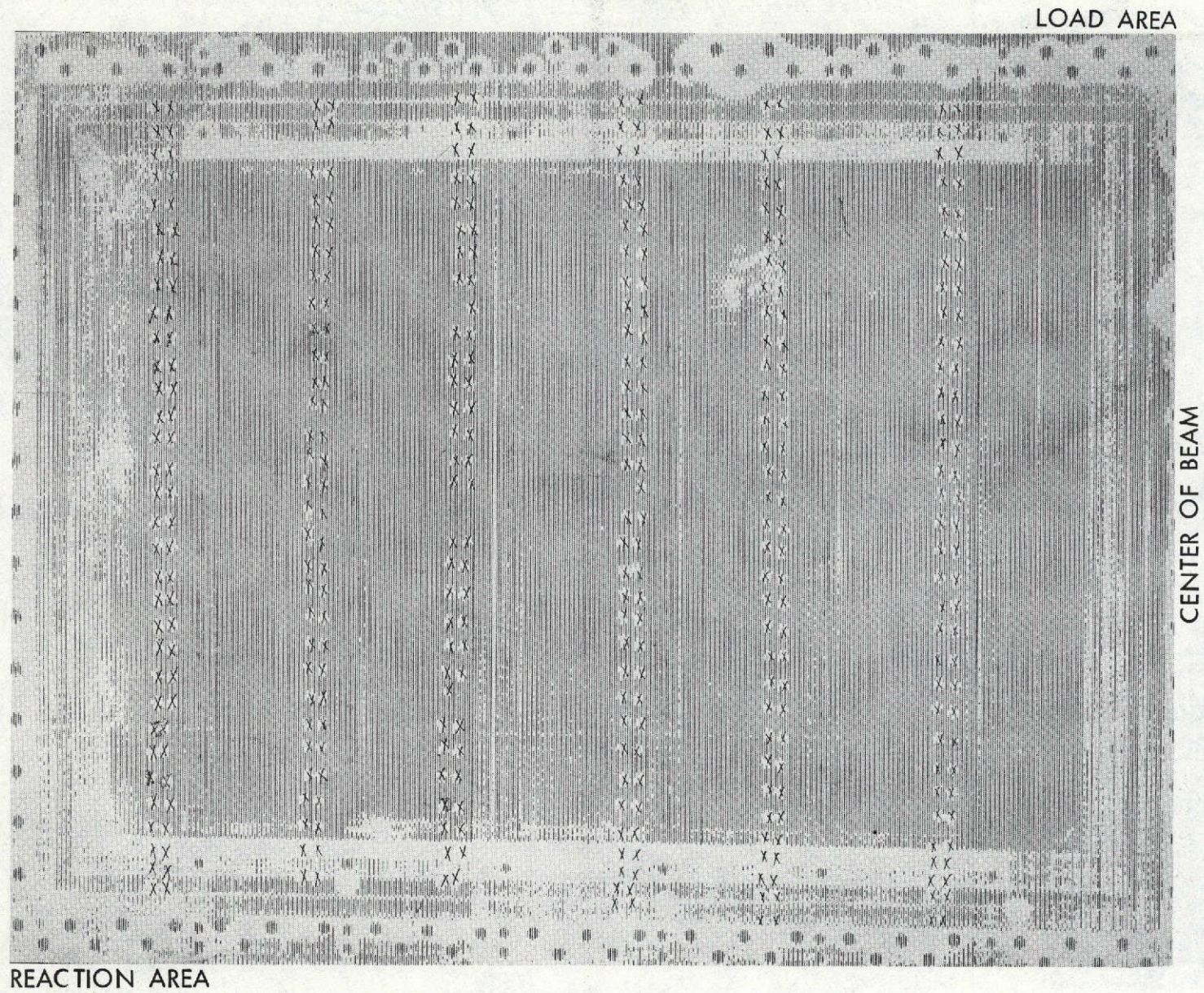
Figure 39: TEST WEB 2 ULTRASONIC SCAN AFTER TESTING

56

the post-test scan X's appear on signatures of tape stickers used for marking purposes; these signatures should be disregarded. Along the edge areas of the web laminate delamination signatures occur around certain holes. These delaminations were produced when the holes were drilled, as discussed in the Phase II Report [2]. Overheating and up-lift forces produced by the drill bit resulted in some delamination of bond lines between the metal cladding and step-lap joint details. Testing did not aggravate any of these delaminated areas.

X-rays taken of the corners of the third test web indicate that the step-lap joint details performed satisfactorily. The B/E reinforced transverse stiffeners also appear to have functioned without premature failure in all testing.

6.0 TEST DATA ANALYSIS

6.1 FAILURE MODE ANALYSIS

Based on analysis of the strain and Moire fringe data, the first and
third web components failed by composite fracturing in the critical
laminate panel areas. The strains in the extreme B/E plies in the
principal compression direction due to membrane and bending exceeded
the assumed design allowable B/E strain of $6000\mu\varepsilon$. The associated
surface strains caused the titanium-cladding to slightly exceed the
proportional limit for biaxial strain conditions.

6.2 FORCE/STRAIN ANALYSIS

The force/strain (F/S) data plotting procedure was employed to estab-
lish the bifurcation buckling loads of the test webs; these buckling
loads are correlated with analytical predictions in Section 8.3. This
procedure, also referred to as the force/stiffness technique [4], was
an effective data analysis method for the shear webs that were tested.
Bifurcation buckling (sudden buckling) did not actually develop in the
first and second webs because large deflection effects produced a
smooth transition from pre-buckling to post-buckling conditions. The

use of the F/S technique allowed definition of the classical theoretical bifurcation buckling load in these tests. The F/S plots also served to define the bifurcation buckling loads in the third web test in which a post-buckled condition did not develop.

Figures 40 to 45 are the F/S plots for the initial and final loadings of the web components. P/ε_B is plotted against P where P is the beam load and ε_B is the web laminate bending strain determined from the principal compression strain given in the Strain Data Section (Section 5.2). The bifurcation buckling load is defined as the linear extrapolation of the prebuckling response to the load axis for the initial load condition. For correlation with analytical buckling predictions, the initial load condition is used wherever possible rather than the final loading. The final loading response is generally different (gives a higher extrapolated buckling load) because of cyclic load effects on initial imperfections and internal load distributions. The development of large deflection and post-buckling response is clearly displayed where the F/S plots diverge from the linear prebuckling condition.

During load holding periods, the third web developed time-dependent response which appears as steps in the F/S plot, Figure 44. The interesting aspect of the F/S plot is that loading after a given hold period produced a return to a hypothetical curve associated with a steady loading rate. This behavior is attributed to creep response occurring in a different mode than the elastic plate flexure mode. As loading is continued, the elastic mode of deformation is restored as the
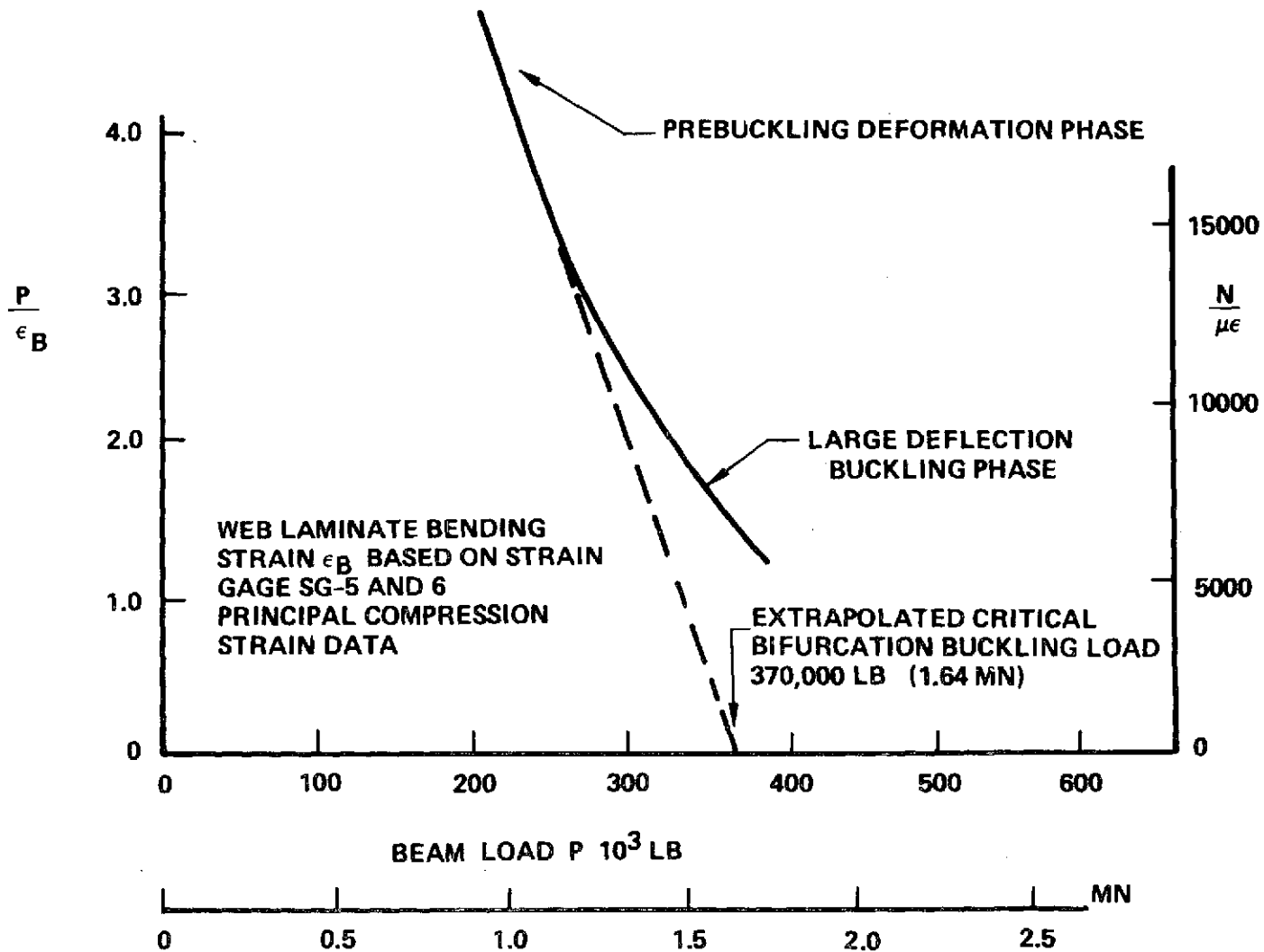
Figure 40: FORCE/STRAIN PLOT FOR TEST WEB 1 INITIAL LOADING
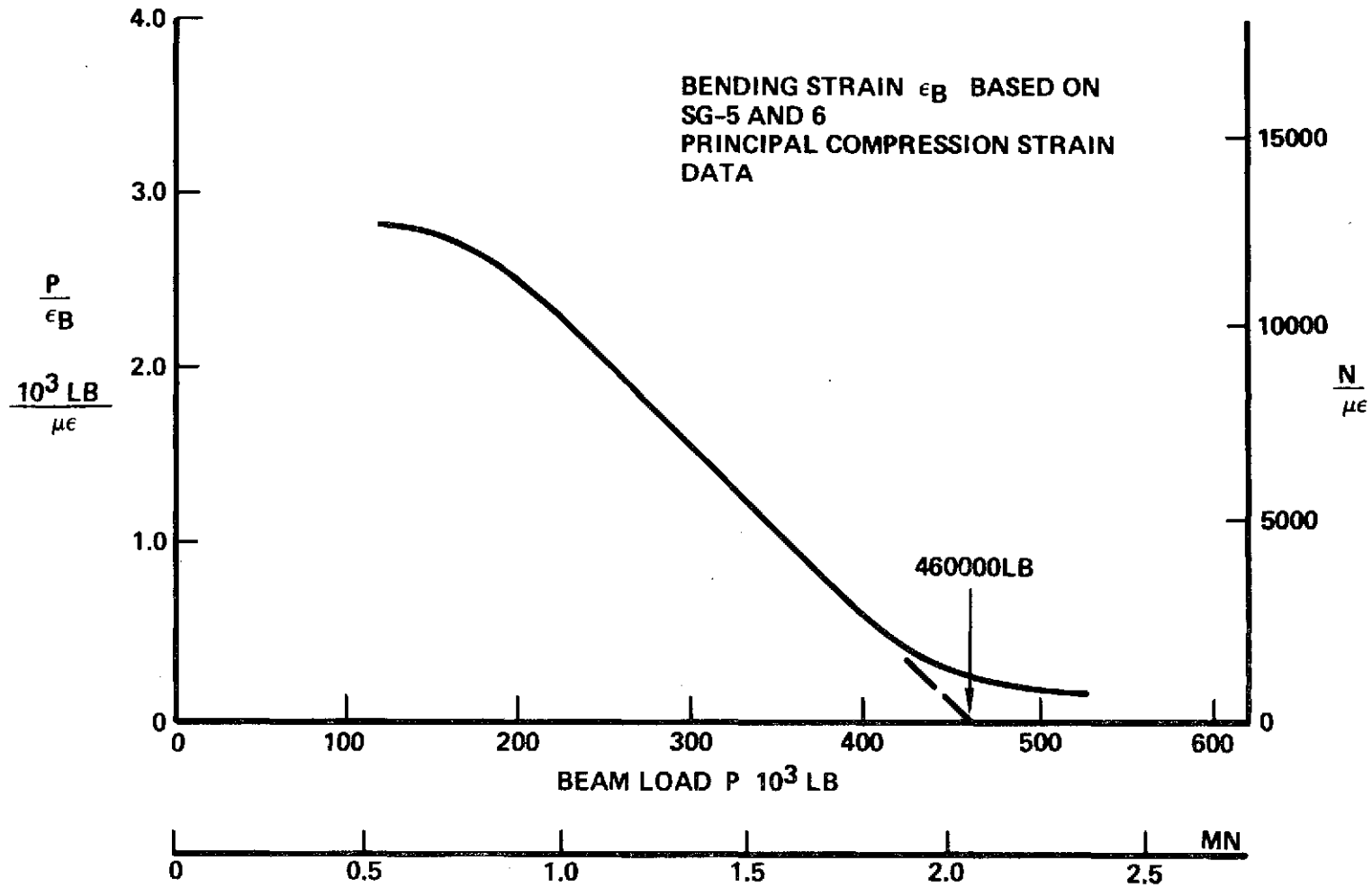
Figure 41: FORCE/STRAIN PLOT FOR TEST WEB 1 FINAL LOADING
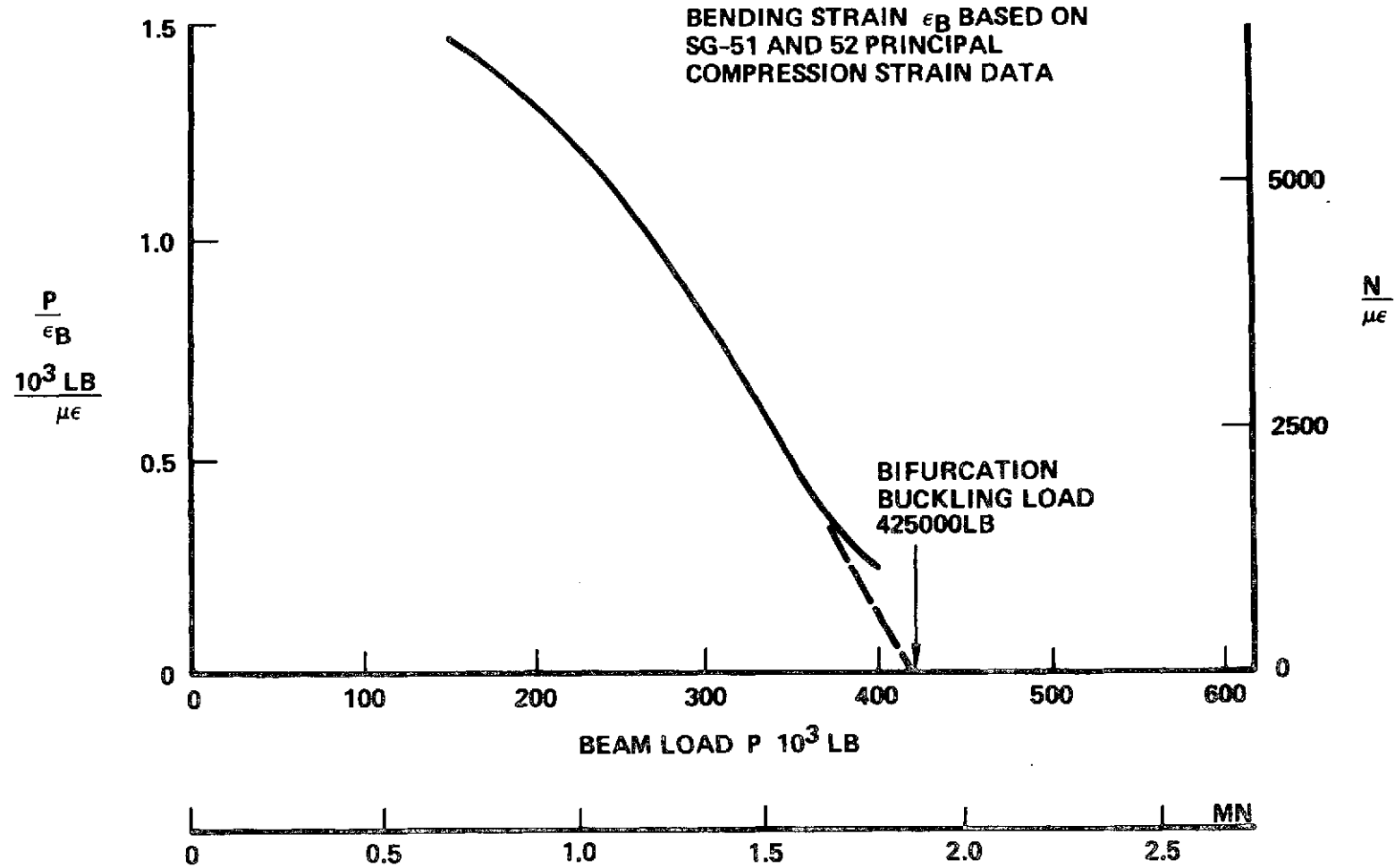
Figure 42: FORCE/STRAIN PLOT FOR TEST WEB 2 INITIAL LOADING
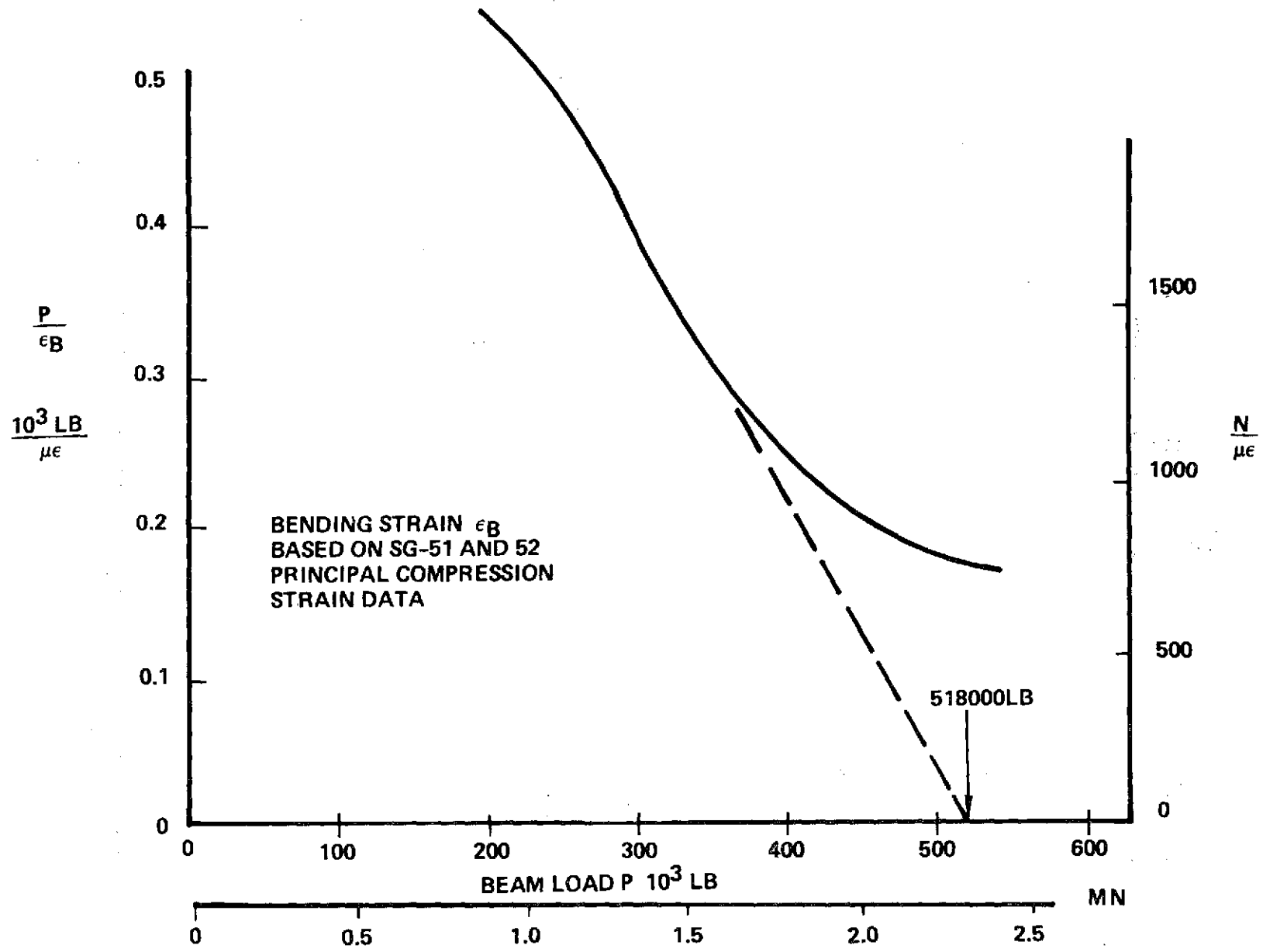
Figure 43: FORCE/STRAIN PLOT FOR TEST WEB 2 FINAL LOADING

63
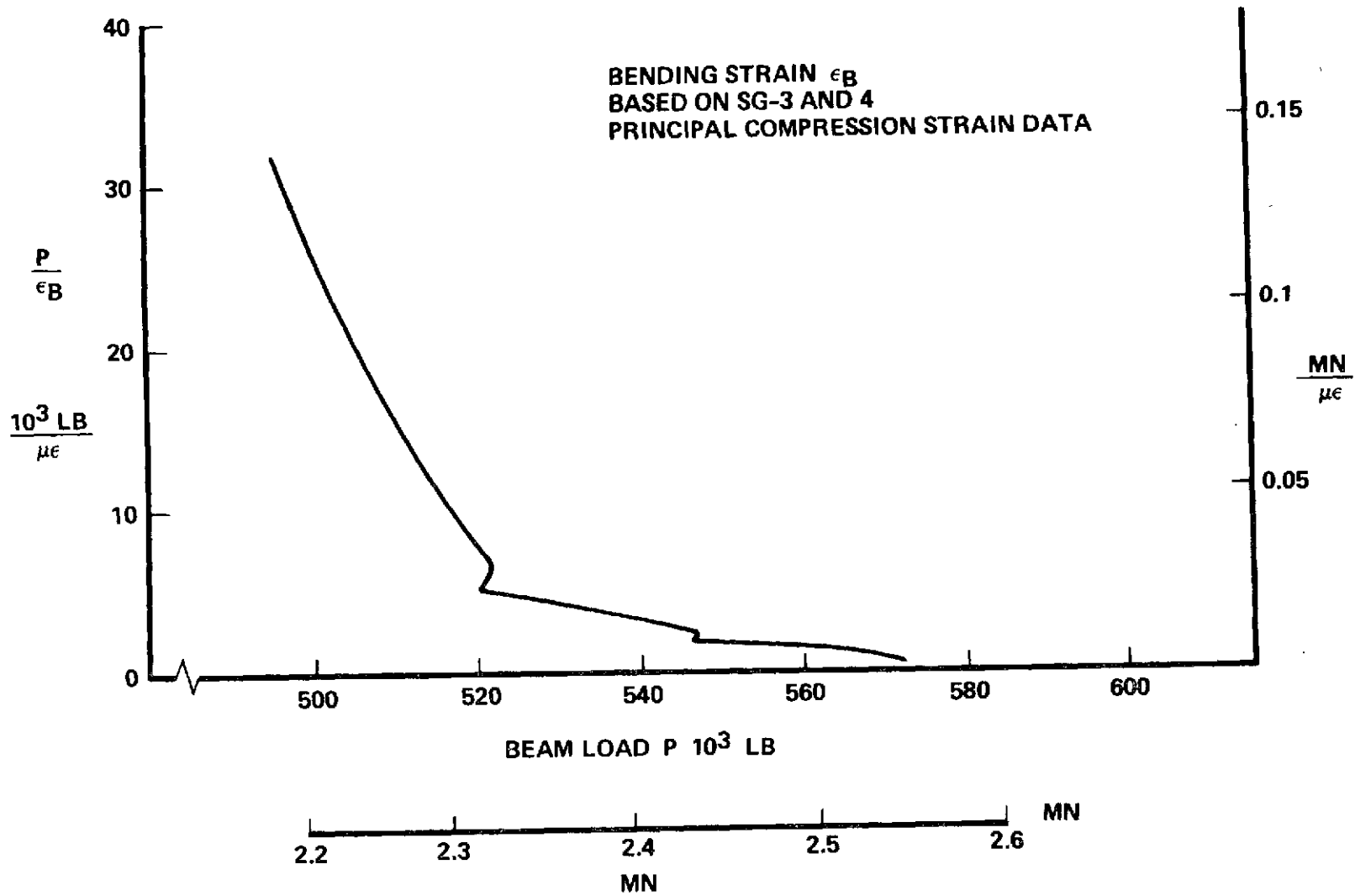
Figure 44: FORCE/STRAIN PLOT FOR TEST WEB 3 FINAL LOADING

64

BENDING STRAIN ϵ_B
BASED ON SG–3 AND 4
PRINCIPAL COMPRESSION STRAIN
DATA

BIFURCATION
BUCKLING LOAD
580,000 LB

$\dfrac{P}{\epsilon_B}$

$\dfrac{10^3 \, LB}{\mu\epsilon}$

$\dfrac{N}{\mu\epsilon}$

BEAM LOAD P 10^3 LB

MN
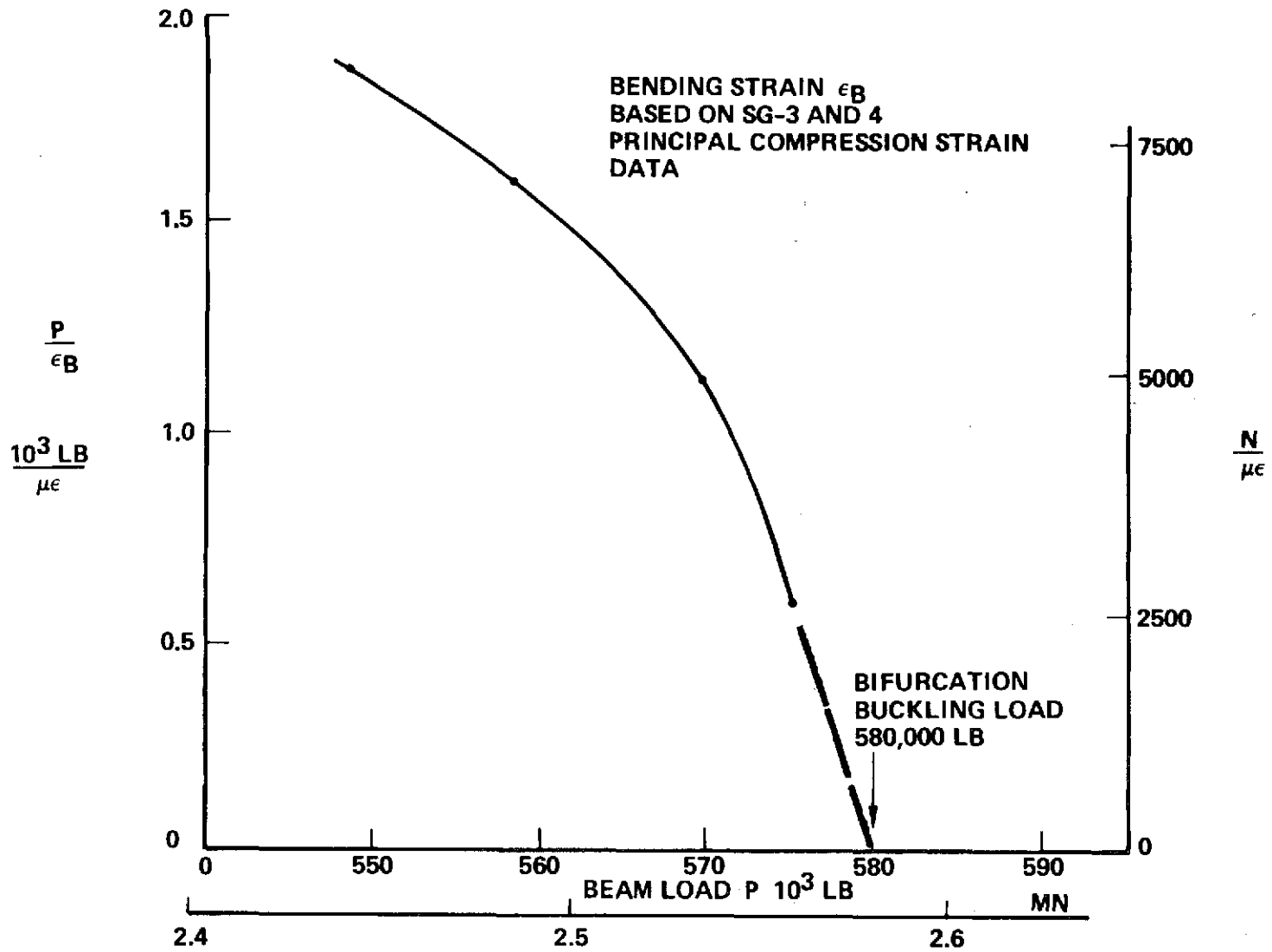
Figure 45: FORCE/STRAIN PLOT FOR TEST WEB 3 FINAL LOADING

dominant mode causing a return to the hypothetical curve. Figure 44

is shown here to illustrate the time dependent response which will be

discussed in Section 6.4. Figure 45 is a magnification of the final

portion of the F/S plot and is the basis of the bifurcation buckling

load definition. The earlier response shown in Figure 44 is not

appropriate for buckling load definition because of the remoteness of

the strain gages from the critical buckle area.

The F/S plot can also be developed directly from Moire fringe data;

Figure 46 is a F/S plot for the third test web. The plot was constructed

by counting fringe orders (N) from a reference point to the critical

buckle peak and then using N as a bending index in place of bending

strain, ϵ_B, used previously.
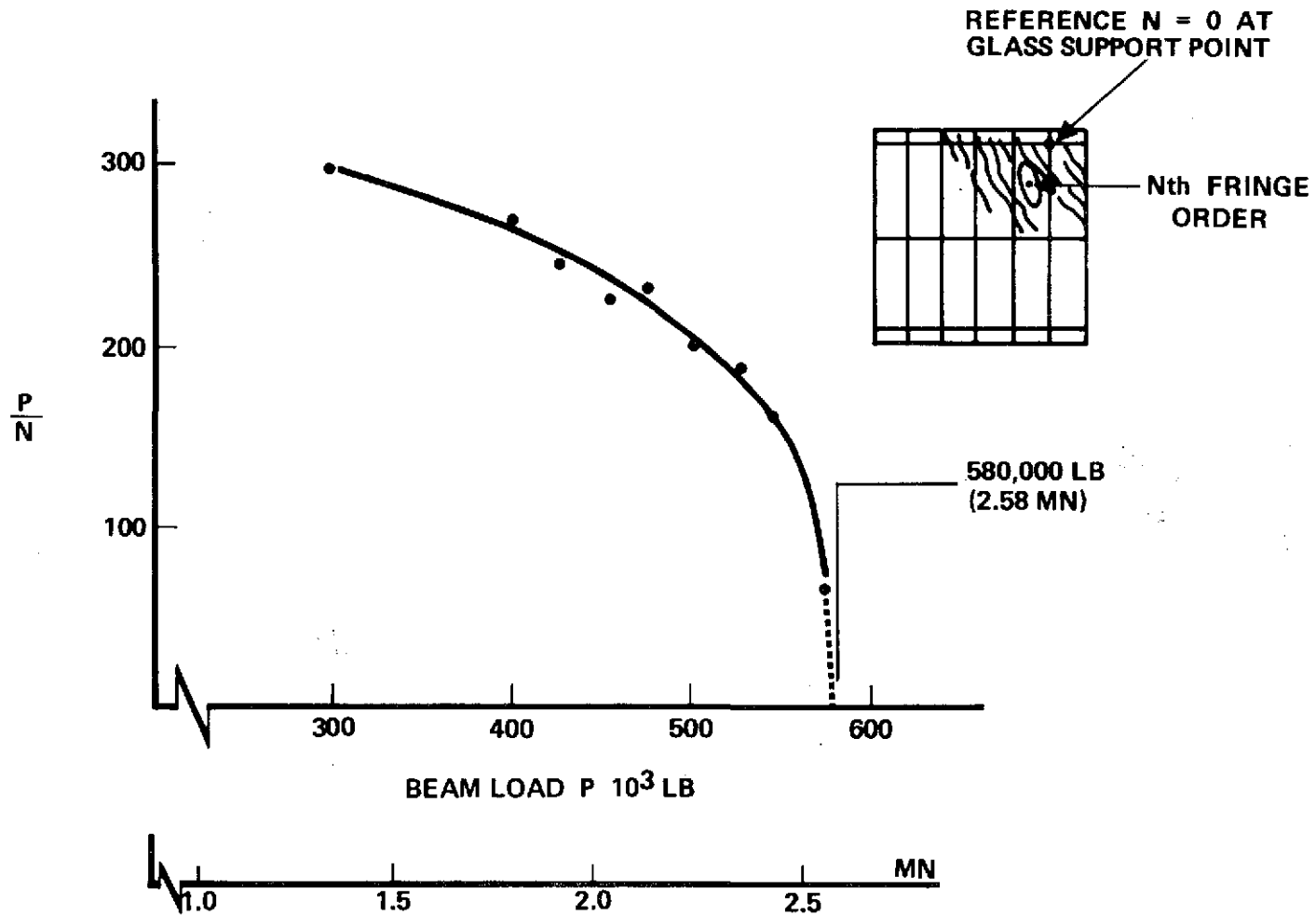
Figure 46: FORCE/STRAIN PLOT FOR TEST WEB 3 FINAL LOADING

6.3 MOIRE FRINGE ANALYSIS

The Moire fringe patterns from the web tests were analyzed by a curve fitted procedure to establish the strain conditions precisely at the critical buckle peaks. This strain data complimented the strain data obtained from the strain gages in close proximity to the critical buckles and was used in subsequent analysis activities.

Figure 47 shows the critical buckle area in the third web at the failure load. The deflected surface was surveyed in the principal compression strain direction to establish coordinates of the fringe orders; both manual surveying and electronic data digitizing equipment (Bendix Digitizer) were employed in the surveys. The coordinate and fringe order calibration data were fitted to a deflection function of the form shown in the figure; the fitting was done by manual and computer aided methods. A wavelength of $\sqrt{2}$ times the stiffener spacing was an assumed deflection function parameter. By differentiating the deflection function twice, the panel bending curvatures were established; local strains in the laminate were computed from the product of bending curvature and a coordinate of the material from the neutral laminate surface.

Figures 48 to 50 show strains computed for the test webs. As shown in the figures, the total strain at a given point in the laminate is the superposition of membrane and computed bending strain from the Moire fringe data. In tests one and two, the membrane strain response is taken as the initial linear strain gage data. For test web 3, the membrane strain response was computed from data generated using the

69

5.0(127) STIFFENER SPACING

45° B/E DIRECTION

CRITICAL BUCKLE AREA

FITTED DEFLECTION FUNCTION

$W = 0.1159 - 0.1076 \cos \frac{\pi x}{5\sqrt{2}}$ (IN)

$W = 2.944 - 2.733 \cos \frac{\pi x}{127\sqrt{2}}$ (MM)

EXTREME B/E SURFACE

$Z_{B/E} = 0.0543$ (1.379)

8 PLIES B/E @ 0.0051 (0.1295)
1.5 PLIES ADHESIVE @ 0.009 (0.2286)

FRINGE ORDER

0 1 2 3

0.0173 (0.439)

x

w

UNITS IN (MM)
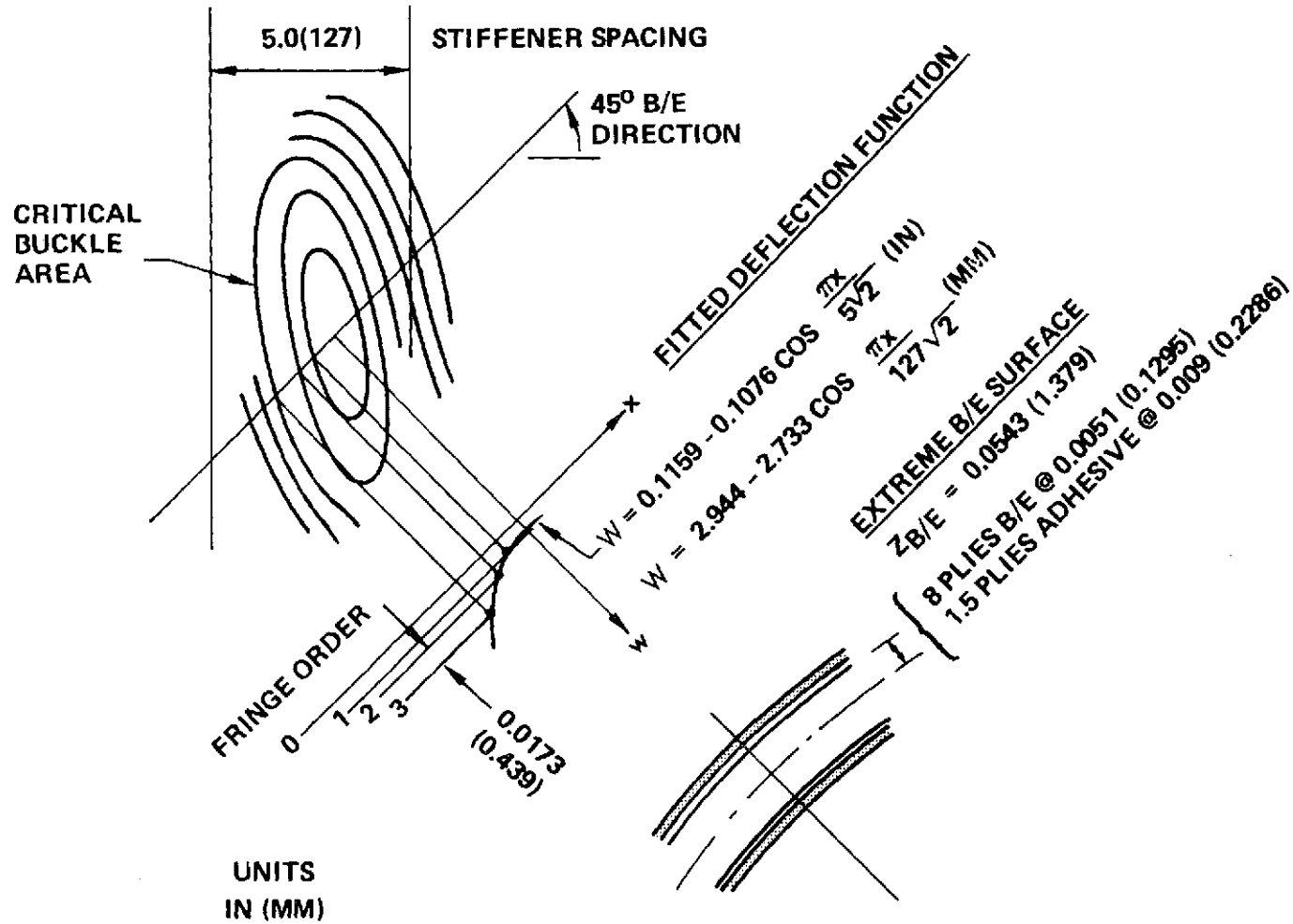
Figure 47: DEFLECTION FUNCTION FITTED TO TEST WEB 3 MOIRE FRINGE DATA
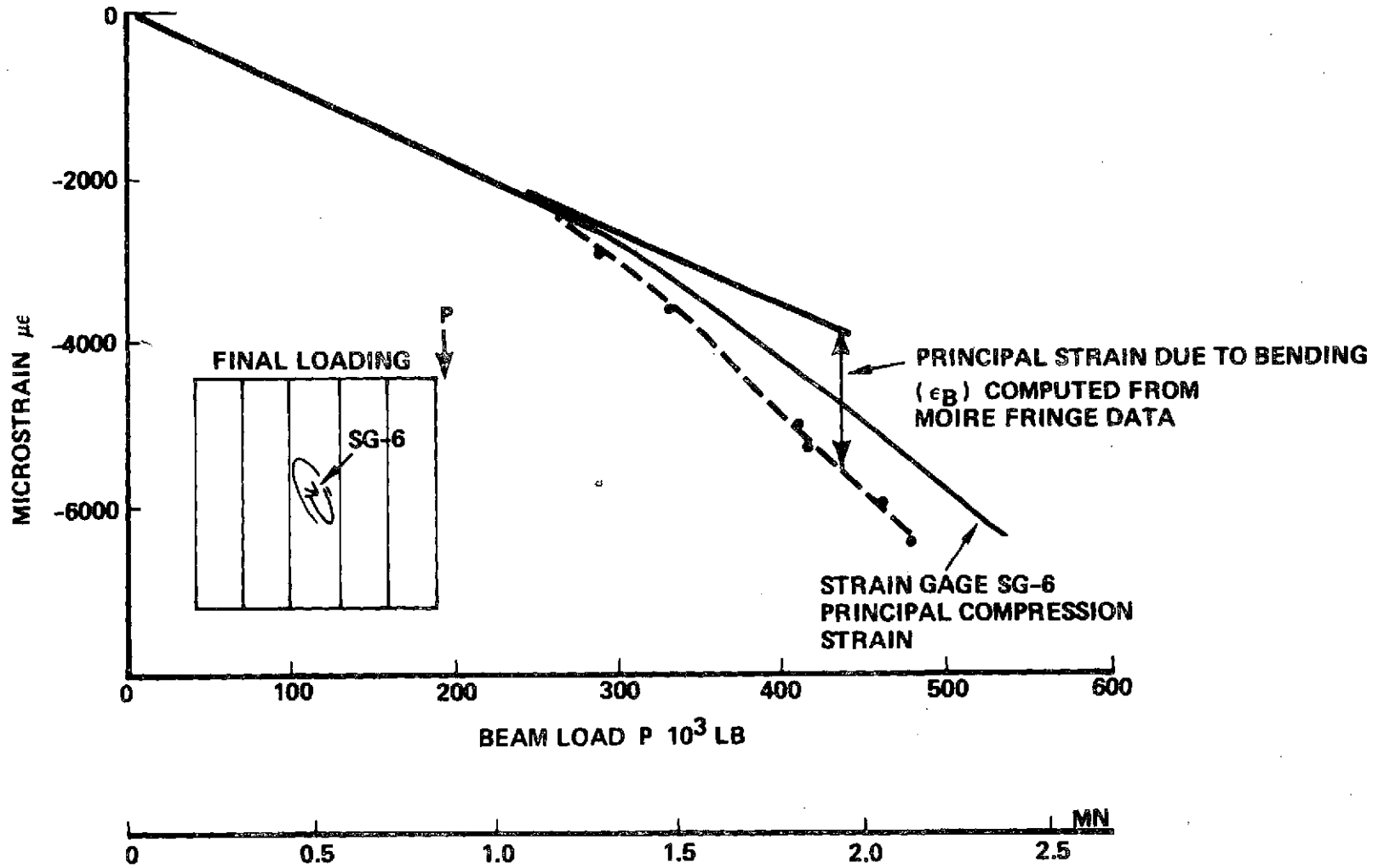
Figure 48: SURFACE CLADDING STRAINS IN TEST WEB 1 CRITICAL BUCKLE AREA
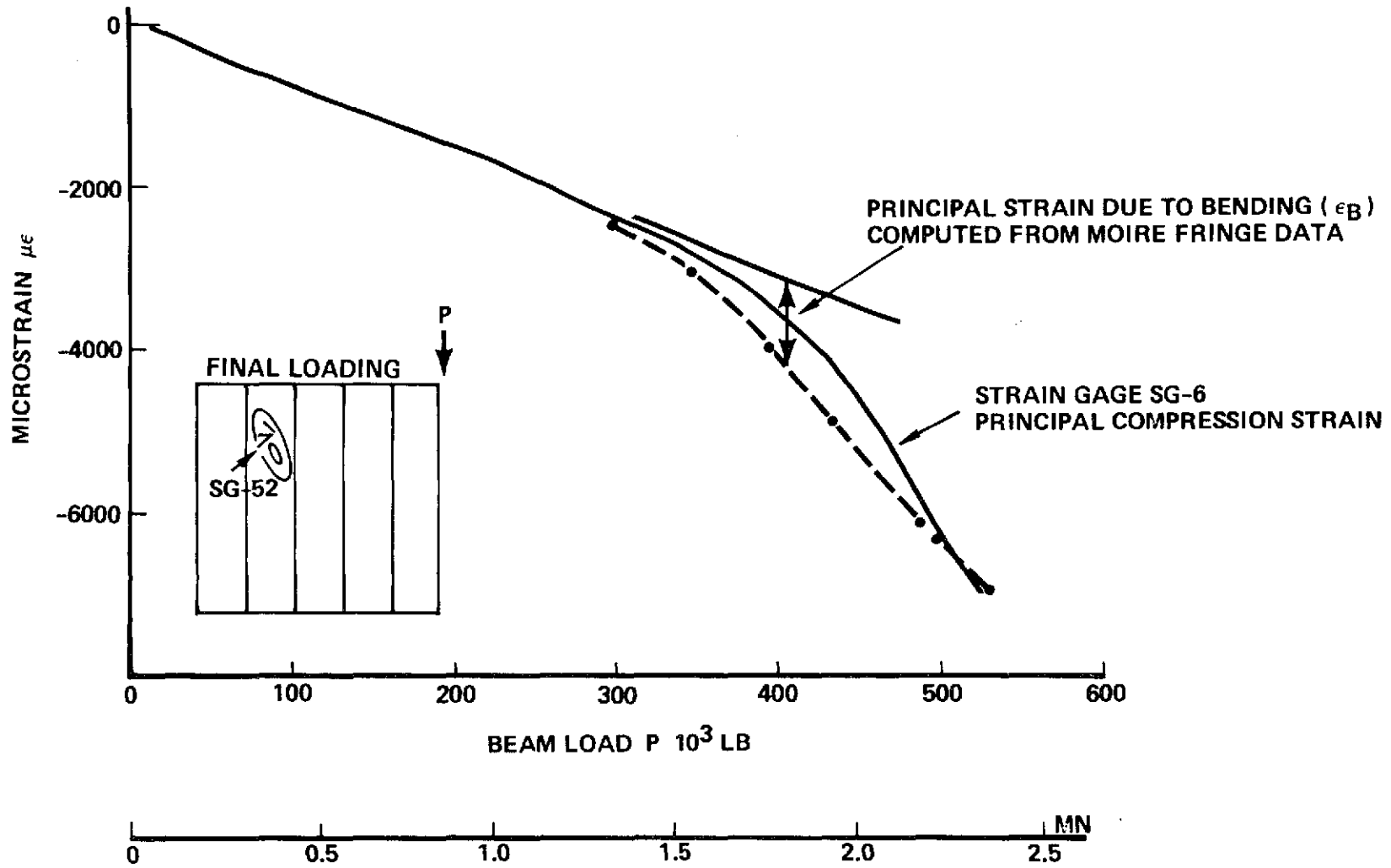
Figure 49: *SURFACE CLADDING STRAINS IN TEST WEB 2 CRITICAL BUCKLE AREA*
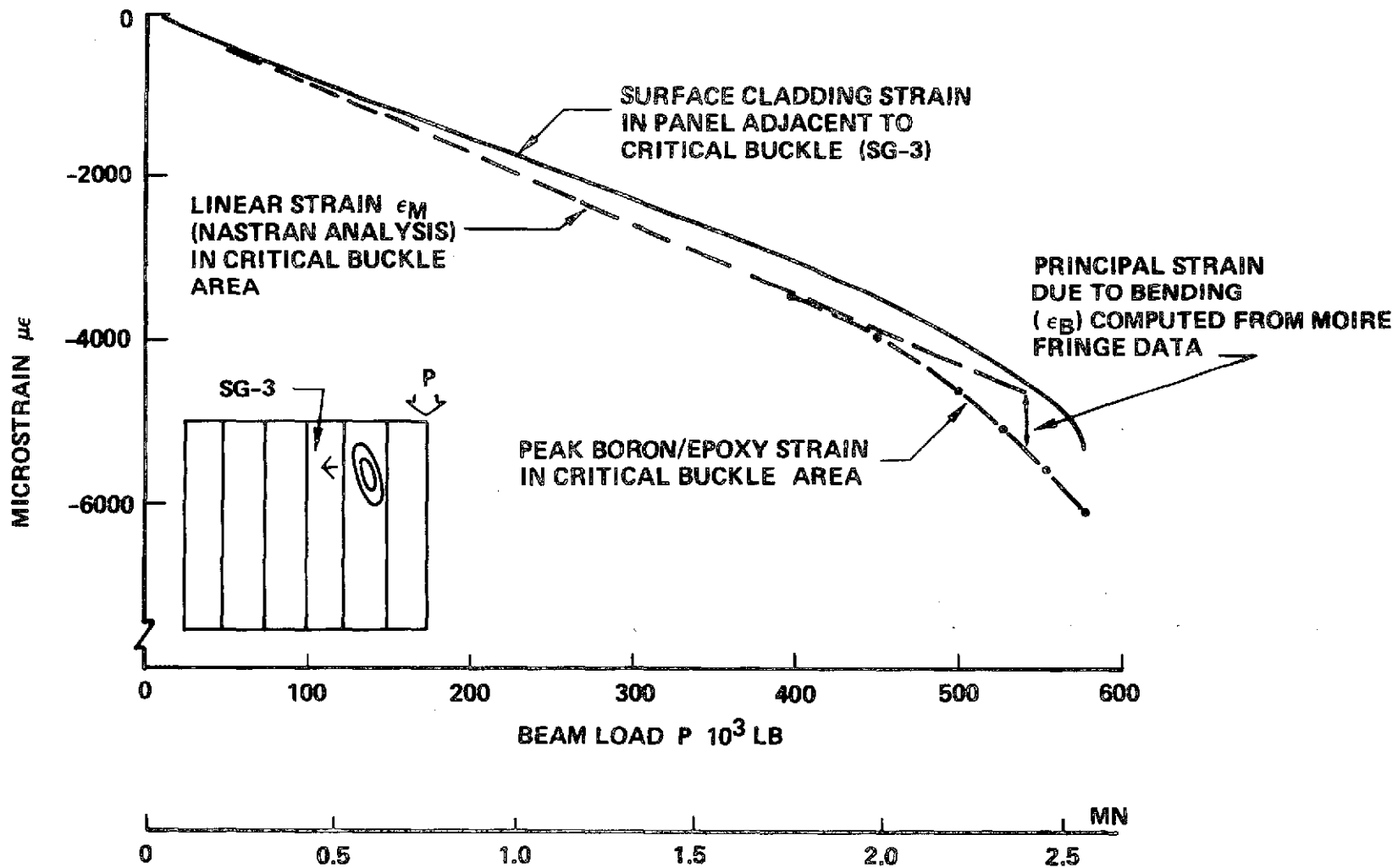
Figure 50: STRAINS IN TEST WEB 3 CRITICAL BUCKLE AREA

NASTRAN code; this was done to account for increased internal loads near the loading area where strain gages were not applied. Good agreement was obtained between the computed strain response and the strain gage data. In general, the computed strains are higher than the measured data because the strain gages were not applied exactly at the peaks of the panel buckles.

6.4 TIME-DEPENDENT RESPONSE

During load holding periods in the third web test, time-dependent web deflection response was evident. Figure 51 shows the load-time history of the final loading. During the hold periods, the various test data were reviewed prior to resumption of loading. The time dependent response is revealed in the F/S data (Section 6.2) and in other data.

Figure 52 represents lateral panel deflection versus load measured by a deflection indicator (linear differential transformer type). The steps in the response indicate lateral deflection growth occurring during load holding periods.

Figure 53 shows the Moire fringe pattern at the beginning of the holding period at 500,000 lb. (2.22 MN). The growth in deflection can be noticed by comparing this pattern with the pattern at the end of the hold period, Figure 54.


73
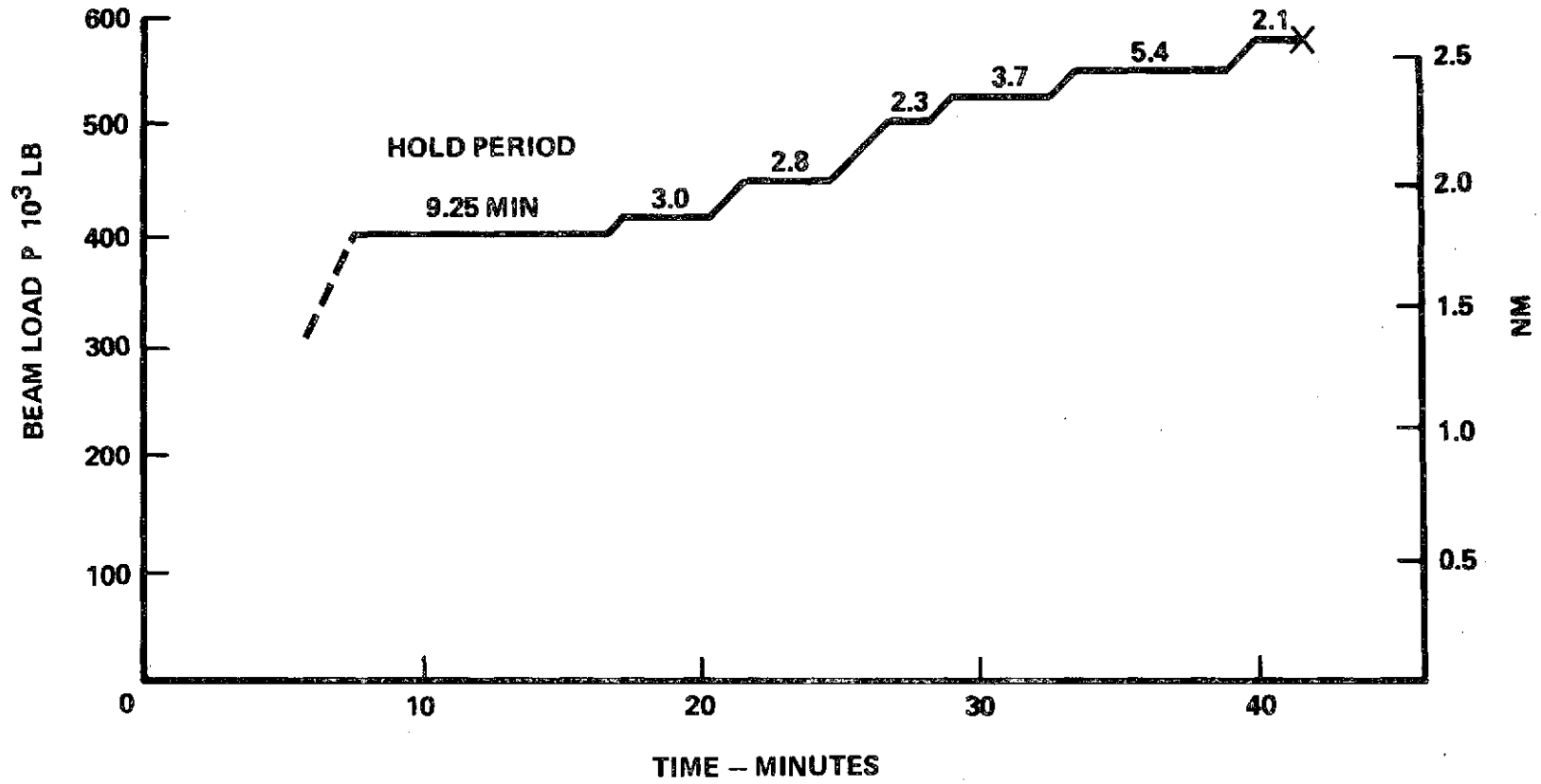
Figure 51: TEST WEB 3 LOAD VS. TIME
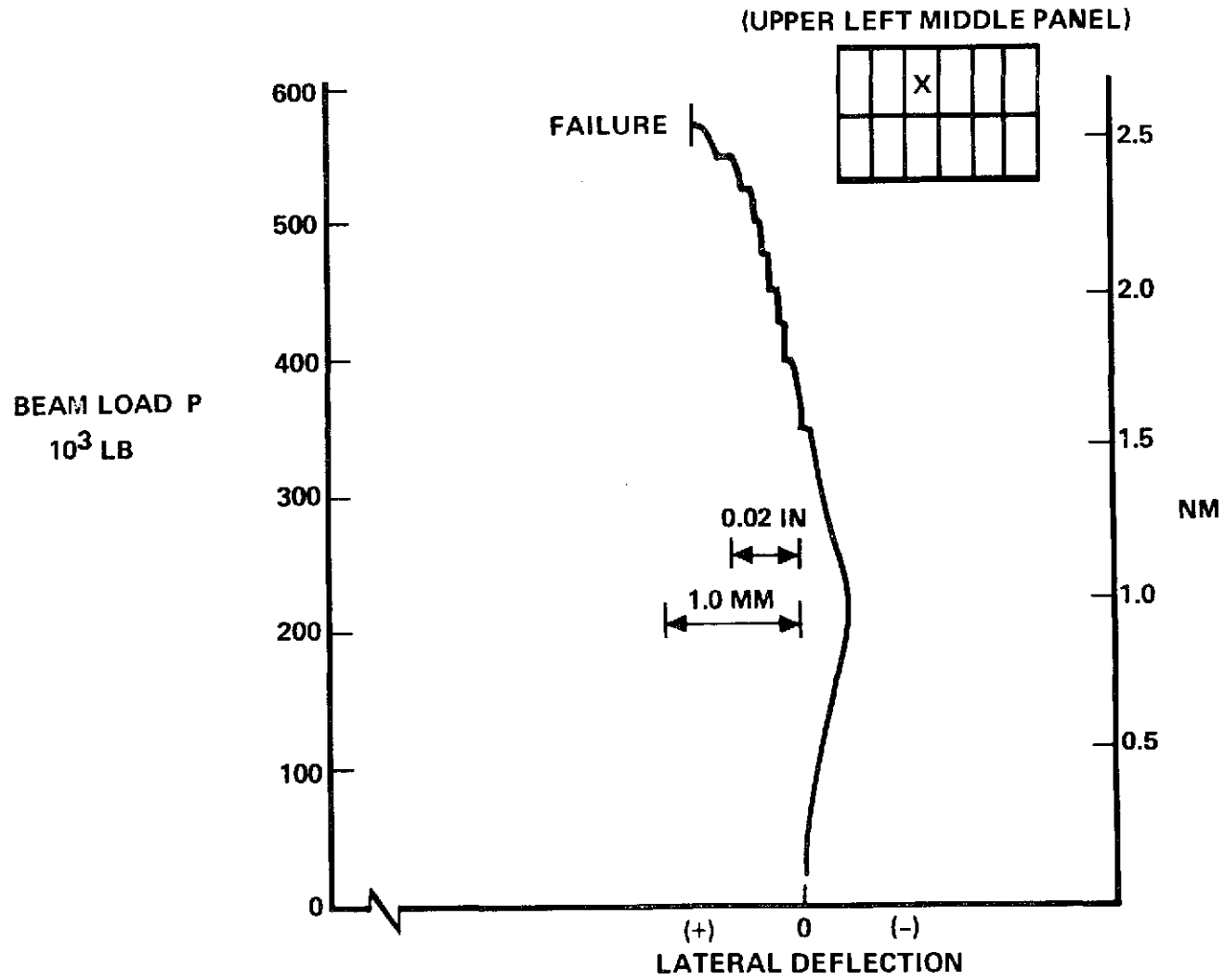
*Figure 52: TEST WEB 3 LATERAL DEFLECTION AT STRAIN GAGE 1 AND 2*

75
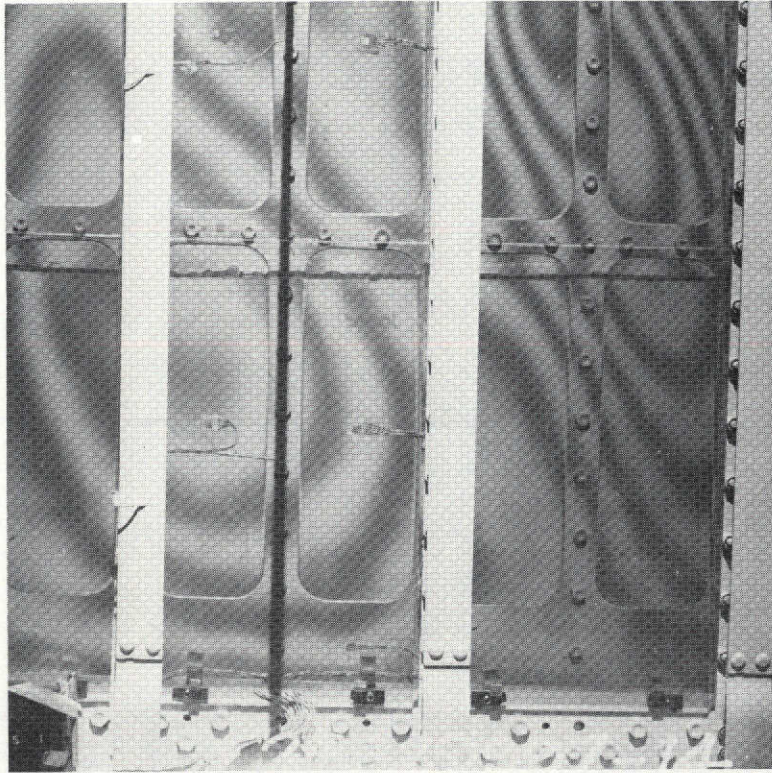
Figure 53: TEST WEB 3 MOIRE FRINGE PATTERN AT 550,000 LB (2.45 MN)
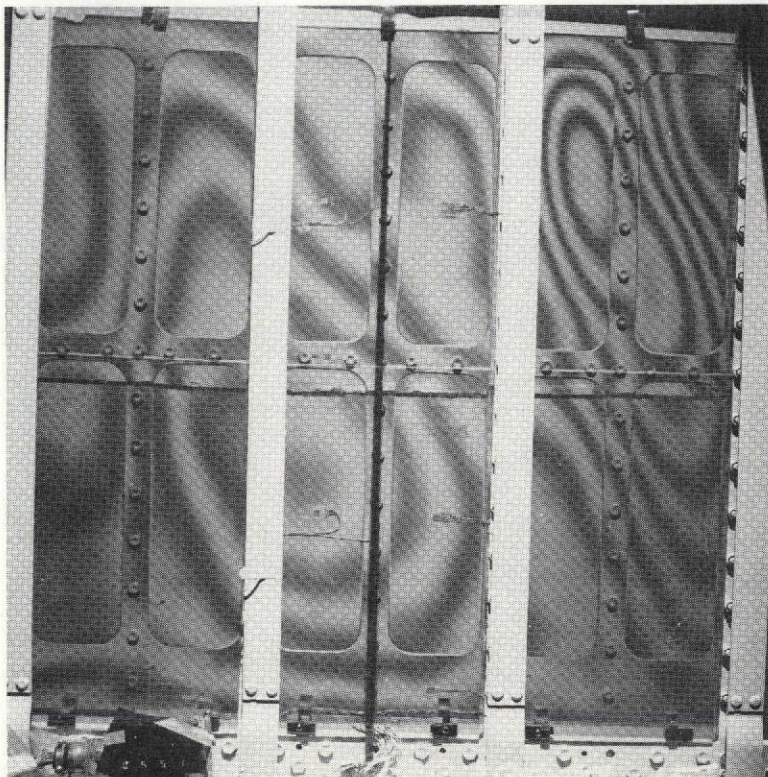
Figure 54: TEST WEB 3 AT 550,000 LB (2.45 MN) AFTER 5 MINUTE LOAD HOLD PERIOD

TEST WEB 3 AT 575,000 LB

$N_x = 9339.5$ LB/IN
(NASTRAN)

$N_{zx} > N_x \frac{\partial w}{\partial x}$ (BIAXIAL AND CURVATURE EFFECTS NEGLECTED)
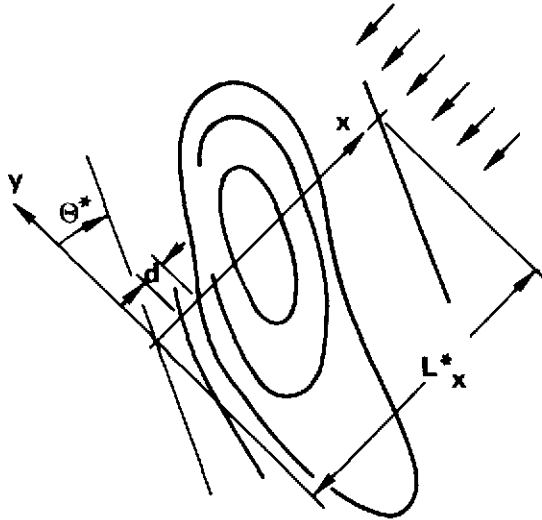
FROM DEFLECTION FUNCTION ANALYSIS:

$$w = A \sin \left\{ \frac{\pi}{L^*_x} (x - \phi^* y) \right\} \quad \text{CORRUGATED MODE}$$

$$\phi^* = \text{TAN } \Theta^*$$

$$\text{MAX} \frac{\partial w}{\partial x} = A \pi / L^*_x$$

$A = 0.121$ IN
$L^*_x = 8.64$ IN
$\Theta^* = 23^o$

$N_{zx} \approx 410.9$ LB/IN   (MAX $T_{zx} = 3317$ LB/IN^2)

FRINGE CALIBRATION

f = 0.0173 IN/ORDER

x,y MODAL COORDINATES ARE
DIFFERENT FROM X,Y BEAM
COORDINATES

FROM DIRECT FRINGE SLOPE ANALYSIS:

$$\text{MAX} \frac{\partial w}{\partial x} = d/f \qquad d = 0.395 \text{ IN}$$

$N_{zx} \approx 409.4$ LB/IN   (MAX $T_{zx} = 3305$ LB/IN^2)

Figure 55: APPROXIMATE TRANSVERSE SHEAR ANALYSIS

While the existence of time-dependent response is not of concern in the thrust structure application, the response may be important to other applications and therefore a brief study of the source of the response was conducted. The time-dependent response was concluded to be primarily due to inter-laminar shear creep in the polymeric parts of the web laminate and, to limited extent, to slippage at stiffener interfaces.

An approximate transverse shear analysis in the critical buckle area was conducted based on the Moire fringe pattern at the failure load (Figure 34) and the principal compression load resultant from the NASTRAN code (discussed in Section 7.0). As illustrated in Figure 55, the critical buckle area can be idealized by a simple corrugated mode whose parameters can be determined by analyzing the fringe pattern. The maximum plate surface slope can then be found by first differentiating the mode slope (deflection function) or by direct calculation of the deflected surface slope. The transverse plate shear is approximated by the product of slope and compression load resultant; this gives a value that is below the actual shear because biaxial and curvature effects are neglected. The maximum inter-laminar shear stress computed from the transverse shear using classical laminate analysis is on the order of 3,300 lb./in.^{2} (22.7 MN/M^2). It is believed that the actual shear stress level is above 3,300 lb./in.^{2} level and that it would then be sufficient to promote creep response in the B/E plies and the adhesive plies in the web laminate. The largest component of the creep response is probably contributed by the adhesive plies; the aggregate adhesive ply thickness was 0.045 in. (1.14 mm) versus a

combined B/E thickness of 0.0816 in. (2.07 mm) so a substantial amount of unreinforced adhesive material was present in the third web laminate. Shen and Rutherford [5] found METLBOND 329 adhesive was susceptible to viscoelastic and microyielding response at low stresses particularly under shear loading.

In order to establish sensitivity to inter-laminar shear creep, several laminate test specimens were cut from remnants of the first test web. The specimen configuration was rectangular and is shown in Figure 56. A typical inter-laminar shear failure appears along the edge of the tested specimen. The specimens were tested in the manner illustrated in Figure 57. The specimens were tested similar to conventional inter-laminar shear techniques except that a two-point loading was used and specimen size and load points were selected to develop measurable deflections. A typical deflection-time test data plot is shown in Figure 57.

Data from the specimen tests were analyzed in terms of shear strain rate as defined in Figure 58. Several load holding time periods were used in the testing and the respective results are plotted in the figure. In keeping with the characteristic response of cross-linked polymers like the epoxy materials in the web laminate, the average strain rate decreases with increasing hold period. The data indicates that measurable creep response can occur at inter-laminar shear stresses down to 3,000 lb./in.^{2} (20.7 MN/M^2) and in load holding periods such as experienced in the third web test.

SPECIMEN SIZE: 2.0 x 5.0 IN.

(5.08 x 12.7 CM.)
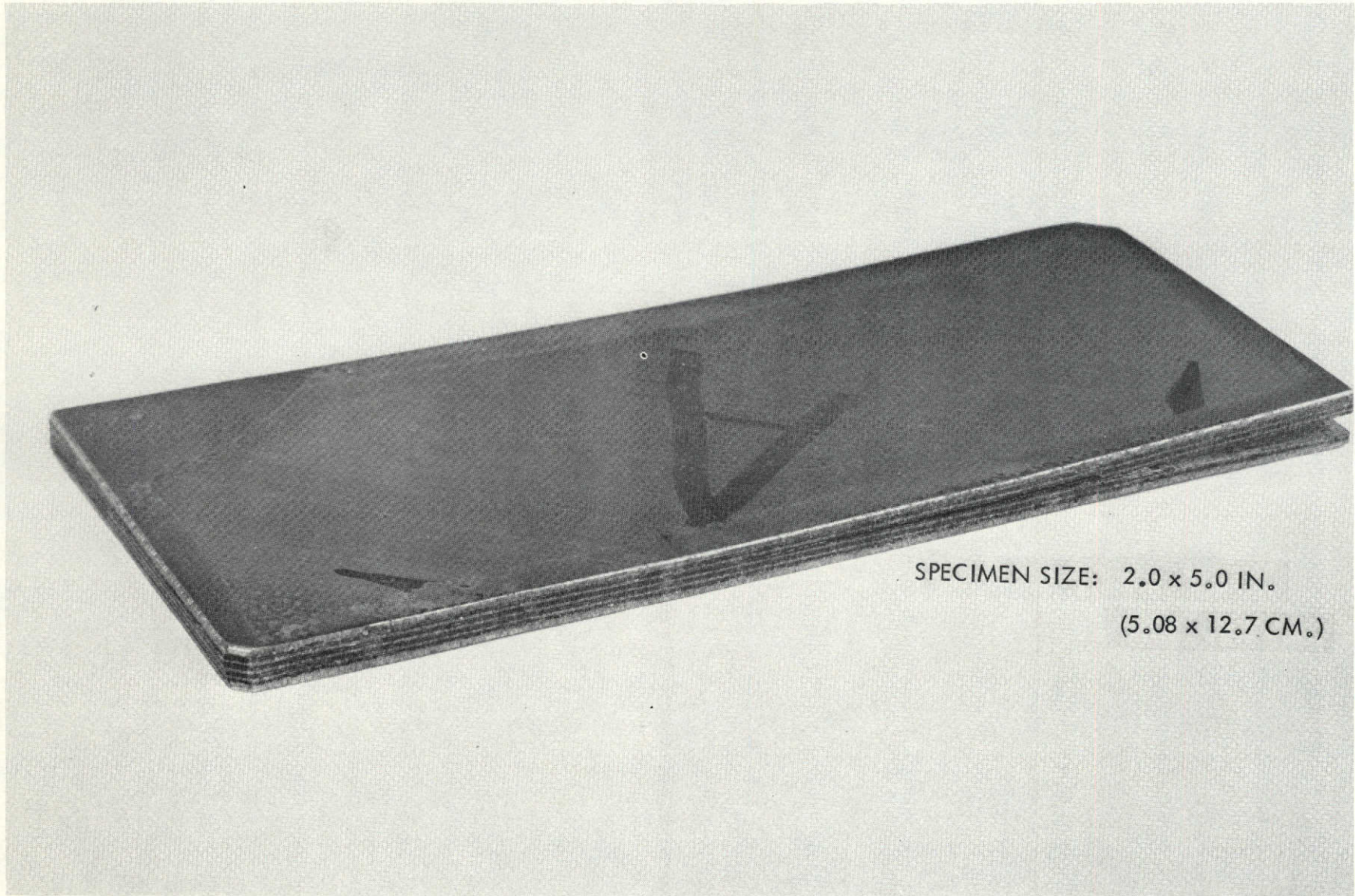
Figure 56: INTERLAMINAR SHEAR CREEP TEST SPECIMEN

TIME
6 MIN

DEFLECTION
0.010 IN
(0.254 MM)

FAILURE

1700 (7562)

1800 LB
(800 IN)

1600 (7117)

1500 (6672)

P = 1400 LB (6227.5 N)

δ

FLEXURAL
DEFLECTION
AT ₵

SHEAR DEFLECTION
AT LOAD POINTS
AND ₵

P/2   P/2

0.5(12.7)

0.98 (24.9)

2.0 IN (50.8 MM)

UNITS
IN (MM)
LB (N)

81
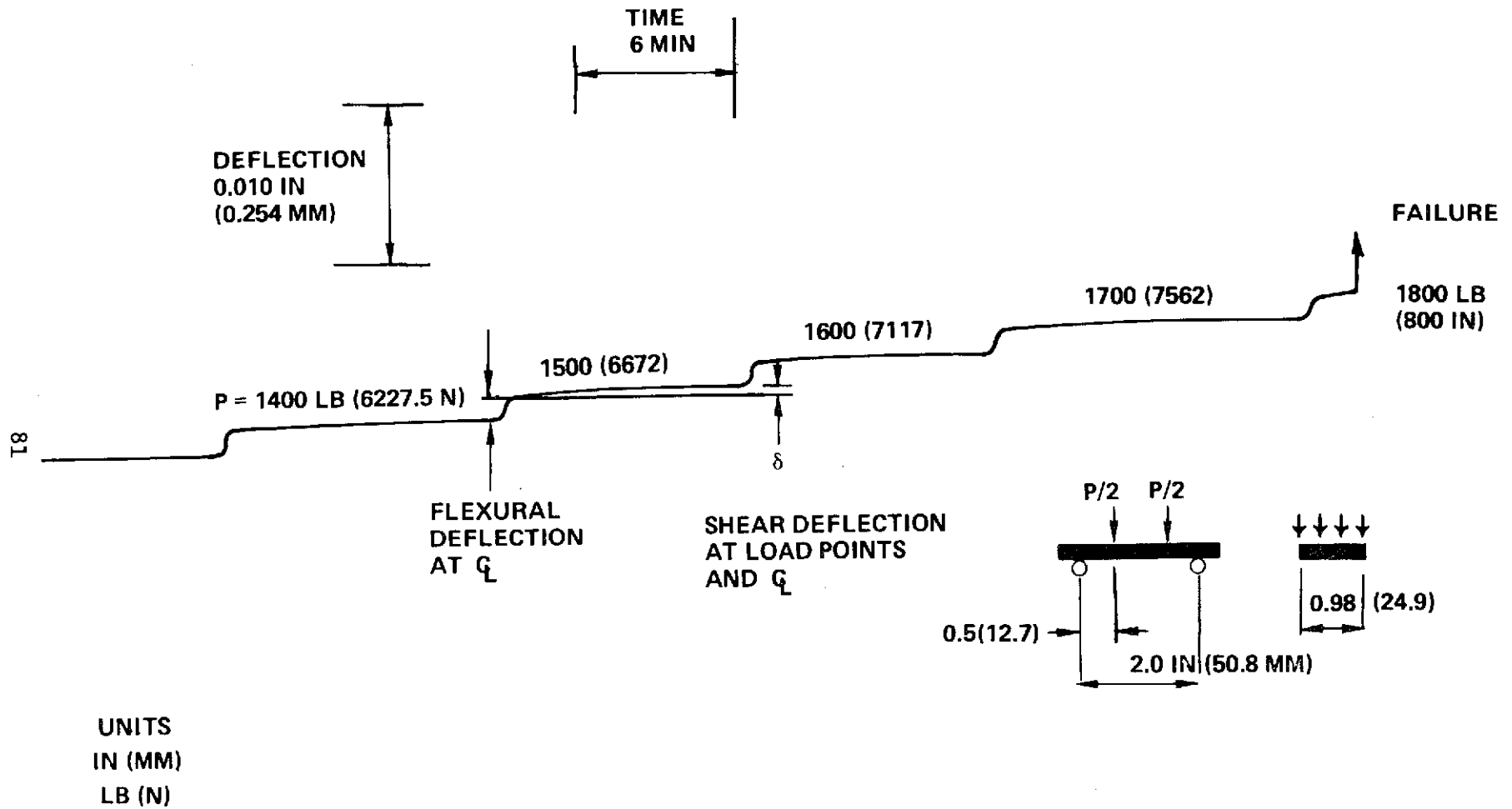
Figure 57: DEFLECTION VS. TIME FOR INTERLAMINAR SHEAR CREEP SPECIMEN NO. 7 FROM TEST WEB 1
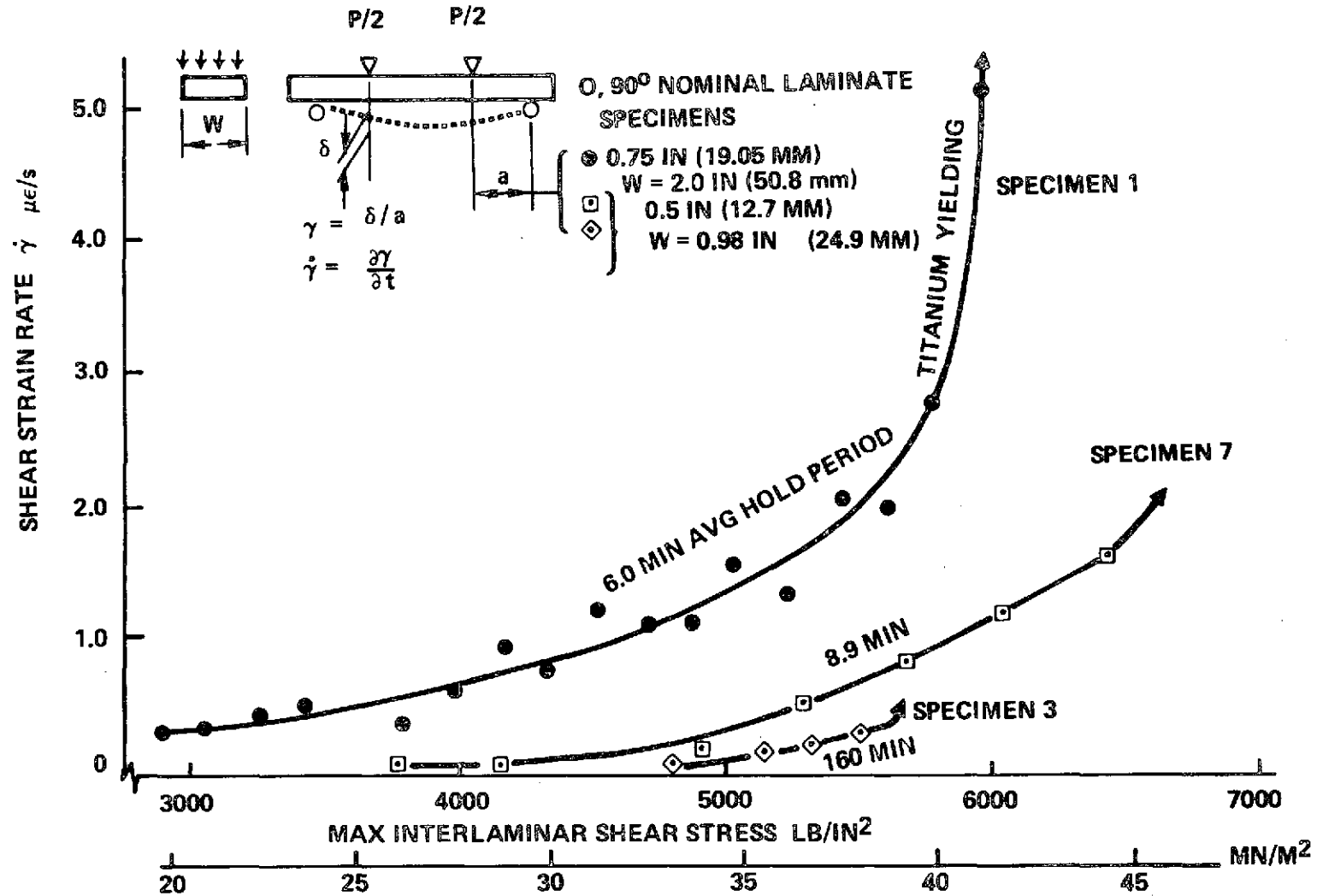
Figure 58: CREEP STRAIN RATES OF SPECIMENS FROM TEST WEB 1

7.0 FINITE ELEMENT STRUCTURAL ANALYSIS

Finite element analyses were conducted to compute membrane strain condition in the test webs. The NASTRAN code, level 15 [6], Boeing Computing Services version with SAIL input preprocessor was used for this purpose. Element properties that were input are shown in Figures 59 and 60 (the elements shown are specifically for test web 2).

Figure 61 presents computed strains for test web 1; the strains agree with measured strains in the initial linear region. The mean computed strains deviate from the linear finite element analysis at higher loading reflecting the development of large deflection ("diagonal tension") effects. The membrane strain results were useful in subsequent analyses of the prebuckling deformations as described in Sections 6.3 and 9.3.

Figure 62 illustrates linear analysis deflection results obtained for the second test web; the deflection pattern is characteristic of a shear web. In comparison with the load/deflection test data (Section 5.1), the predicted stiffnesses of the test beam assemblies are within 5% of the actual test values.

Finite element buckling analyses were also conducted using the NASTRAN code. Computed buckling loads for a single panel of the test web 1 orthotropic laminate were reasonably accurate only with a fine idealization consisting of triangular elements (CTRIA1); computed buckling loads are compared to an analytical solution by Sekerzh-Zen'Kovich [7]

REINFORCED LAMINATE
T = 0.248   I = 0.00075

$$\text{MEMBRANE } G_{ij} = 10^6 \begin{bmatrix} 10.4 & 4.63 & 0 \\ & 10.4 & 0 \\ S & & 5.29 \end{bmatrix}$$

$$\text{BENDING } G_{ij} = \begin{bmatrix} 14.85 & 4.90 & 0 \\ & 14.85 & 0 \\ S & & 5.70 \end{bmatrix}$$

$\overline{X}$

$\overline{Y}$

$\overline{Z}$

PLATE
COORDINATE AXES

P/2

ROLLER SUPPORTS
AT PLANE UP
SYMMETRY

• ALL PLATE ELEMENTS
ARE CTRIA1 TYPE

36 IN (0.91 M)

48 IN (1.22 M)

TITANIUM AND ALUMINUM
EDGE PLATE MATL
T = 0.734   I = 0.0117

$$\text{MEMBRANE } G_{ij} = 10^6 \begin{bmatrix} 13.25 & 3.97 & 0 \\ & 13.25 & 0 \\ S & & 4.65 \end{bmatrix}$$

$$\text{BENDING } G_{ij} = 10^6 \begin{bmatrix} 12.00 & 3.62 & 0 \\ & 12.00 & 0 \\ S & & 4.18 \end{bmatrix}$$

ROLLER BEAM
SUPPORT

NOMINAL WEB LAMINATE
T = 0.1932 IN I = 0.000601 IN^3

$$\text{MEMBRANE } G_{ij} = 10^6 \begin{bmatrix} 8.04 & 4.25 & 0 \\ S & 8.04 & 0 \\ & & 4.25 \end{bmatrix}$$

$$\text{BENDING } G_{ij} = 10^6 \begin{bmatrix} 11.67 & 4.50 & 0 \\ & 11.67 & 0 \\ S & & 5.17 \end{bmatrix}$$

Figure 59: TEST WEB 2 NASTRAN FINITE ELEMENT PLATE ELEMENTS

- ALL BEAM ELEMENTS ARE CBAR TYPE
- ALL BEAM ELEMENTS HAVE THEIR WEBS PERPENDICULAR TO THE SHEAR WEBS
- STIFFENERS HAVE NO ECCENTRICITY

UPPER AND LOWER BEAM FLANGES

14.5 IN²
4.60 IN²
4.60 IN²
18.40 IN²

11.25
2.175
2.175
8.70

8.00
0.785
0.785
3.14

4.75
0.1675
0.1675
0.67

A
I₁
I₂
J

END POST FLANGES

$A = 9.75$ $I_1 = 34.3$ $J_2 = 1.83$ $J = 5.49$

ALUMINUM CENTER POST
A = 6.0
I₁ = 13.5
I₂ = 1.4
J = 4.2

B/E REINFORCED STIFFENERS
A = 0.266 (REF. MATL. IS UNI. B/E)
I₁ = 0.059
I₂ = 0.
J = 0.
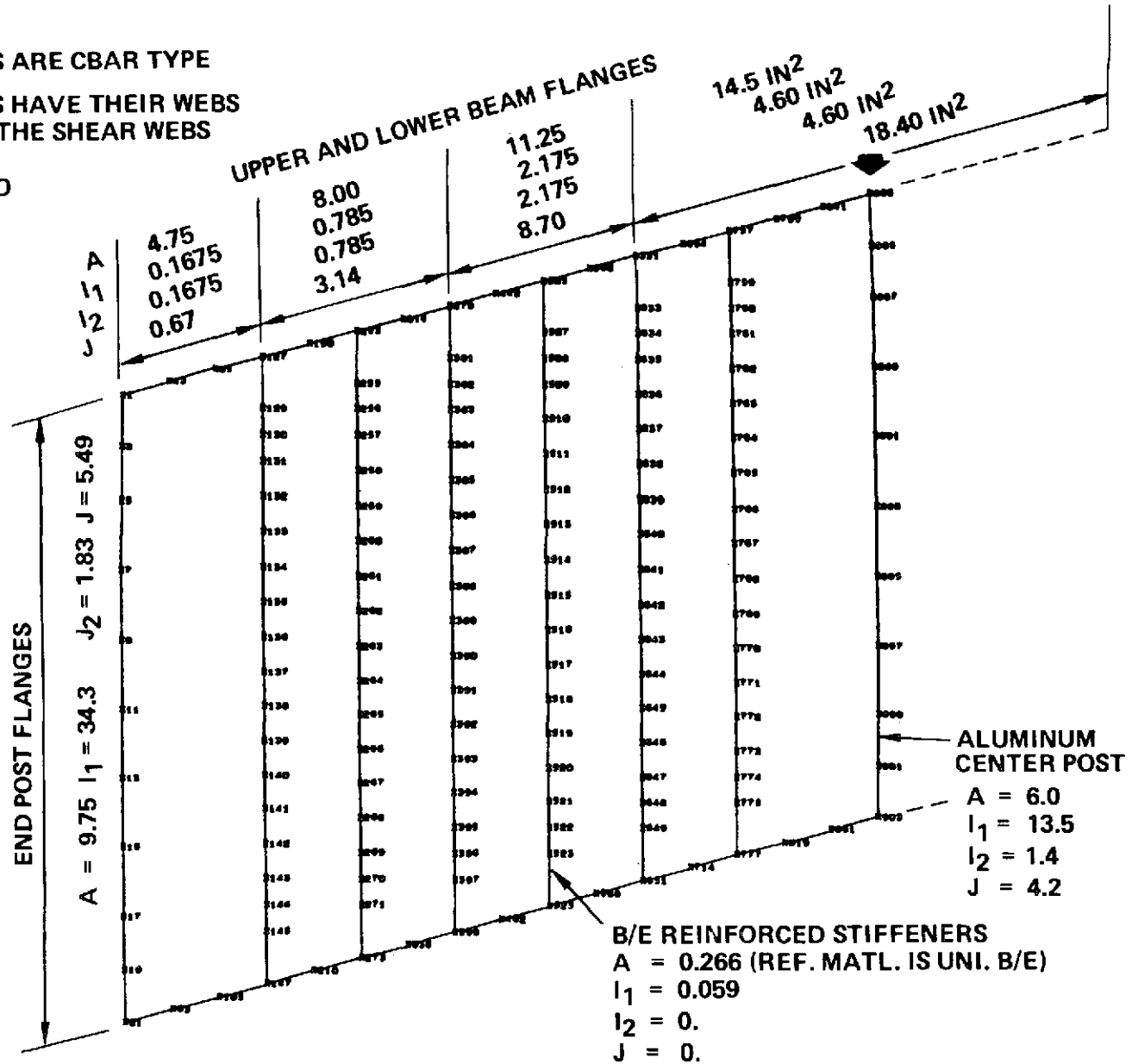
Figure 60: TEST WEB 2 NASTRAN FINITE ELEMENT BEAM ELEMENTS

85

SG-5 ON NEAR SURFACE
SG-6 ON FAR SURFACE } AT CENTER OF CENTER PANEL

8050
(8135-- NASTRAN PREDICTION)

γ

ε_{MAX}

3800 (3861)

ε_{MIN}

-4400 (-4273)

FAILURE AT 540000 LB

BEAM LOAD - 10^3 LB

MICROSTRAIN

10000

8000

6000

4000

2000

0

-2000

-4000

0   100   200   300   400   500   600
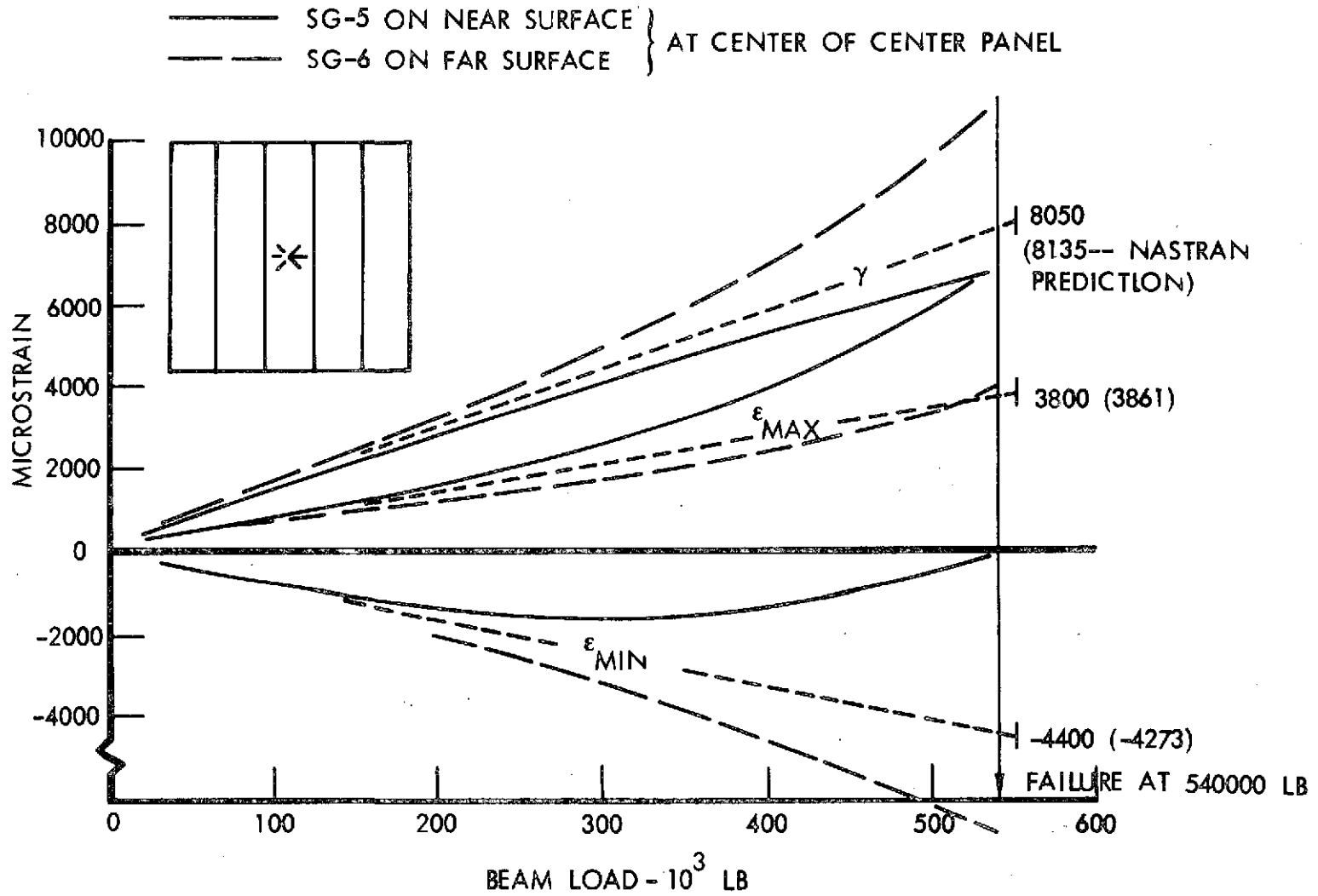
Figure 61: TEST WEB 1 STRAINS COMPARED WITH NASTRAN ANALYSIS RESULTS

100,000 LB
(4.429 MN)

Δ = 1.655 IN
(42.04 MN)
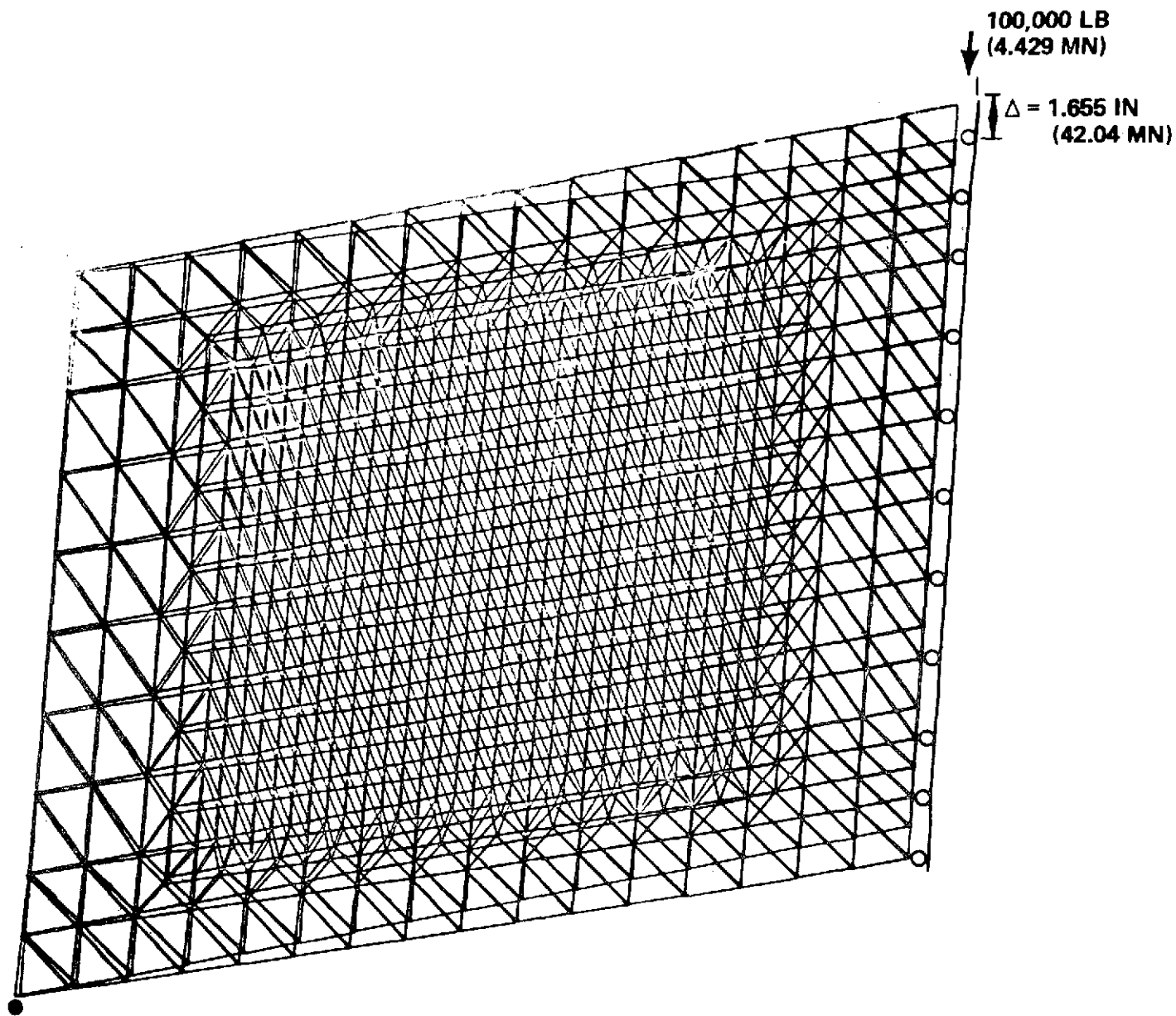
Figure 62: LINEAR DEFLECTION RESPONSE OF TEST WEB 2 FINITE ELEMENT MODEL

in Figure 63. This same idealization was used in the test beam assembly models. However, as indicated in Figure 64, the computed buckling loads for various stiffening eccentricity assumptions were in considerable error relative to the extrapolated test bifurcation load defined by the F/S data in Section 6.2. A plot of the computed critical mode shape for test web 2 appears in Figure 65; the plotted shape has similar mode inclination as the mode displayed by the test Moire fringe pattrns given in Section 5.3. The finite element buckling analysis was not pursued further because of excessive computing cost associated with the large test web model.
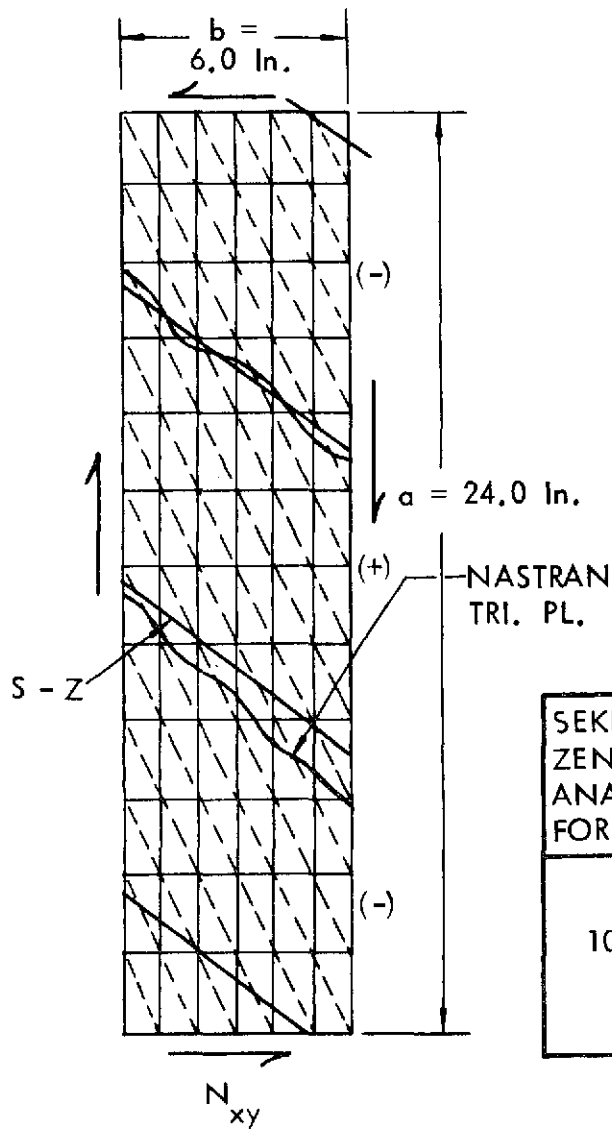
**NASTRAN ORTHOTROPIC PLATE
FINITE ELEMENT MODEL OF TEST
WEB 1 LAMINATE**

$T = 0.188$ In   Simple Supports

Membrane Properties

$$G_{ij} = \begin{bmatrix} 8.093E6 & 4.424E6 & 0 \\ S. & 8.093E6 & 0 \\ & & 4.96E6 \end{bmatrix}$$

Bending Properties

$$G_{ij} = \begin{bmatrix} 11.45E6 & 4.386E6 & 0 \\ & 11.45E6 & 0 \\ S. & & 5.027E6 \end{bmatrix}$$

COMPUTED CRITICAL SHEAR LOADS (N_{xy} Lb/In)

SEKERZH-ZEN'KOVICH ANALYSIS FOR $a/b = \infty$	WEBBUC CODE (RAYLEIGH-RITZ)	NASTRAN ANALYSIS		$\dfrac{\text{NASTRAN}}{\text{WEBBUC}}$
10556.1	10676.7 (Symmetric Mode) 5 x 15 Series	Quad. Plates (C QUAD 1)	14184.5	1.33
		Triangular Plates (C TRIA 1)	11158.7	1.05

Figure 63: NASTRAN BUCKLING ANALYSIS CORRELATIONS

b = 6.0 In.

a = 24.0 In.

(−)

(+) — NASTRAN TRI. PL.

S − Z

(−)

N_{xy}

FINITE ELEMENT MODEL	FEATURES	$\dfrac{P_{CR}\ \text{NASTRAN}}{P_{CR}\ \text{TEST}}$
A	ECCENTRIC STIFFENING	1.61
B	NON-ECCENTRIC STIFFENING	1.36
C	NON-ECCENTRIC STIFFENING STIFFENERS HAVE NO STIFFNESS IN JOGGLED END AREAS	1.25

Figure 64: NASTRAN BUCKLING ANALYSIS OF TEST WEB 2
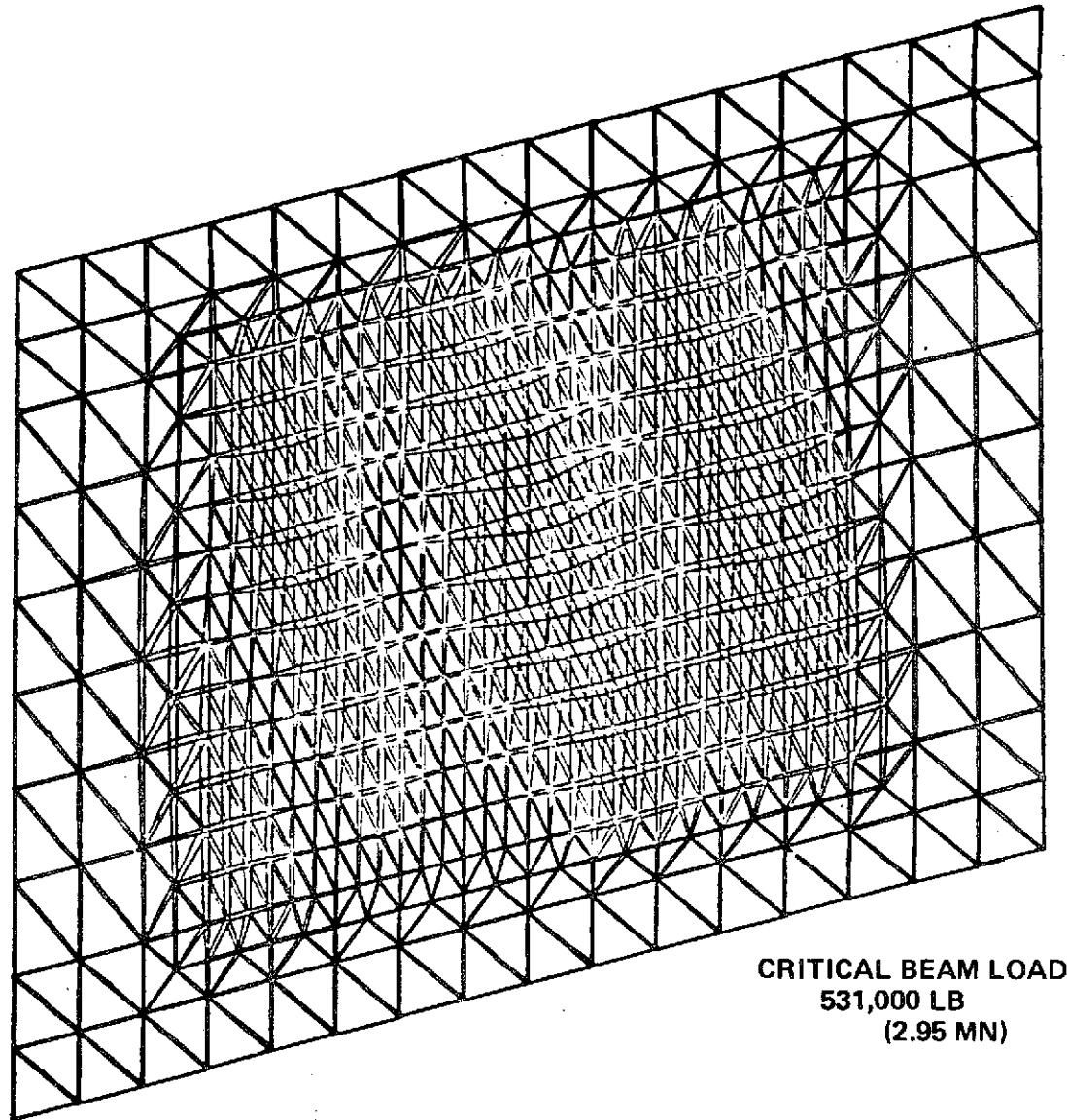
CRITICAL BEAM LOAD
531,000 LB
(2.95 MN)

Figure 65: CRITICAL BUCKLING MODE FOR TEST WEB 2 FINITE ELEMENT MODEL

8.0   BUCKLING ANALYSIS/TEST CORRELATIONS

The results of the three web tests were correlated with the results from computer-aided buckling analysis of simplified web configurations. The purpose of this study was to determine criteria for effective web height and effective stiffening which might be useful to other applications.

8.1   STRUCTURAL STIFFNESSES

The structural stiffnesses used in the buckling analyses are presented in Figure 66. These stiffnesses were computed by classical laminate analysis [8] and conventional engineering analysis. Bending stiffness tests were conducted on specimens cut from the first and third test webs to verify selected computed values. Also, bending tests were performed on selected stiffeners from the test webs to verify the computed bending stiffnesses. The calculated torsional stiffness for the stiffeners on the first test web was verified by torsion testing. In calculating stiffener stiffnesses, none of the web laminate nor web-to-stiffener eccentricity effects were included.

TEST WEB	WEB NOMINAL LAMINATE				TRANSVERSE STIFFENERS		LONGITUDINAL STIFFENER
	D_{11} LB–IN (NM)	D_{12}	D_{22}	D_{33}	EI_T LB–IN^2 (NM^2)	GJ_T	EI_L
1	6023.1 (680.5)	2270.5 (256.5)	6023.1 (680.5)	2610.1 (294.9)	1.483E6 (4256.)	7500 (21.5)	NONE
2	7024.3 (793.6)	2705.9 (305.7)	7024.3 (793.6)	3105.4 (350.9)	1.77E6 (5080.)	20000 (57.4)	NONE
3	4536.4 (512.5)	1749.9 (197.7)	4536.4 (512.5)	2008.9 (227.0)	1.64E6 (4706.)	15000 (43.0)	2.41E6 (100% EFFECTIVE VALUE) (6926.)

Figure 66: STRUCTURAL STIFFNESSES USED IN BUCKLING ANALYSES

8.2 RITZ BUCKLING ANALYSIS

An existing Ritz energy buckling solution was adapted to the analysis of the test webs. This solution was developed in support of the Boeing SST Program for use in computing bifurcation loads of transversely stiffened orthotropic shear webs [9, 10]. Coding for this solution was extended to treat the conditions shown in Figure 67. The modified code is called the WEBBUC code and was verified by analyses of the design configurations shown in Figures 68 and 69. The accuracy of the buckling solution is dependent on the number of terms taken in the assumed deflection function in the Ritz method; consequently, numerical tests of the type shown in Figure 69, which pertain to an analysis of test web 1, were conducted to establish requirements for the size of the computed buckling determinant. Since the Ritz method is presented in the literature, discussion concerning its theoretical aspects will not be given in this report.

8.3 BUCKLING ANALYSIS/TEST CORRELATIONS

Numerous analyses were performed using the WEBBUC code in which the height of an effective, simply supported web was varied. Figures 70 to 72 show the computed critical shear buckling loads versus effective web height for the respective test webs. Also shown are the test shear loads given by dividing the bifurcation buckling loads, defined by the F/S data (Section 6.2), by the total web height.

94

- RITZ ENERGY METHOD

  - EXTENSION OF SST RESEARCH TO TREAT BEAM BENDING LOAD AND LONGITUDINAL STIFFENERS

LINEAR BEAM BENDING STRAIN (UP TO PURE COMPRESSION)

UNIFORM SHEAR LOAD

LONGITUDINAL STIFFENERS (ARBITRARY LOCATION, EI, EA)

TRANSVERSE STIFFENERS (EI, GJ, EΓ)

ORTHOTROPIC WEB PLATE (D$_{IJ}$)

$$w = \Sigma\Sigma \ a_{ij} \ Sin\frac{i\pi x}{L} \ Sin\frac{j\pi y}{H}$$

$i = I,M$
$j = I,N$
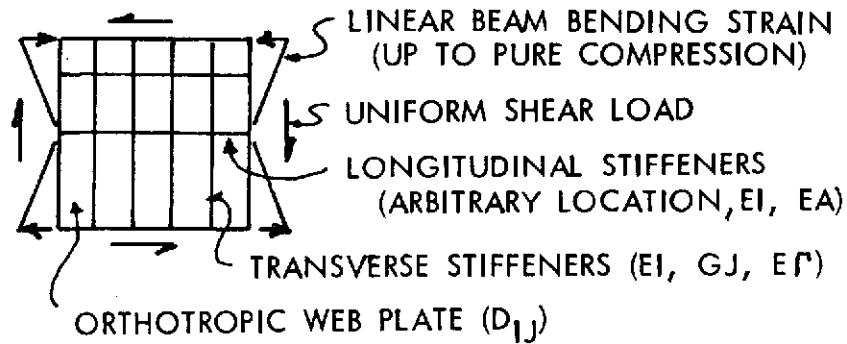
(SIMPLE SUPPORTS)

$$\psi = \frac{\partial}{\partial a_{ij}} (V - T) = 0$$

(MINIMIZED TOTAL ENERGY EQUATIONS)

- WEBBUC CODE

  - CRITICAL EIGENVALUE FOUND BY NEWTON METHOD
  - BUCKLING DETERMINANT $|\Psi|$ EVALUATED BY DIRECT SYMMETRIC CHOLESKI METHOD

Figure 67: SHEAR WEB RITZ BUCKLING ANALYSIS FEATURES

STIFFENED ISOTROPIC PLATE PROBLEMS	WEBBUC CODE		K_{CR} LITERATURE	STRUCTURAL PARAMETERS			
	BUCKLING COEF. K_{CR}	DET. ORDER		PANEL ASPECT RATIO	γ_T	γ_L	β_L
	81.45	38	80 STEIN & FRALICH REF [11] 72.5 COOK & ROCKEY REF [12] (L = ∞)	5.0	74.32	0	0
	149.8	96	126 COOK & ROCKEY REF [12] (L = ∞)	5.0	74.32	20	0
	11.081	25	11.1 TIMOSHENKO REF [13]	2.0	0	5	0.1
	14.443	25	14.5 TIMOSHENKO REF [13]	3.0	0	5	0.1 -33
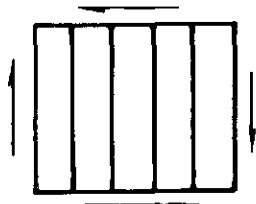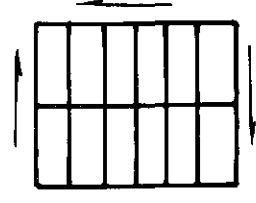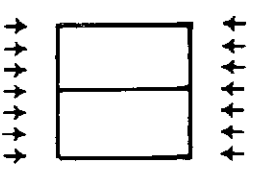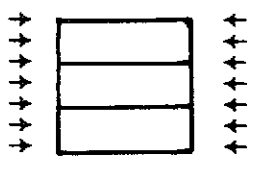
Figure 68: WEBBUC CODE SOLUTION COMPARISONS
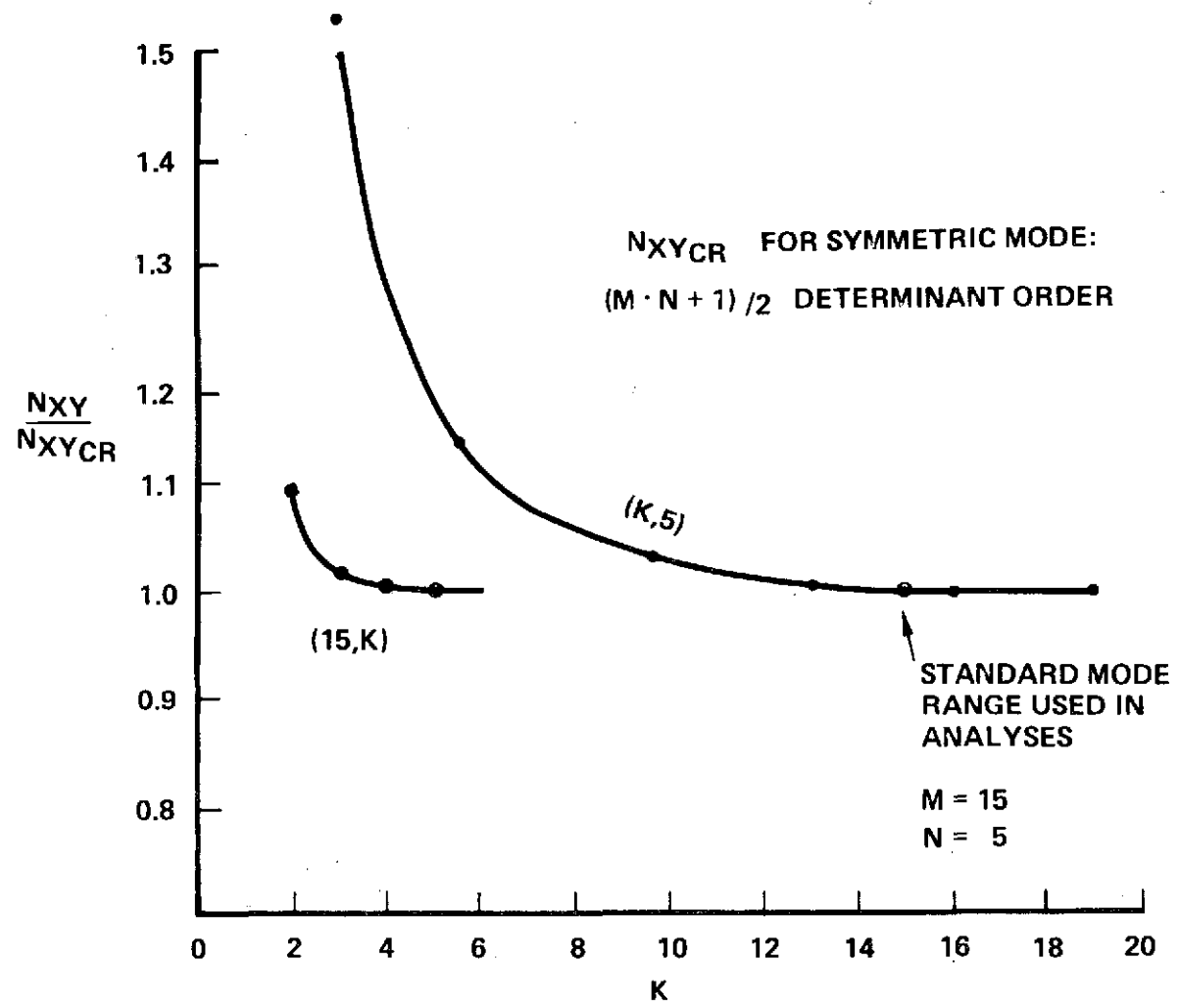
Figure 69: WEBBUC CODE SOLUTION CONVERGENCE TEST

WEBBUC CODE RESULTS
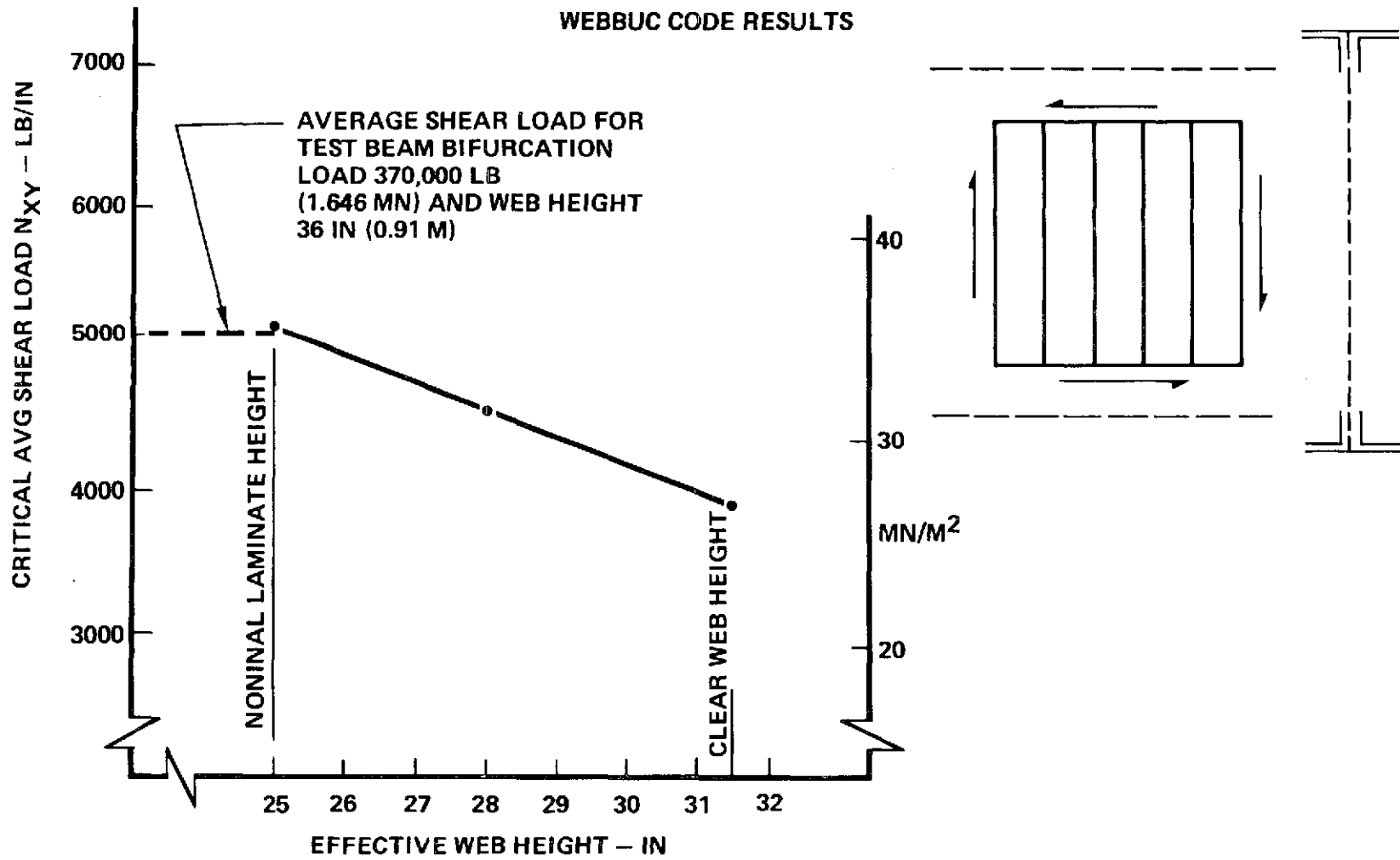
Figure 70: *RITZ ANALYSIS/TEST CORRELATION FOR TEST WEB 1*

86
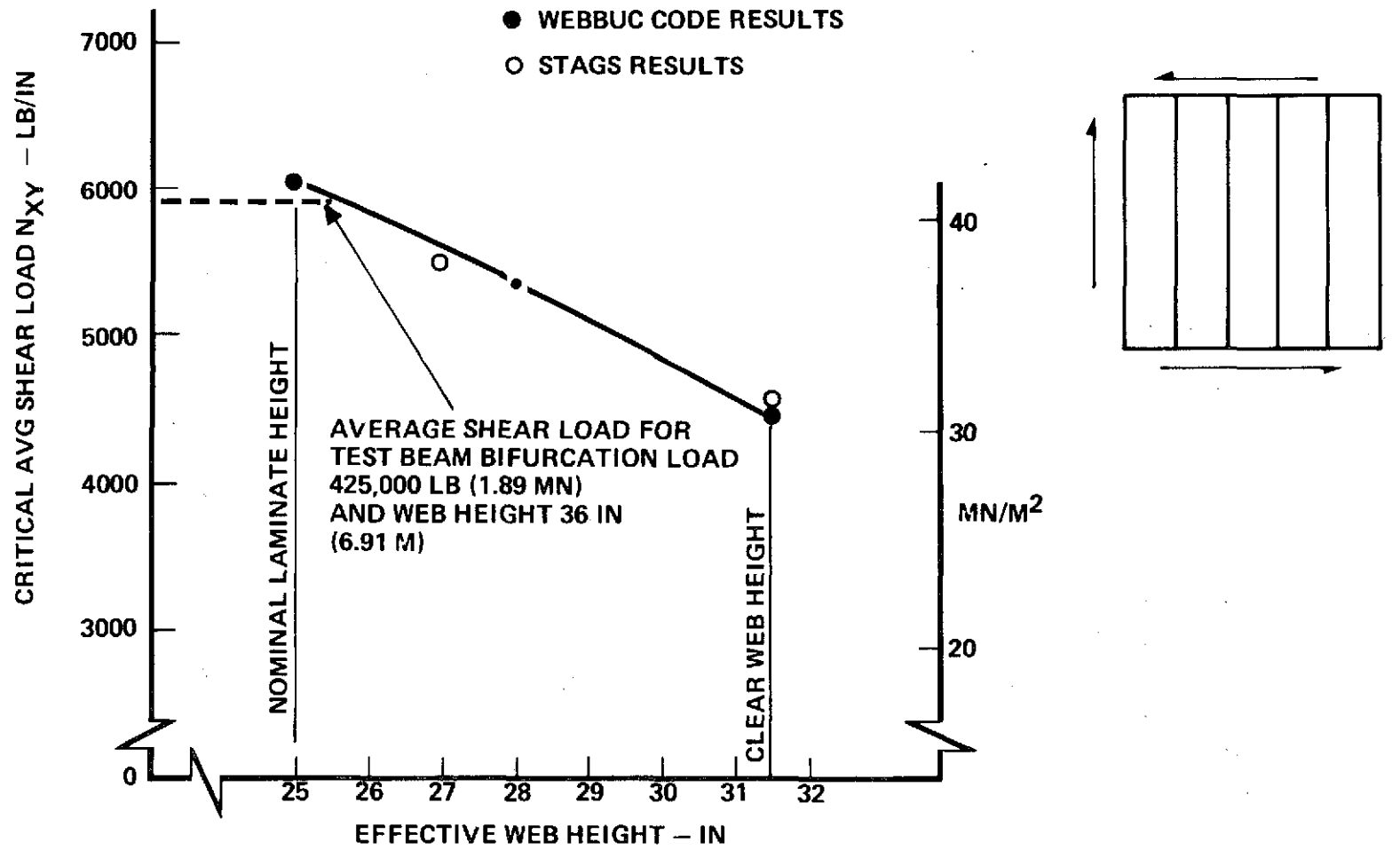
Figure 71: BUCKLING ANALYSIS/TEST CORRELATION FOR TEST WEB 2
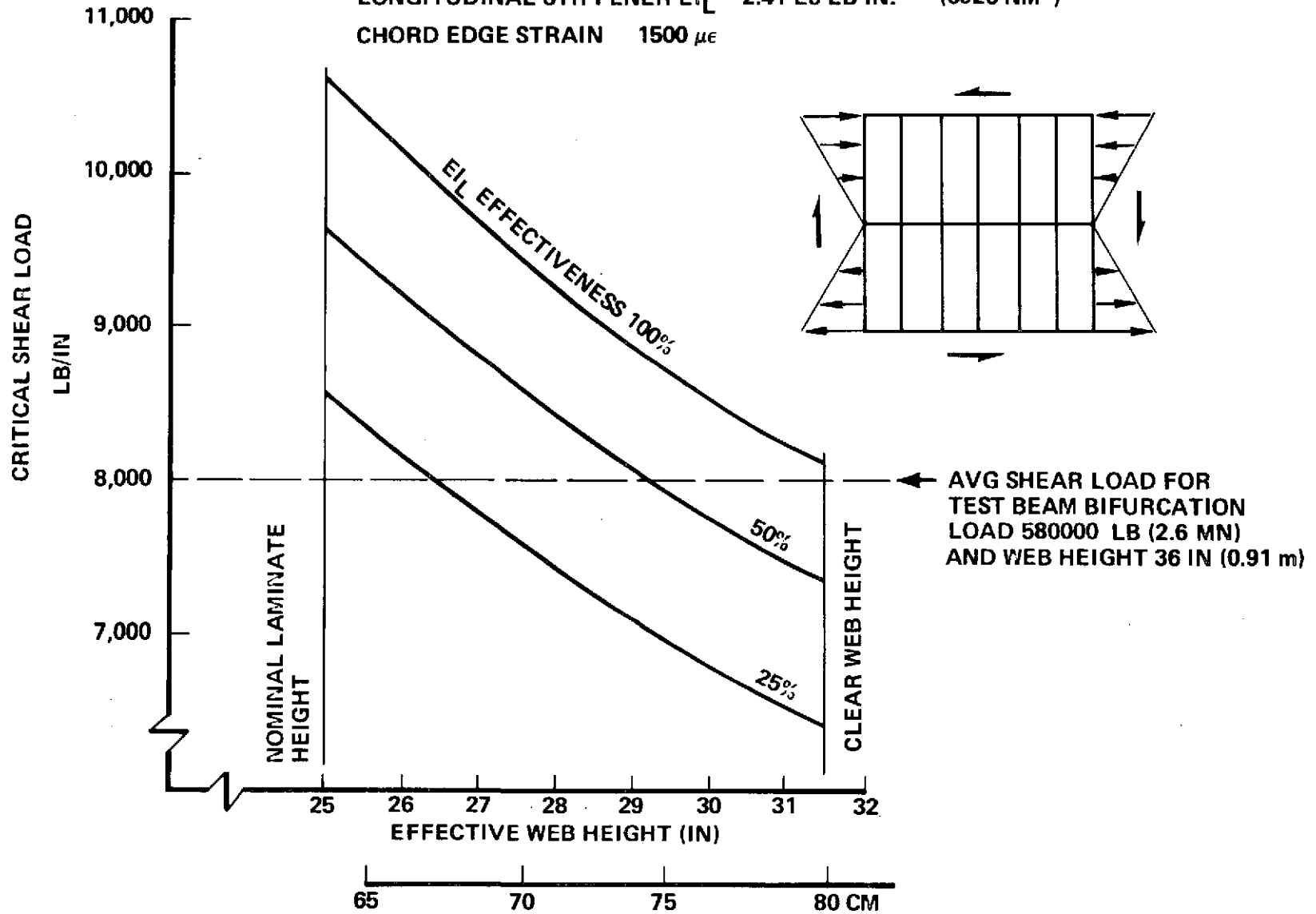
Figure 72: RITZ ANALYSIS/TEST CORRELATION FOR TEST WEB 3

Both test webs 1 and 2 appear to have effective web heights on the order of the nominal laminate panel height. The reason for this is buckling occurs in the central portion of the high aspect ratio panels and is not significantly influenced by the web edge conditions.

Test web 3, having a longitudinal stiffener, had smaller panels and the test data indicates panel deflections occurred near the beam chords, therefore the effective web height lies between the nominal laminate height and the clear height between chord angles. Because of the large cut-outs that were present in the longitudinal stiffener, the stiffness of this stiffener was not fully effective. Assuming a 50% longitudinal stiffener effectiveness results in an effective web height of 29 inches when comparing the test versus the predicted buckling loads in Figure 72. This correlation is, of course, subject to interpretation. In a future analysis situation, one would be conservative by computing the buckling load based on the full clear web height and some reduced effective longitudinal stiffener stiffness.

In all of the correlation studies, it was found that satisfactory correlation could only be obtained when stiffener stiffnesses were calculated on the basis of an uncoupled stiffener section, neglecting the web laminate parts and web-to-stiffener eccentricity. An explanation of this is that the stiffener/web assembly fasteners were non-hole filling and were not tightly torqued (to preclude damaging the web laminate) which does not provide a strong shear-tie. During buckling deformation, slippage probably occurred between the stiffeners

101

and the web so that the stiffeners were loaded primarily in bending. In a production program, studies of fastening methods should be undertaken to improve stiffener/web interaction.

As indicated in Figure 72, beam bending loads were included in the buckling analyses for test web 3. The effects of beam bending on the test results was determined to be insignificant in a shear/bending load interaction study. Figure 73 shows the results of this study. While the test webs had low beam bending loads, the effects of load interaction must not be neglected in buckling analysis of "shear resistant" production webs which will frequently have high beam chord strains.

In Figure 71, linear buckling analysis results from the STAGS code [14] are shown. The STAGS code which is based on a finite difference energy solution approach, became operational later in the program and its use in analysis of production hardware is recommended. A particular advantage of the STAGS code is its capability to perform non-linear pre- and post-buckling analyses in an efficient manner. For the analyses shown, the input structural properties (orthotropic laminate stiffnesses, etc.) were the same as used in the WEBBUC code analyses.

The graph shows:
- Y-axis (left): $N_{XB_{CR}}$ — LB/IN, ranging 0 to 12,000
- Y-axis (right): MN/M^2, marked 50, 60, 70
- X-axis (bottom): $N_{XY_{CR}}$ — LB/IN, 0 to 10,000
- X-axis (lower): MN/M^2, 0 to 60

BENDING LOAD MAGNITUDE IN TEST

D_{11W} = 6023.1 LB IN
EI_T = 2.0E6
GJ_T = 20,000
EI_L = 0.74E6
75th ORDER DETERMINANT
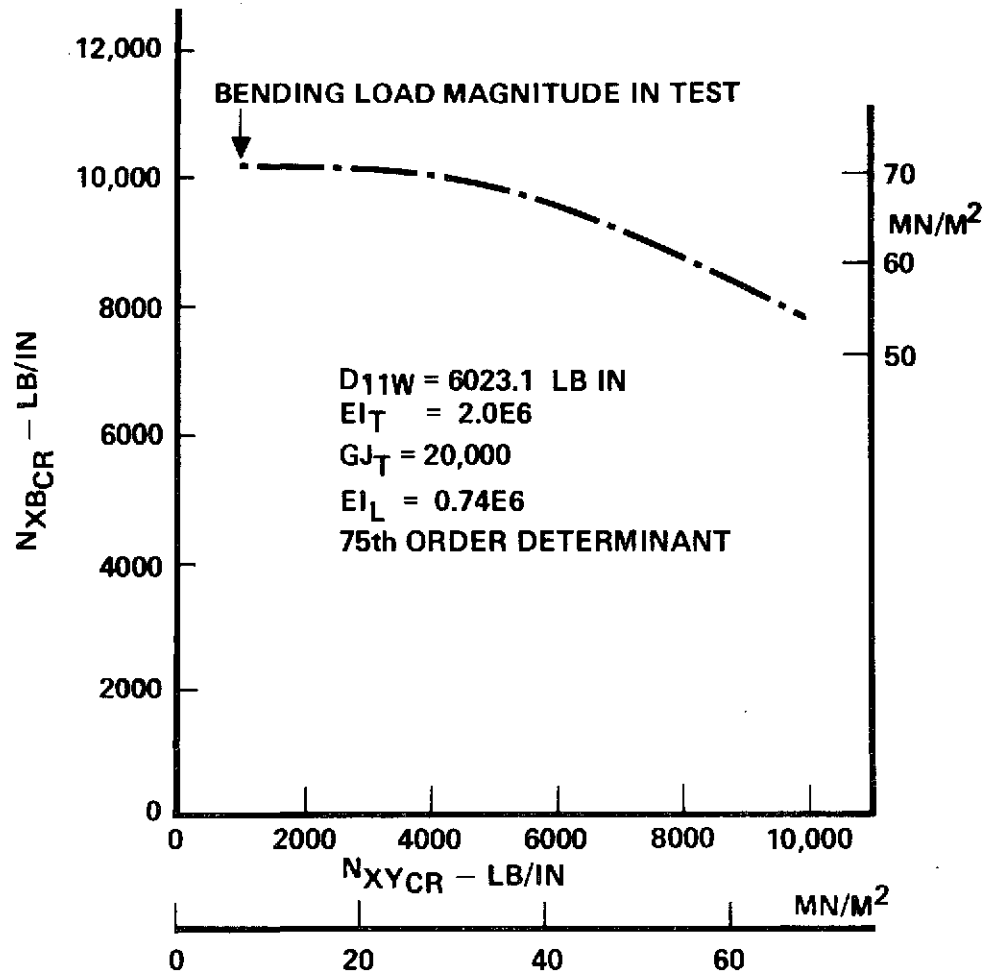
WEBBUC CODE RESULTS

H = 28 IN
L = 30

TEST WEB 3 CONFIG-URATION
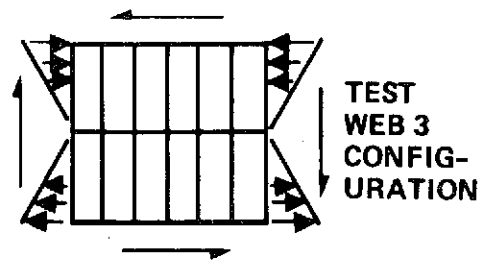
Figure 73: BENDING/SHEAR BUCKLING INTERACTION ANALYSIS RESULTS

9.0 DESIGN ANALYSIS METHODS

Design Analysis methods were established in Phase III to provide a basis for analyzing the composite reinforced shear web concept in applications different from the test conditions in this program. The methods presented in the Phase I Summary Report, while suitable for design screening purposes were revised and amended to include treatment of all important responses experienced during the web component tests. The methods given herein are approximate and are reported with the intention of providing guidelines for analysis of preliminary designs for other applications of the design concept. While the methods were used in this program in a computer-aided design code (OPTRAN), the methods are suitable for manual analysis. Appendix C presents all of the analyses that are required for preliminary design analysis; the following discusses the methods developed in Phase III.

9.1 SHEAR BUCKLING ANALYSIS

The shear buckling analysis method given in Phase I (in which smeared stiffening was assumed) was found to be inadequate on the basis of the test results and therefore was revised to treat single central longitudinal stiffening and discrete stiffening. The analysis, given in Figure 74, was developed by curve fitting the data of Cook and Rockey [12]. For a given design, the shear buckling coefficient is first found for the case of no longitudinal stiffening (K_{SI}). This coefficient is then multiplied by a magnification parameter (η) to produce

104
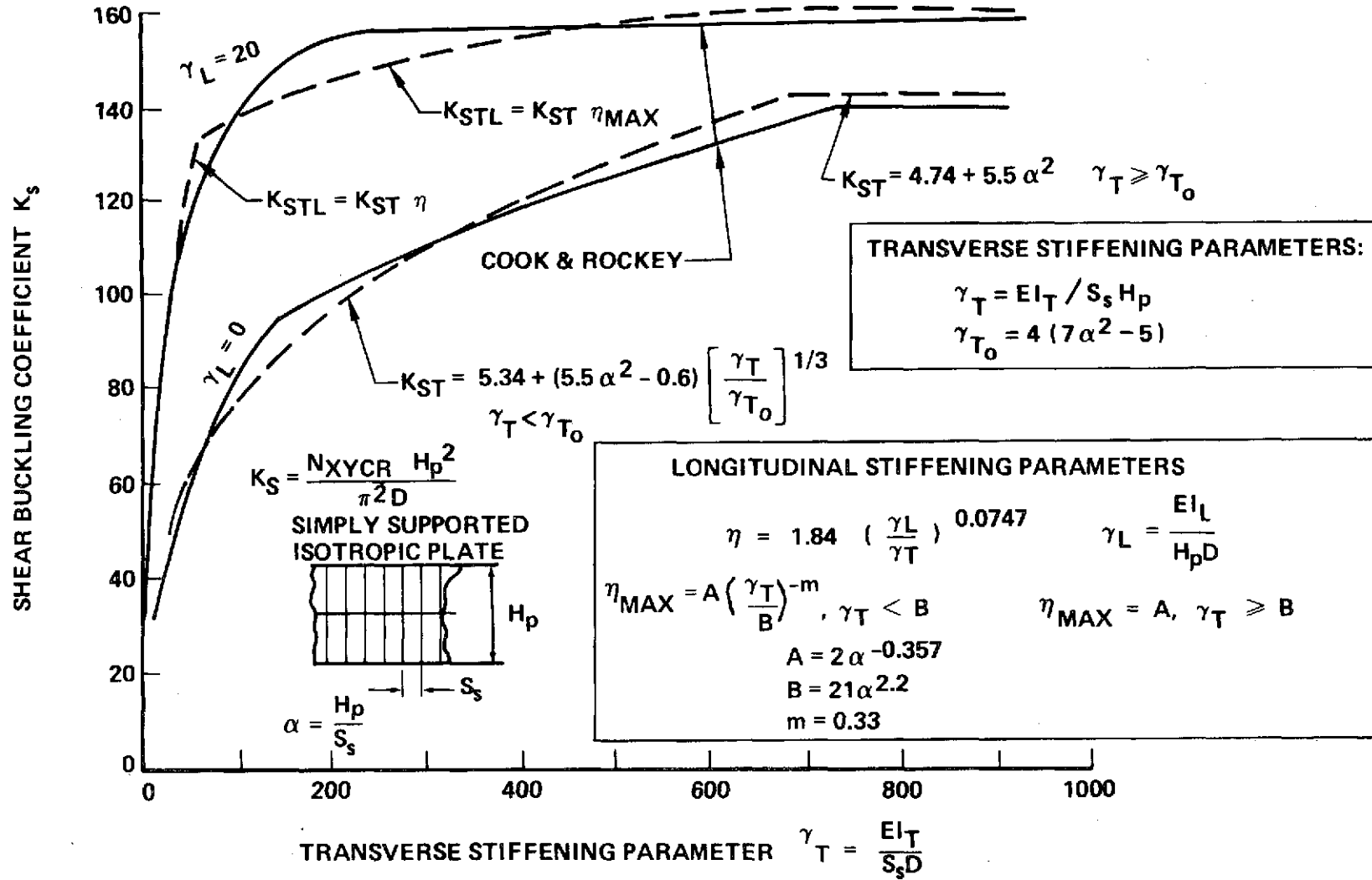
Figure 74: SHEAR BUCKLING COEFFICIENT RELATIONS

the shear buckling coefficient for the case with longitudinal stiffening (K_{STL}). The buckling coefficients are a function of effective web depth (Hp), transverse stiffener spacing (Ss), transverse stiffener bending stiffness (EI_T), longitudinal stiffener bending stiffeners (EI_L), and web plate bending stiffeners (D_{11}). A comparison of the fitted-equations with data from Cook and Rockey [12] for cases with and without longitudinal stiffening are shown in Figure 74; also shown is the equation used to calculate critical shear buckling load. While the data fit is reasonably good for preliminary analysis of the shear web configurations studied in this program, the fit should be checked for other cases against the original Cook and Rockey data or data from another source (for example, the STAGS code).

9.2 BENDING BUCKLING ANALYSIS

The analysis of local panel buckling under beam bending loads is accomplished with the data given in Figure 75. The WEBBUC code described in Section 8.1, was used to compute buckling coefficients for high panel aspect ratios not treated in the literature (Bleich [15]). As in the analysis of shear buckling, the computation of critical bending buckling load is by a relation from isotropic plate theory. This simplifying approach is slightly conservative for the metal-clad laminates developed in this program because the metal-clad laminates have excess twisting stiffness (D_{33}) compared to isotropic plates with equivalent bending stiffnesses.

$$K_B = \frac{100}{(\zeta / .1425)^{1.858}}$$

$$K_B = \frac{88.57}{(\zeta / .1425)^{1.858}} + 4.886 - 6.585\,\zeta$$

$$+ 10.85\,\zeta^2 - 3.568\,\zeta^3$$

$$N_{XB} = \frac{K_B\,\pi^2 D}{S_s{}^2 b^2}$$

SIMPLY SUPPORTED
ISOTROPIC PANEL
WEBBUC CODE RESULTS
49th ORDER DETERMINANT

BLEICH

K_B

10^2

10^1

10^0

10^{-1} 10^0 10^1

PANEL ASPECT RATIO ζ = b/a

107
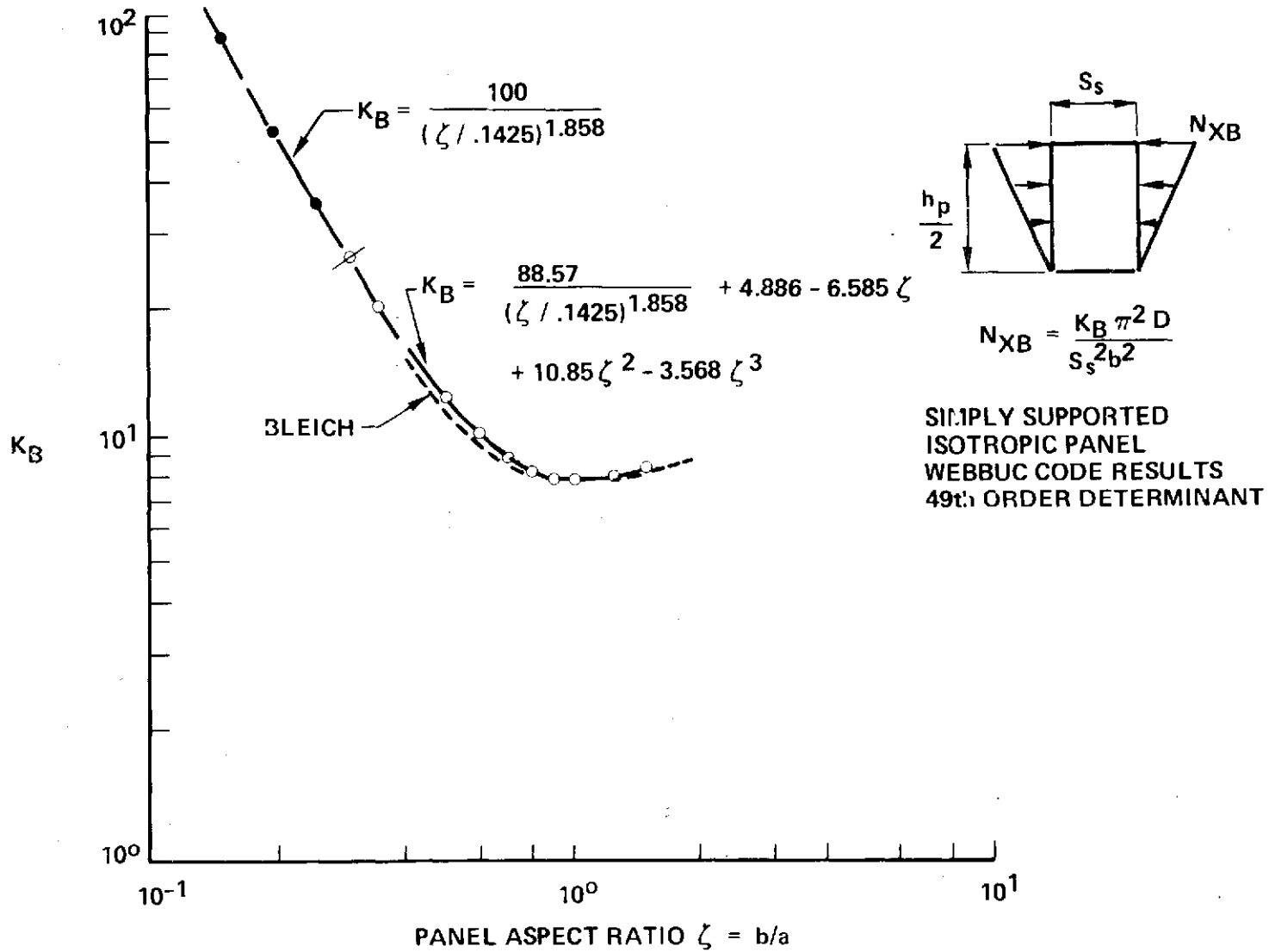
Figure 75: PANEL BUCKLING COEFFICIENTS FOR BENDING

9.3 PRE-BUCKLING BENDING STRAIN ANALYSIS

The problem of pre-buckling bending strains can be treated in a manner analogous to the imperfect column problem. That is, given an initial mode shape, find the resultant deflected shape under load. The method is simple for a column, but in the case of a shear web, it is complicated by (1) the presence of initial imperfections unlike the critical mode shape, (2) need for critical mode shape definition, and (3) large deflection effects. An approximate analysis was established for the purposes of this program by adopting the following assumptions:

1. The initial imperfection has the same shape as the critical theoretical bifurcation buckling mode.

2. The magnitude of initial imperfection of a fabricated panel is the deviation from a mean flat surface.

3. The critical buckling mode is a skewed local panel buckling mode (stiffeners are unbuckled and form the vertical panel nodal lines)

4. The pre-buckling magnification of initial deflection is a function of the critical theoretical buckling load interaction criterion.

Figure 76 illustrates the skewed mode shape model that was adopted; this mode shape has been used in classical shear plate buckling analysis (Timoshenko [13]). The associated plate bending curvatures are obtained from the deflection surface equation by double differentiation with respect to the panel coordinates; the important maximum curvatures occur at the buckle peak.
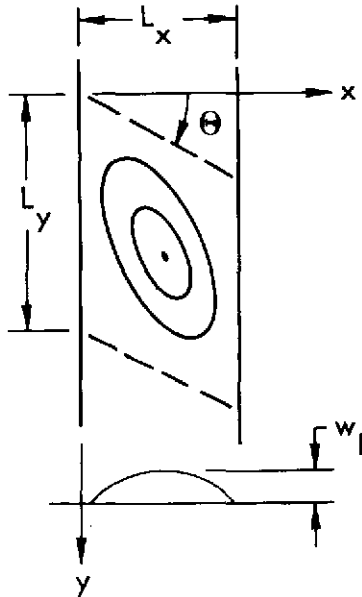
INITIAL DEFLECTION SURFACE:

$$w = w_1 \sin \frac{\pi y}{L_y} \sin \frac{\pi}{L_x}(x - \phi y) \qquad \phi = \tan \Theta$$

CURVATURES AT BUCKLE CENTER:

$$K_x = \frac{\partial^2 w}{\partial x^2} = -w_1 \left(\frac{\pi}{L_x}\right)^2$$

$$K_y = \frac{\partial^2 w}{\partial x^2} = -w_1 \left[\left(\frac{\pi}{L_y}\right)^2 + \phi^2 \left(\frac{\pi}{L_x}\right)^2\right]$$

$$K_{xy} = \frac{\partial^2 w}{\partial x \partial y} = 0$$

INTERACTION CRITERION:

$$R = R_S^2 + R_B^2 \leq 1.0 \qquad R_S = \frac{N_{xy}}{N_{xyCR}} \qquad \text{ETC.}$$

PRE-BUCKLING CURVATURES DUE TO LOADING:

$$K_x = -w_1 \left(\frac{\pi}{L_x}\right)^2 \left[\frac{1}{1-R^{1/2}} - 1\right] \qquad \text{ETC.}$$

Figure 76: PRE-BUCKLING ANALYSIS RELATIONS

The resultant curvature strains are given by the product of initial curvatures and a magnification factor of the form:

$$\frac{1}{1 - R^{1/2}} - 1$$

where the first term is the load function and the (-1) term compensates for the unloaded initial condition. The use of square root with the critical buckling load interaction criterion parameter (R) is required because of the squared terms in the classical shear + bending interaction relation (given in Appendix C).

The total strains in the laminate materials are found by superposition of the membrane web strains and the curvature-induced strains, as shown in Figure 77, taking into consideration the material coordinate from the laminate's neutral surface. Strains in the composite plies are calculated in the respective ply coordinates by classical laminate analysis. Stresses in the metal-cladding are given directly by the product of the elastic coefficient matrix and the total cladding strain vector.

The prebuckling strain analysis method was checked with the web component test results. Figure 78 lists the estimated local panel buckle parameters used in the analysis. W_I, L_y and θ were determined for each test web from the Moire fringe patterns at final load levels. The P_{cr} values are the extrapolated bifurcation loads from the F/S plots and are used in place of $R^{1/2}$ in the magnification factor. The material coordinates (Z_M) were established from the data in Figure 11.

110

BENDING STRAIN COMPONENTS AT A MATERIAL POINT

$$\varepsilon_{im}^{B} = K_i \, Z_m$$

o   TOTAL STRAIN = MEMBRANE STRAIN + BENDING STRAIN COMPONENTS

$$\varepsilon_i = \varepsilon_i^{M} + \varepsilon_{im}^{B}$$

o   TRANSFORM X-Y STRAINS TO PLY COORDINATES

o   METAL CLADDING STRESSES

$$\sigma_i = a_{ij} \, \varepsilon_j$$

Z_m

111
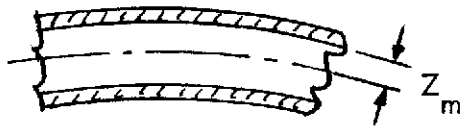
Figure 77: PRE-BUCKLING STRAIN ANALYSIS RELATIONS

TEST WEB	W_i IN (MM)	L_x IN (MM)	L_y IN (MM)	θ DEG	Z_m IN (MM)		P_{cr} 10^3 LB (MN)
1	0.016 (0.406)	6 (152.4)	18 (457.2)	66	0.0911 (2.31)	CLADDING SURFACE	460 (2.05)
2	0.014 (0.356)	6 (152.4)	19 (482.6)	65	0.0966 (2.45)	CLADDING SURFACE	518 (2.30)
3	0.003 (0.076)	5 (127.0)	14 (355.6)	60	0.0543 (1.38)	EXTREME B/E SURFACE	580 (2.58)

θ

L_y (ESTIMATED FROM MOIRE FRINGE PHOTOGRAPHS)

L_x ASSUMED EQUAL TO STIFFENER SPACING
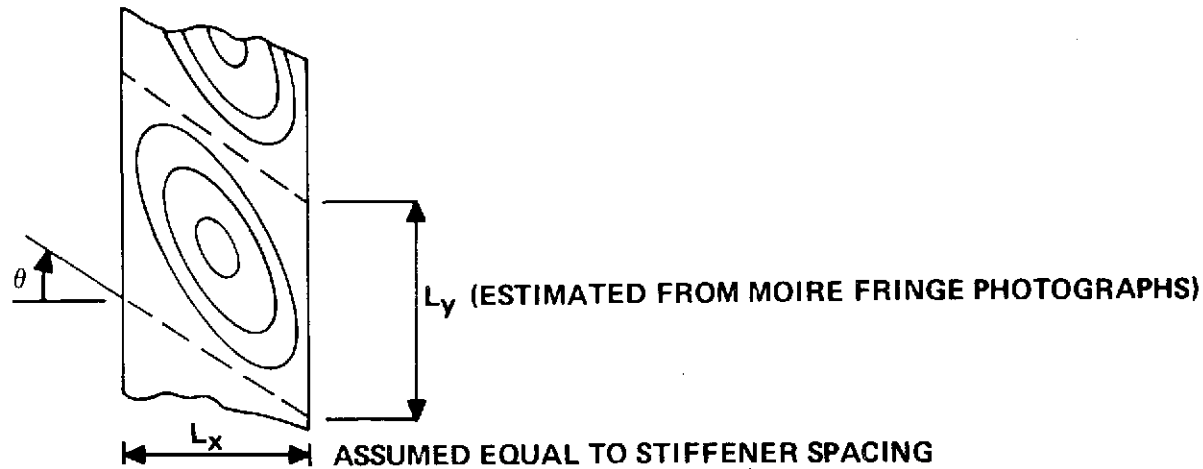
Figure 78: ESTIMATED LOCAL PANEL BUCKLE PARAMETERS

Figures 79 to 81 show the predicted prebuckling strains compared to the actual strains (computed from the Moire fringe data and presented in Section 6.3) for the respective test webs. The agreement between the predicted versus the actual strain is good in the pre-buckled regimes of each test (before large deflection effects appear). In the case of the third web, the comparisons suggest the initial imperfection level is on the order of ± 0.003 in. (0.076 mm). A reduction in initial imperfection, while producing a proportional change in bending strain, does not produce a large change in load at a constant critical strain level of, say, $6000 \mu\epsilon$.

9.4 BEAM CHORD CRUSHING LOAD

An analysis was included for transverse web "crushing" loads due to beam chord curvature associated with beam flexure. The analysis requires an assumption of chord load which is used with chord strain and web depth in a simple relation (shown in Figure 86), to yield the transverse web crushing load. The web crushing load is used, as shown in Appendix C, in the computation of web material stresses and strains but is not considered to be important in the analysis of web buckling loads.
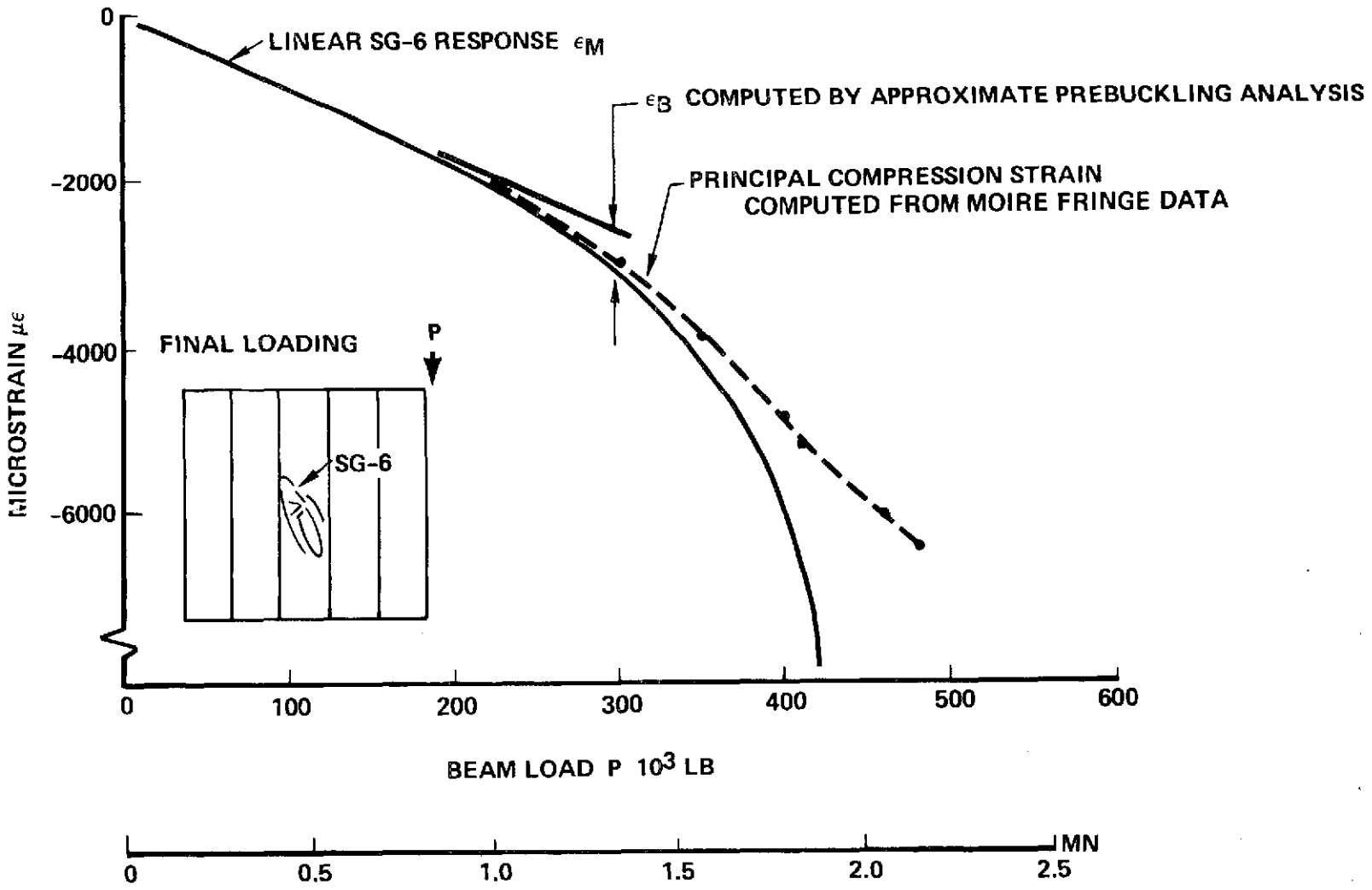
Figure 79: COMPUTED SURFACE CLADDING STRAINS IN TEST WEB 1 CRITICAL BUCKLE AREA
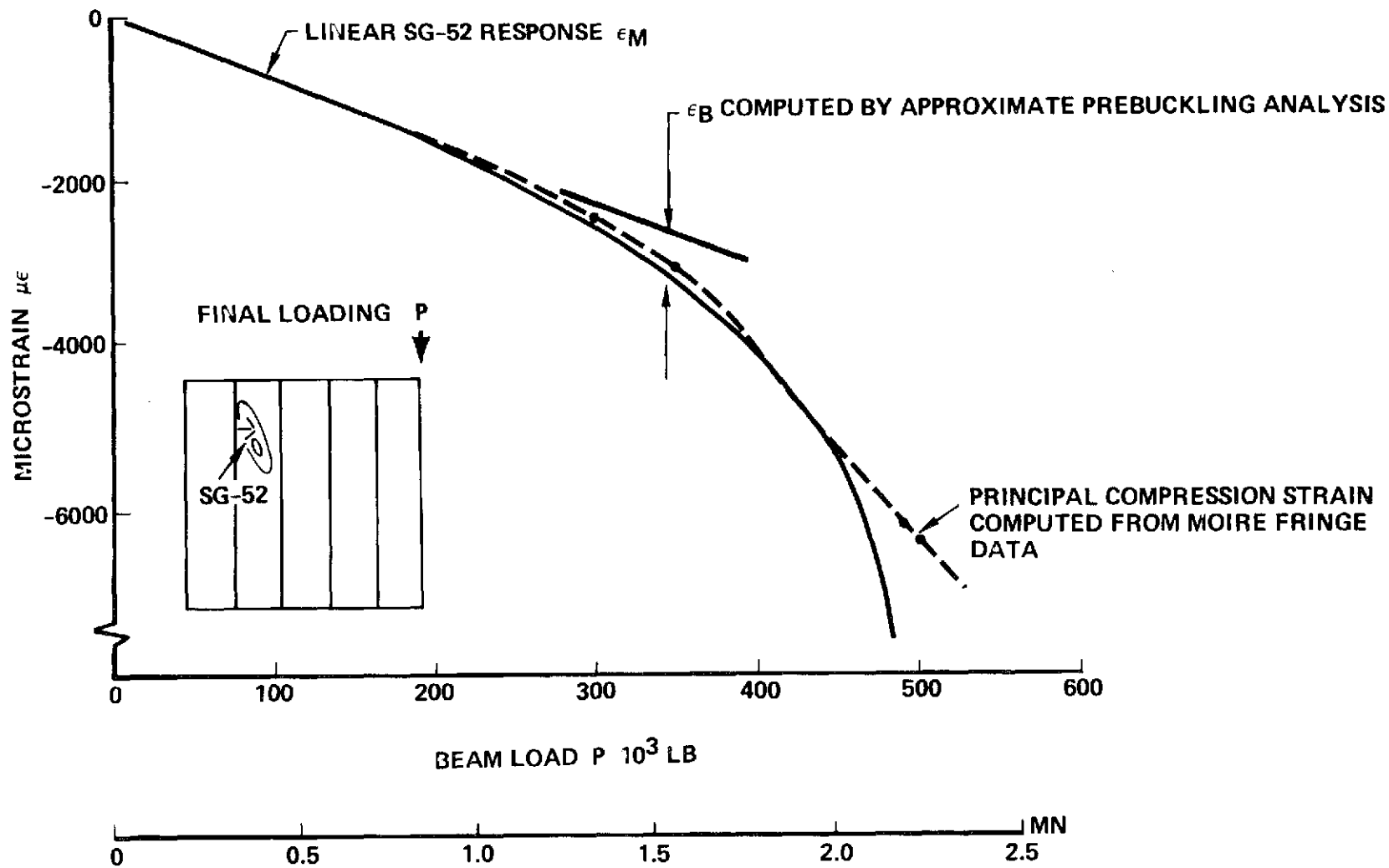
Figure 80: *COMPUTED SURFACE CLADDING STRAINS IN TEST WEB 2 CRITICAL BUCKLE AREA*

115
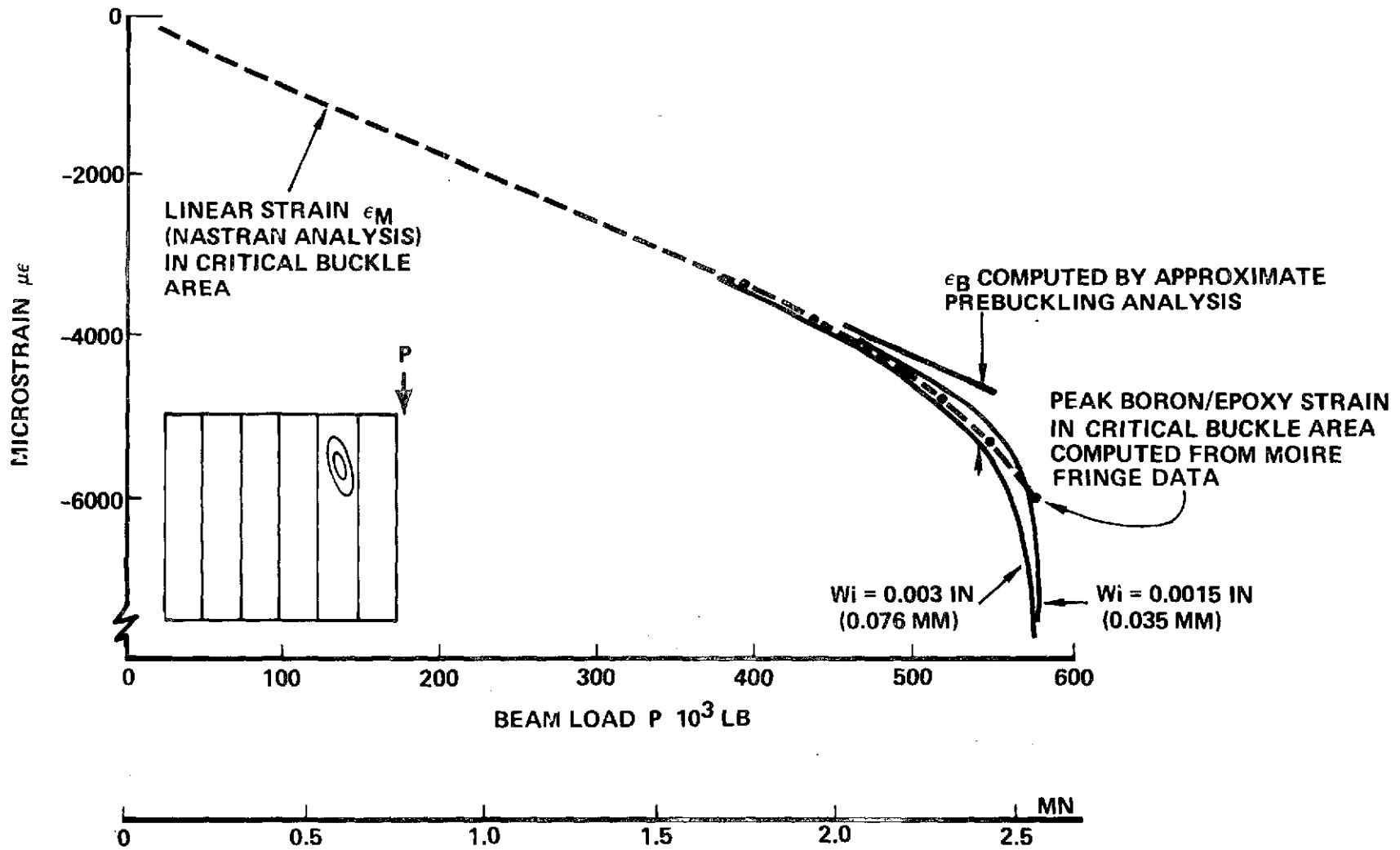
Figure 81: COMPUTED STRAINS IN TEST WEB 3 CRITICAL BUCKLE AREA

10.0 COMPUTER-AIDED DESIGN WEIGHT TRADES

10.1 MODIFIED SHEAR WEB OPTRAN CODE

The OPTRAN code for stiffened metal clad composite shear webs employed
in Phase I for concept screening [1, 16] was revised with the analysis
methods discussed in the preceding section. The revised code was then
used to study the behavior of the third test web and to establish final
weight trades for production hardware. Figure 82 summarizes the fea-
tures of the modified OPTRAN code. Details concerning the OPTRAN code
may be found in the Phase I Report and the analyses that specialize the
code for stiffened metal-clad composite webs are presented in Appendix
C. The OPTRAN code was selected for use in this program's computer-
aided design activities because of convenience; other multivariable
optimization codes in use by various organizations (such as AESOP [17]),
may also be adapted to perform the type of studies conducted in this
program.

The general shear web model that was treated by the computer-aided
design method, as followed in this program, is illustrated in Figures
83 to 85. The OPTRAN code is used to optimize the "long" web model for
minimum weight consistent with a prescribed set of material properties,
failure mode constraints and fabrication dimension limits. Longitu-
dinal stiffening (a single metal central stiffener) or all-metal
construction are design problem options. In the final form, the shear
web model has a maximum of 9 design variables that can be optimized.

117

o   OPTRAN CODE USED IN PHASE I REVISED TO TREAT PREBUCKLING

   -   APPROXIMATE PREBUCKLING BENDING STRAIN ANALYSIS
       FOR ASSUMED INITIAL IMPERFECTION AND BUCKLE MODE
       SHAPE

o   IMPROVED CODE MODULES

   -   MEMBRANE LOADS

   -   LOCAL PANEL BUCKLING UNDER BEAM BENDING LOADING

   -   GENERAL INSTABILITY UNDER SHEAR LOADING WITH ONE
       OR NO LONGITUDINAL STIFFENER.

o   9 DESIGN VARIABLES

o   FAILURE MODE CONSTRAINTS

   -   CLADDING YIELDING   ⎫
                              ⎬   CHECKED AT 2 LOCATIONS
   -   COMPOSITE STRAIN   ⎭

   -   STIFFENER FASTENER HOLE TEARING

   -   GENERAL INSTABILITY (COUPLED PLATE/STIFFENER BUCKLING)

Figure 82: MODIFIED OPTRAN CODE FEATURES

$V = H(N_{xy})$ INPUT SHEAR LOAD

S_s

REINFORCED STEP-LAP JOINT
AREA (REINF. NOT SIZED)

TRANSVERSE
STIFFENER

LONGITUDINAL
STIFFENER

H_e

$\mathsf{C_L}$ N.A.

NOMINAL
LAMINATE
H PANEL

H

$H/2$

$\pm 45°$ B/E

BAY

FLG.AREA
(NOT SIZED)
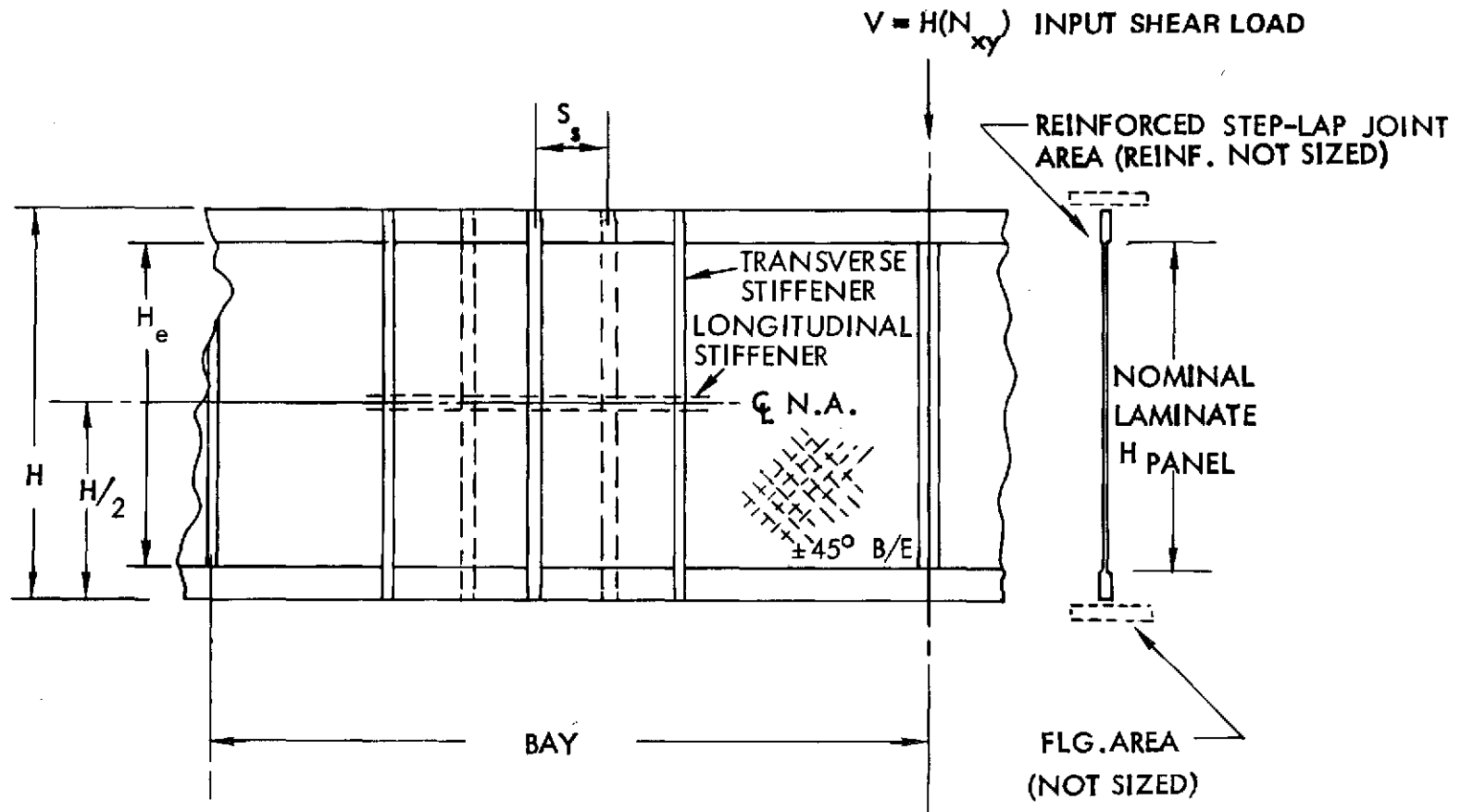
TOTAL NUMBER OF VARIABLES = 9 $(S_s,\ H_s,\ T_s,\ T_{sr},\ T_{cl},\ T_{clr},\ T_{cl},\ H_{ls},\ T_{ls})$

Figure 83: SHEAR WEB OPTRAN CODE MODEL

F = FIXED CONSTANT

W_s = 1.5 (38.1)F

UNIDIRECTIONAL B/E

T_{sf}

T_{sfcl} = 0.020 (F)

T_s

H_s

W_{sf} = 1.0 (25.4)F

T_s

T_{clr}

T_{cl}

T_{co}

N_{ps} PLYSETS

T_{co} = 0 FOR ALL METAL DESIGN CASE

SEC A-A

LAY-UP OF ONE PLY SET

T_{adh} = 0.009(0.2286)F
VENDOR STOCK THICKNESS

+45
−45
+45
−45
adh
−45
+45
−45
+45

$T_{B/E}$ = 0.0051(0.1295)F
VENDOR STOCK THICKNESS

UNITS
IN (mm)

120
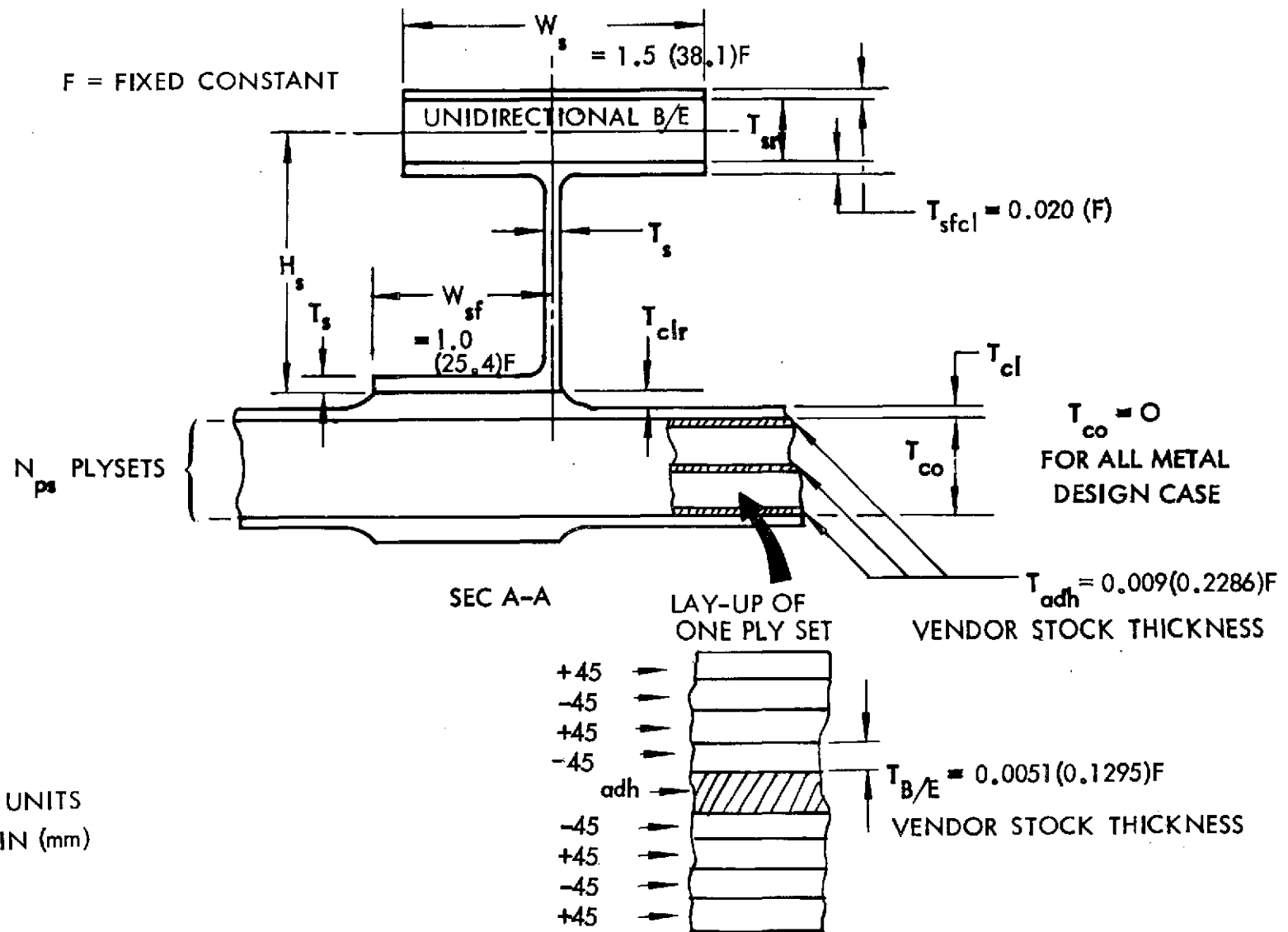
Figure 84: LAMINATE AND TRANSVERSE STIFFENER SECTION MODELS

$$W_{LS} = 1.25 \ (31.75) \ F$$

H_{LS}

T_{LS}
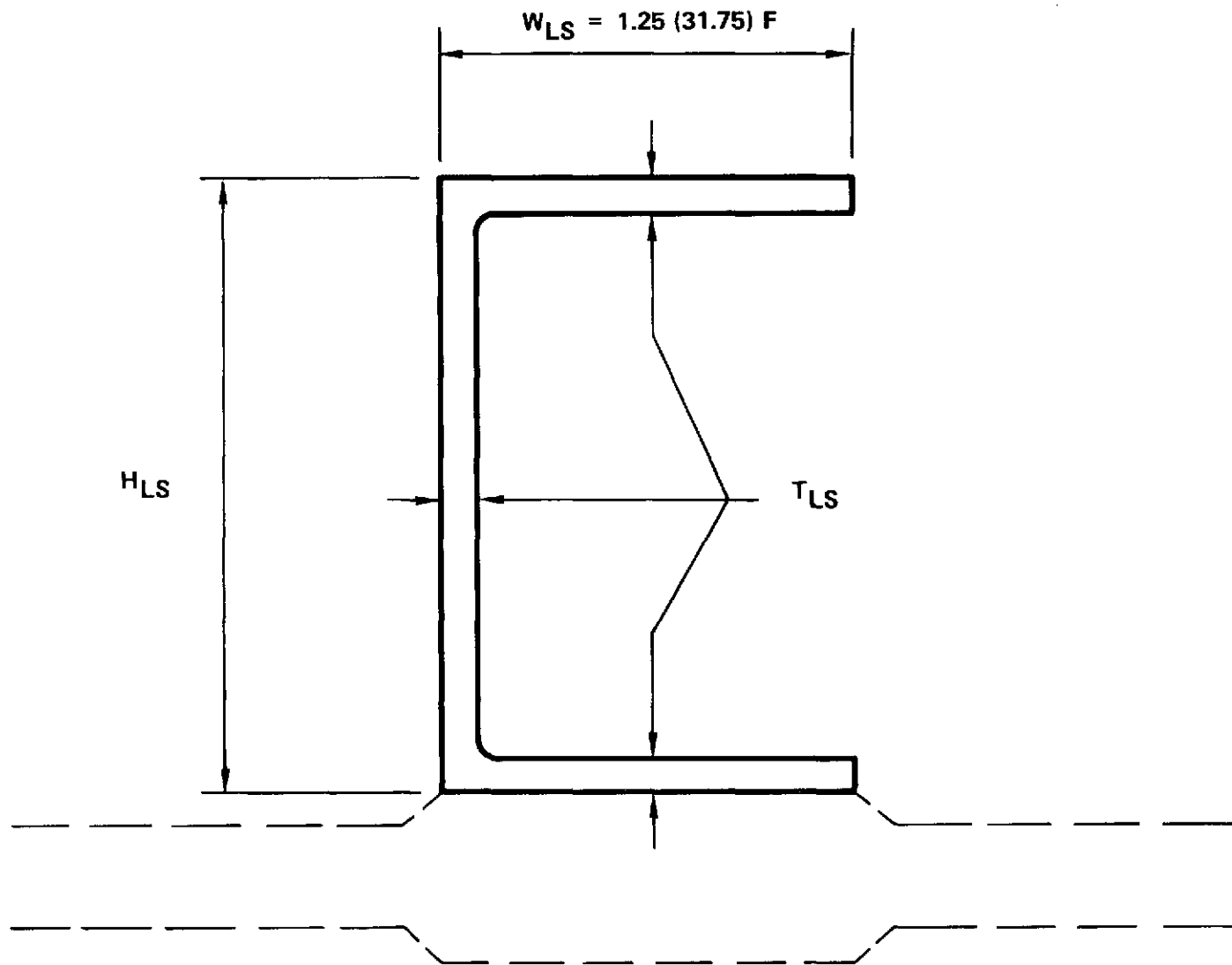
Figure 85: LONGITUDINAL STIFFENER SECTION MODEL

Only the nominal design section details that are shown are optimized and weights are computed assuming the web has a depth equal to the full depth H. Design details normally considered as weight penalties, such as edge joints, are not optimized.

The central location of the longitudinal stiffener is dictated by the dominance of shear buckling in the application that was studied. Other applications in which bending loads are dominant would benefit from a, say, 1/5 height location of the longitudinal stiffener (as is commonly done in bridge girder webs). An all-metal stiffener section was adopted for the longitudinal stiffener because composite reinforcement of the stiffener would not offer significant overall web weight savings. Aluminum was selected for the metal parts of the transverse stiffeners, as discussed in the Phase I Report, and the longitudinal stiffener because of light loads in these parts.

Another point concerning modeling philosophy is that the model shown here represents a compromise between manufacturing practicality, analysis capability, and minimum weight objectives. Weight savings by means of other detail options are certainly possible (for example: tapered cladding gage, alternate composite ply orientations, tapered stiffeners). However, the additional development efforts required by other options are not believed to be warranted in view of the high efficiency already offered by the model in the specific application studied in this program.

Figure 86 shows the "shear resistant" web loads that are input data to the OPTRAN code. The bending strain loads at the beam chords are corrected linearly to levels at the assumed edge of the nominal laminate panel and at interior panel points for use in structural analyses.

Figure 87 illustrates the assumed deflection mode shape that is used in the pre-buckling strain analysis. The pre-buckled strains are analysed at a location shown in Figure 88; this location was selected based on recognition of beam bending loads and their possible influence on shifting the panel buckle towards the compression chord (as occurred in the third web test, see Figure 34). In addition to the buckle peak area, strain analysis is conducted at the nominal laminate panel edge where the membrane strains are maximum. Out-of-plane web plate bending strains are assumed to be zero at the nominal panel edge.
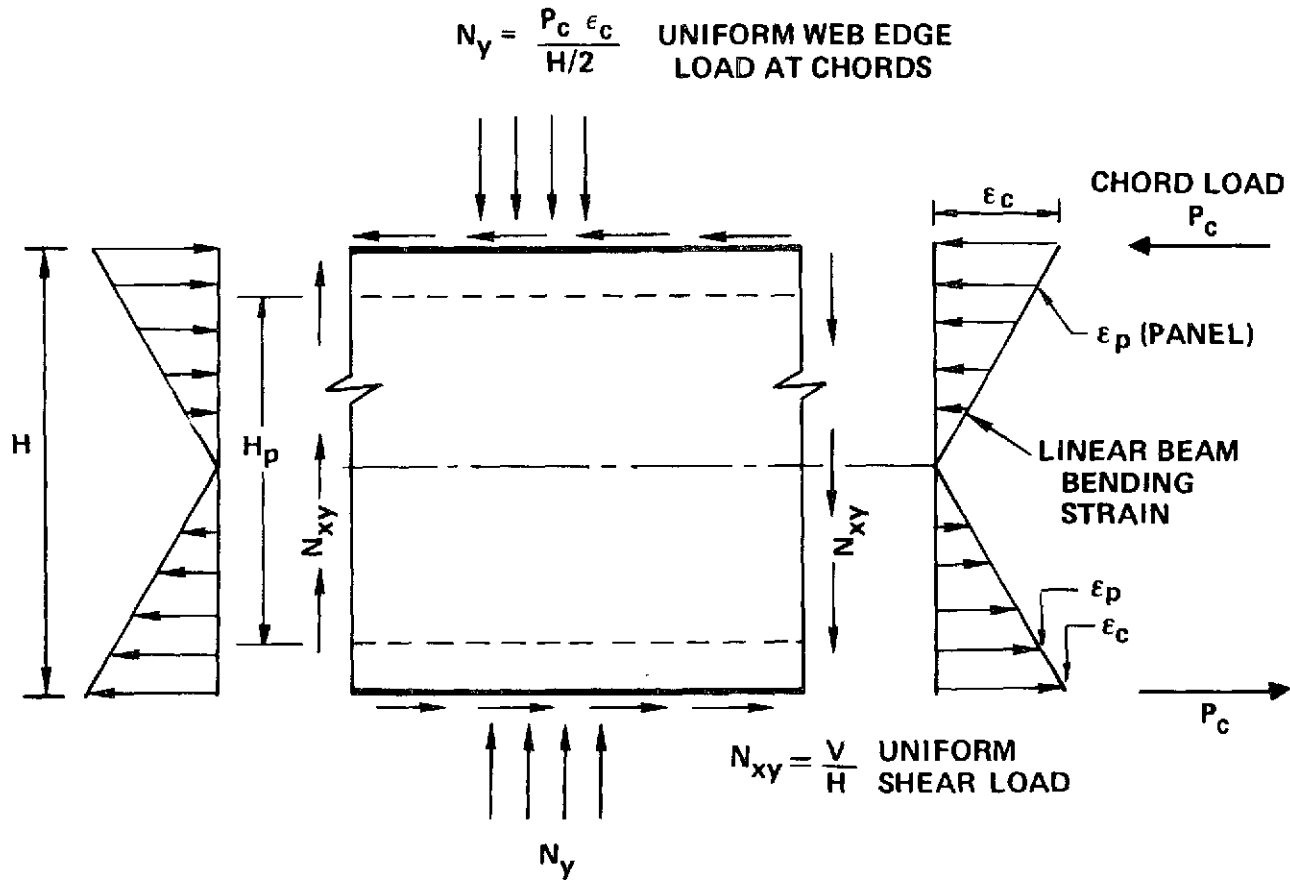
Figure 86: *SHEAR RESISTANT WEB LOADS*

INITIAL IMPERFECTION

$$W_{\cdot} = W_i \; SIN \; \frac{\pi Y}{L_Y} \; SIN \; \frac{\pi}{L_X} \; (x - \phi y)$$

$$\phi = TAN \; \theta$$

ASSUMED $\theta = 60^o$

$$L_Y = S_S$$

$$L_X = \frac{H_P}{2}$$
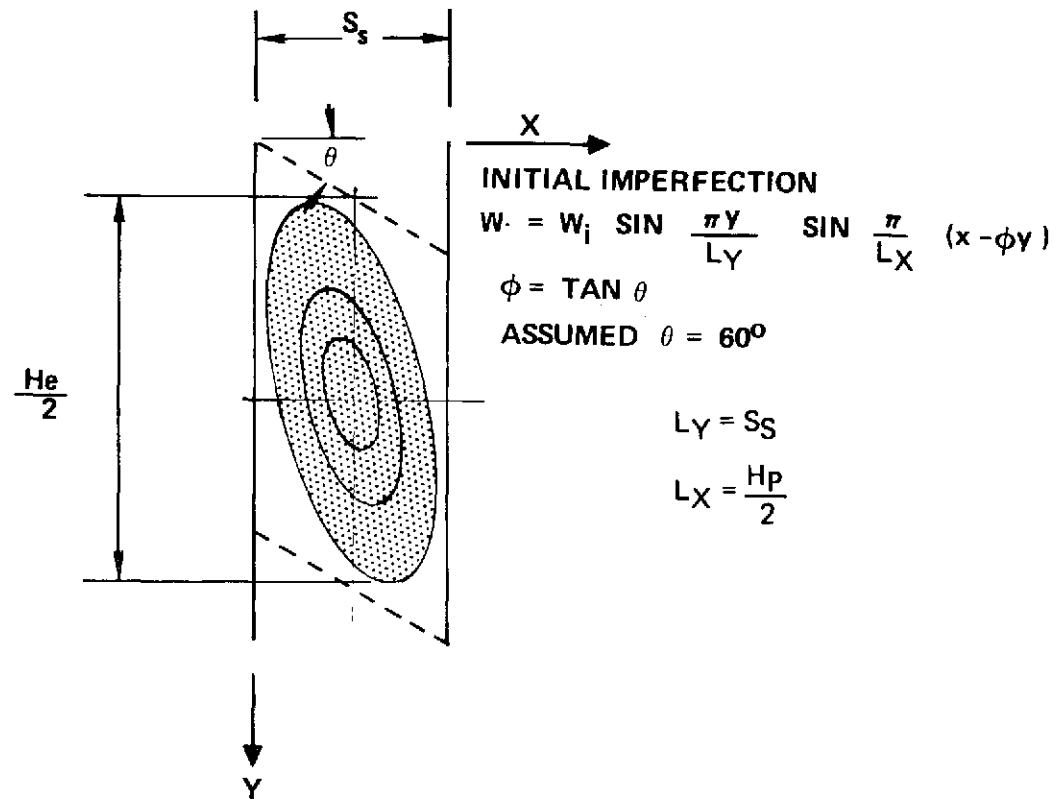
Figure 87: ASSUMED PRE-BUCKLED PANEL MODE SHAPE

EFFECTIVE SIMPLY SUPPORTED NOMINAL
LAMINATE PANEL

CHECK MEMBRANE
STRAINS

CHECK MEMBRANE
PLUS LOCAL PANEL
BENDING STRAINS

REINFORCED
WEB EDGES

TRANSVERSE STIFFENER SPACING
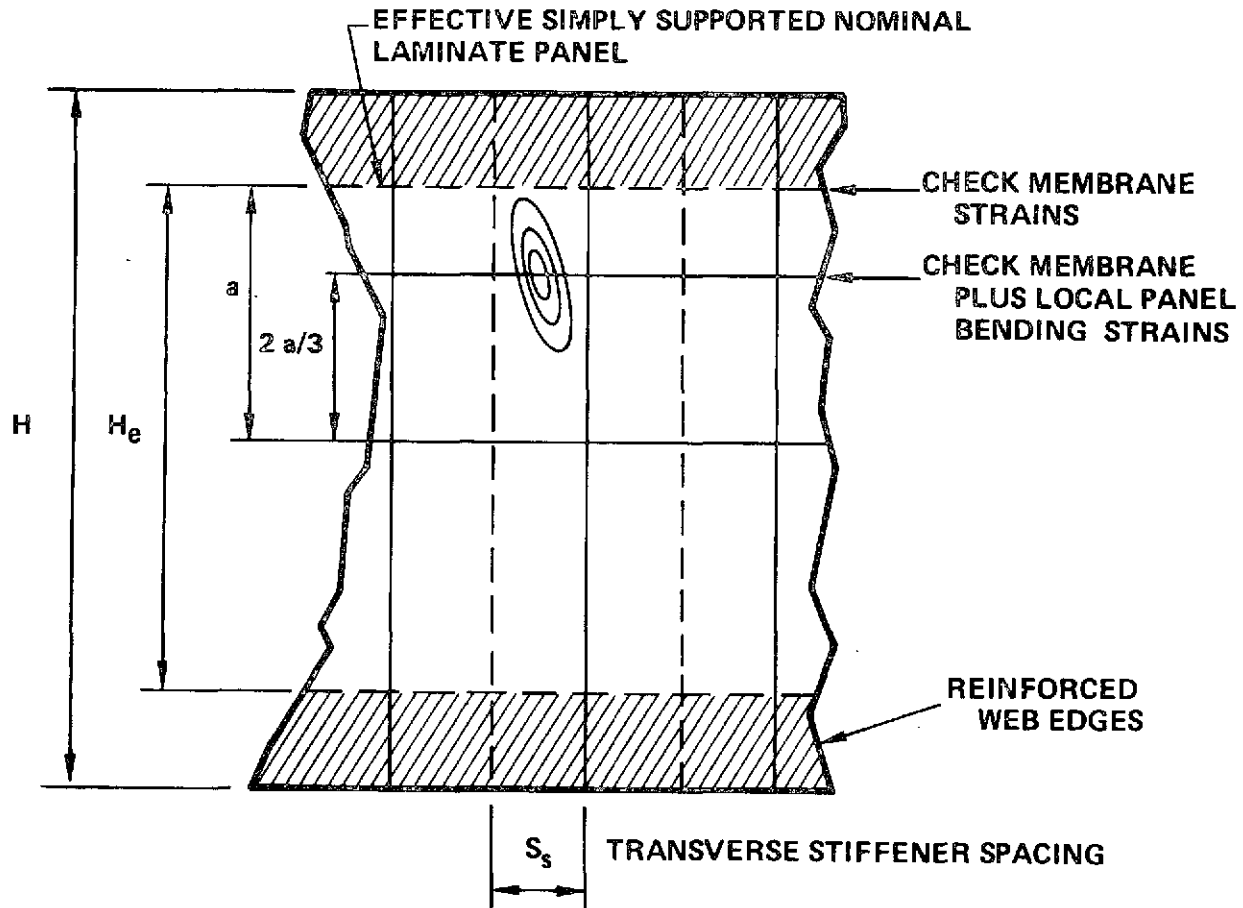
Figure 88: LAMINATE STRAIN ANALYSIS LOCATIONS

10.2 COMPUTED DESIGN/TEST WEB CORRELATIONS

Comparisons of the third test web with designs generated by the modified OPTRAN code appear in Figure 89. The computed optimum designs are constrained at various stiffener spacing values; the third test web spacing was 5 inches. Designs were generated with and without longitudinal stiffening; the option having longitudinal stiffening offers least weight. The longitudinal stiffener section was constrained to the actual test section and a 50% effective stiffness was assumed for this stiffener in the optimizations. The treatment of discrete ply set thickness (number of fabrication subassemblies are defined by the use of the integer variable NPS) produces the discontinuities in the optimum weight plots.

A number of combinations of effective web height (nominal laminate height) and initial imperfections were studied to arrive at the test/computed design correlation shown in Figure 89. The data from only one test makes a highly quantitative correlation difficult because of the number of structural parameters and complex response that are involved. However, the correlation that is shown appears reasonable based on the following considerations:

1. The effective web height of 26 inches (66.0 cm) that was used in the computations is close to the 29 inch effective web height correlation at 50% longitudinal stiffener effectiveness given in Figure 72.
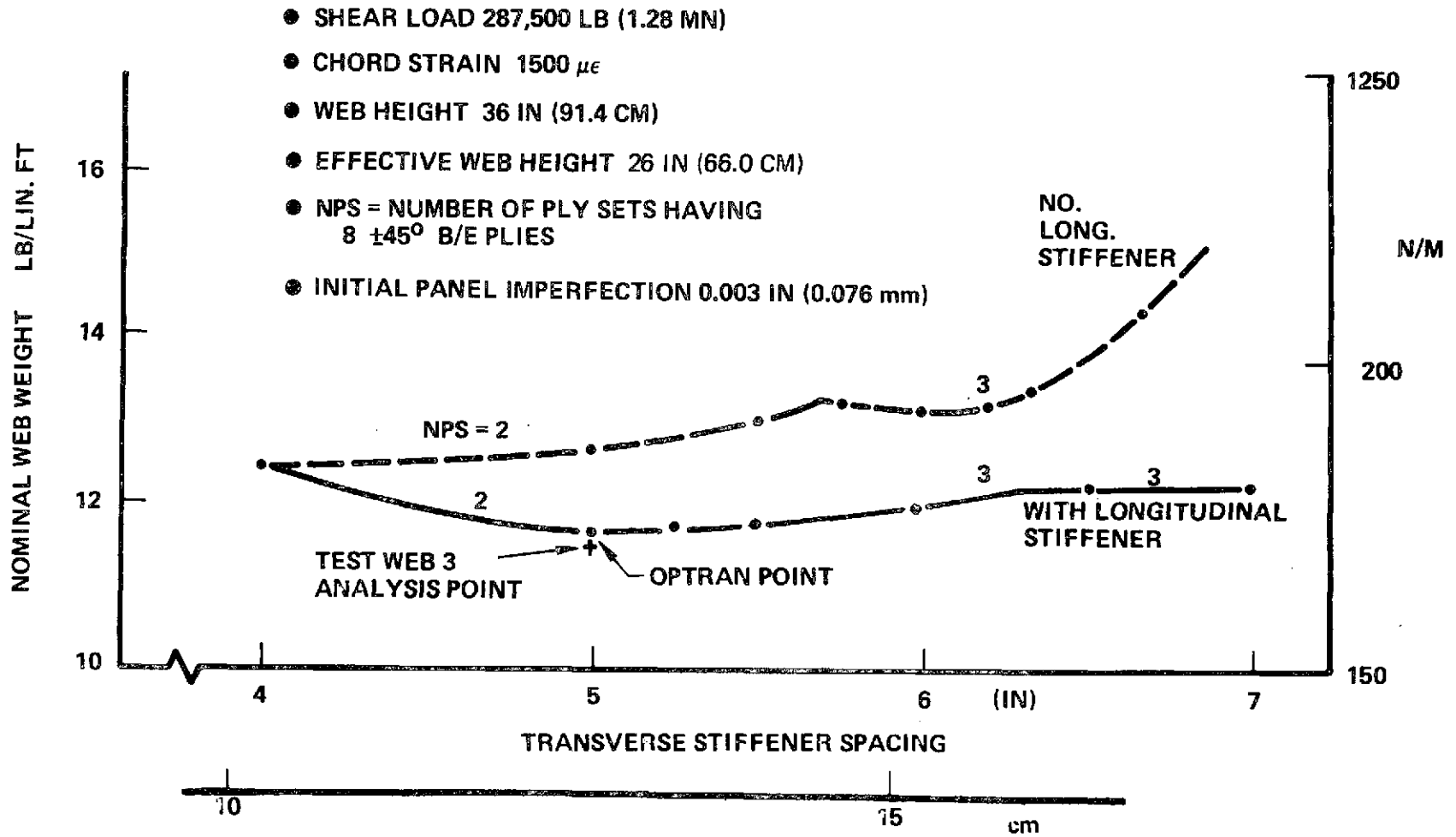
Figure 89: OPTRAN WEIGHT TRADES FOR TEST WEB 3 CONFIGURATION

2. The assumed initial imperfection magnitude of 0.003 in. (0.076 mm) is within the fringe order sensitivity for the Moire fringe pattern in the critical panel area at zero load shown in Figure 30. After web assembly, surveys made with a feeler gage and a straight edge in the critical area indicate that the deviation from flatness was on the order of the assumed imperfection level.

3. The computed optimum design weight is slightly greater than the actual weight of the nominal test web section. The weight increase is due to an increase in stiffener material which results in a computed design that is conservative.

The structural analysis data associated with the computed optimum design that correlates with the third test web is given in the following listing. The analyses coded in the OPTRAN code that produced the structural data are presented in Appendix C.

DESIGN CONDITIONS

Total web height H	36 in.	(91.4 cm)
Nominal Laminate panel height H_p	26 in.	(66.0 cm)
Ultimate shear load V	287500. lb.	(1.28 MN)
Chord Strain ε_C	1500 $\mu\varepsilon$	

Initial panel imperfection parameters

Magnitude	w_i=0.003 in.	(0.076 mm)
Mode skew angle parameter	θ=60°	
Mode wave length	L_y=13 in.	(33.0 cm)

MATERIALS

Web Laminate:

6AL-4V mill annealed titanium cladding

B/E composite in $\pm 45°$ ply sets of 8 plies each

METLBOND 329 adhesive plies

Transverse Stiffeners:

7075-T6 aluminum J-section

B/E undirectional reinforcement

Longitudinal Stiffener:

7075-T6 aluminum channel section

OPTIMUM WEIGHTS	LB/ Lineal Ft. of Beam	N/M
Web Laminate:		
B/E	2.56	(37.4)
Nominal Cladding	2.63	(38.4)
Cladding Reinforcement		
at stiffeners	0.94	(13.7)
Adhesive plies	1.23	(18.0)
Transverse Stiffeners:		
Aluminum section	3.48	(50.8)
B/E reinforcement	0.19	(2.77)
Longitudinal Stiffeners	0.61	(8.9)
Total Weight	11.64	(169.9)

MARGINS OF SAFETY

Buckled nominal laminate panel area:

Cladding yielding	0.08
Composite strain	0.00

Unbuckled nominal laminate
panel edge area:

Cladding yielding	0.26
Composite strain	0.24
General web instability	0.08

Web tearing at stiffener
fastener holes   0.21

OPTIMUM VARIABLE VALUES

Web laminate:

Number of ply sets NPS	2		
Cladding Thickness T_{CL}	0.019 in.	(0.48 mm)
Cladding Reinforcement T_{CLR}	0.030 in.	(0.76 mm)

Transverse Stiffener

Spacing S_S	5.0 in.	(12.7 cm)
Height H_S	1.74 in.	(4.42 cm)
Gage T_S	0.25 in.	(3.18 mm)
B/E thickness T_{SR}	0.021 in.	(0.53 mm)

Longitudinal Stiffener

Height H_{LS}	1.75 in.	(4.45 cm)
Gage T_{LS}	0.125 in.	(3.18 mm)

ANALYSIS DATA

Nominal laminate stiffeners:

Membrane $A_{ij} = 10^6 \begin{bmatrix} 1.42 & 0.77 & 0 \\ 0.77 & 1.42 & 0 \\ 0 & 0 & 0.87 \end{bmatrix}$ lb/in

$= 10^8 \begin{bmatrix} 2.49 & 1.35 & 0 \\ 1.35 & 2.49 & 0 \\ 0 & 0 & 1.52 \end{bmatrix}$ N/M

Bending $D_{ij} = \begin{bmatrix} 4414 & 1711 & 0 \\ 1711 & 4414 & 0 \\ 0 & 0 & 1968 \end{bmatrix}$ lb/in

$= \begin{bmatrix} 498.9 & 193.3 & 0 \\ 193.3 & 498.9 & 0 \\ 0 & 0 & 222.3 \end{bmatrix}$ N/M

Transverse Stiffener

$EI_T = 2.53E6 \quad lb/in^2$ (7261 NM^2)

$EA_T = 5.04E6 \quad lb/in$ (14464 NM^2)

Longitudinal Stiffener

100% $EI_L = 2.41E6 \quad lb/in^2$ (6926 NM^2)

Total nominal laminate thickness 0.165 in. (4.19mm)

Total nominal cladding thickness 0.038 in. (0.97mm)

Total adhesive thickness 0.045 in. (1.14mm)

Total B/E thickness 0.0816 in. (2.07mm)

Net percentage of B/E in nominal laminate

$$\xi = 76.9\%$$

Net percentage of B/E in reinforced laminate
at stiffener fasteners

$$\xi_R = 45.6\%$$

Buckled panel curvatures:

$$\kappa_x = 0.00457$$

$$\kappa_y = 0.0446$$

$$\kappa_{xy} = 0$$

Coordinates from neutral laminate surface:

Cladding

$$Z_{CL} = 0.0823 \text{ in.} \qquad (2.09\text{mm})$$

Extreme B/E ply

$$Z_{BE} = 0.0543 \text{ in.} \qquad (1.38\text{mm})$$

Transformed strains in extreme B/E ply in critical buckled panel area

membrane $\qquad \bar{\varepsilon}_{BP}^{M} = \begin{bmatrix} -4658 \\ 4501 \\ 292 \end{bmatrix} \quad \mu\varepsilon$

due to bending $\qquad \bar{\varepsilon}_{BP}^{B} = \begin{bmatrix} -1335 \\ -1335 \\ 1087 \end{bmatrix} \quad \mu\varepsilon$

combined $\qquad \bar{\varepsilon}_{BP}^{T} = \begin{bmatrix} -5992 \\ 3166 \\ 1378 \end{bmatrix} \quad \mu\varepsilon$

Maximum composite strains

Buckled panel	-5992	$\mu\varepsilon$
Panel edge	-4822	$\mu\varepsilon$

von Mises effective cladding stresses

Buckled panel	116990.	lb/in^2	(806.6 N/M^2)
Panel edge	100200.	lb/in^2	(690.9 N/M^2)

Shear buckling analysis parameters

$\alpha = 5.20$

$A = 1.11$ $\quad\quad\quad\quad$ $B = 802.8$ $\quad\quad\quad\quad$ $m = 0.33$

$\gamma_{T_o} = 737$

$\gamma_T = 114.5$ $\quad\quad\quad\quad$ $\gamma_L = 12.3$ $\quad\quad\quad\quad$ $K_{ST} = 84.7$

$\eta = 1.56$ $\quad\quad\quad\quad$ $\eta_{max} = 1.69$ $\quad\quad\quad\quad$ $K_{SLT} = 132$

Critical shear buckling load

$N_{xycr} = 8540$ $\quad$ lb/in $\quad\quad\quad$ (1.50 MN/M)

Critical bending buckling load
(maximum panel load at nominal panel edge)

$N_{pxcr} = -4580$ $\quad$ lb/in $\quad\quad\quad$ (0.80 MN/M)

Panel Shear load

$N_{xy} = 7972$ $\quad$ lb/in $\quad\quad\quad$ (1.40 MN/M)

Panel Bending load (maximum)

$N_{px} = 1082$ $\quad$ lb/in $\quad\quad\quad$ (1.89 MN/M)

General Instability Interaction

$$R_S = \frac{N_{xy}}{N_{xycr}} = 0.934$$

$$R_B = \frac{N_{px}}{N_{xpcr}} = 0.236$$

$$R_S{}^2 + R_B{}^2 = 0.9275 < 1.0$$

Composite strain in reinforced laminate near stiffener fastener holes

$$\bar{\varepsilon}_R = 3220$$

10.3 SHEAR WEB WEIGHT TRADES

After establishing the test/analysis correlation, weight trades were conducted with the OPTRAN code for conditions more representative of production hardware; these conditions are shown in Figure 90. The essential differences between this study and the test/computed design correlation study discussed in Section 10.1 is that (1) a higher chord strain level was assumed, and (2) the longitudinal stiffener section was allowed to vary. In addition, the options of all-aluminum transverse stiffening, all-metal web construction and other design perbutations were included as optimization cases. In all weight trade cases studied, an aluminum longitudinal stiffener was specified and an effective web height of 26 in. (66.0 cm) was assumed.

Figure 90 shows the computed results that compare composite reinforced and all-metal construction. At the same level of initial imperfection, the composite-reinforced shear web concept, which is similar to the third test web design configuration, offers about 31% savings in nominal web weight at the test shear load level. The composite design cases that the plotted curve represents were all governed by the (1) failure mode of composite fracture in the pre-buckled panel areas and (2) minimum titanium cladding gage of 0.019 in (0.483 mm). The all-metal webs were governed by yielding in the pre-buckled panel areas as defined by the von Mises effective stress equalling the 0.2% offset yield stress for the titanium web plate (defined in the Structural Analysis Equations Appendix C).

INITIAL PANEL IMPERFECTION 0.003 IN (0.076 mm)
CHORD STRAIN 4000 $\mu\epsilon$

HEIGHT 36 IN (91.4 CM)
EFFECTIVE HEIGHT 26 IN (66.0 CM)
SINGLE ALUMINUM LONGITUDINAL STIFFENER
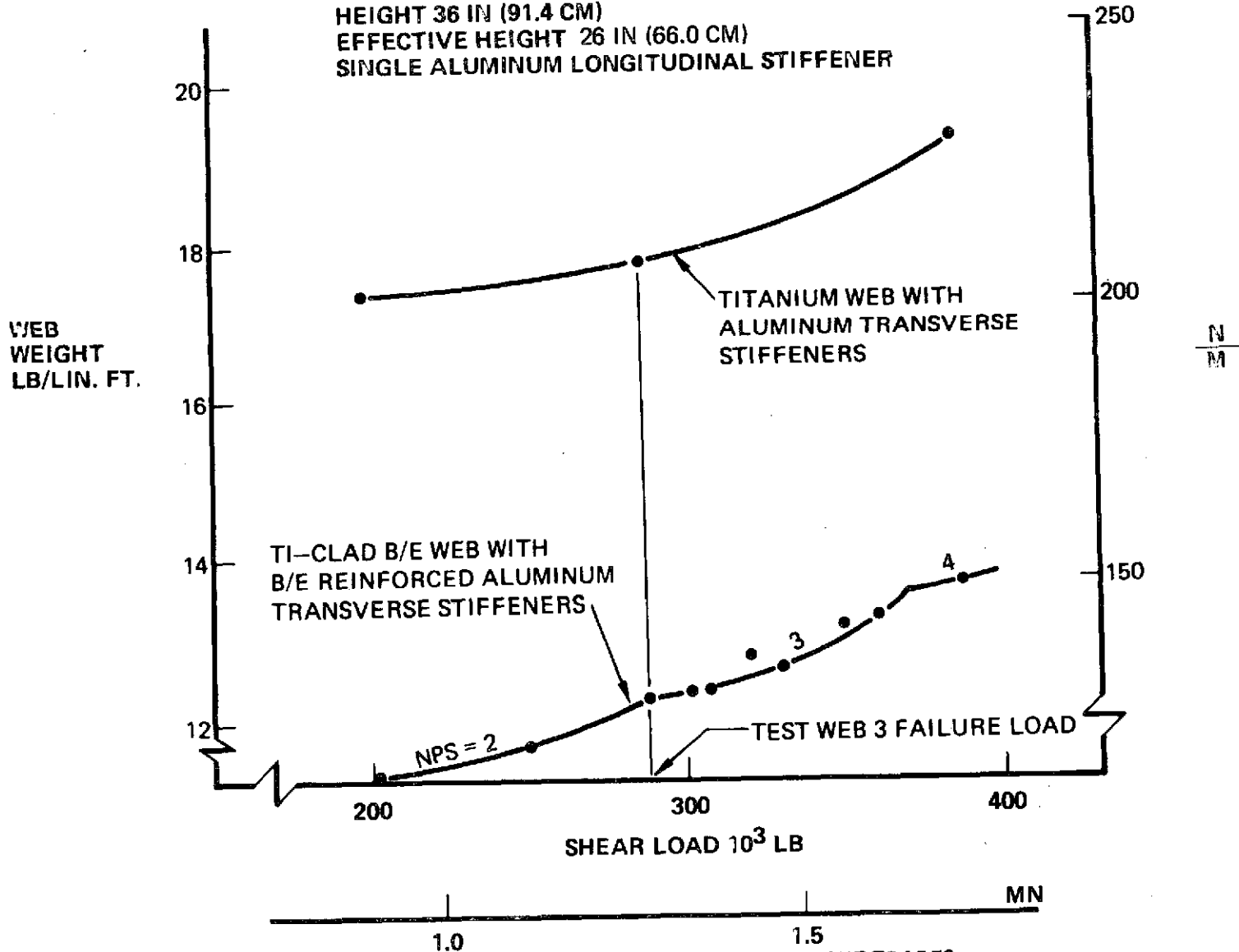
Figure 90: SHEAR RESISTANT WEB OPTRAN WEIGHT TRADES

Figure 91 presents weight trades for composite-reinforced design options
having (1) very small minimum cladding thickness constraint, (2) dif-
ferent initial imperfection levels, (3) different chord strains, and
(4) all-aluminum stiffeners. The design conditions were similar to those
in the test/computed design correlation study except for the parameters
shown and that all web variables were allowed to be optimized. For the
case with relaxed constraint on minimum cladding gage (Case 2), the
decrease in nominal weight from the baseline case (Case 1) is 0.9% which
is small. For the perturbations studied of this type, in no case did
the cladding gages tend to optimize at "zero" thickness. In addition
to having a fabricable cladding gage on the order of 0.020 in (0.508 mm),
the baseline case requires 33% less B/E in the web laminate than design
cases which allow thinner cladding gages. This large difference in B/E
requirement is partly due to the use of the discrete ply-set variable
NPS in defining the OPTRAN web laminate model; NPS changes from 2 to 3
in going from Case 1 to Case 2.

As indicated in Figure 91, an order of magnitude change in the initial
imperfection level produces a significant change in nominal web weight.
The design case (Case 3) having an initial imperfection of 0.030 in
(0.762 mm) has 8.8% greater weight than the baseline case. The sensi-
tivity to initial imperfection was found to be greater in other design
cases having higher beam chord strain levels.

The use of all-aluminum stiffeners does not significantly alter web
weight. As shown in Figure 91, the all-aluminum stiffener design case

DESIGN CASE PERBUTATION	WT LB/FT (N/M)	% CHANGE	VALUES OF SELECTED OPTIMUM DIMENSIONS
(1) BASELINE CASE: 　　Ti-CLAD B/E WEB LAMINATE 　　MIN T_{CL} = 0.019 IN (0.482 mm) 　　w_i = 0.003 IN (0.076 mm) 　　ϵ_c = 1500 $\mu\epsilon$ 　　B/E REINF. ALUM. 　　　TRANSVERSE STIFFENER 　　ALUM. LONGO. STIFFENER	11.4 (166)	—	NPS = 2 T_{CL} = 0.019 IN (0.482 mm) S_S = 5.36 IN (13.6 cm)
(2) MIN. T_{CL} = 0.0001 IN (0.0025 mm)	11.3 (164)	-0.9%	NPS = 3 T_{CL} = 0.003 IN (0.576 mm) S_S = 5.01 IN (12.7 cm)
(3) w_i = 0.03 IN (0.76 mm)	12.4 (180)	+8.8%	T_{CL} = 0.025 IN (0.635 mm) S_S = 5.29 IN (13.4 cm)
(4) w_i = 0.06 IN (1.52 mm)	12.7 (185)	+11.4%	NPS = 3 S_S = 6.8 IN (17.3 cm)
(5) ϵ_i = 4000 $\mu\epsilon$	12.2 (178)	+7.0%	NPS = 2 S_S = 4.61 IN (11.8 cm)
(6) ALL ALUM. STIFFENERS	11.9 (173)	+4.4%	NPS = 2 T_{CL} = 0.023 IN (0.584 mm) S_S = 5.39 IN (13.7 cm)

Figure 91: SHEAR RESISTANT WEB OPTRAN PARAMETER TRADES

138

(Case 6) has 4.4% greater nominal weight than the baseline case having B/E reinforced transverse stiffeners. In comparison with an all-metal shear web case, the composite web having all-aluminum transverse stiffeners offers 28% nominal weight saving whereas the case having B/E reinforced transverse stiffeners gives 31% weight saving. The reasons for the low sensitivity of design weight to B/E stiffener reinforcement are (1) the lack of extensional coupling between the stiffener and the web plate that is assumed in the analysis, and (2) the relatively low combined stiffener weight. The effectiveness of composite stiffener reinforcement could be enhanced by (1) providing additional composite reinforcement in the attachment leg area, (2) altering the stiffener section configuration, and/or (3) increasing the stiffener/web interaction by using interference fit fasteners.

11.0 EVALUATION CONCLUSIONS

As summarized in Figure 92, the general evaluation conclusions of the titanium-clad B/E reinforced shear web design concept are that it is practical and efficient for the specific application that was studied. The metal-clad web laminate is an interesting concept because of the protection offered by the cladding to the polymeric laminate parts and the low-cost tooling and inspection operations needed in its fabrication. The element test results of Phase I and the web component tests indicate that the concept will be reliable in service with respect to low-cycle fatigue and flaw growth resistance. However, the concept has low post-buckling strength and therefore, its use in production hardware will require that special analytical and element test techniques be employed to accurately predict design strength. Specifically, improved pre-buckling analysis methods and design aids must be developed before the concept can be routinely applied in structural designs.

The theoretical nominal weight savings of the baseline composite-reinforced design (test web 3 concept) is about 31% relative to all-metal titanium/aluminum construction, as determined by an optimization method in which the different design concepts were treated in a uniform analytical manner. Based on analysis of detailed design drawings in Phase I, this weight saving is reduced by penalties for edge joints, etc., to 24%. The weight saving could be improved somewhat by development of alternate stiffener fastening methods, alternate stiffener configurations, and tapered laminate concepts, although the

TI-CLAD BORON/EPOXY SHEAR WEB CONCEPT IS:

o PRACTICAL

WEB LAMINATE IS EASY TO FABRICATE
LOW-COST TOOLING
INSPECTABLE
METAL-CLADDING PROTECTS COMPOSITE PARTS IN FABRICATION AND SERVICE

o RELIABLE IN ORBITER DESIGN ENVIRONMENT

FATIGUE RESISTANT
NOT FLAW-GROWTH CRITICAL
ELEMENT TEST PROGRAM EFFECTIVE IN ESTABLISHING DESIGN CONFIDENCE

o EFFICIENT

31% NOMINAL WEIGHT SAVINGS RELATIVE TO A SHEAR RESISTANT ALL-METAL
WEB FOR THE TEST WEB AND CONFIGURATION DESIGN CASE

24% WEIGHT SAVING FOR DETAILED DESIGNS

STRUCTURAL EFFICIENCY OF COMPOSITE REINFORCED WEB LAMINATE DEPENDENT ON
PREBUCKLING DEFORMATION

o CONSIDERABLE ANALYTICAL EFFORT REQUIRED

o PREBUCKLING ANALYSIS METHODS NEED TO BE DEVELOPED AND/OR EVALUATED

COMPOSITE REINFORCED STIFFENER DESIGN OPTIONS NEED FURTHER EVALUATION
IN A PRODUCTION PROGRAM

o RESIDUAL CURVATURE PRESENT ASSEMBLY PROBLEMS

o OPTIMUM REINFORCED CONFIGURATION IS A FUNCTION OF ATTACHMENT METHOD

o FIRST GENERATION HARDWARE WOULD BE COST/EFFECTIVE WITH ALL-ALUMINUM
SECTIONS IN MANY CASES

28 % NOMINAL WEIGHT SAVINGS FOR THE TEST WEB -3 CONFIGURATION
DESIGN CASE

Figure 92: EVALUATION CONCLUSIONS

cost-effectiveness of these approaches is doubtful. The use of all-aluminum stiffening in lieu of B/E reinforced transverse stiffening is attractive for near-term production hardware because of anticipated reduction in fabrication problems and costs at the expense of a small reduction in weight savings (the 31% weight saving indicated for the web with B/E reinforced stiffeners reduced to 28% with all-aluminum stiffeners).

12.0 REFERENCES

1. "Evaluation of a Metal Shear Web Selectively Reinforced With
    Filamentary Composites for Space Shuttle Application--Phase I
    Report". J. H. Laakso and D. K. Zimmerman, Prepared under NASA/LRC
    Contract NASI-10860, Boeing Aerospace Company Document D180-15104,
    September 1972.

2. "Evaluation of a Metal Shear Web Selectively Reinforced With
    Filamentary Composite for Space Shuttle Application--Phase II
    Report", J. H. Laakso and D. K. Zimmerman, Prepared under NASA/LRC
    Contract NASI-10860, Boeing Aerospace Company Document D180-15323,
    February 1973.

3. B.C. Dykes, "Analysis of Displacements in Large Plates by the
    Grid-Shadow Moire Technique", Paper 14, Proceedings of the Fourth
    International Conference on Experimental Stress Analysis, Cambridge,
    England, 1970.

4. M. D. Musgrove and B. E. Greene, "Advanced Beaded and Tubular
    Structural Panels", Paper 73-370, AIAA/ASME/SAE 14th Structures,
    Structural Dynamics, and Materials Conference, Williamsburg,
    Virginia, March 20-22, 1973.

5. H. K. Shen and J. L. Rutherford, "Time Dependent Properties of
    Adhesives--Final Report", Prepared under Naval Air Development
    Center Contract N00156-70-C-1246, Singer Aerospace and Marine
    Systems Report KD-71-23, November 1971.

6. NASA SP-222, "NASTRAN User's Manual", September 1970.

7. Ya. I. Sekerzh - Zen'kovich, "Calculating the Stability of Plywood Sheets as an Anisotropic Plate", Trudy TsAGI, No. 76, 1931 (in Russian).

8. NASA CR-224, "Strength Characteristics of Composites", S. W. Tsai, April 1965.

9. FAA Report FAA-SS-72-11, "SST Technology Follow-on Program - Phase I--Intermediate Shear Beam Analysis", V. M. Barevics, J. D. Hoy and R. E. Sheerer, Prepared under Contract to the Federal Aviation Administration Supersonic Transport Office, The Boeing Company, Commercial Airplane Group, Document D6-60211, May 1972.

10. Boeing Document AS-2794, "Analysis and Computer Programs for Intermediate Shear Webs (Tension Field) and Shear Resistant Webs", R. E. Sheerer, R. M. Mello and B. T. Lindquist, 1971.

11. NACA TN 1851, "Critical Shear Stress of Infinitely Long, Simply Supported Plate With Transverse Stiffeners", M. Stein and R. W. Fralich, April 1949.

12. K. C. Rockey and I. T. Cook, "Shear Buckling of Orthogonally Stiffened, Infinitely Long Simply Supported Plates--Stiffeners Having Torsional and Flexural Rigidities", The Aeronautical Quarterly, February 1969, pp. 75-87.

13. S. P. Timoshenko and J. M. Gere, *Theory of Elastic Stability*, Second
     Edition McGraw-Hill, 1961.

14. B. O. Almroth, et al, "User's Manual for the STAGS Computer Code",
     Lockheed Missiles and Space Compant Report LMSC D266611 (STAGS A),
     October 1972.

15. F. Bleich, *Buckling Strength of Metal Structures*, McGraw-Hill,
     1952.

16. J. H. Laakso, "Design Synthesis of a Boron/Epoxy Reinforced Metal
     Shear Web", Paper 72-395, AIAA/ASME/SAE 13th Structures, Structural
     Dynamics and Materials Conference, San Antonio, Texas, April 10-12,
     1972.

17. NASA CR-73200, "An Introduction to Multivariable Search Techniques
     for Parameter Optimization (and Program AESOP)", D. S. Hague and
     C. R. Glatt, The Boeing Company, April 1968.

18. W. Prager and P. G. Hodge, *Theory of Perfectly Plastic Solids*,
     John Wiley, 1951.

19. *Boeing Design Manual*, Section 318.5, "Shear Buckling Resistant
     Beams", (unreleased), The Boeing Company.

APPENDICES

APPENDIX A   STRAIN GAGE DATA

APPENDIX B   MOIRE FRINGE PATTERN DATA

APPENDIX C   STRUCTURAL ANALYSIS EQUATIONS

APPENDIX D   TEST WEB 3 DETAIL DESIGN DRAWINGS

APPENDIX A   STRAIN GAGE DATA

Presented in this appendix are the strain gage data that were acquired

in the final loadings of the web component tests. The data for each web

is preceded with a schematic showing the gage locations. Data given

for the rosette gages were processed into principal strain form. Cer-

tain low level strain data contains discontinuities because of recording

interruptions, data system noise, and/or time dependent structural

response.
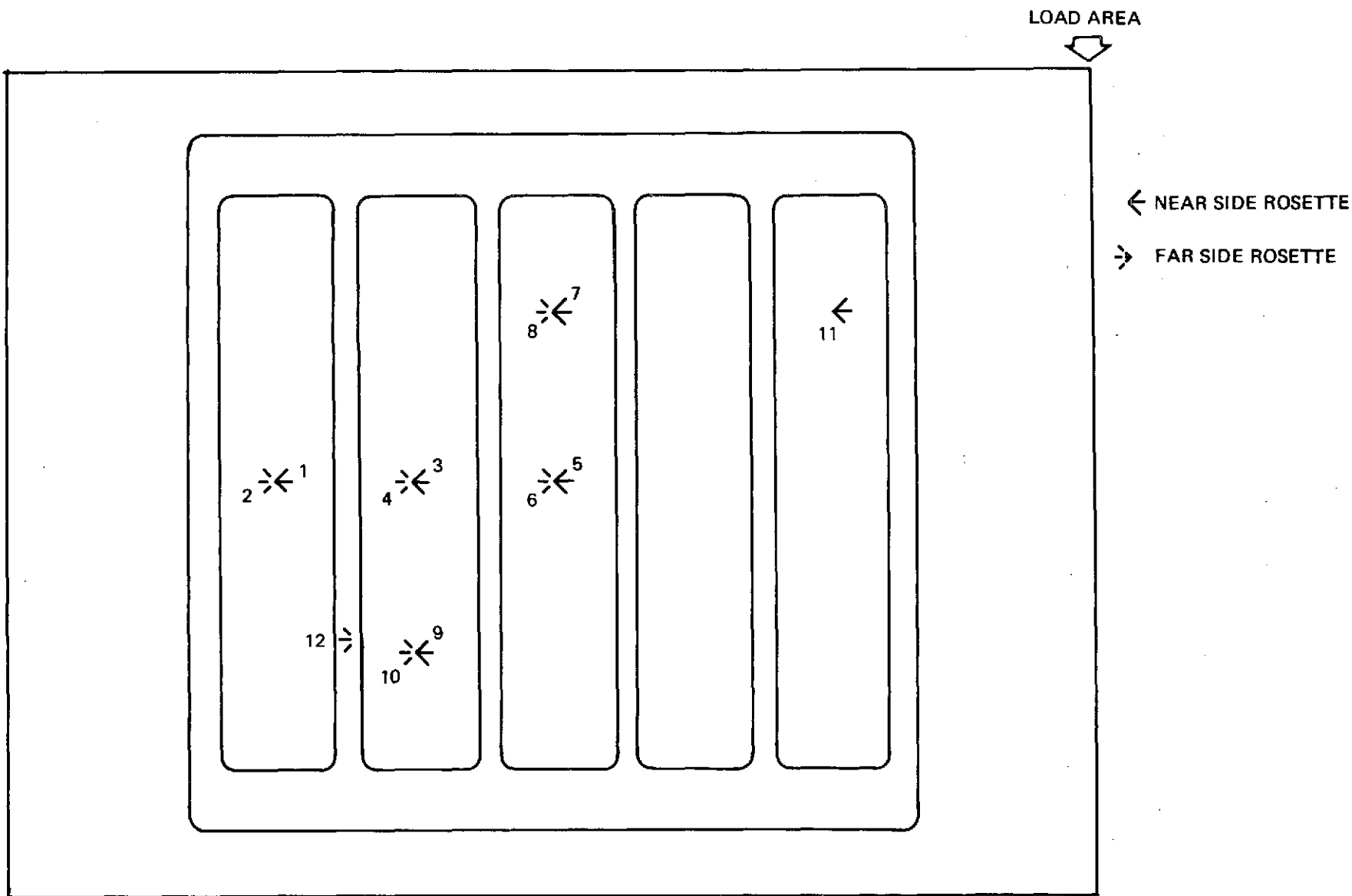
Figure A-1 : TEST WEB 1 STRAIN GAGE LOCATIONS
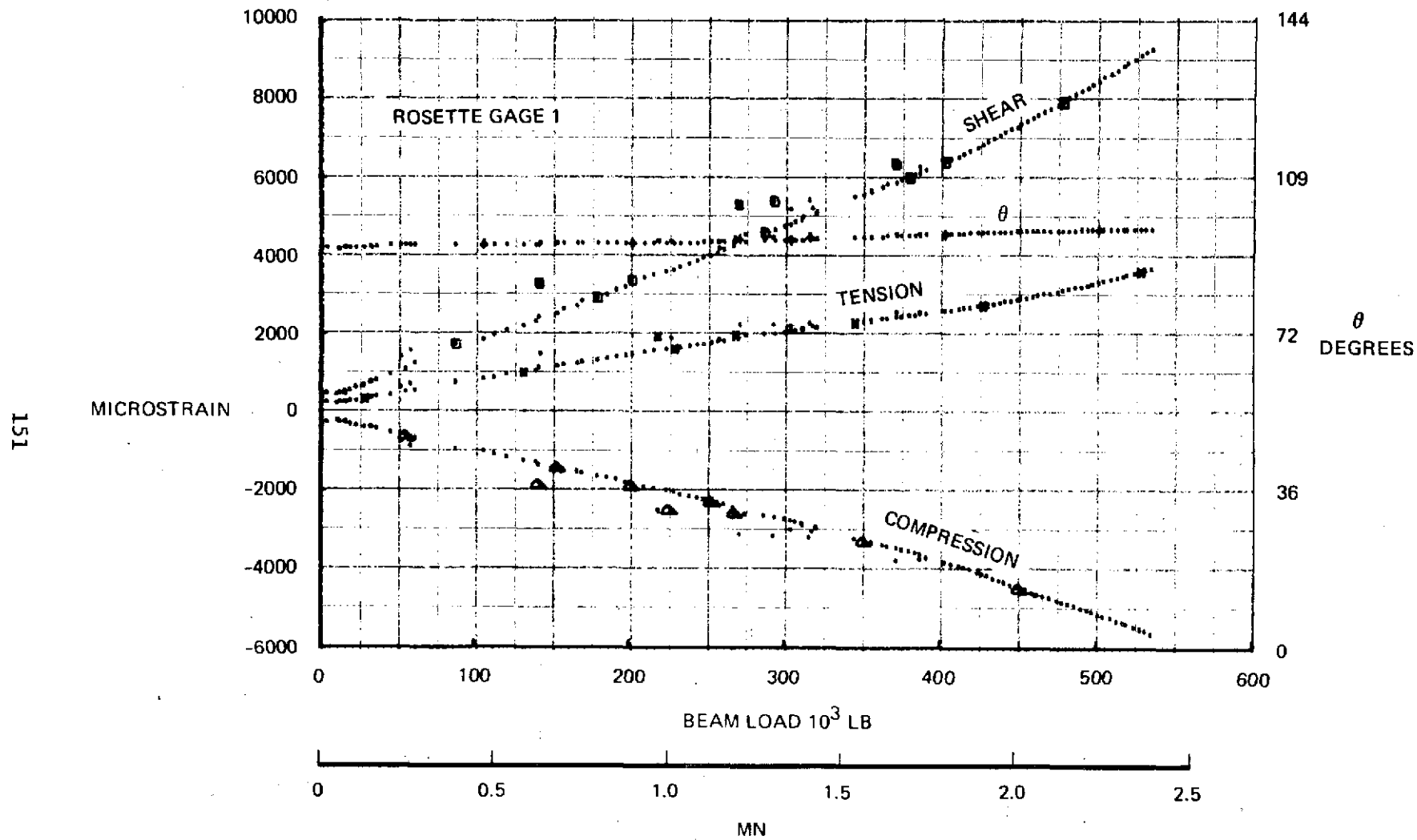
Figure A-2 : TEST WEB 1 PRINCIPAL STRAIN DATA
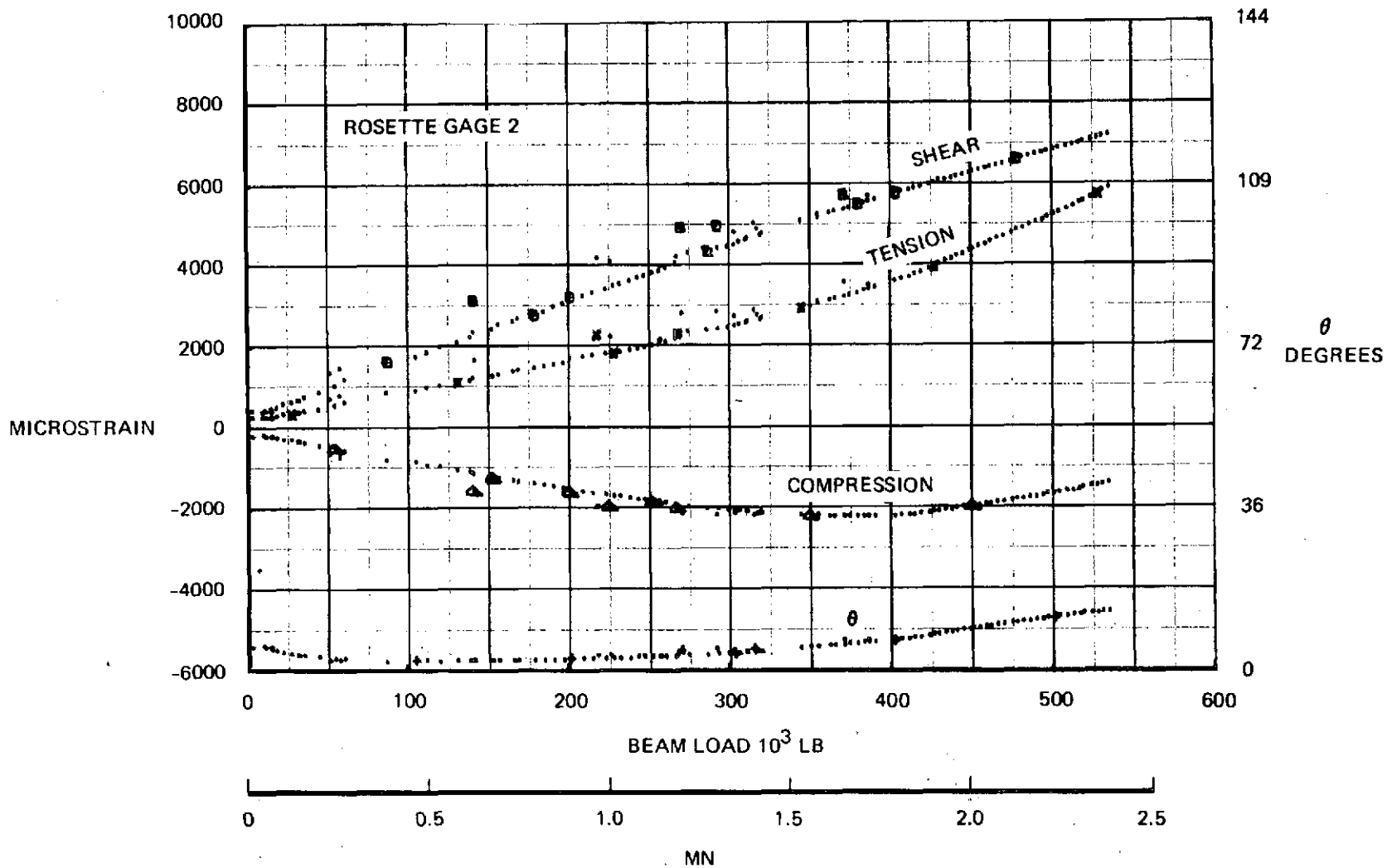
Figure A-3: TEST WEB 1 PRINCIPAL STRAIN DATA
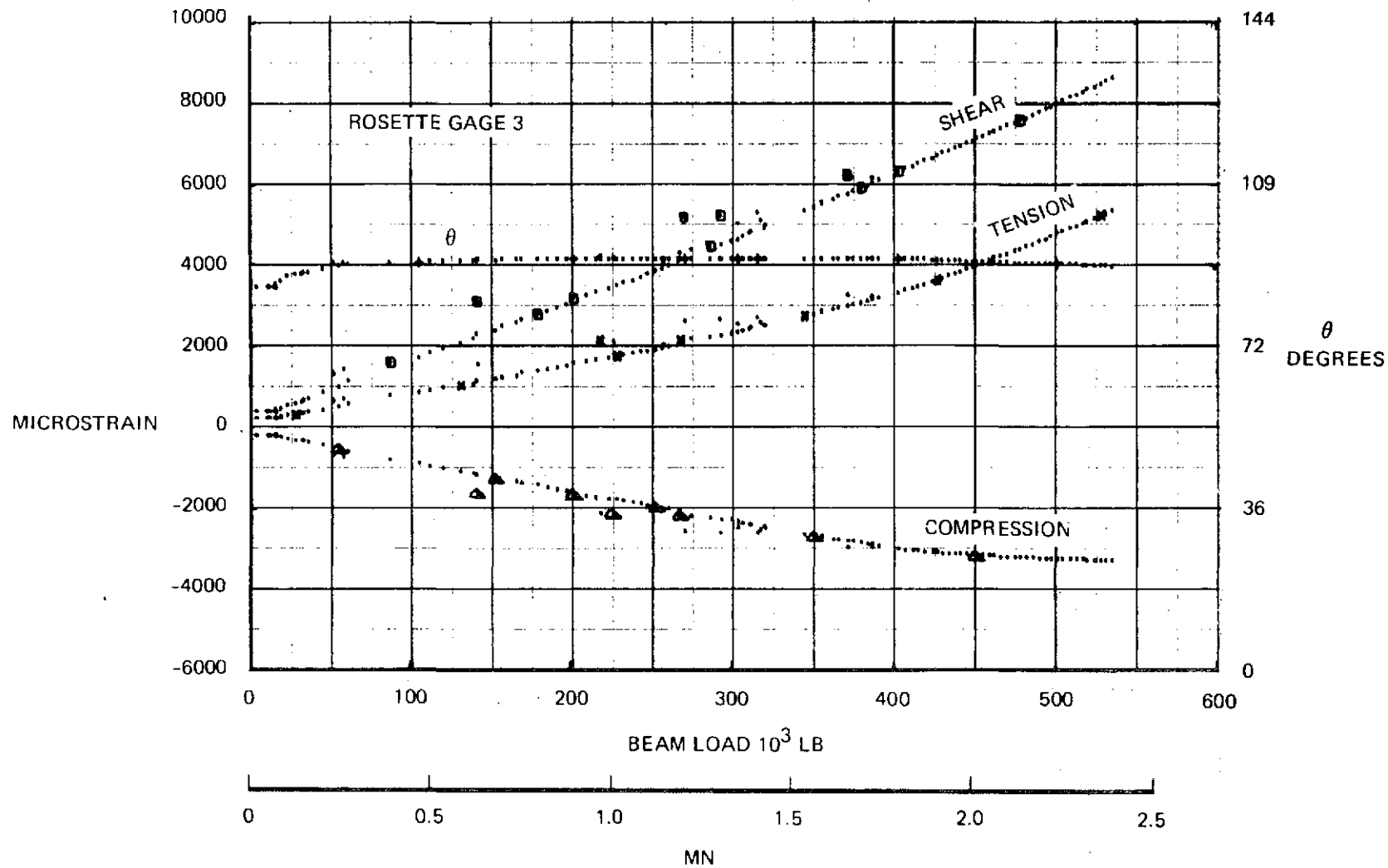
Figure A-4 : TEST WEB 1 PRINCIPAL STRAIN DATA
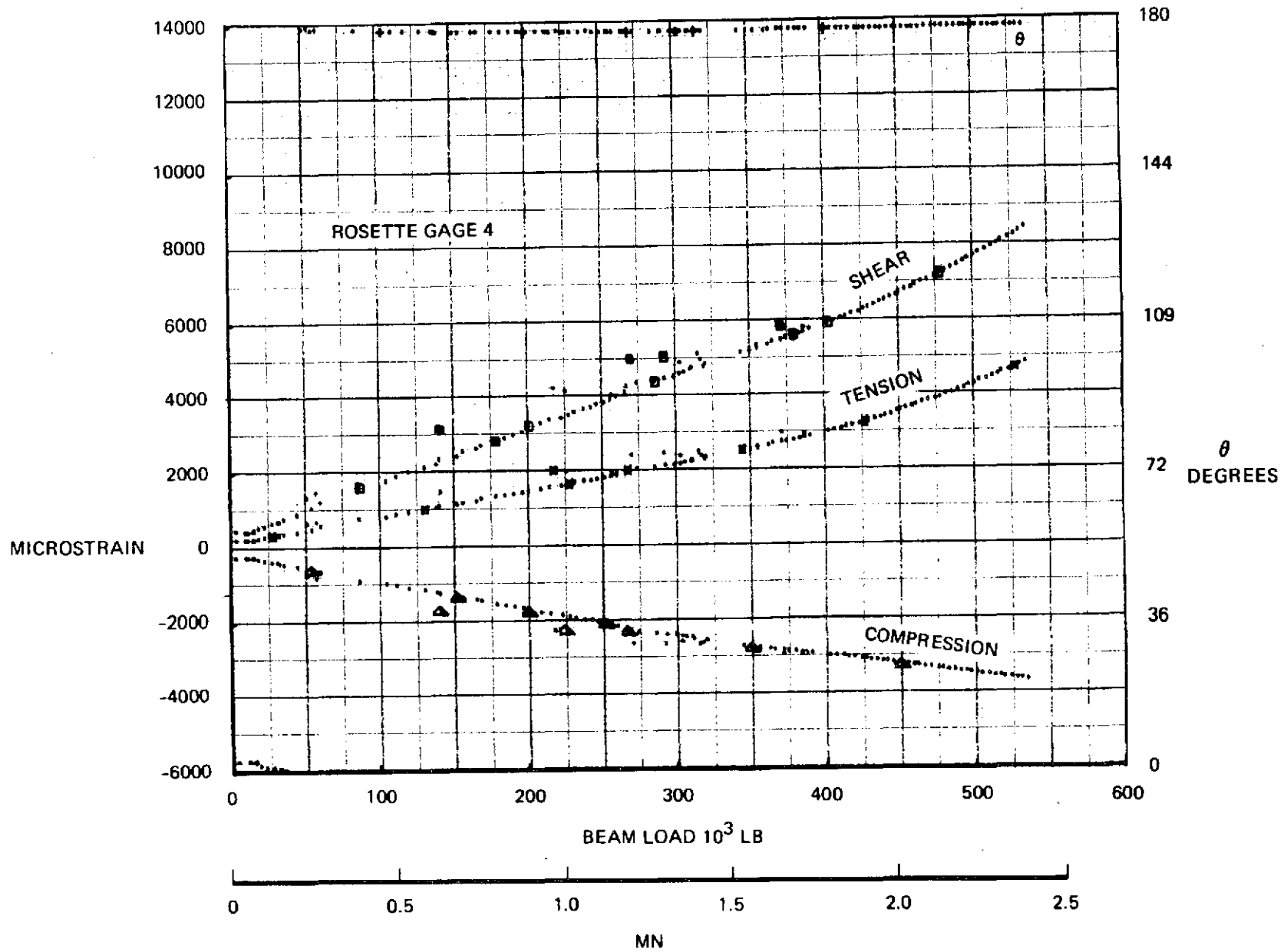
Figure A-5 :   TEST WEB 1 PRINCIPAL STRAIN DATA
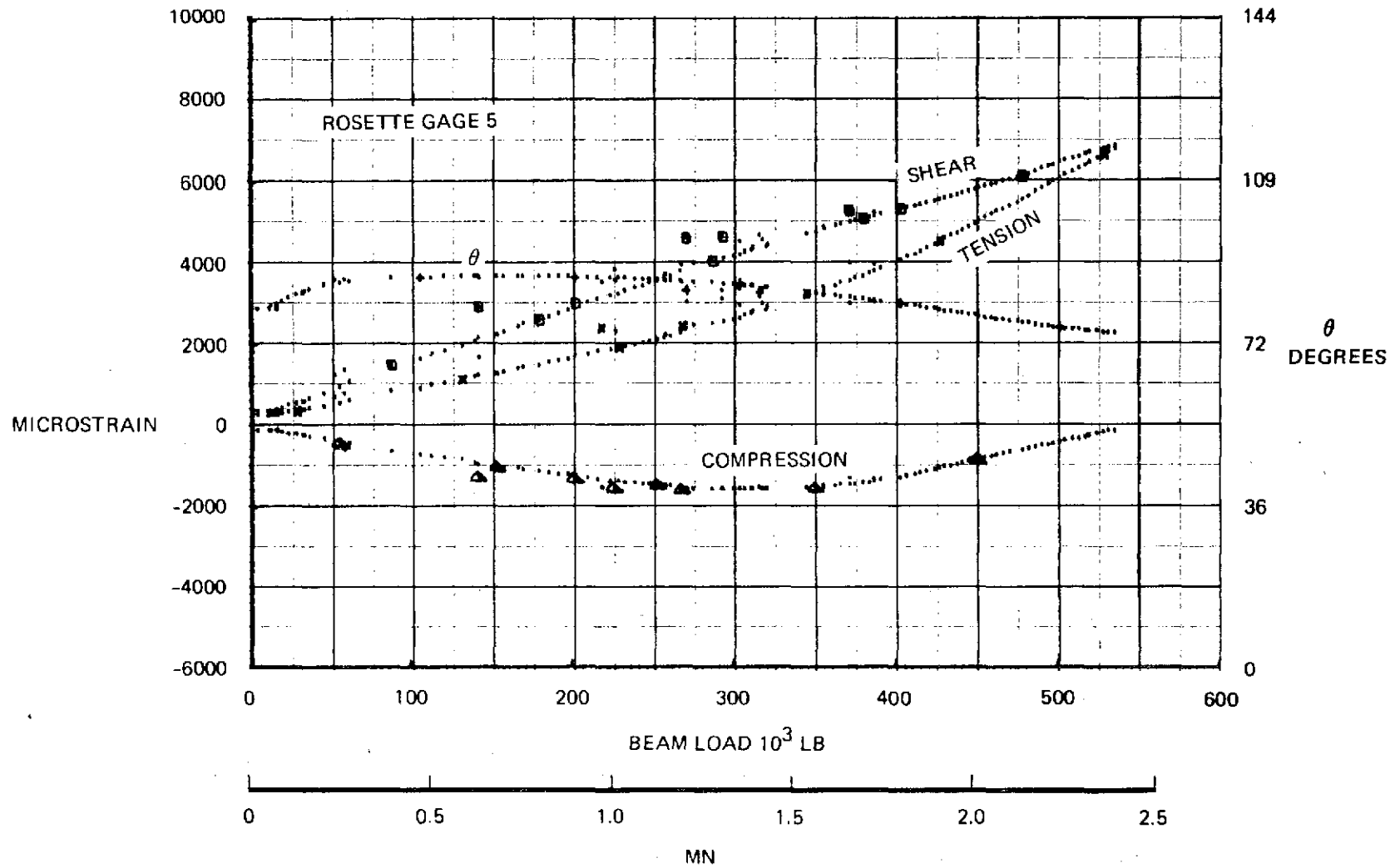
Figure A-6 :   TEST WEB 1 PRINCIPAL STRAIN DATA
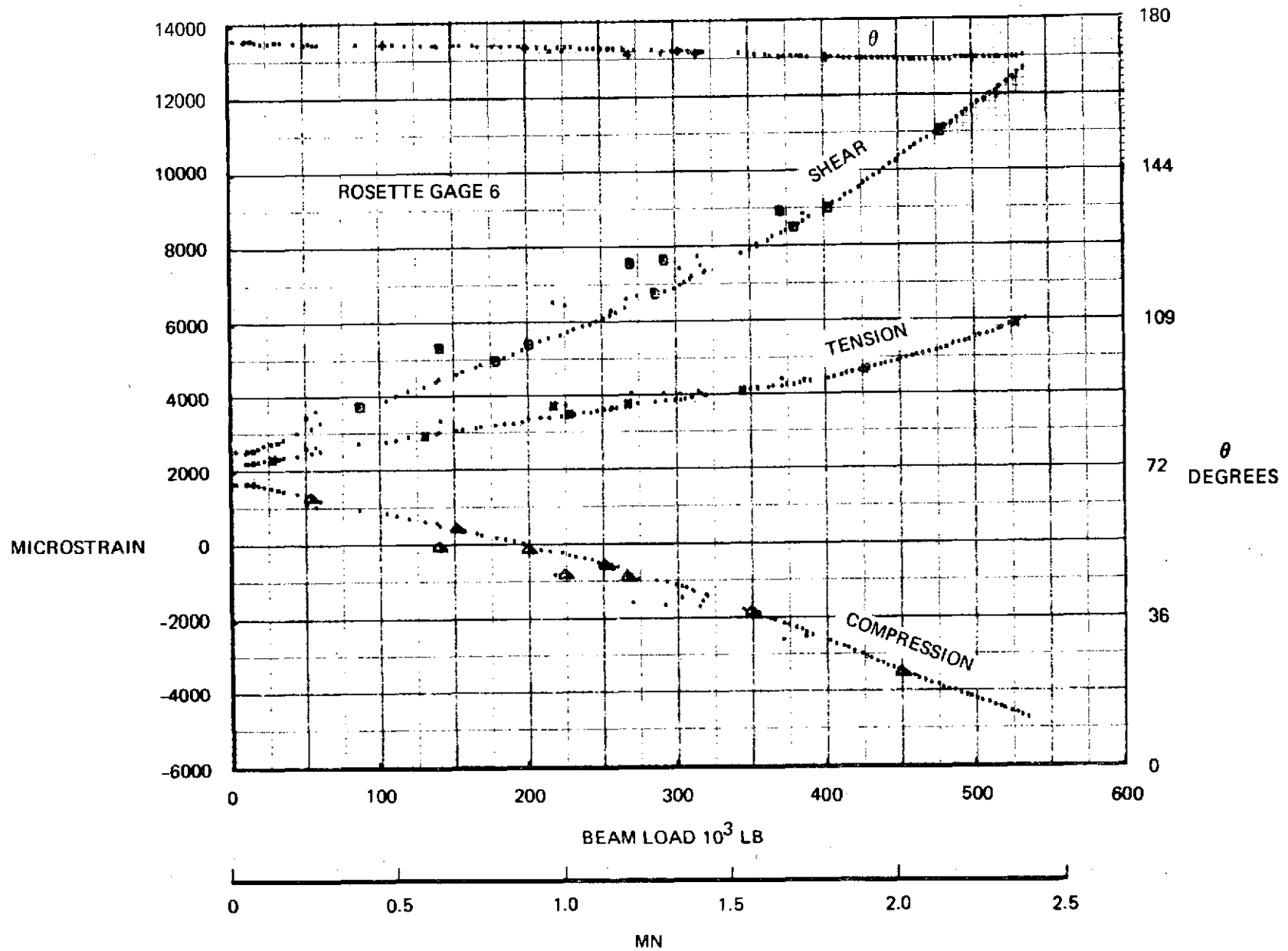
Figure A-7: TEST WEB 1 PRINCIPAL STRAIN DATA
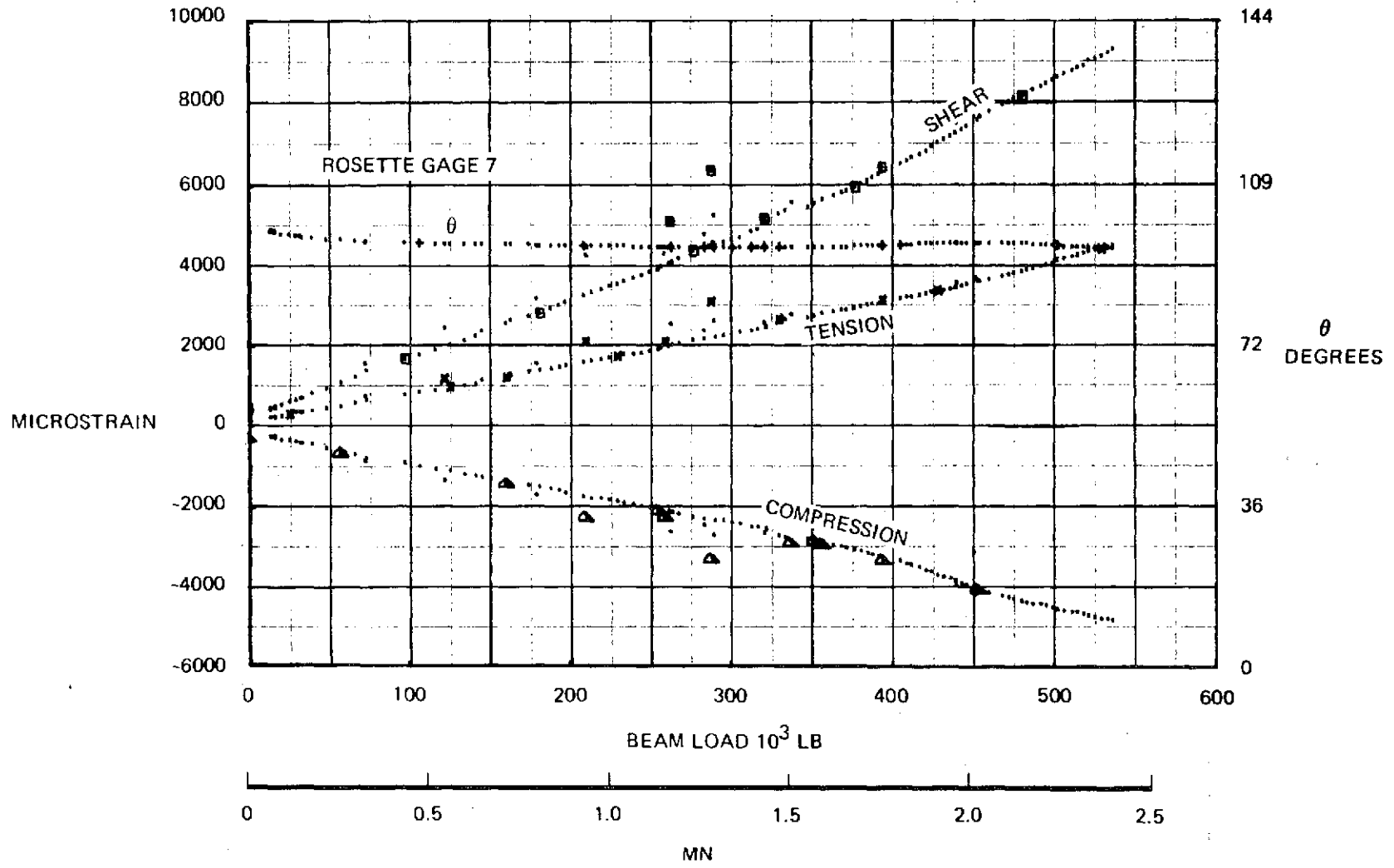
Figure A-8 : TEST WEB 1 PRINCIPAL STRAIN DATA

157
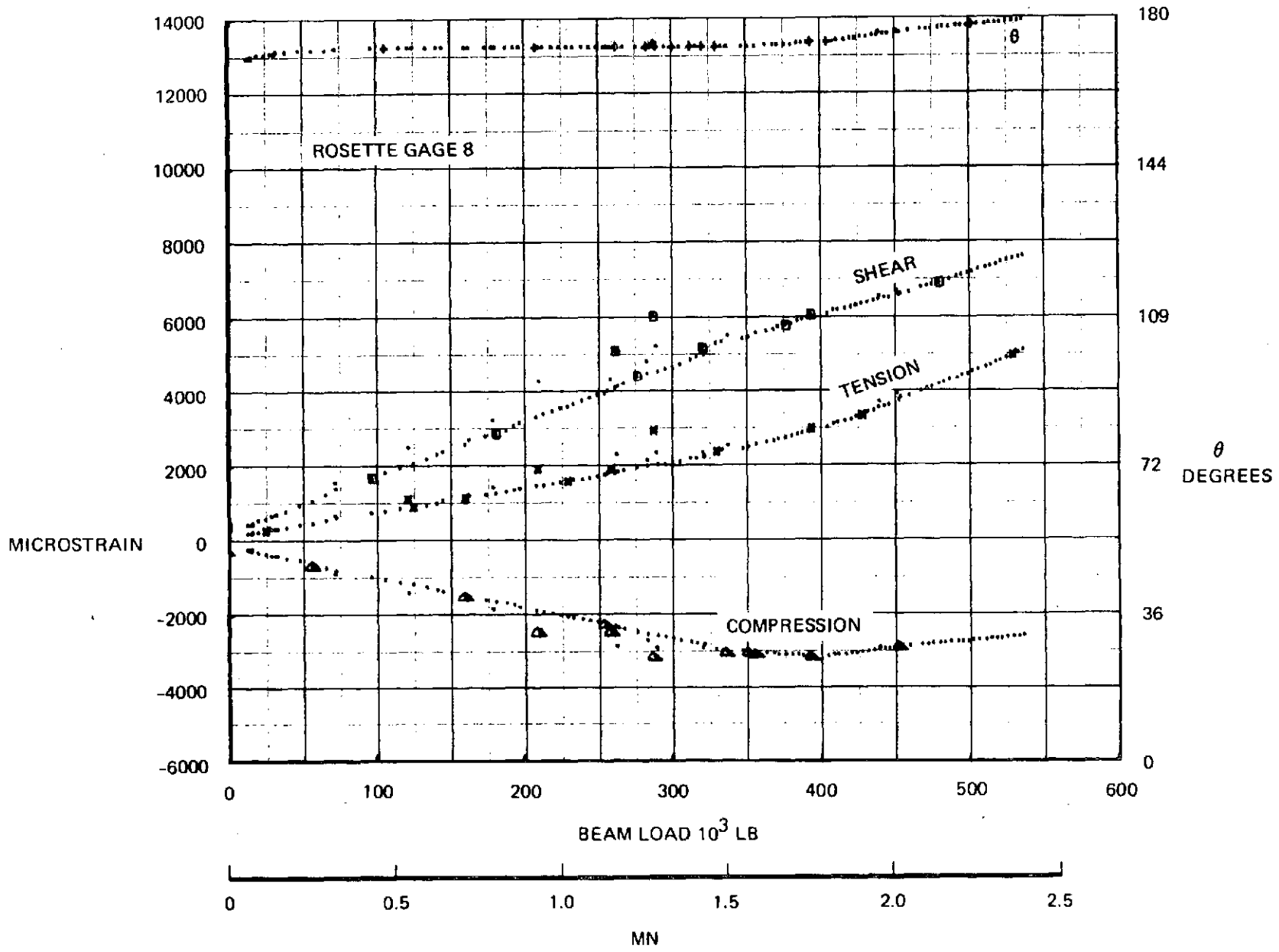
Figure A-9 : TEST WEB 1 PRINCIPAL STRAIN DATA
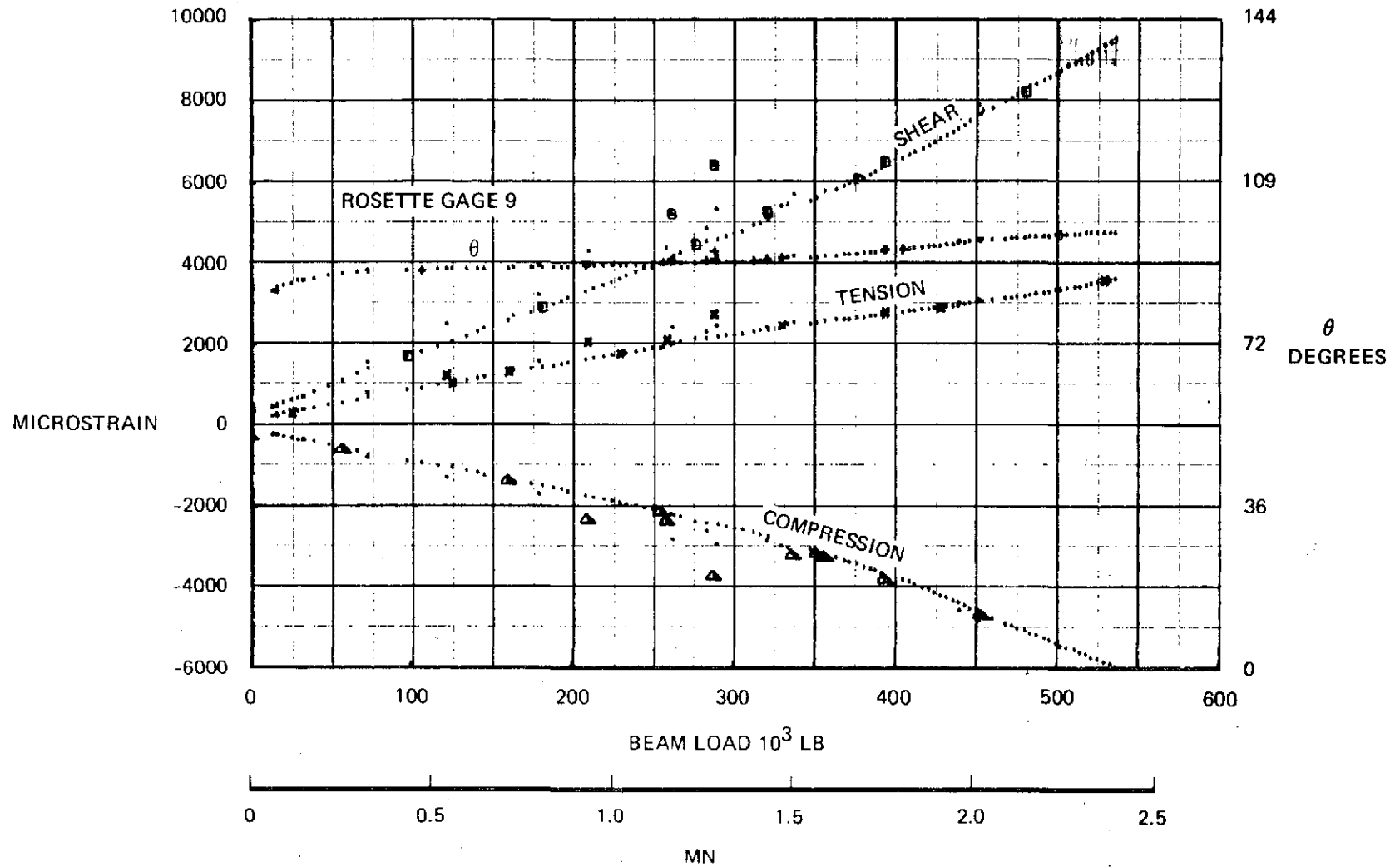
Figure A-10 : TEST WEB 1 PRINCIPAL STRAIN DATA
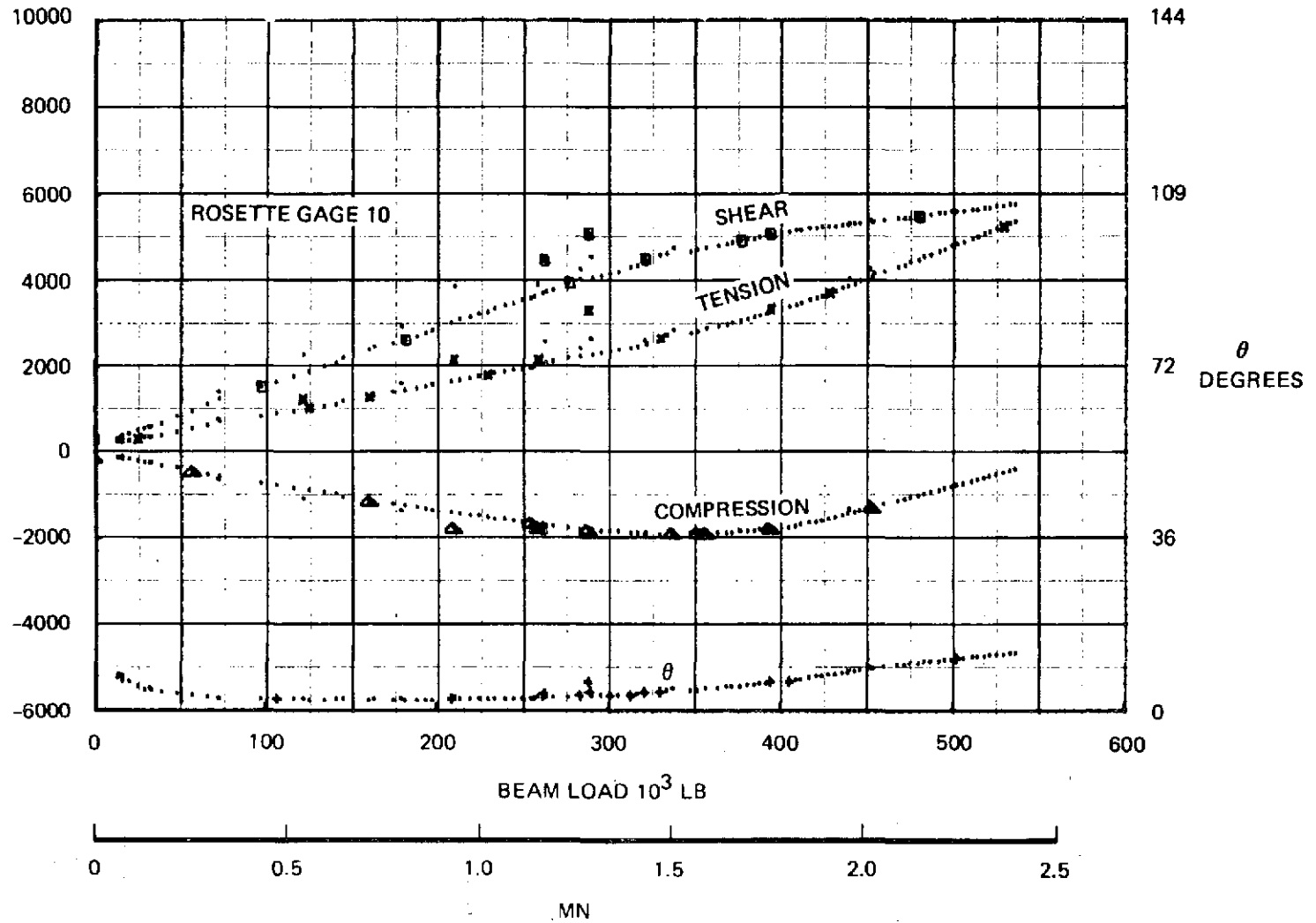
Figure A-11 : TEST WEB 1 PRINCIPAL STRAIN DATA
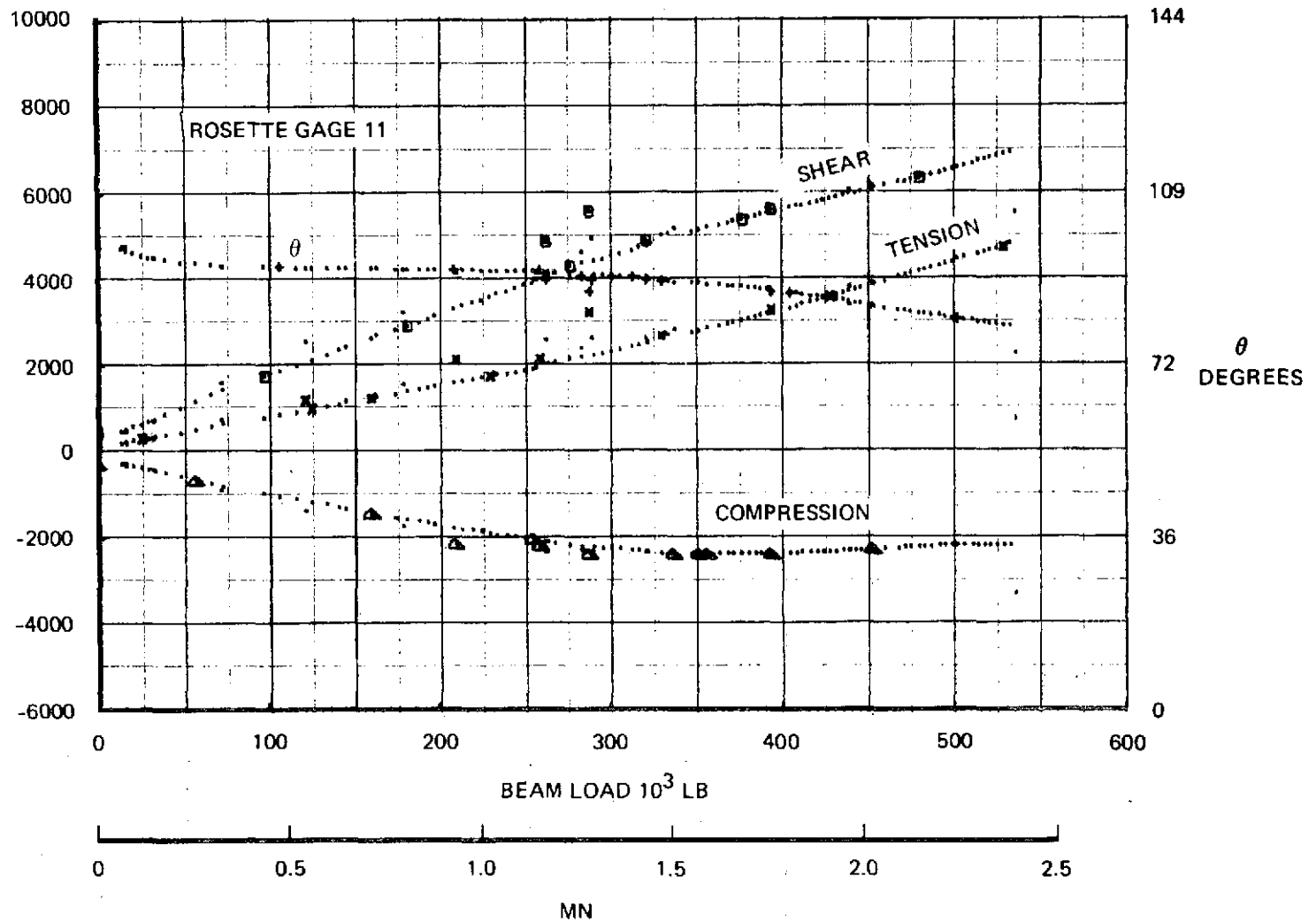
Figure A-12 : TEST WEB 1 PRINCIPAL STRAIN DATA
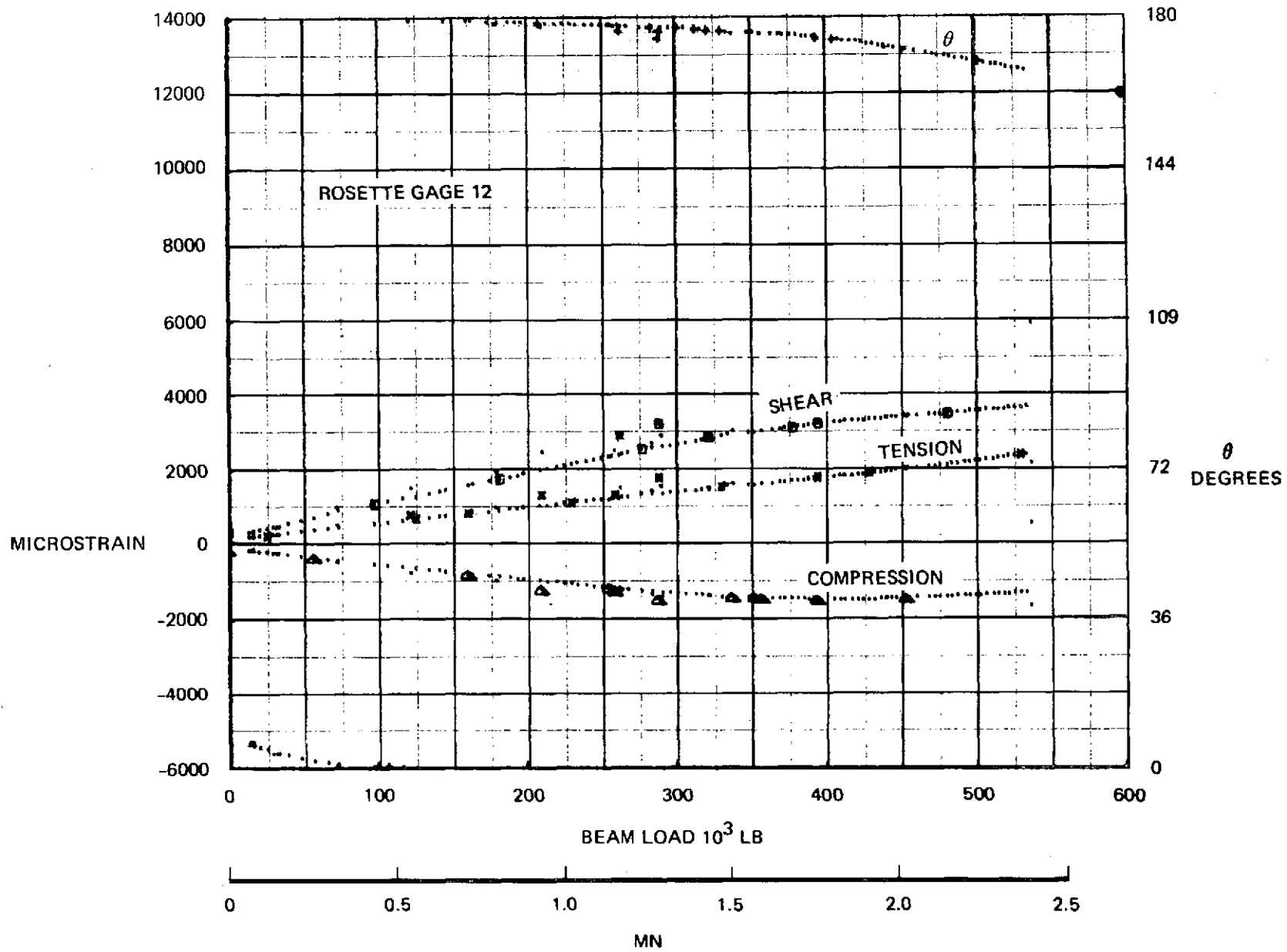
Figure A-13 : TEST WEB 1 PRINCIPAL STRAIN DATA

162

NEAR SIDE GAGES

ROSETTE   ←

SINGLE   ▬

FAR SIDE GAGES

ON STIFFENER FLANGE

ON WEB LAMINATE

52 →<← 51   2 →<← 1   54 →<← 53

4 →<← 3   6 →<← 5

10 →<← 9
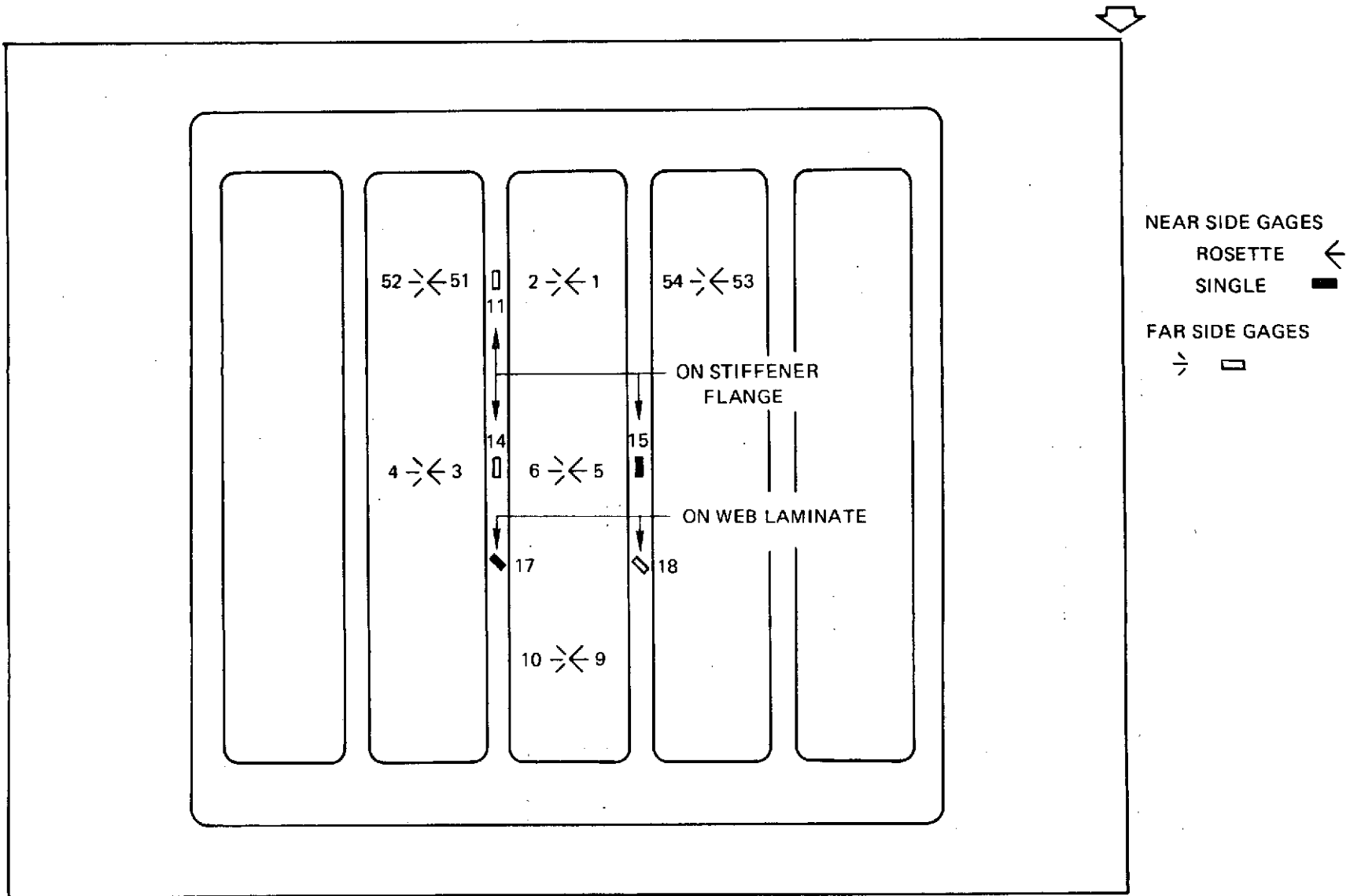
Figure A-14 : TEST WEB 2 STRAIN GAGE LOCATIONS

163
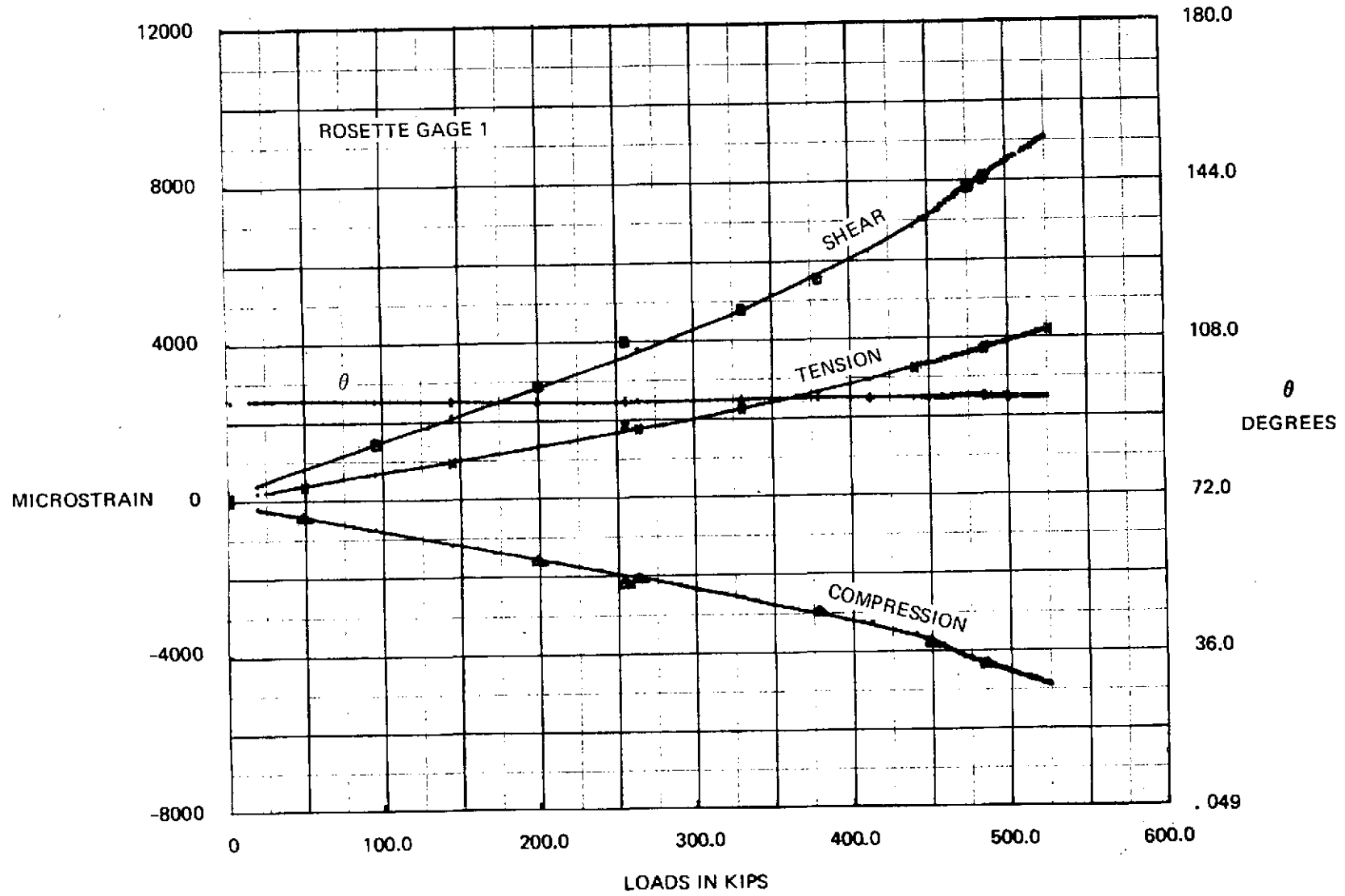
Figure A-15 : TEST WEB 2 PRINCIPAL STRAIN DATA

164
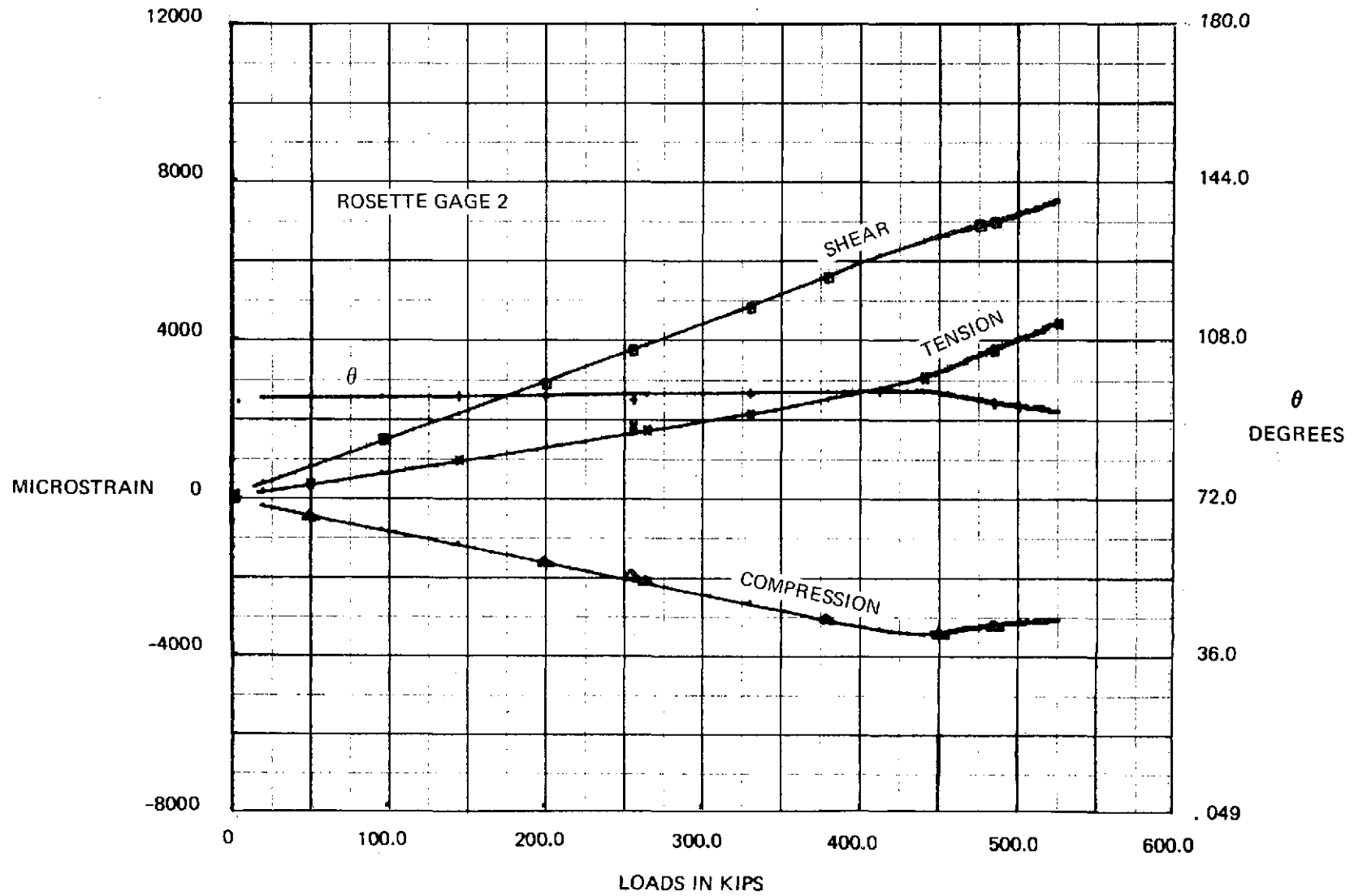
Figure A-16 : TEST WEB 2 PRINCIPAL STRAIN DATA
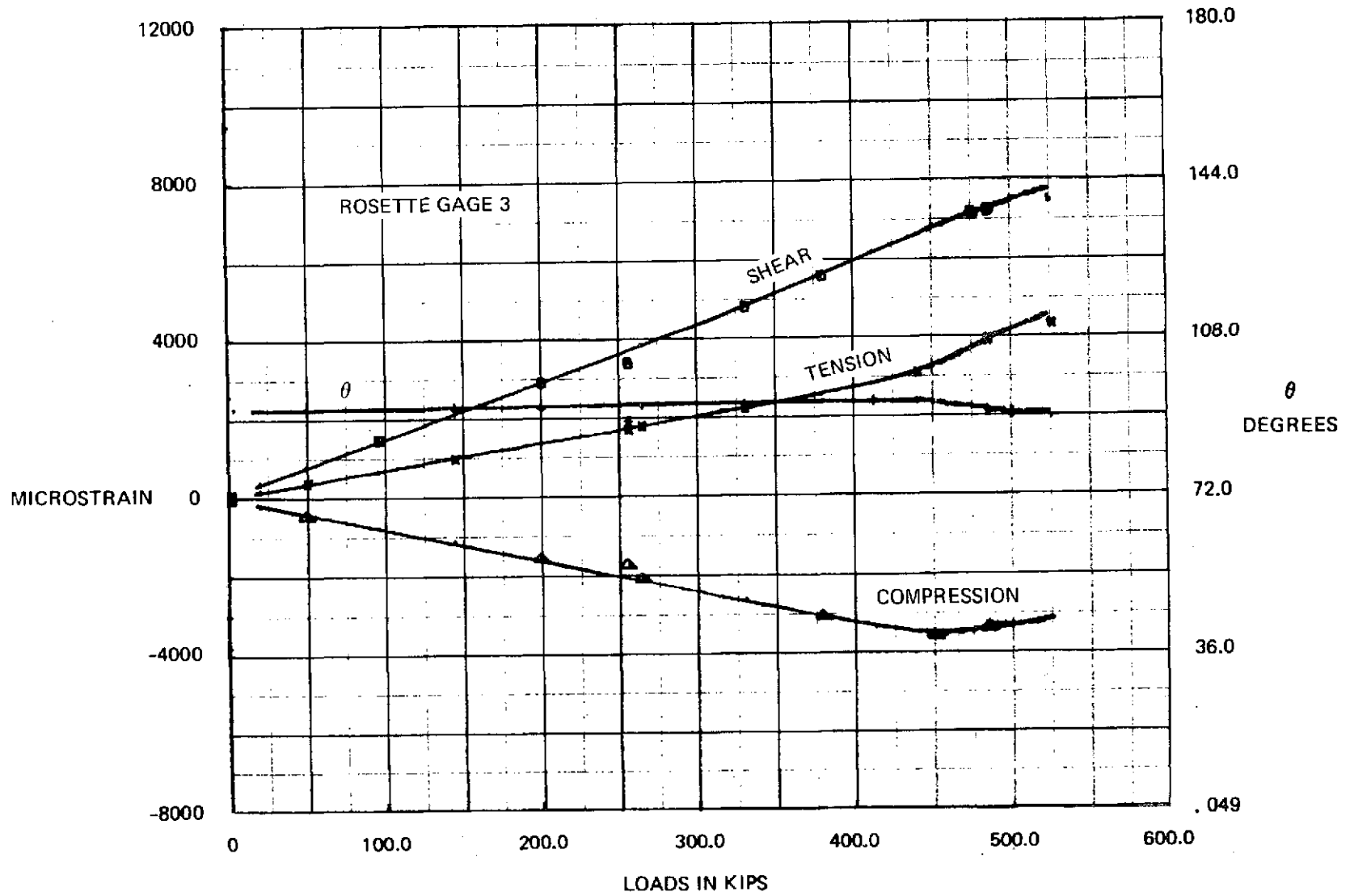
Figure A-I7 :   TEST WEB 2 PRINCIPAL STRAIN DATA
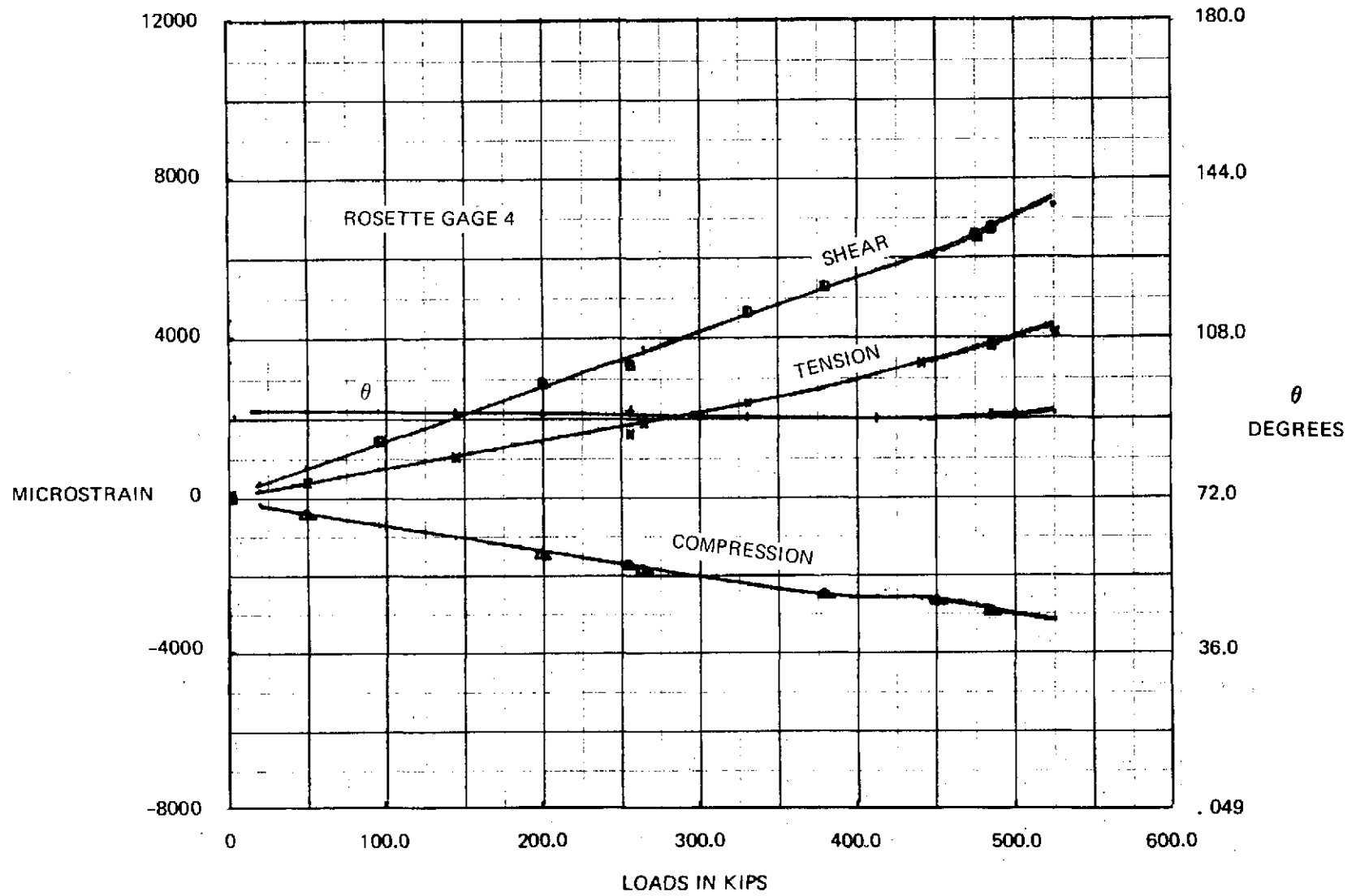
Figure A-l8 : TEST WEB 2 PRINCIPAL STRAIN DATA
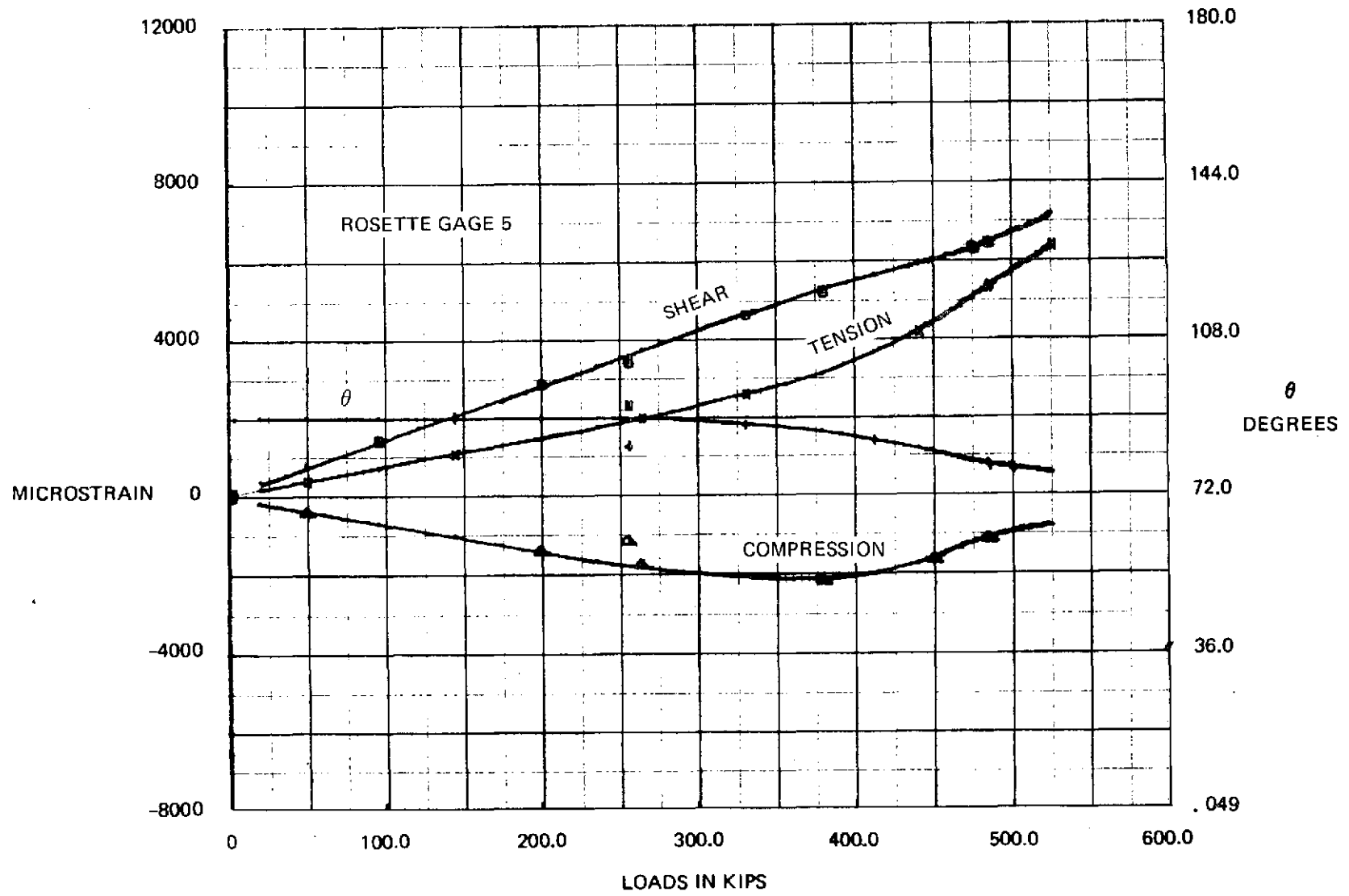
Figure A-19 : TEST WEB 2 PRINCIPAL STRAIN DATA
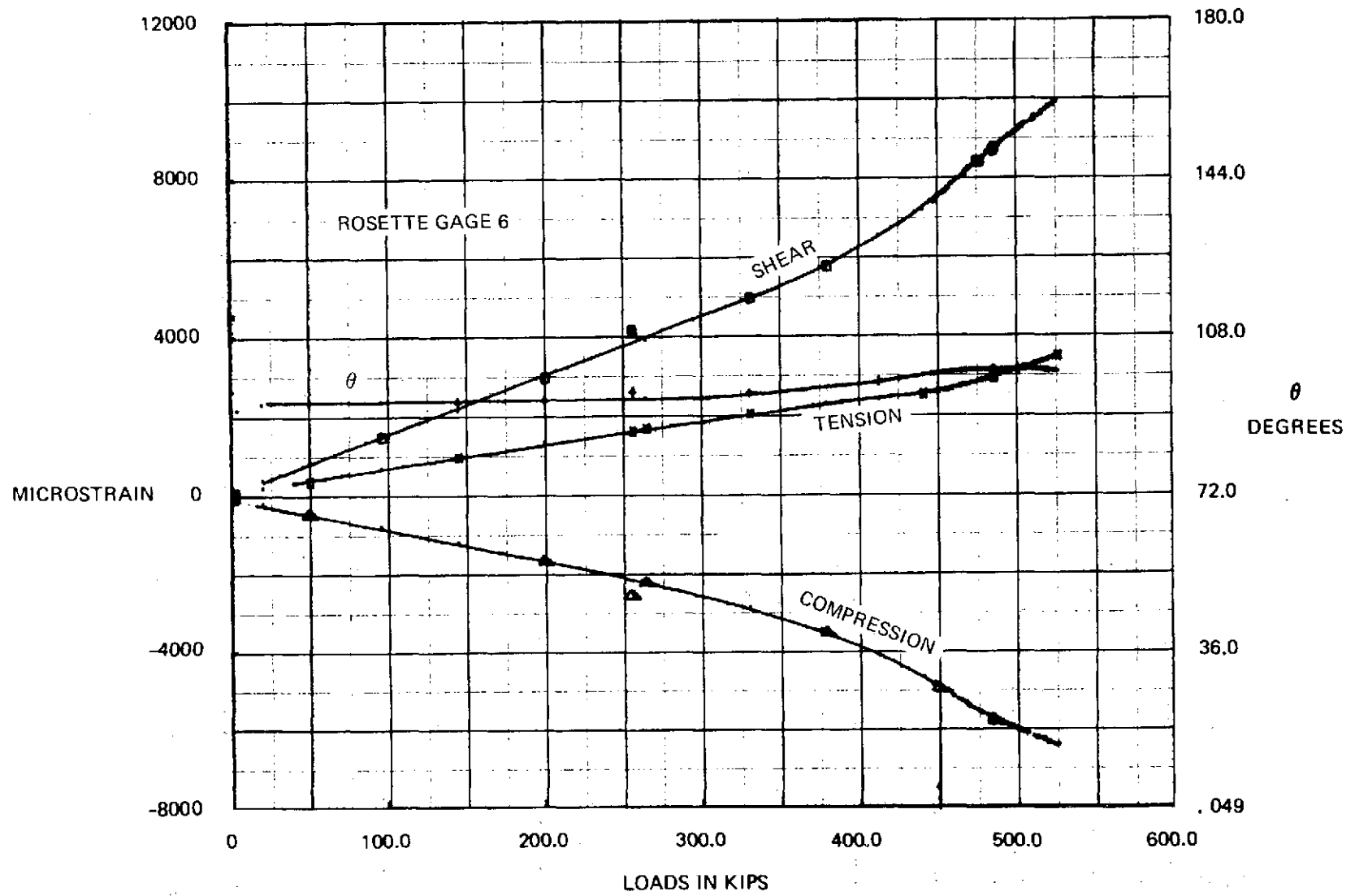
Figure A-20 : *TEST WEB 2 PRINCIPAL STRAIN DATA*

169
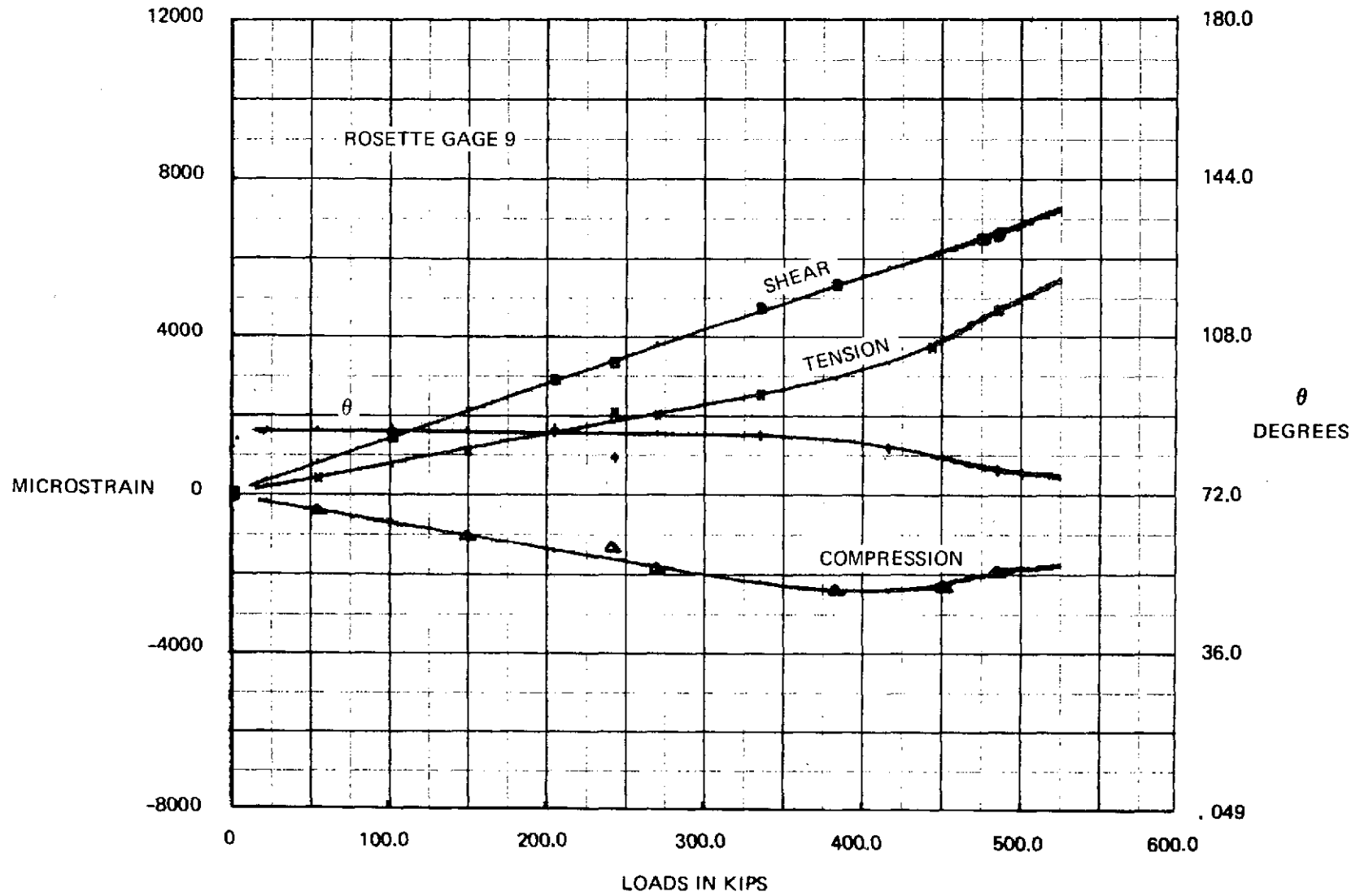
Figure A-21 : TEST WEB 2 PRINCIPAL STRAIN DATA
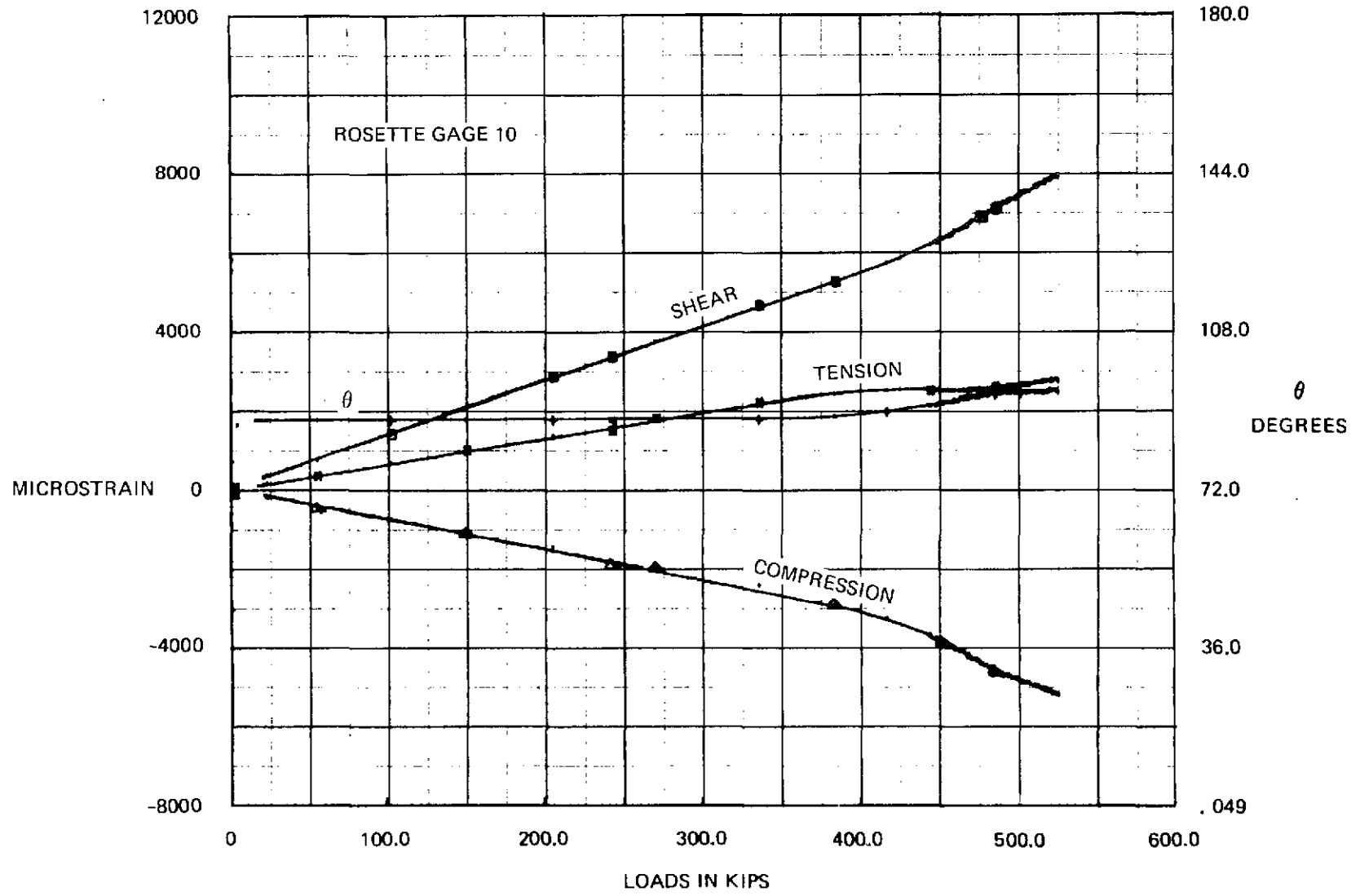
Figure A-22 : TEST WEB 2 PRINCIPAL STRAIN DATA
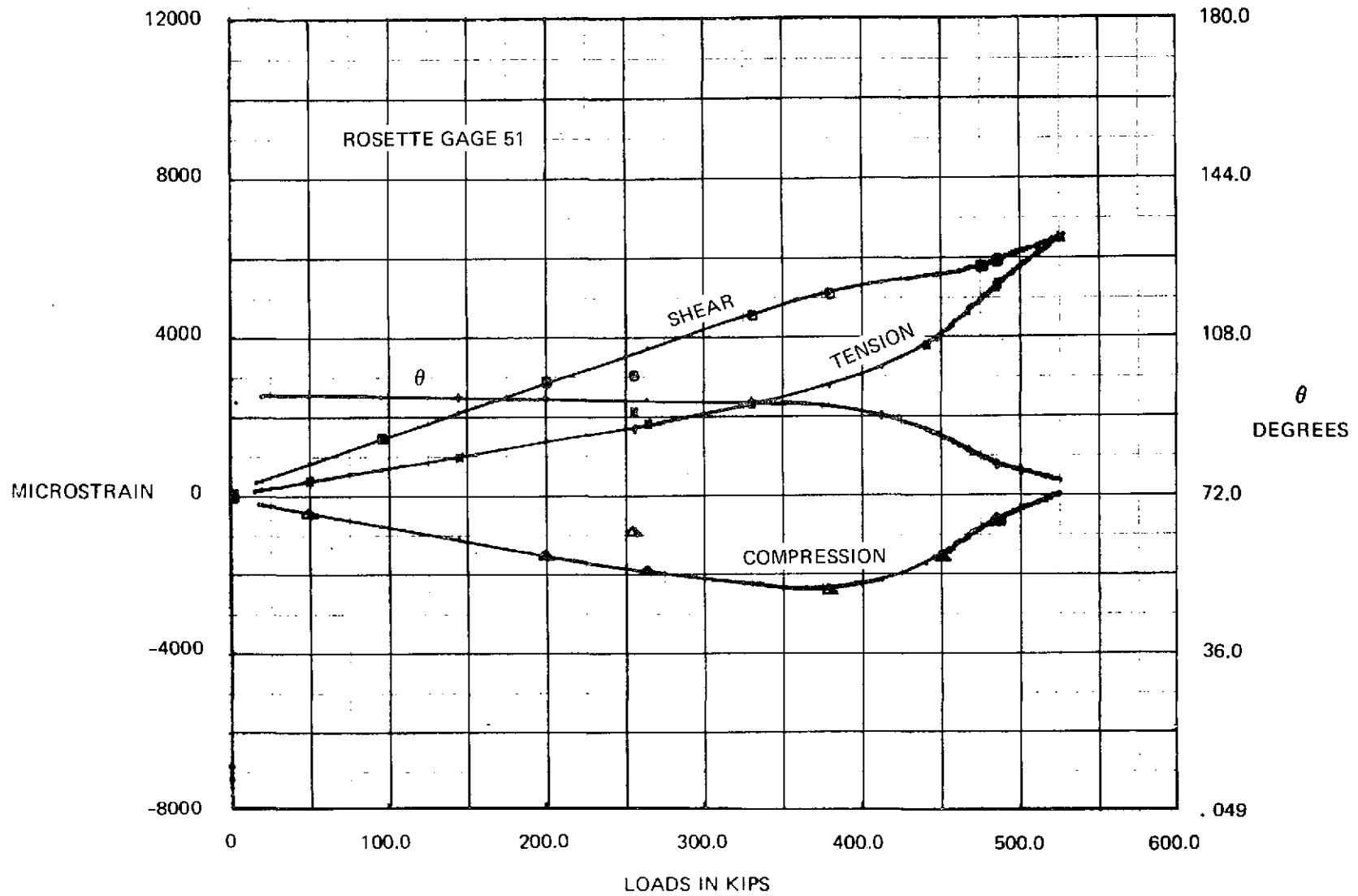
Figure A-23 : TEST WEB 2 PRINCIPAL STRAIN DATA

172
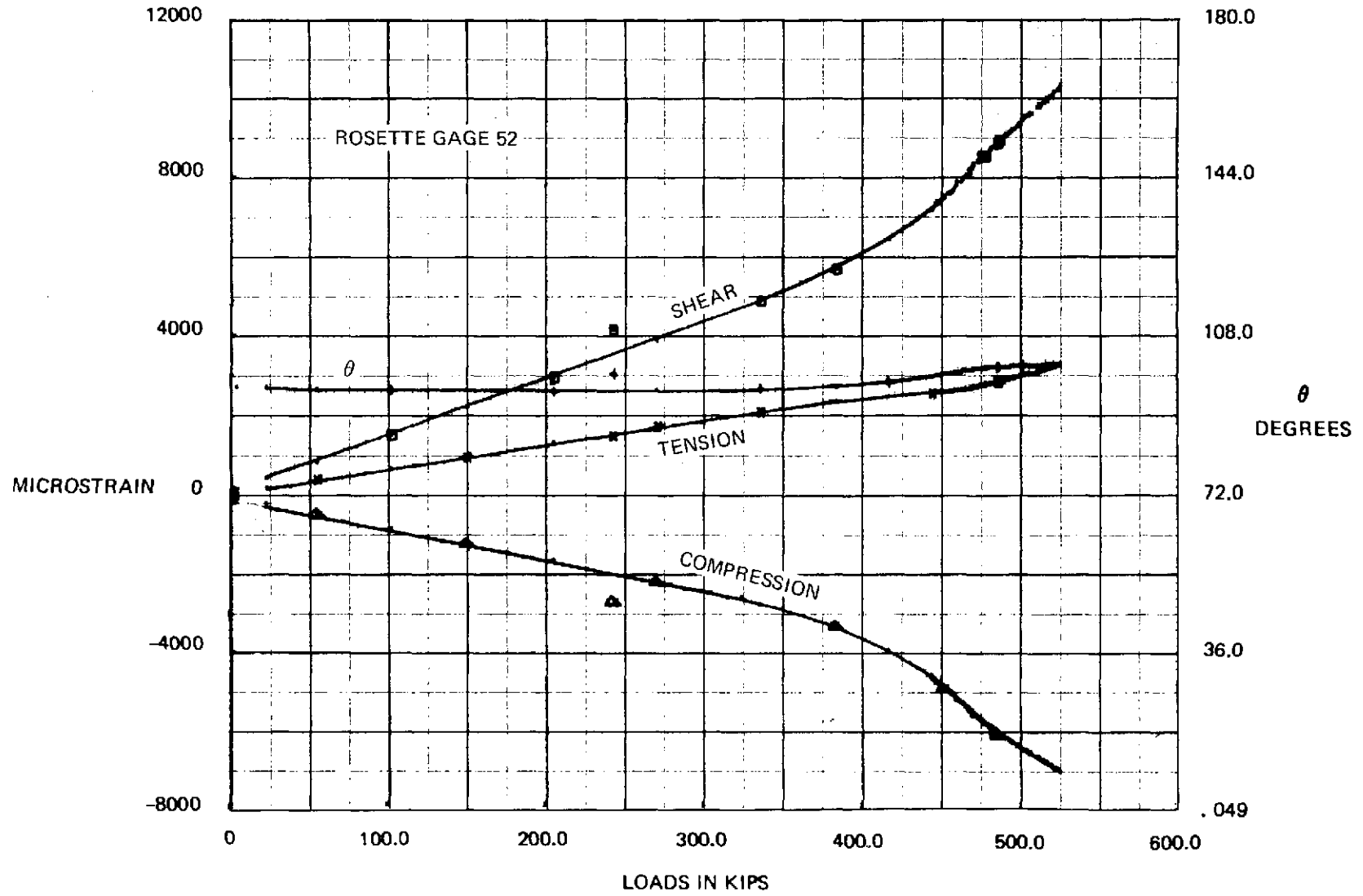
Figure A-24 : TEST WEB 2 PRINCIPAL STRAIN DATA

173
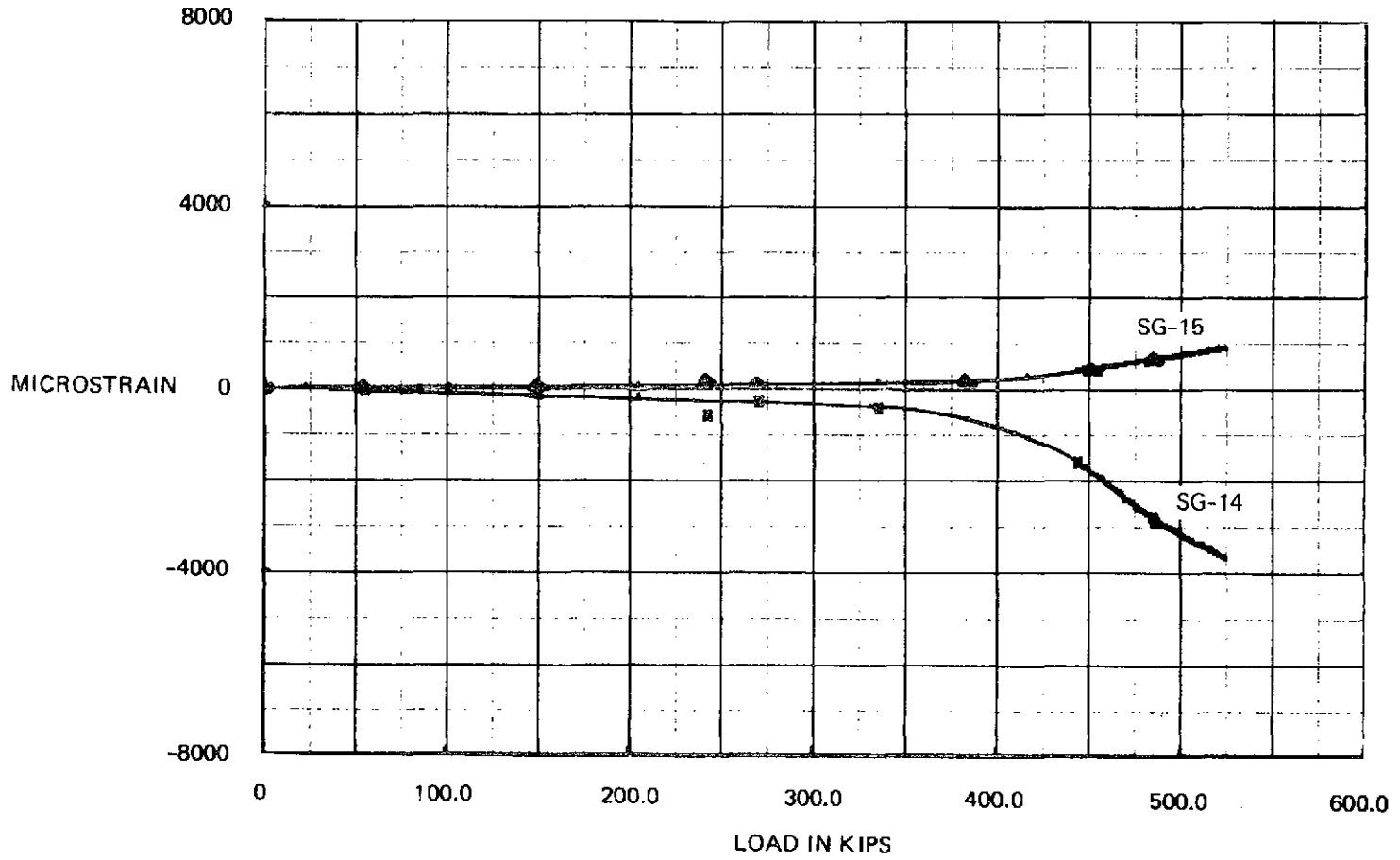
Figure A-25 :   TEST WEB 2 STRAIN DATA
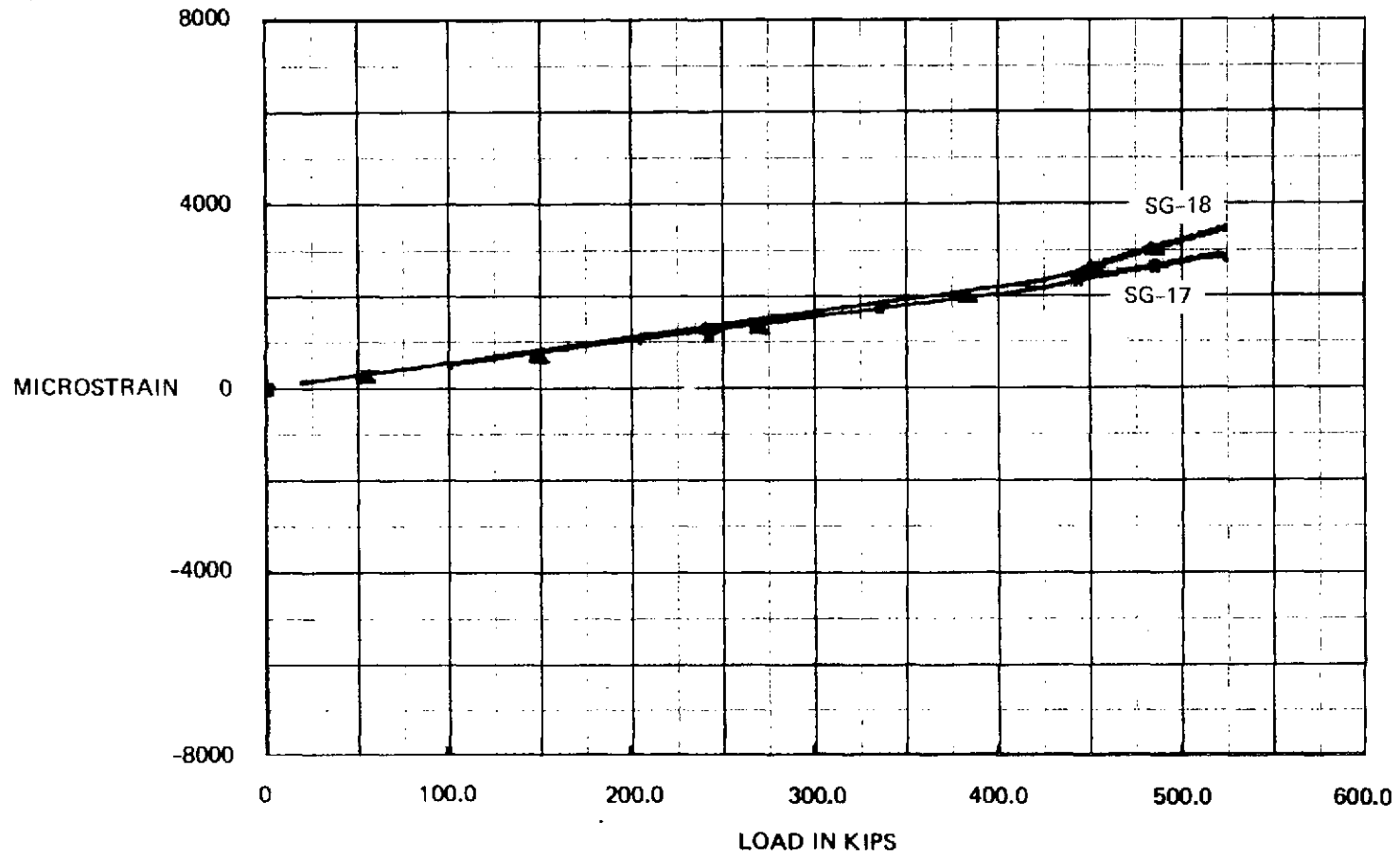
Figure A-26 : *TEST WEB 2 STRAIN DATA*
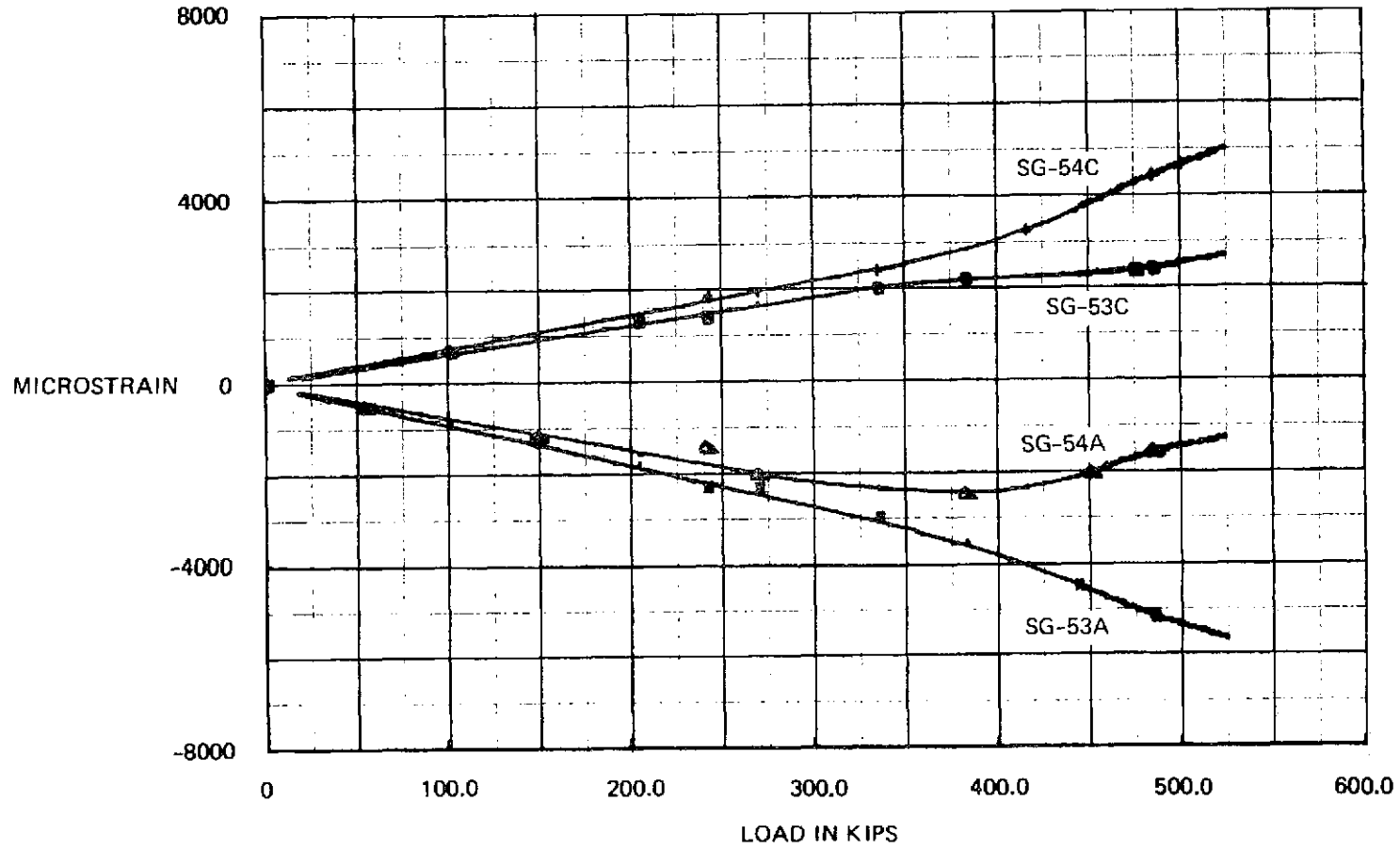
Figure A-27 : TEST WEB 2 STRAIN DATA

NEAR SIDE ON STIFFENER FLANGE
FAR SIDE ON WEB LAMINATE

NEAR SIDE ON WEB LAMINATE
FAR SIDE ON STIFFENER FLANGE

NEAR SIDE GAGES

ROSETTE ←

SINGLE ▬

FAR SIDE GAGES

□
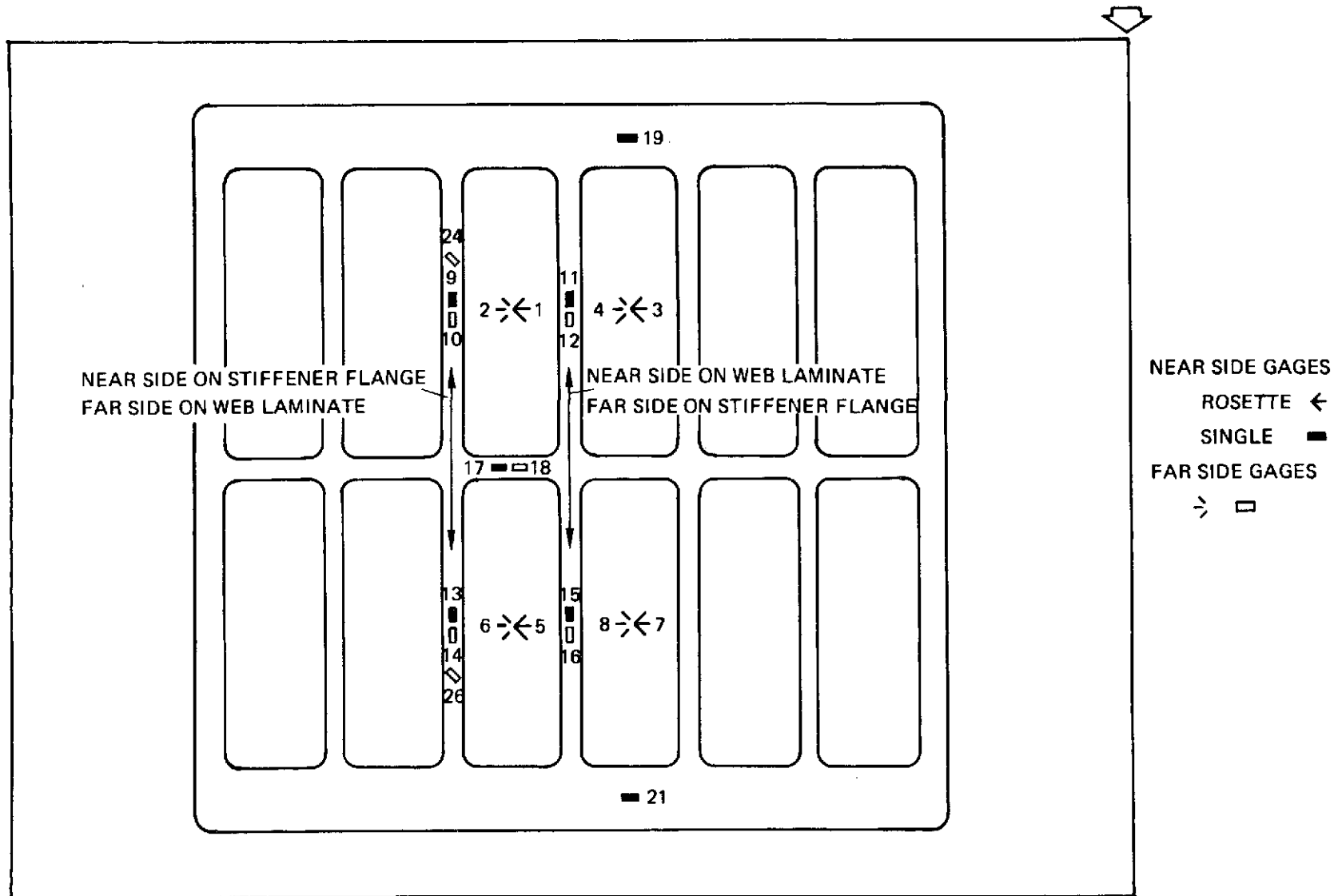
Figure A-28 :   TEST WEB 3 STRAIN GAGE LOCATIONS
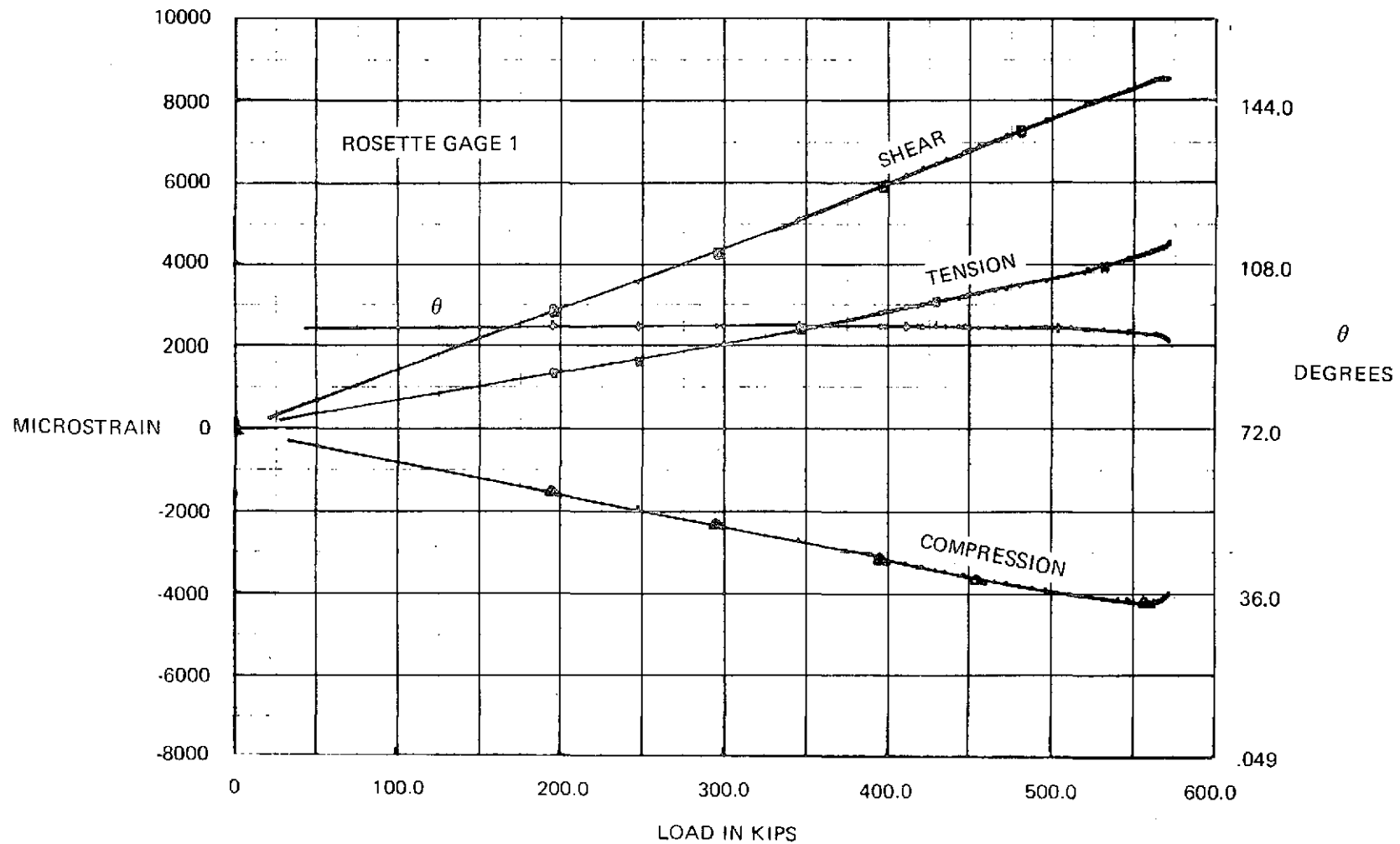
Figure A-29 : TEST WEB 3 PRINCIPAL STRAIN DATA

178
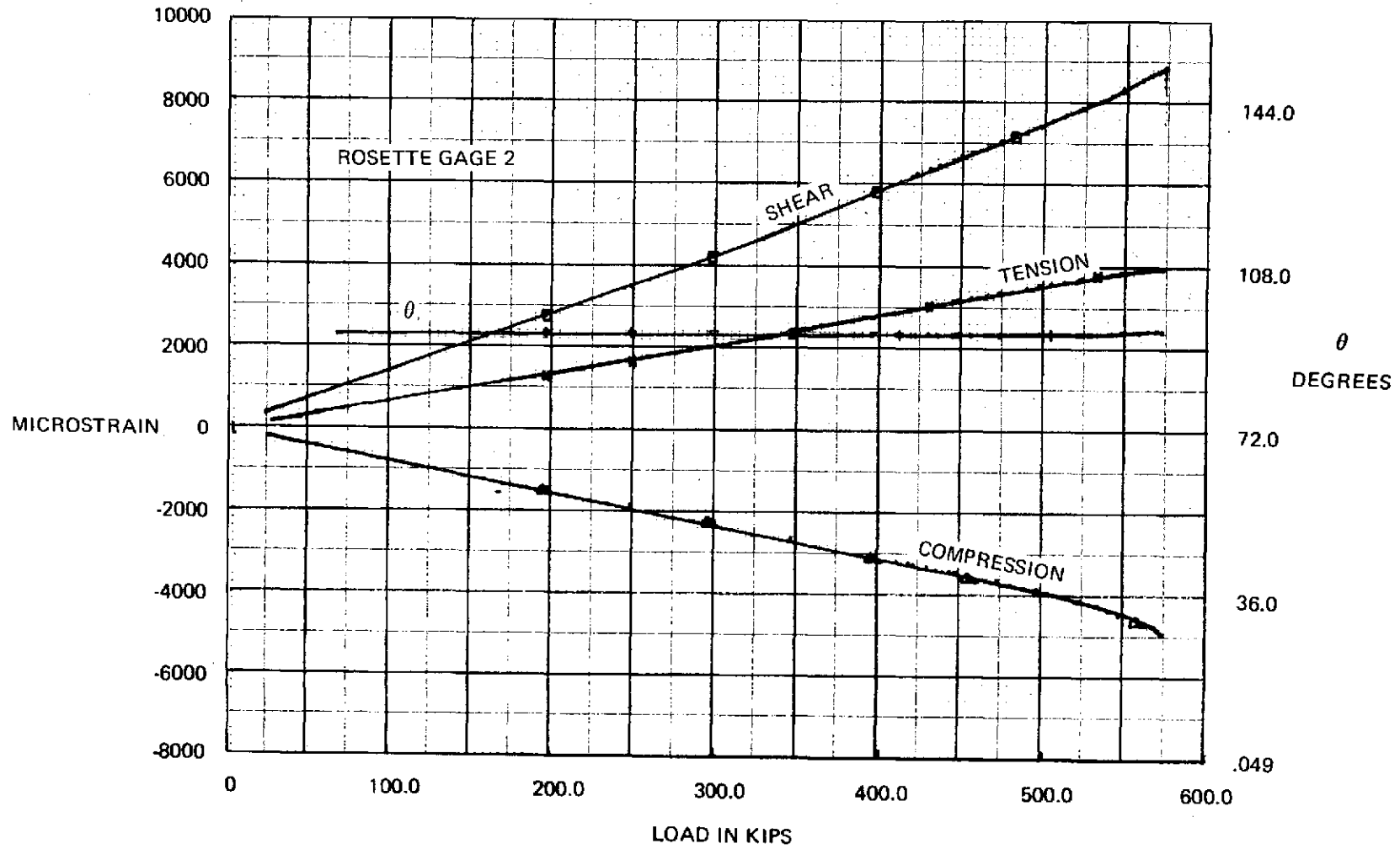
Figure A-30 : TEST WEB 3 PRINCIPAL STRAIN DATA
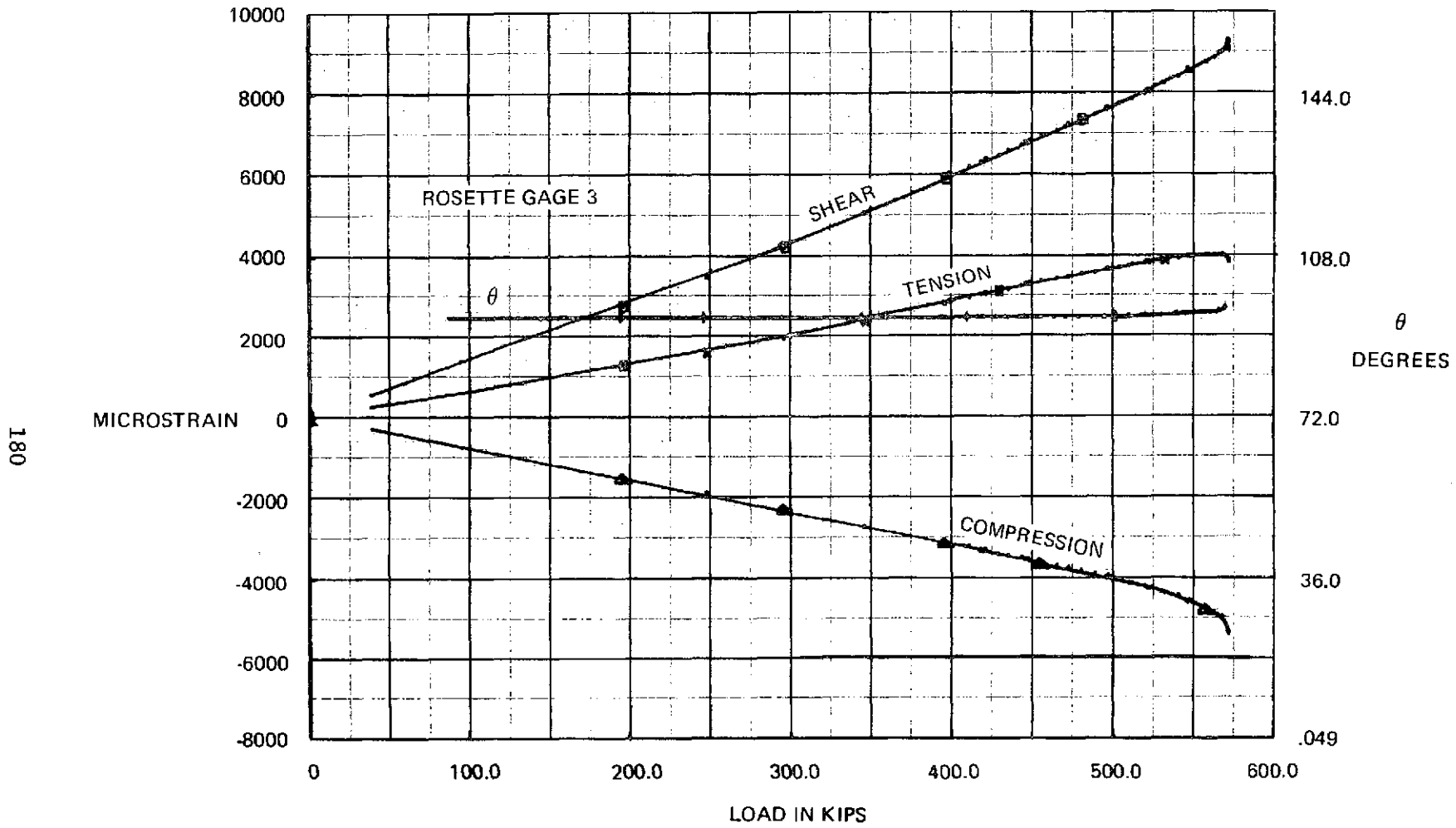
Figure A-31 : TEST WEB 3 PRINCIPAL STRAIN DATA
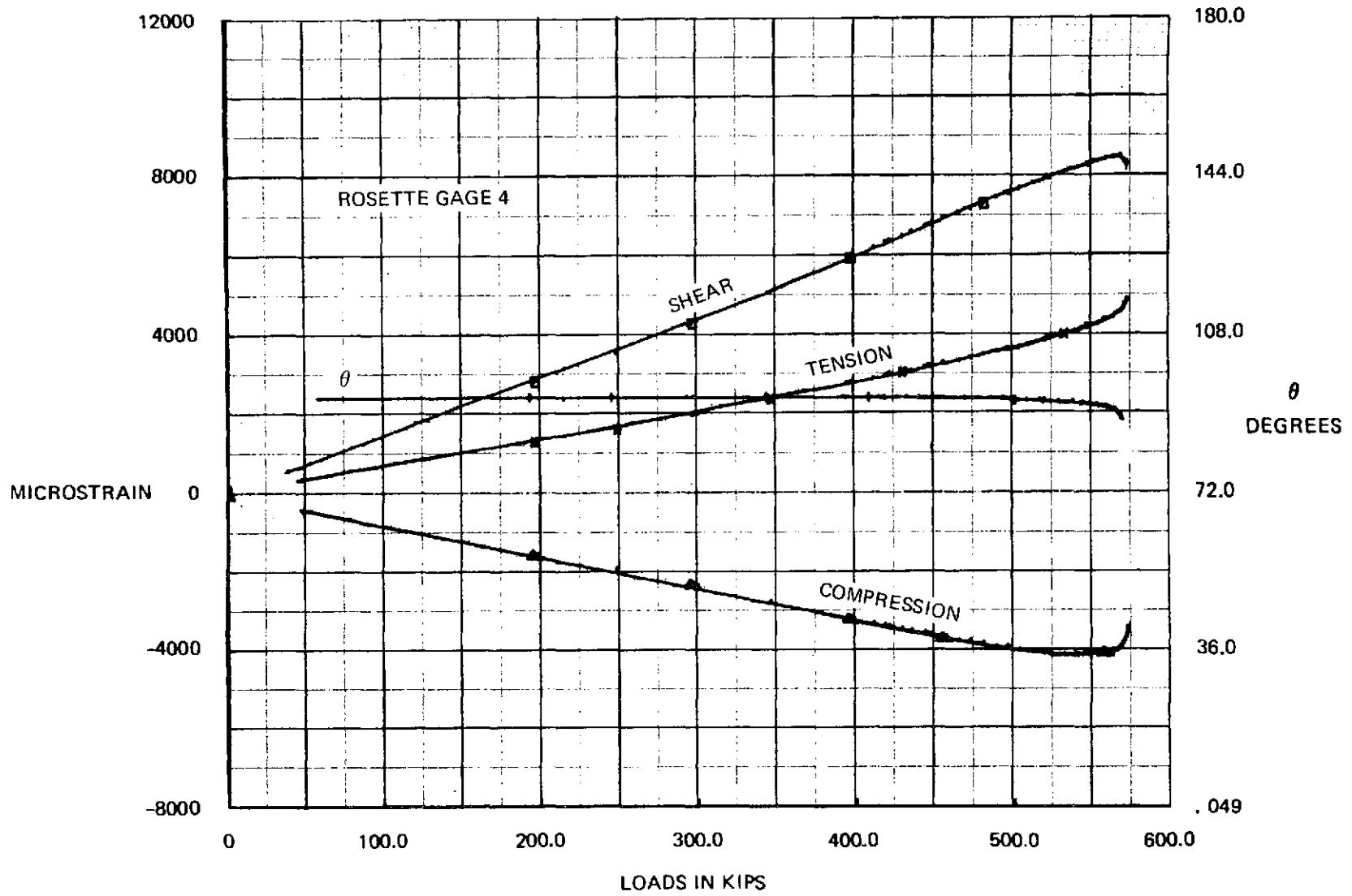
Figure A-32 : TEST WEB 3 PRINCIPAL STRAIN DATA

181
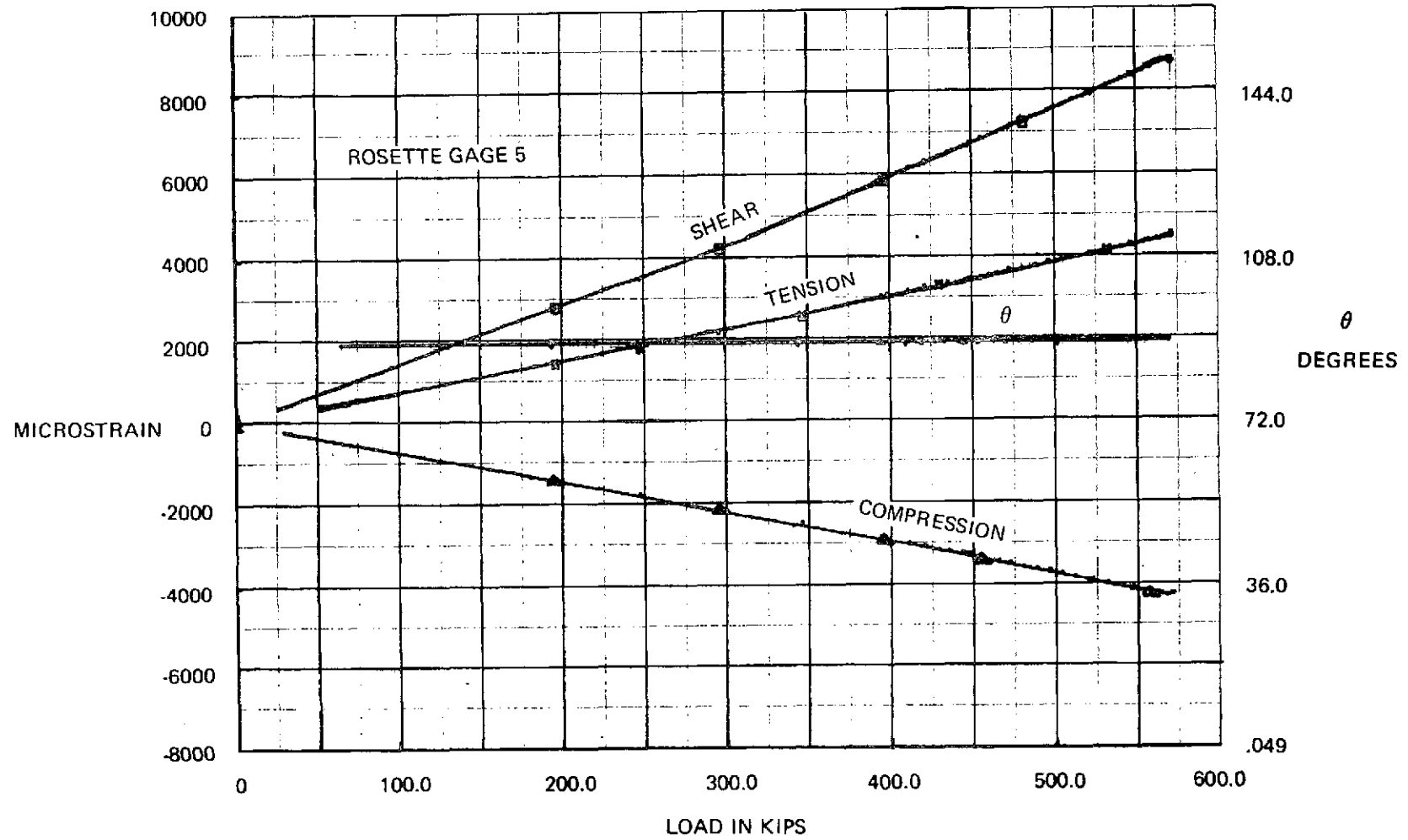
Figure A-33 : TEST WEB 3 PRINCIPAL STRAIN DATA
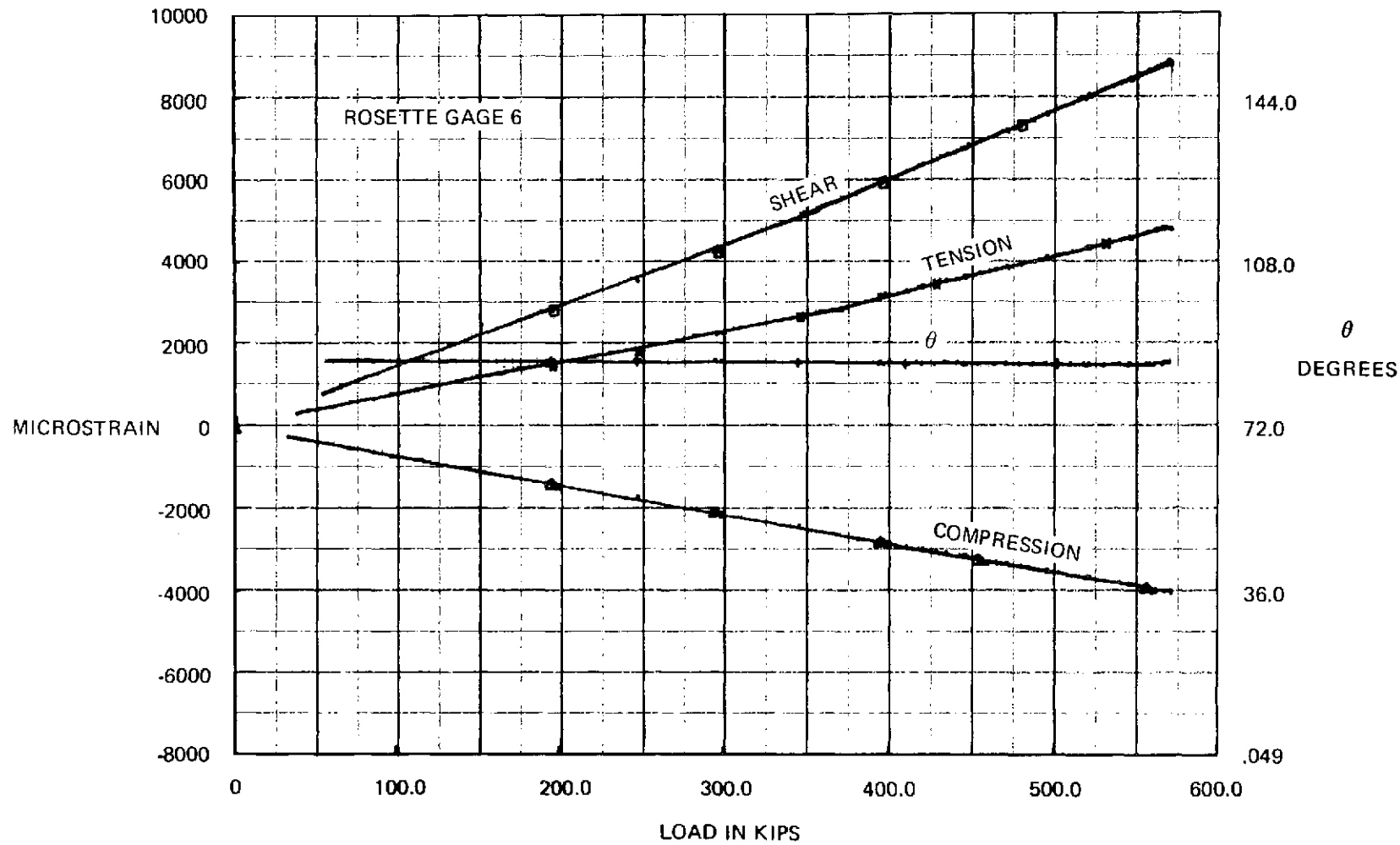
Figure A-34 : TEST WEB 3 PRINCIPAL STRAIN DATA
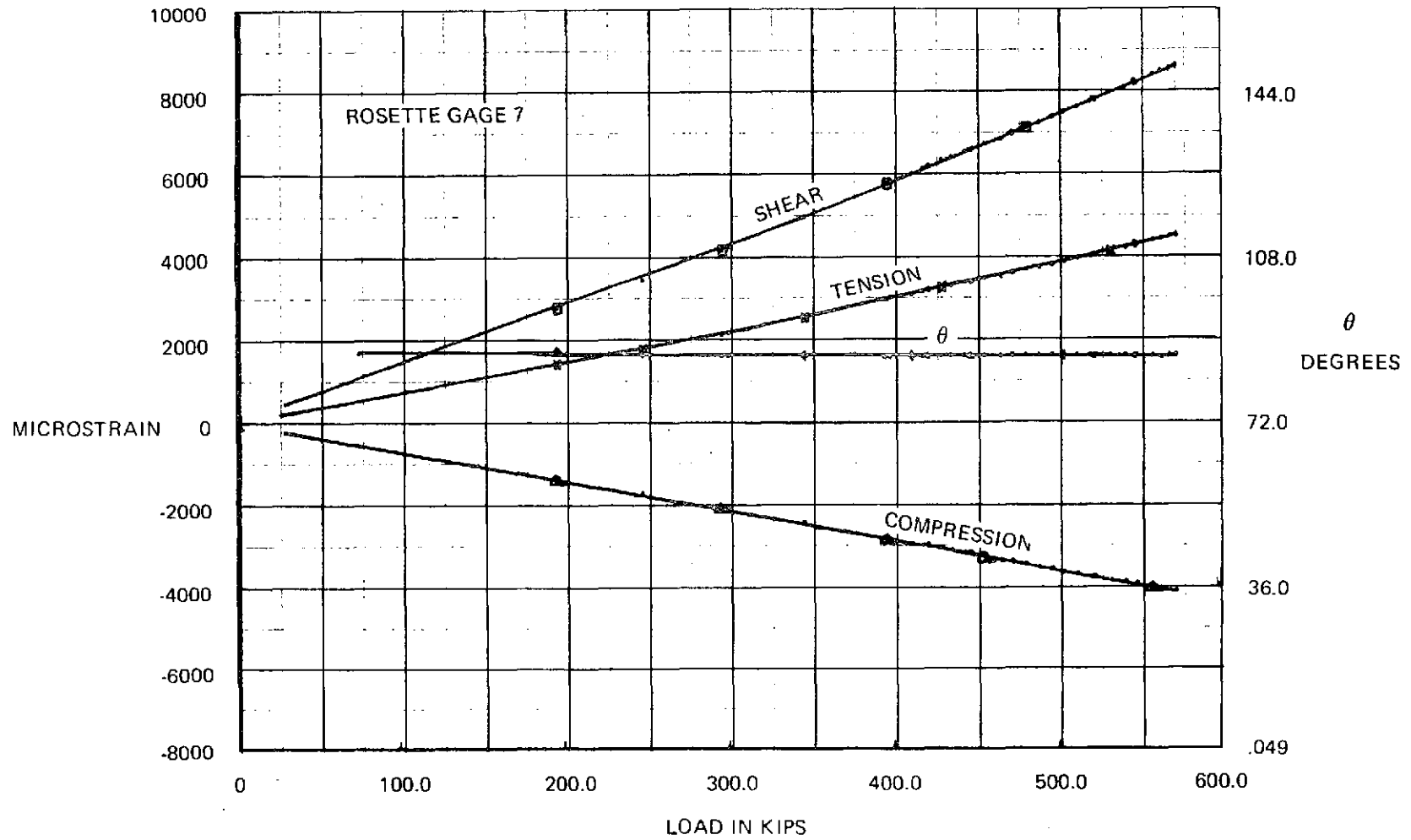
Figure A-35 : TEST WEB 3 PRINCIPAL STRAIN DATA
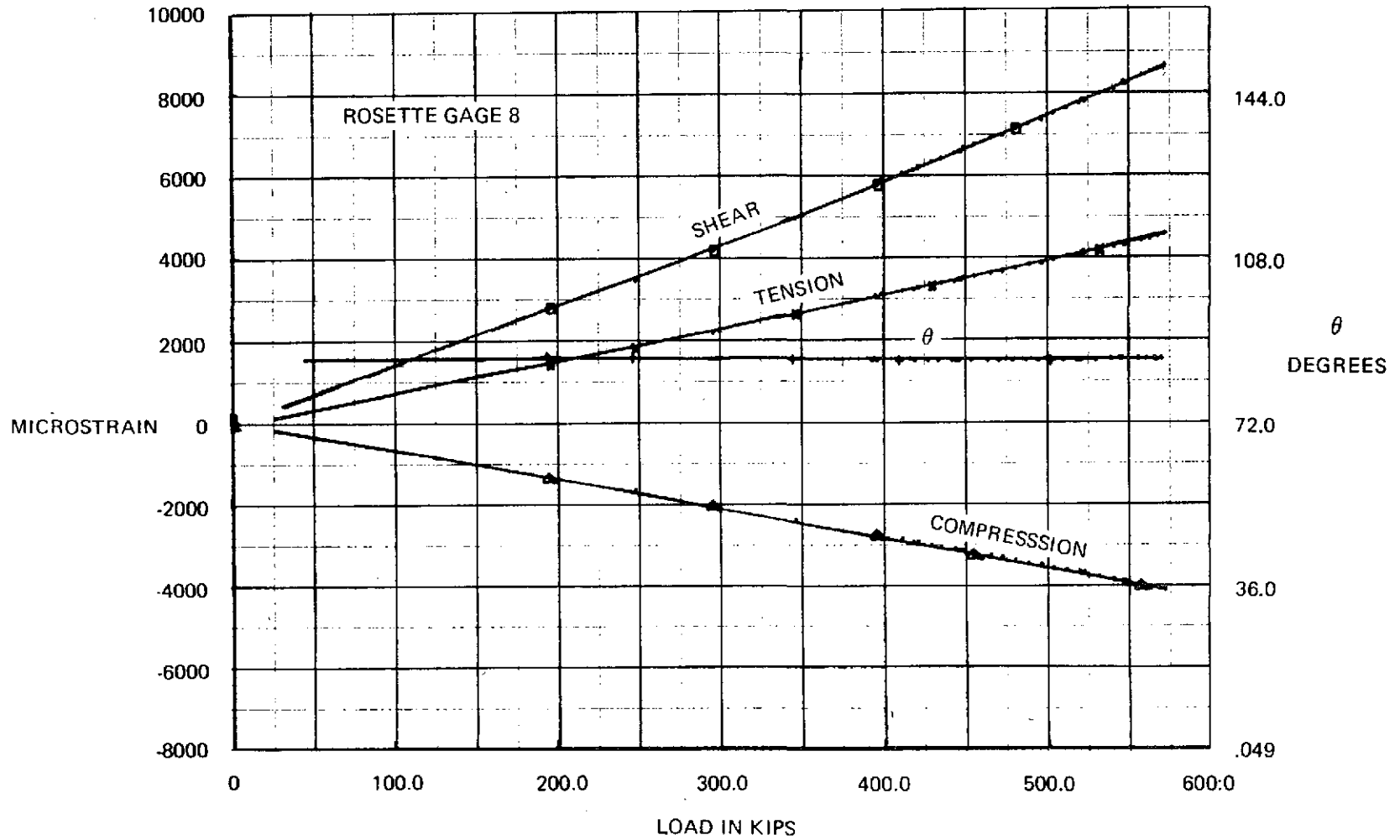
Figure A-36 : TEST WEB 3 PRINCIPAL STRAIN DATA

185
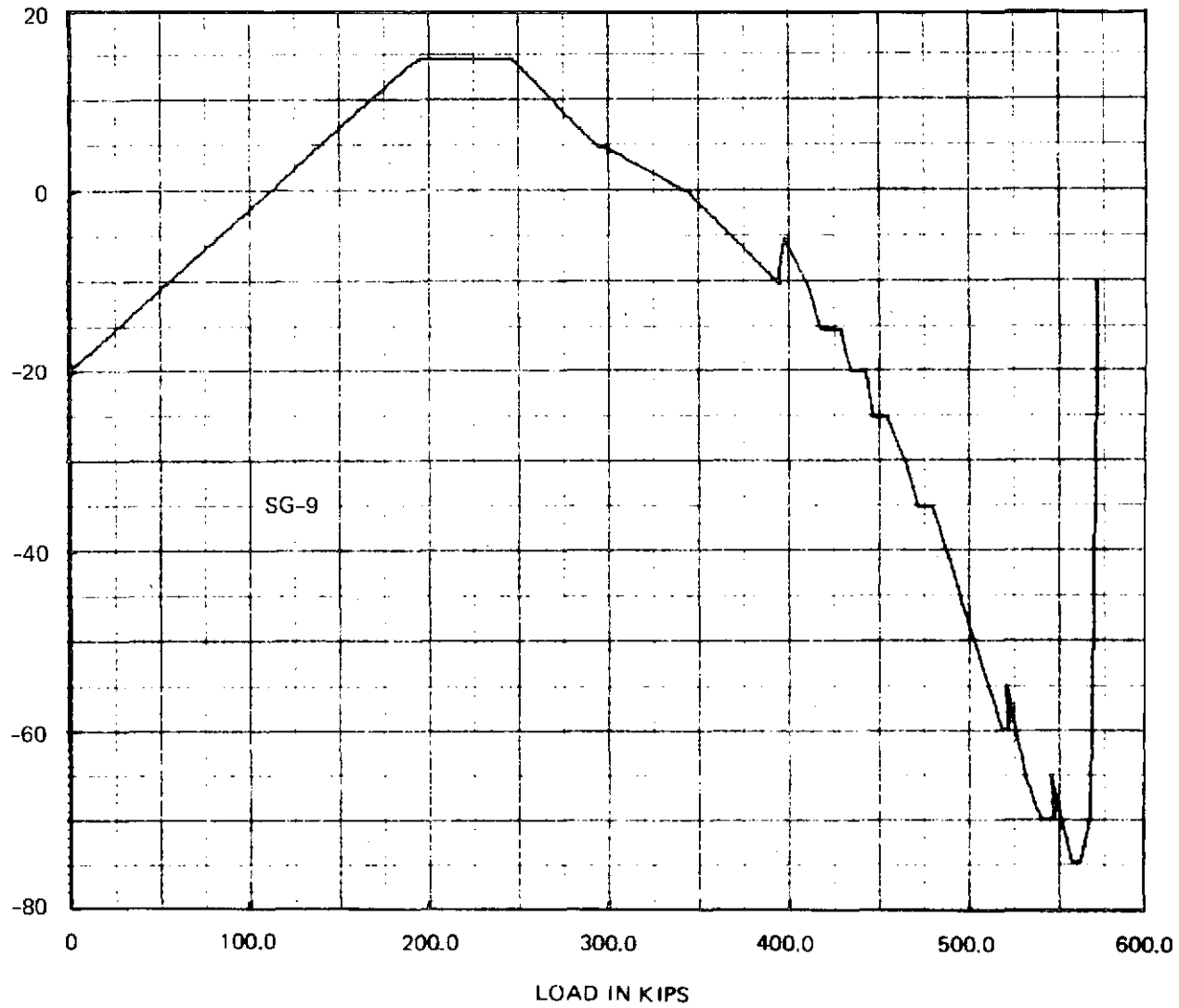
Figure A-37 : TEST WEB 3 PRINCIPAL STRAIN DATA

MICROSTRAIN

LOAD IN KIPS
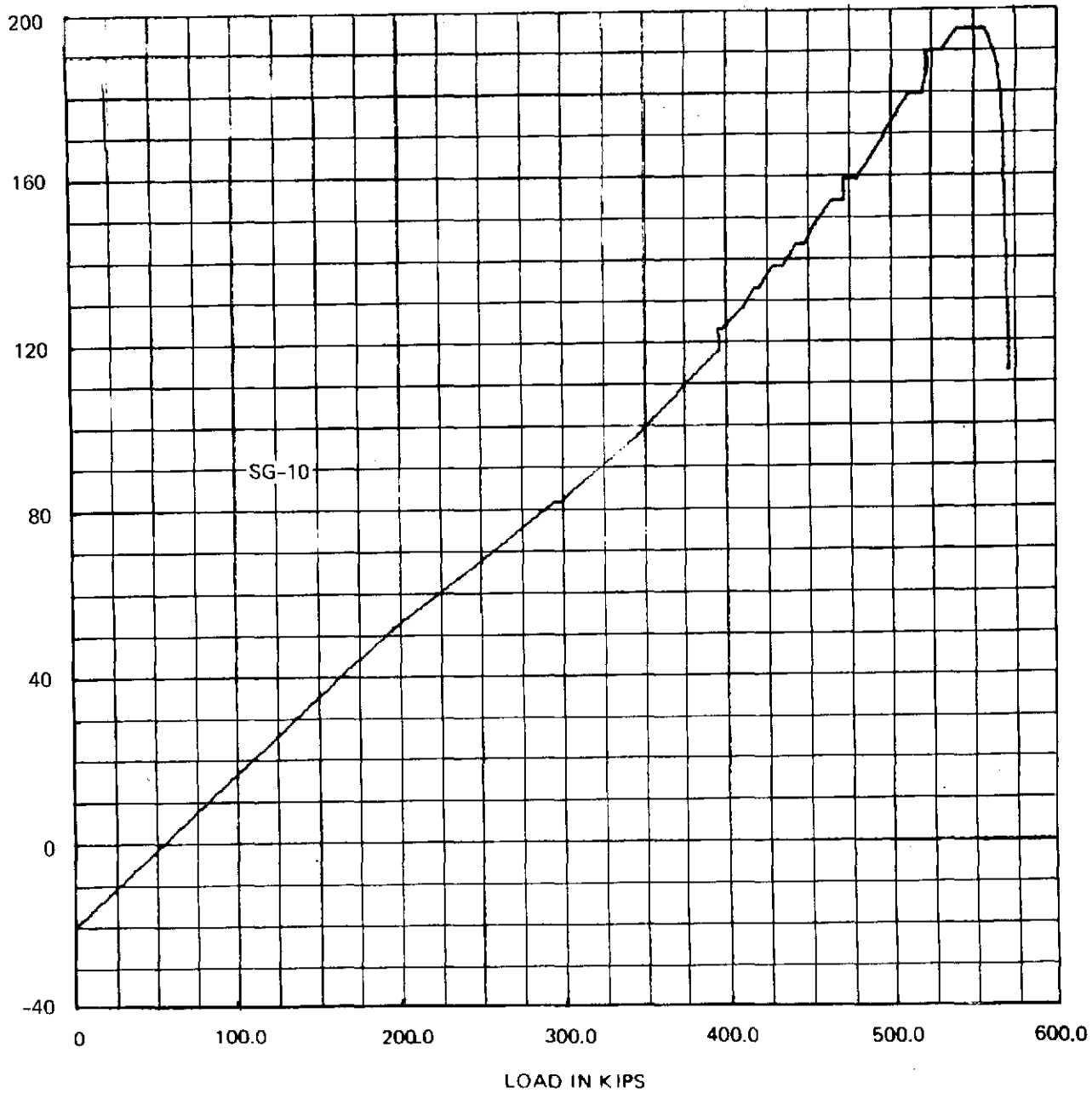
Figure A-38 : TEST WEB 3 PRINCIPAL STRAIN DATA

187

C3

MICROSTRAIN

SG-11

LOAD IN KIPS
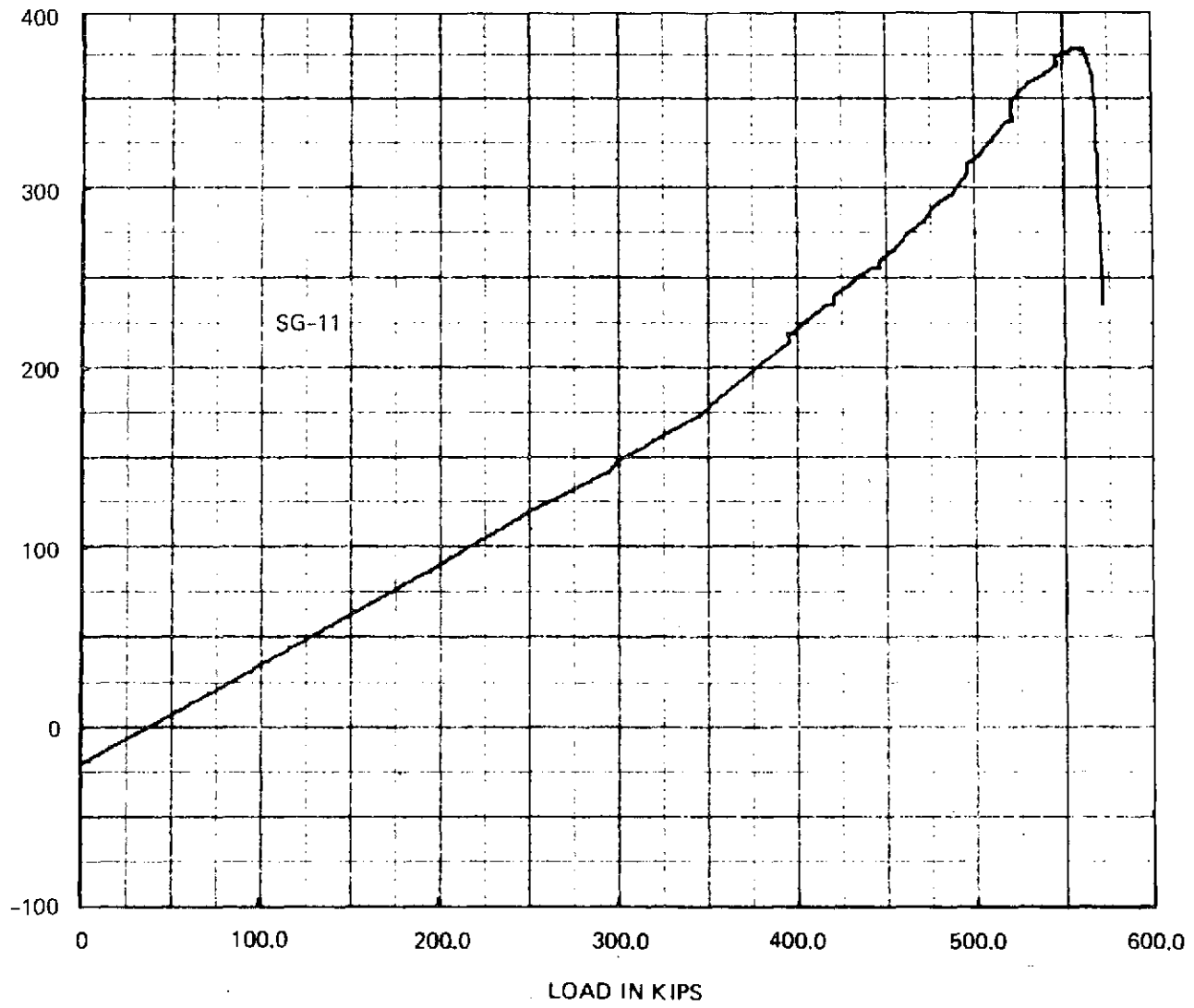
Figure A-39 :   TEST WEB 3 PRINCIPAL STRAIN DATA

MICROSTRAIN

LOAD IN KIPS
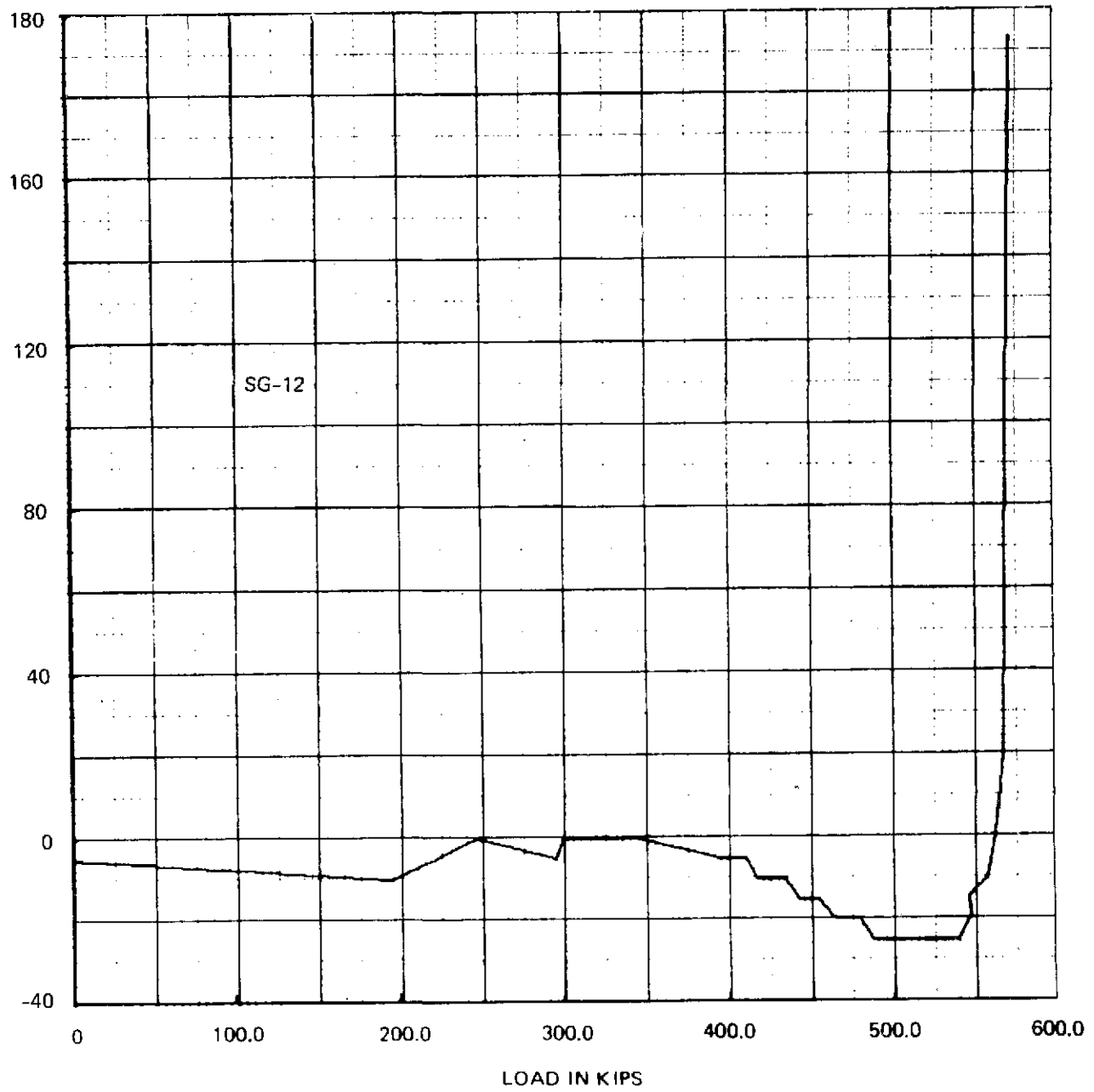
Figure A-40 : TEST WEB 3 PRINCIPAL STRAIN DATA

189

MICROSTRAIN

LOAD IN KIPS
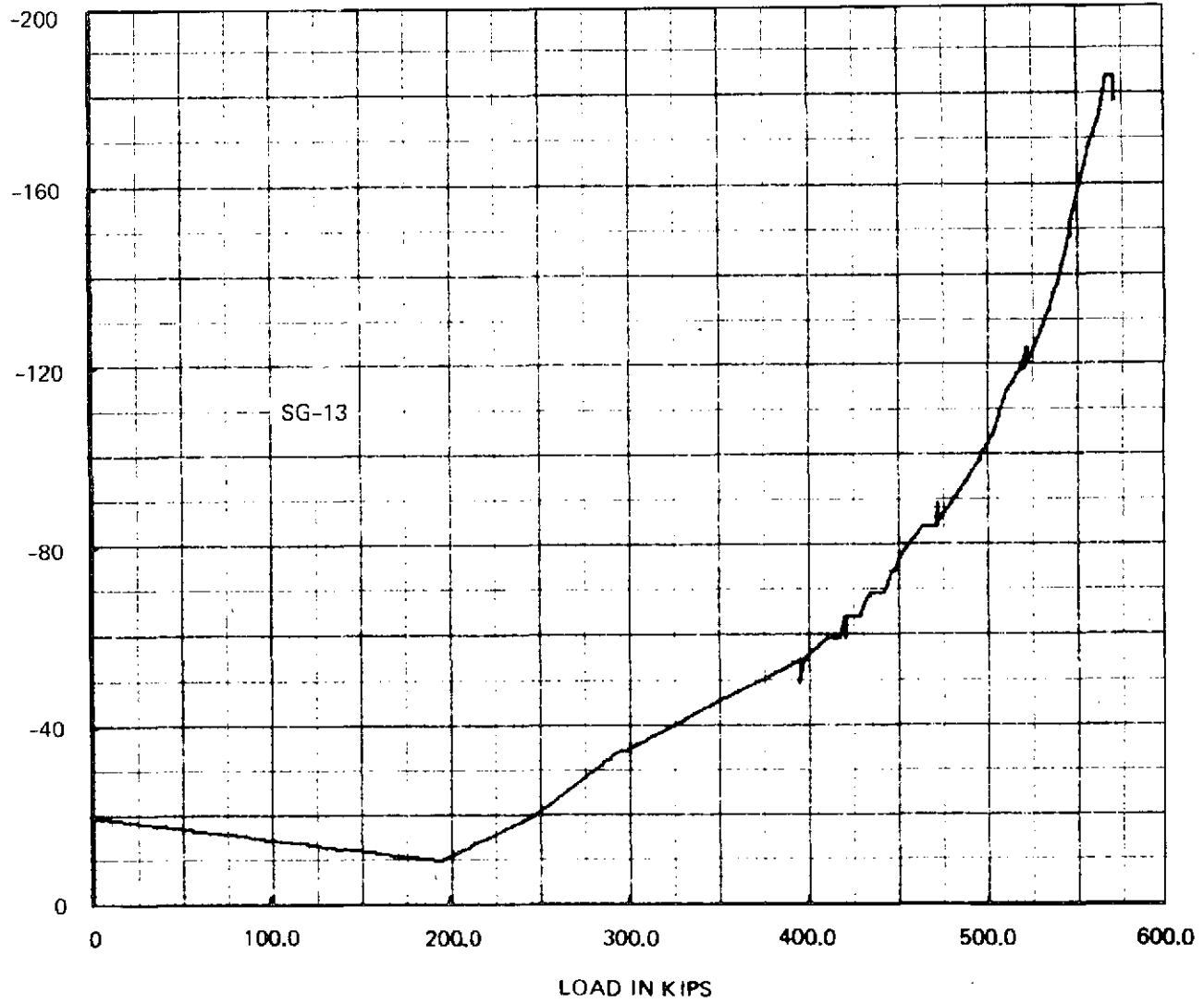
Figure A-41 : TEST WEB 3 PRINCIPAL STRAIN DATA
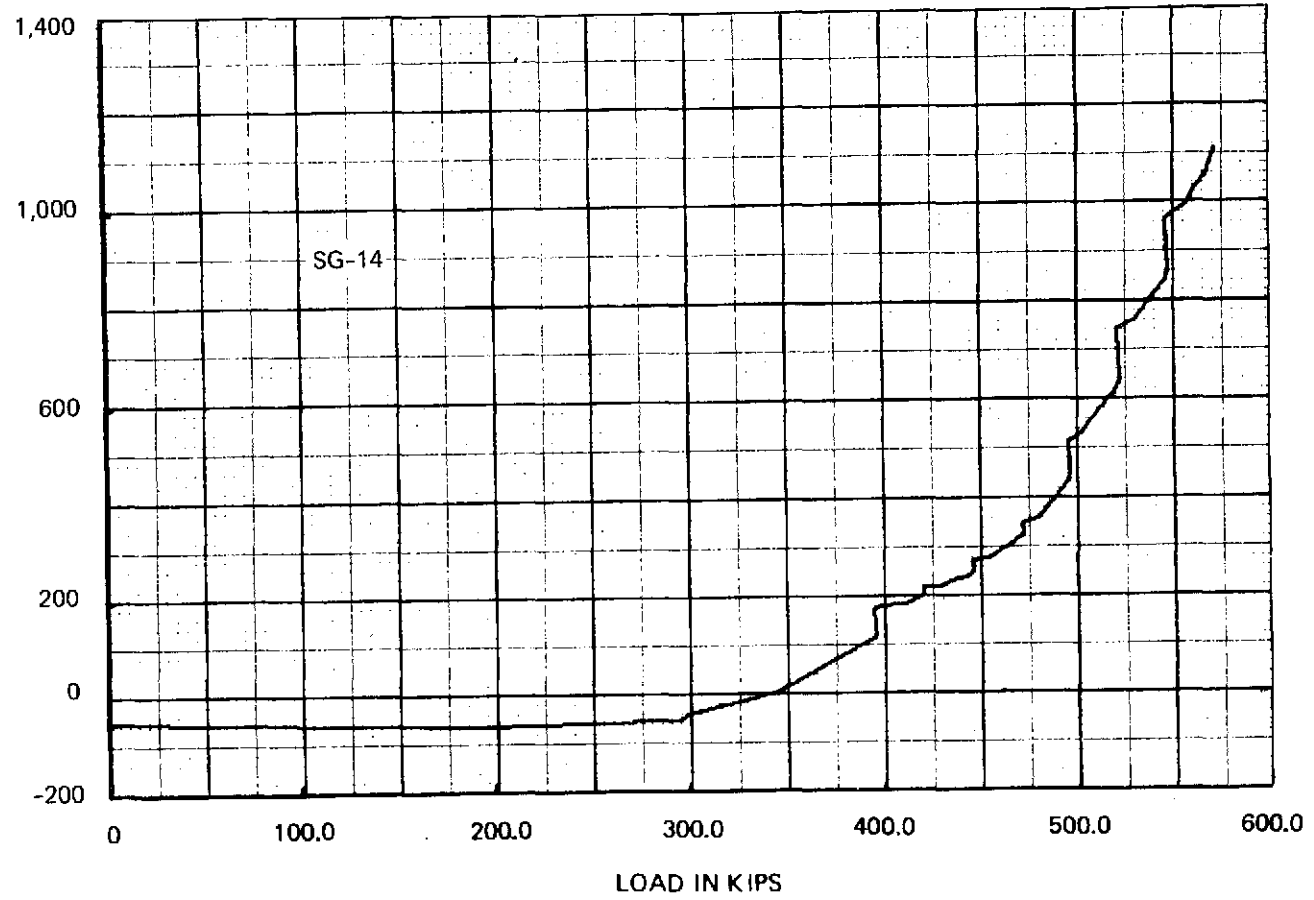
Figure A-42 : TEST WEB 3 PRINCIPAL STRAIN DATA

MICROSTRAIN

LOAD IN KIPS
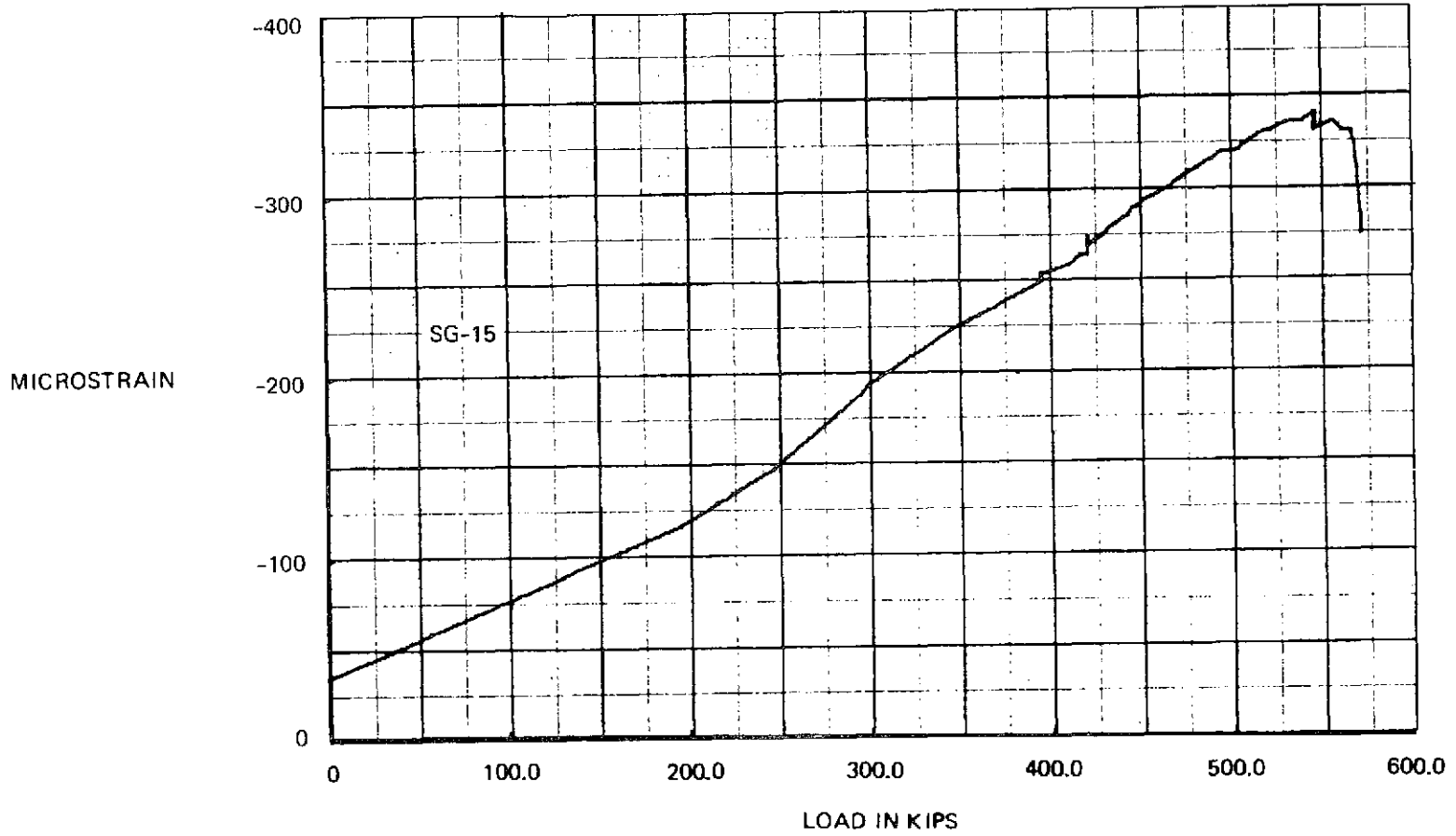
Figure A-43 : TEST WEB 3 PRINCIPAL STRAIN DATA

MICROSTRAIN

193
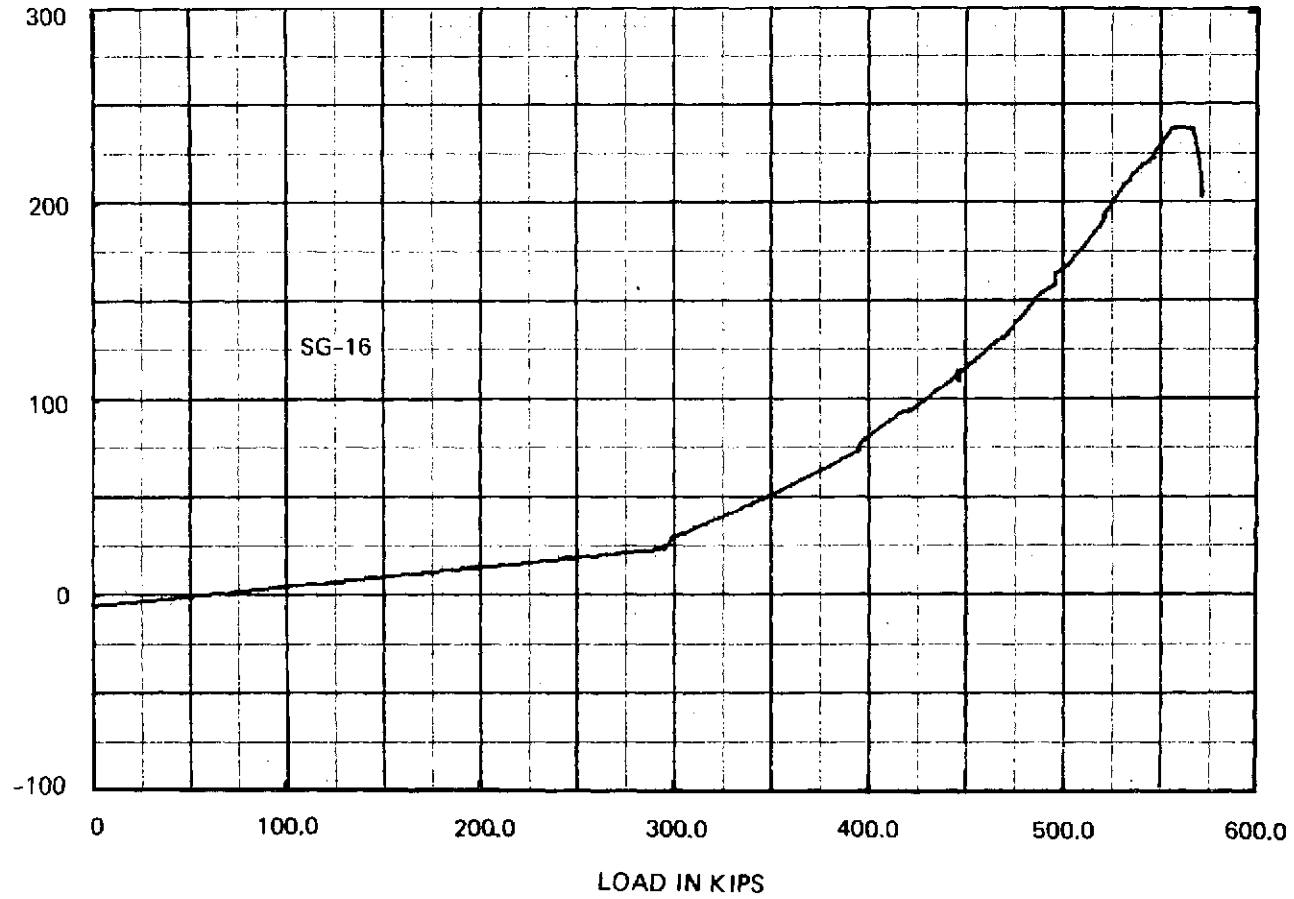
Figure A-44 : TEST WEB 3 PRINCIPAL STRAIN DATA
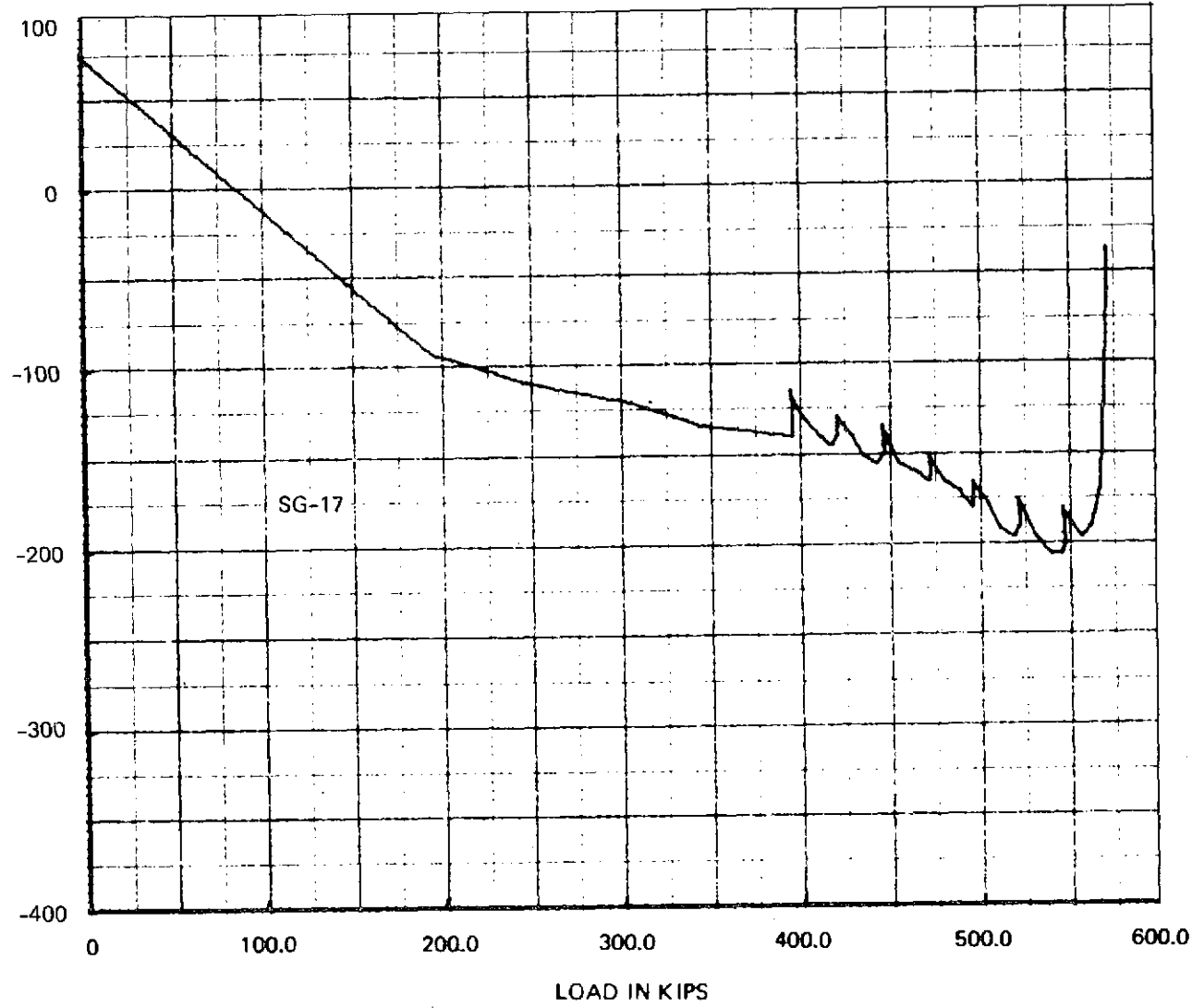
Figure A-45 : TEST WEB 3 PRINCIPAL STRAIN DATA
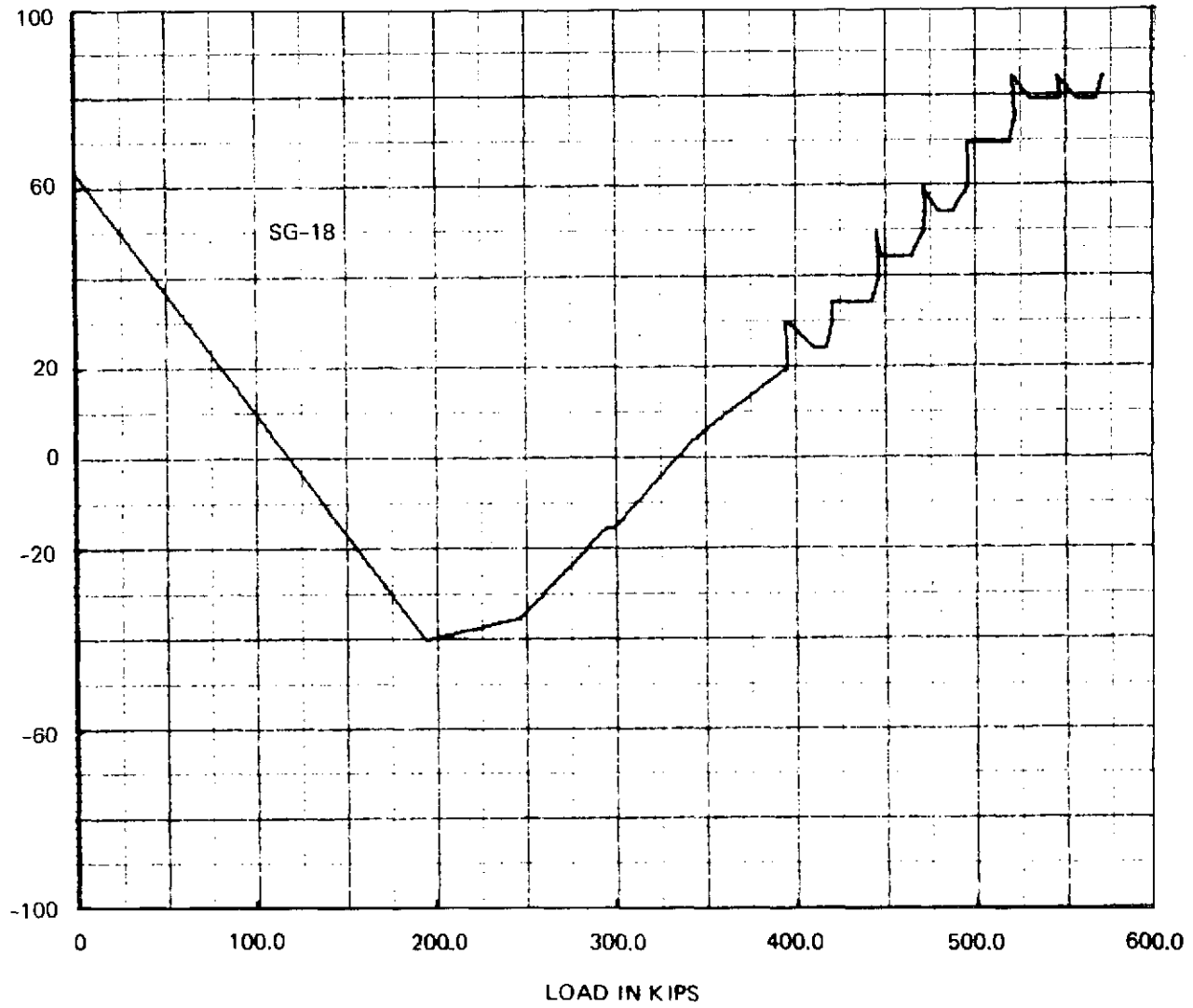
Figure A-46 : TEST WEB 3 PRINCIPAL STRAIN DATA
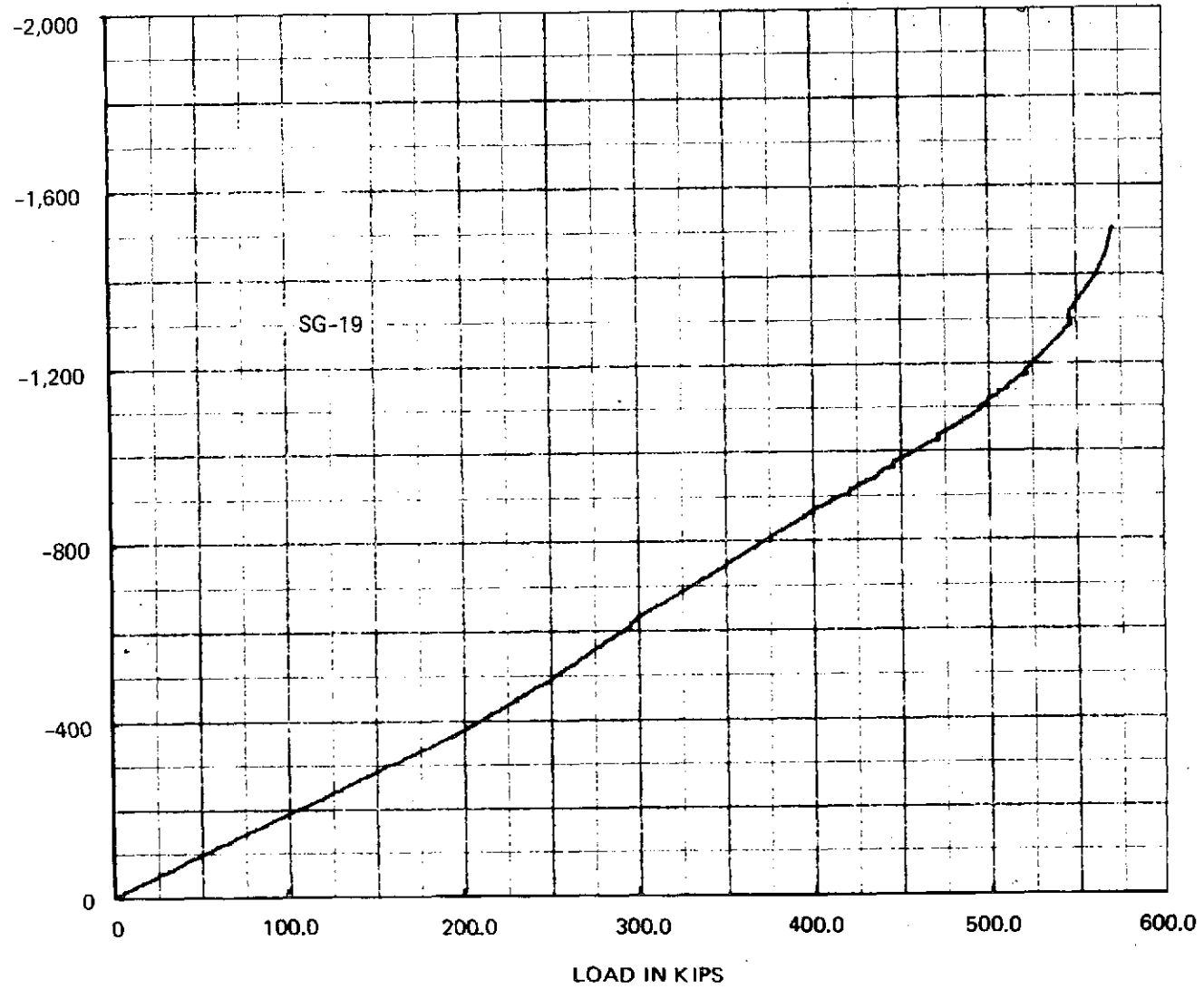
Figure A-47 : TEST WEB 3 PRINCIPAL STRAIN DATA

MICROSTRAIN

LOAD IN KIPS

197
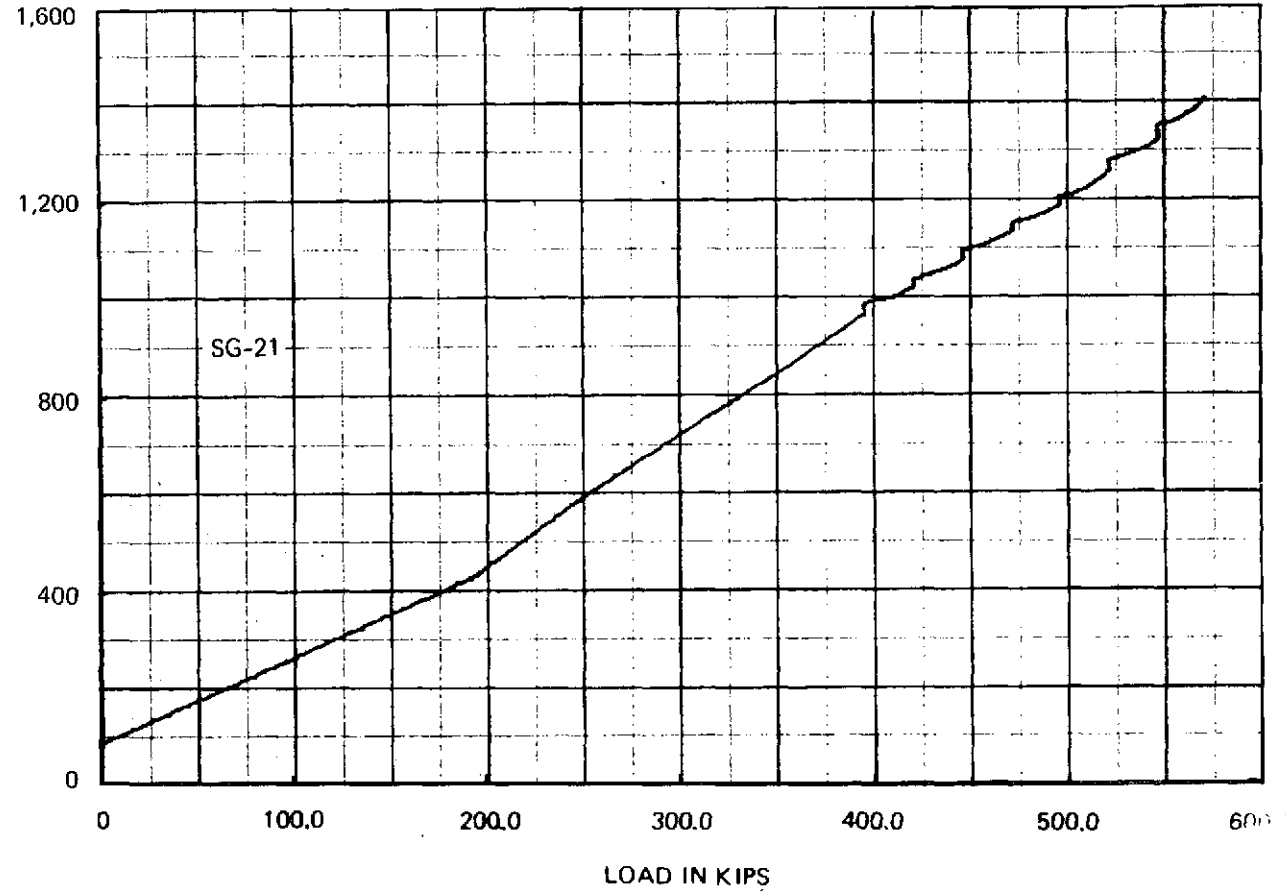
Figure A-48 : TEST WEB 3 PRINCIPAL STRAIN DATA
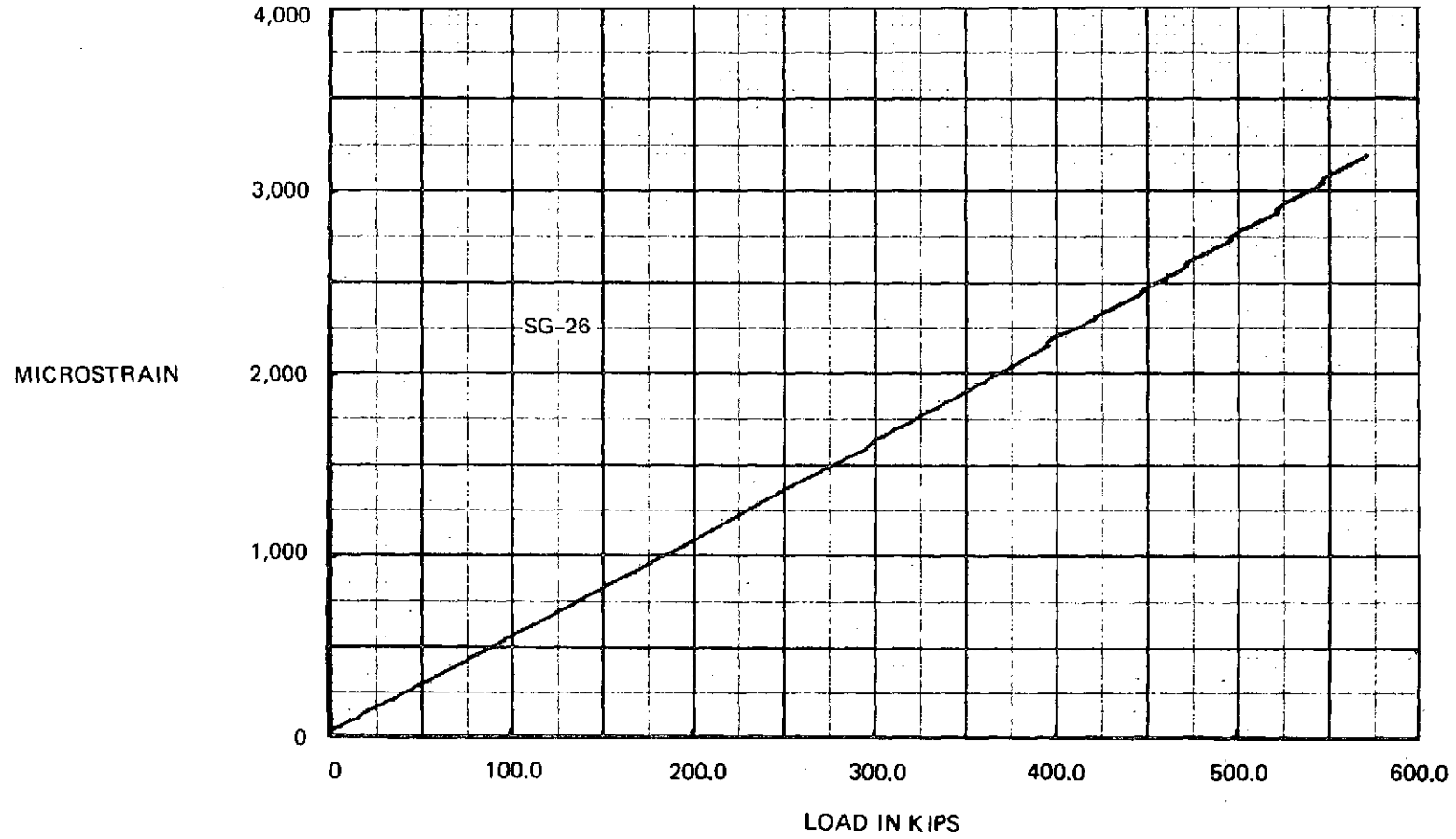
Figure A-49 : TEST WEB 3 PRINCIPAL STRAIN DATA
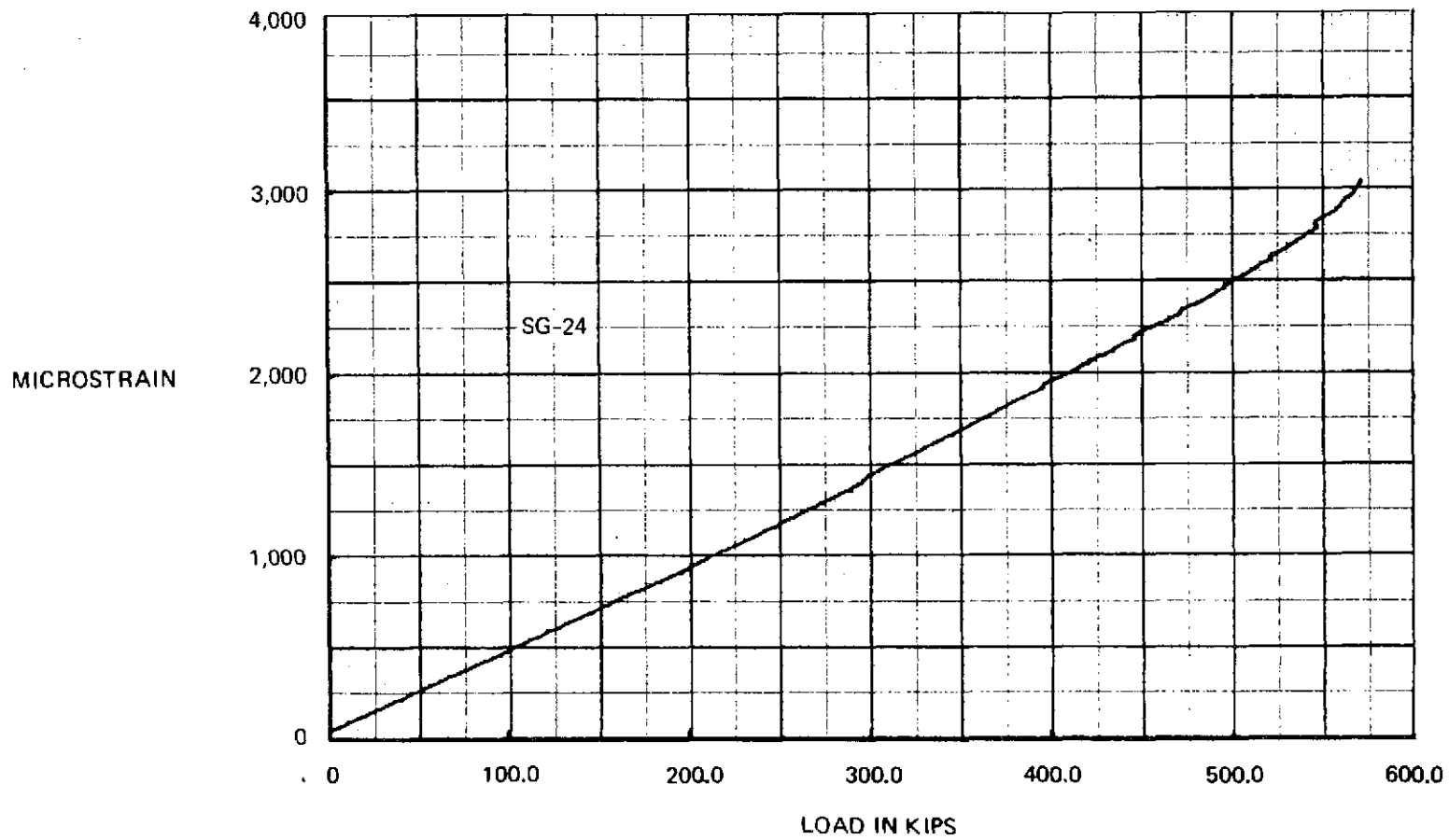
Figure A-50 : TEST WEB 3 PRINCIPAL STRAIN DATA

APPENDIX B   MOIRE FRINGE DATA

The sequential moire fringe patterns for the final loading of the
second and third test web components are given in this appendix.   The
loaded patterns are preceded by zero biased patterns which were produced
by shimming the lower glass supports 0.25 in. (6.35 mm) outward.   The
biased patterns are used for establishing fringe order calibration
factors and initial web imperfections.
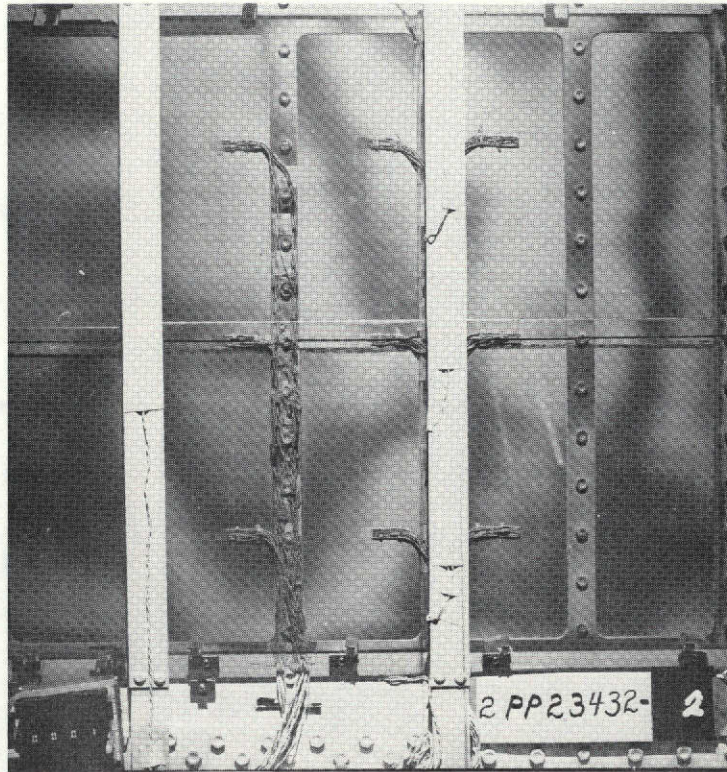
Figure B-1: TEST WEB 2 AT ZERO LOAD WITH BIASED GRID PANES
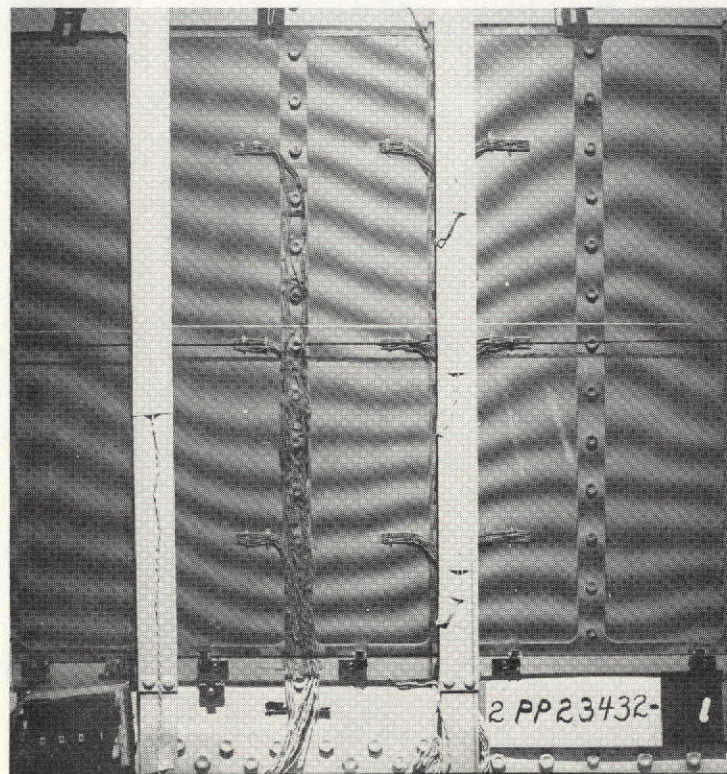
Figure B-2: TEST WEB 2 AT ZERO LOAD BEFORE LOAD CYCLING
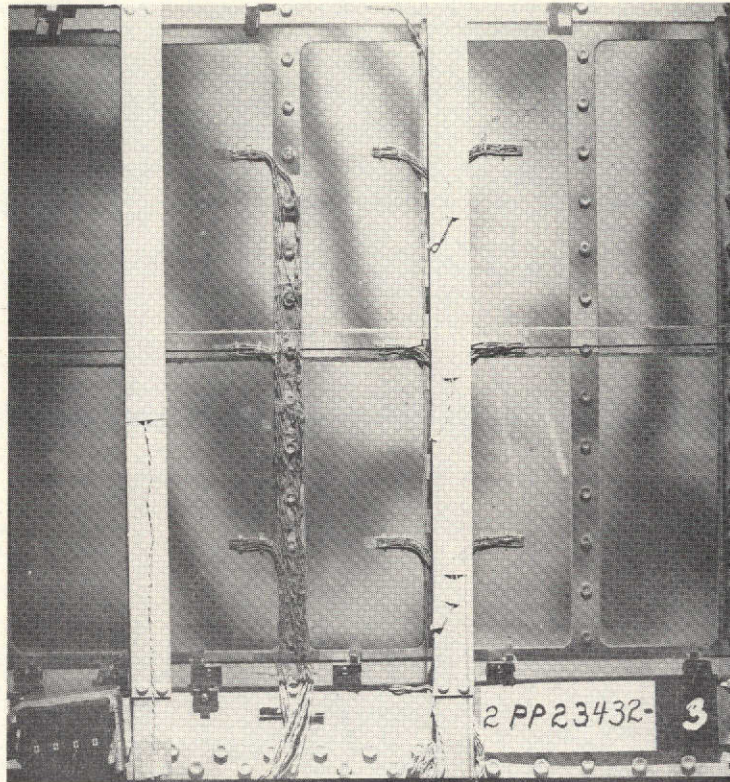
Figure B-3: TEST WEB 2 AT ZERO LOAD AFTER LOAD CYCLING
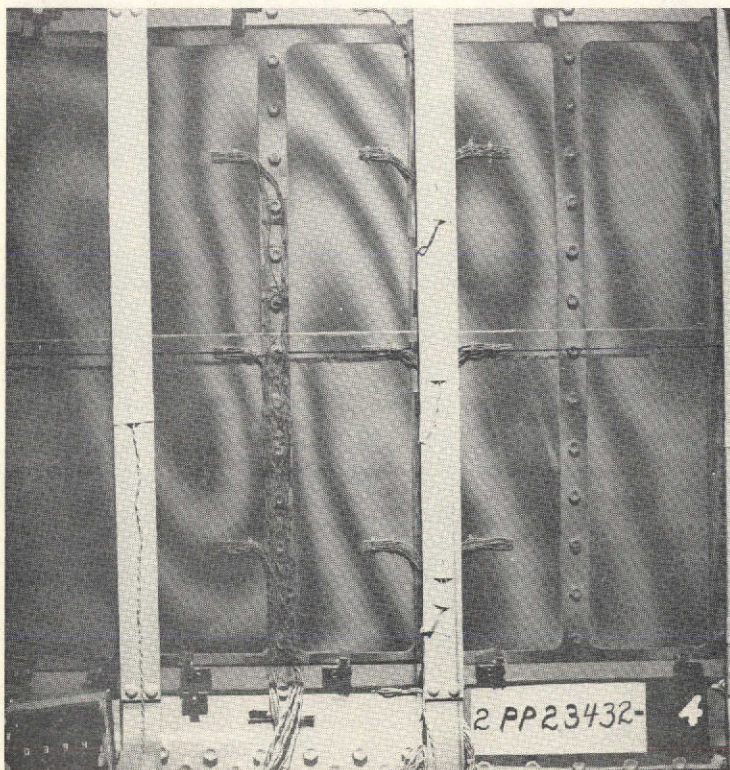
Figure B-4: TEST WEB 2 AT 394,000 LB (1.75 MN) IN 11TH LOADING

203
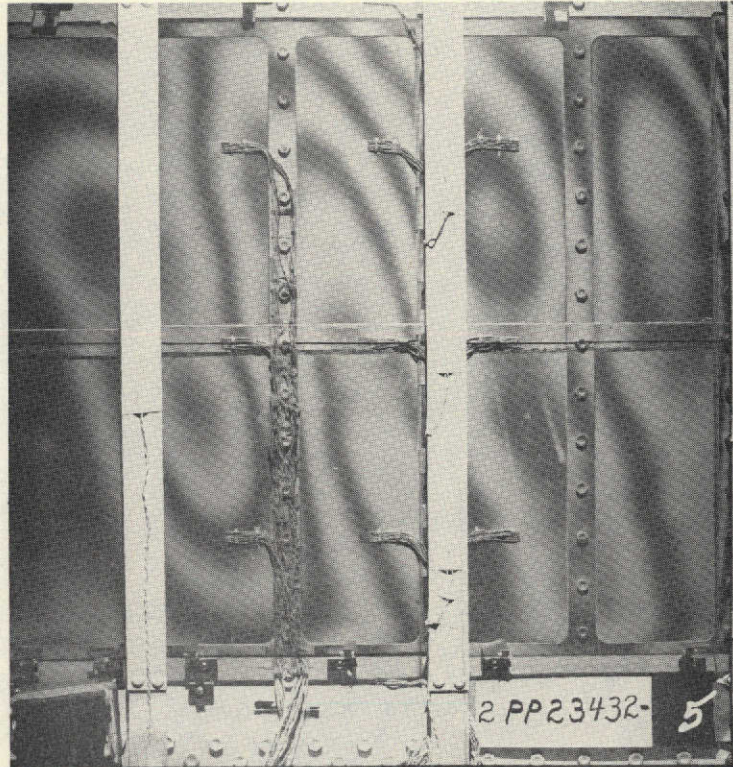
Figure B-5: TEST WEB 2 AT 400,000 LB (1.78 MN) IN 400TH LOADING
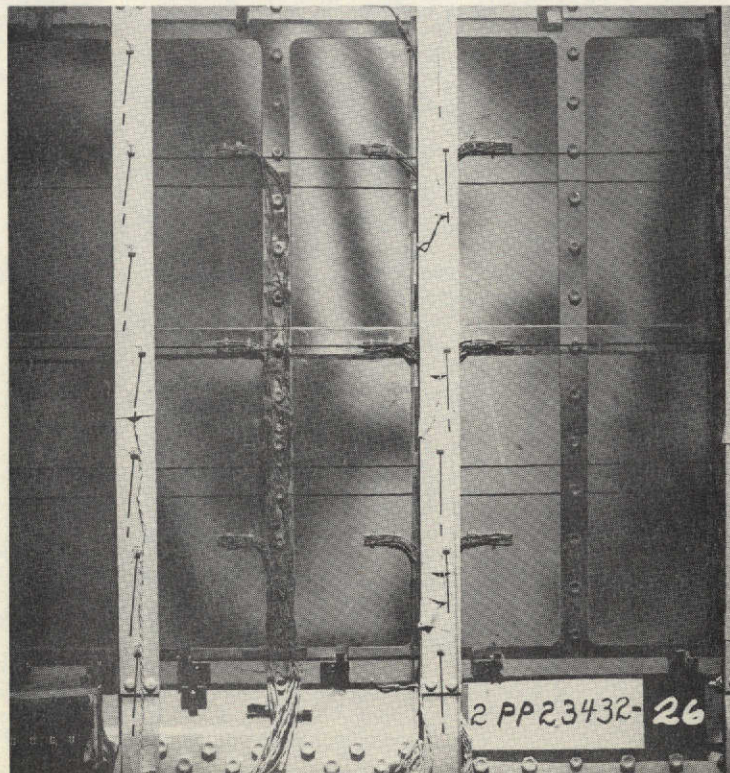
Figure B-6: ZERO LOAD PRIOR TO 409TH LOADING

204
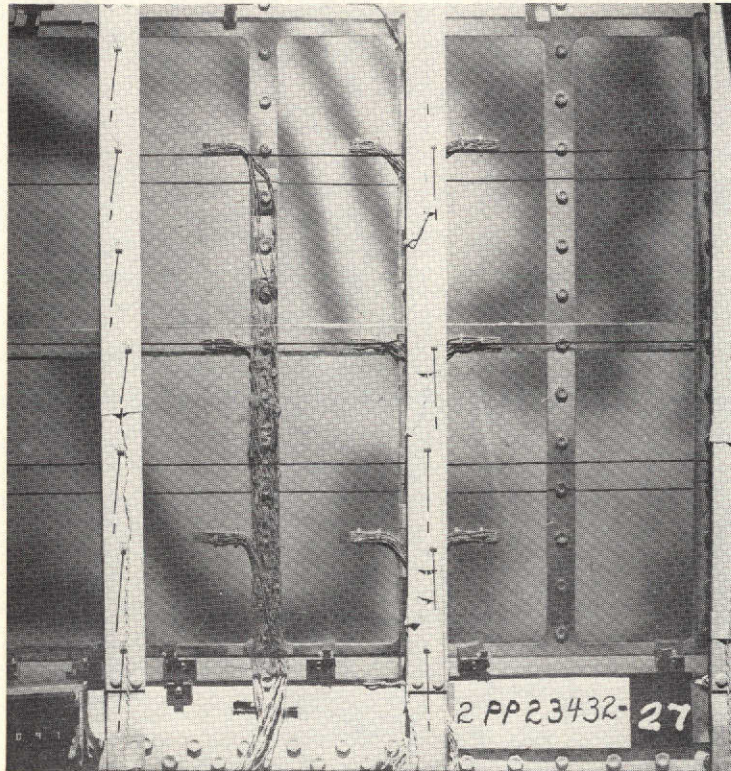
Figure B-7: 97000 LB (0.43 MN) IN 409TH LOADING
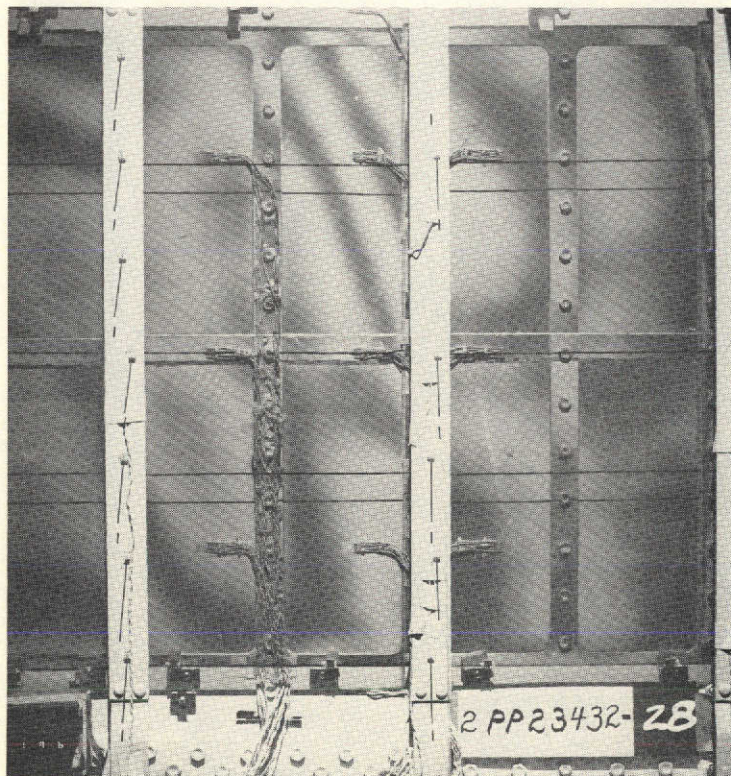
Figure B-8: 196,000 (0.87 MN) IN 409TH LOADING
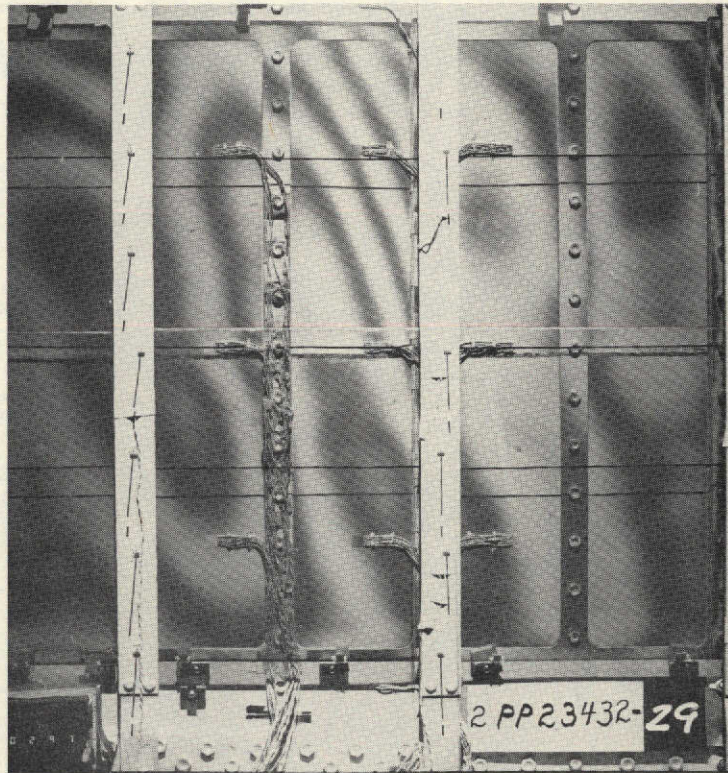
Figure B-9: 297,000 LB (1.32 MN) IN 409TH LOADING
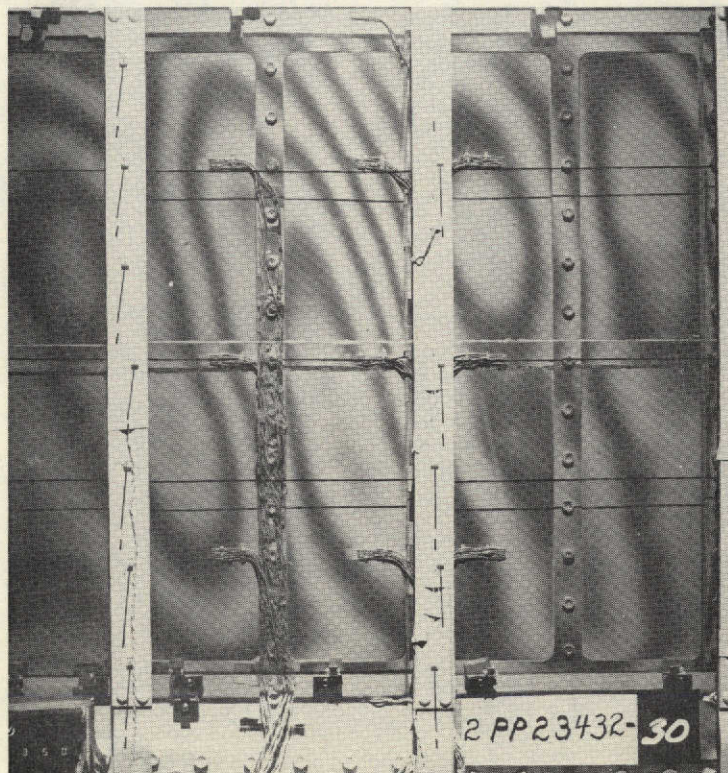
Figure B-10: 350,000 LB (1.56 MN) IN 409TH LOADING
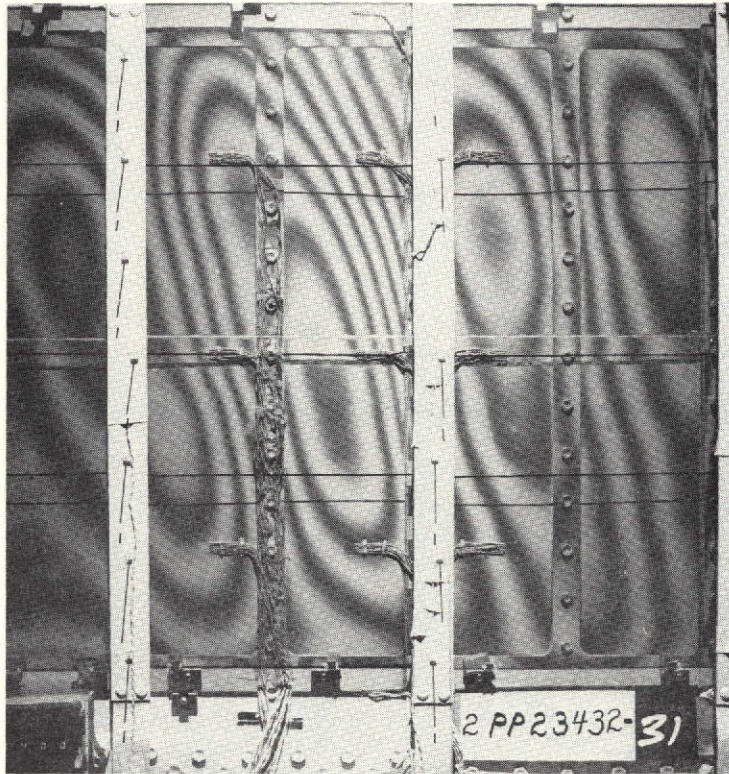
Figure B-11: 400,000 LB (1.78 MN) IN 409TH LOADING
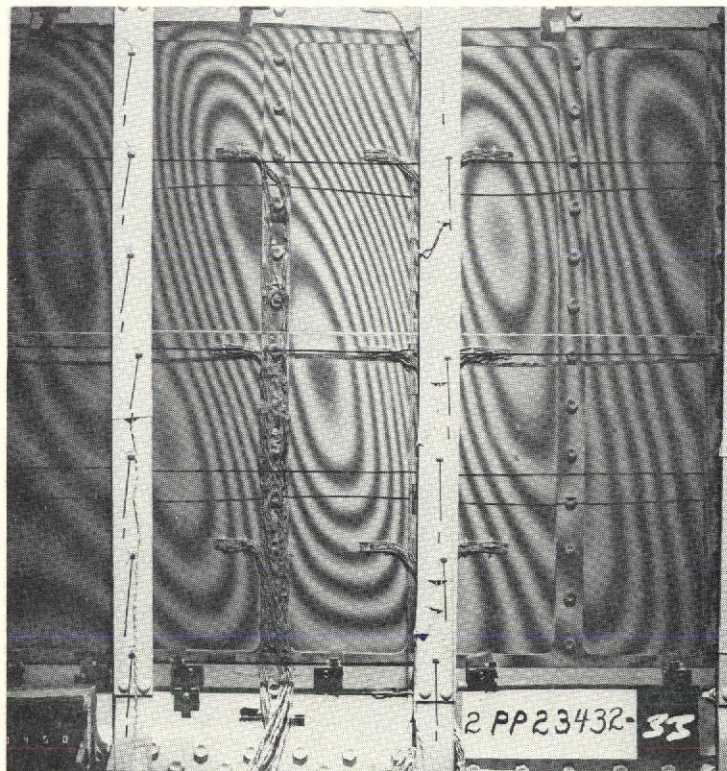
Figure B-12: 450,000 LB (2.00 MN) IN 409TH LOADING
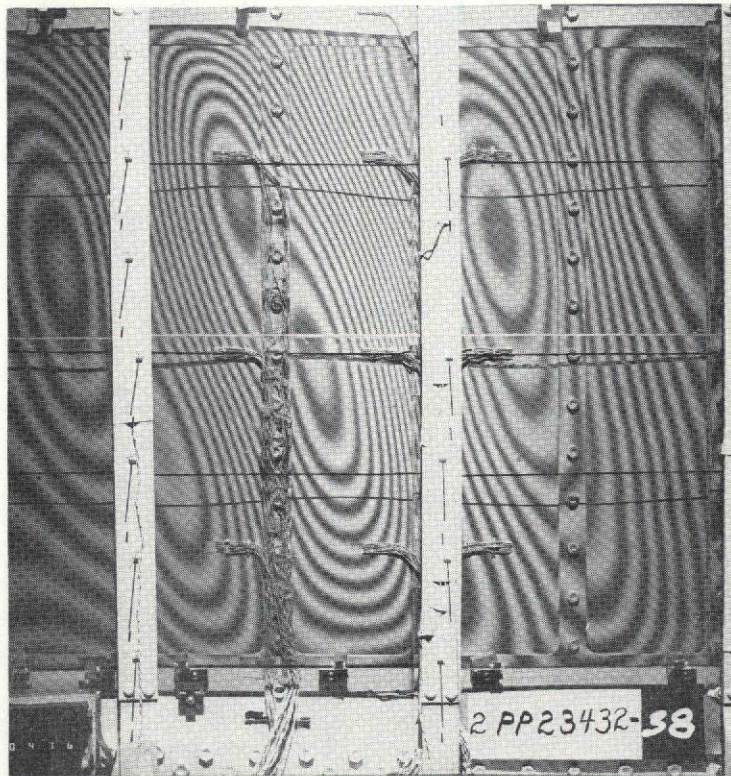
Figure B-13: 476,000 LB (2.12 MN) IN 409TH LOADING
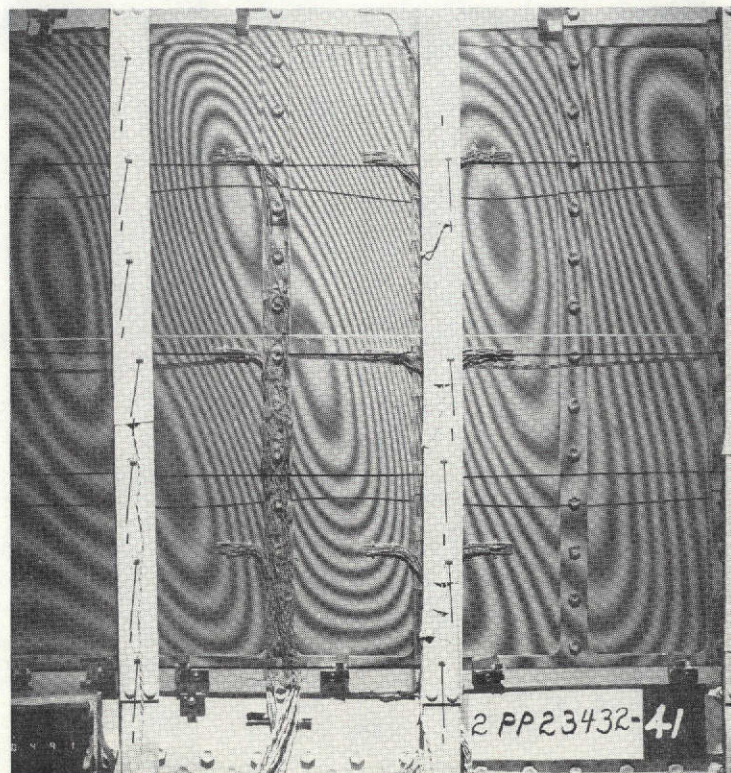
Figure B-14: TEST WEB 2 AT 491,000 LB (2.18 MN) IN 409TH LOADING
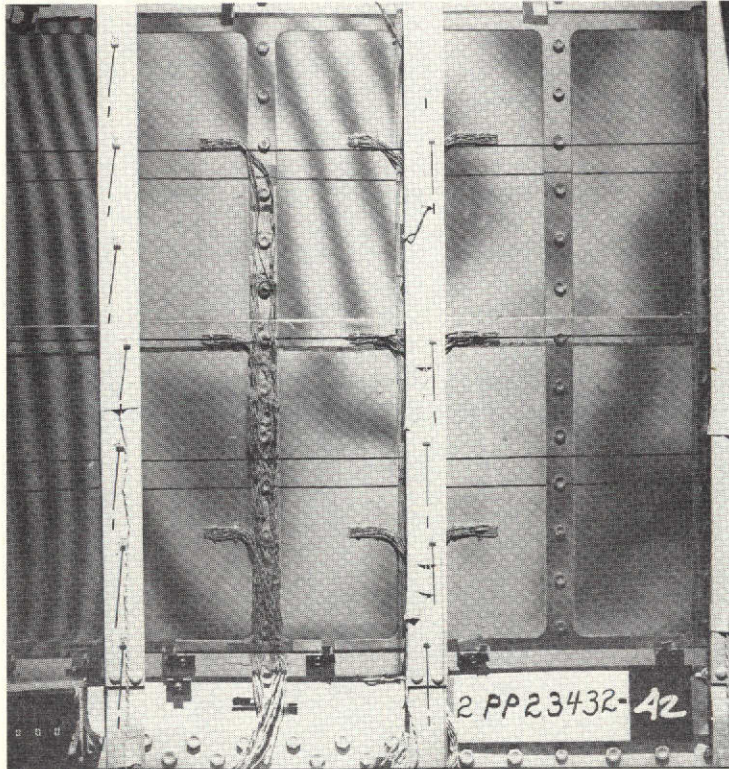
Figure B-15: TEST WEB 2 AT ZERO LOAD PRIOR TO FINAL 410TH LOADING
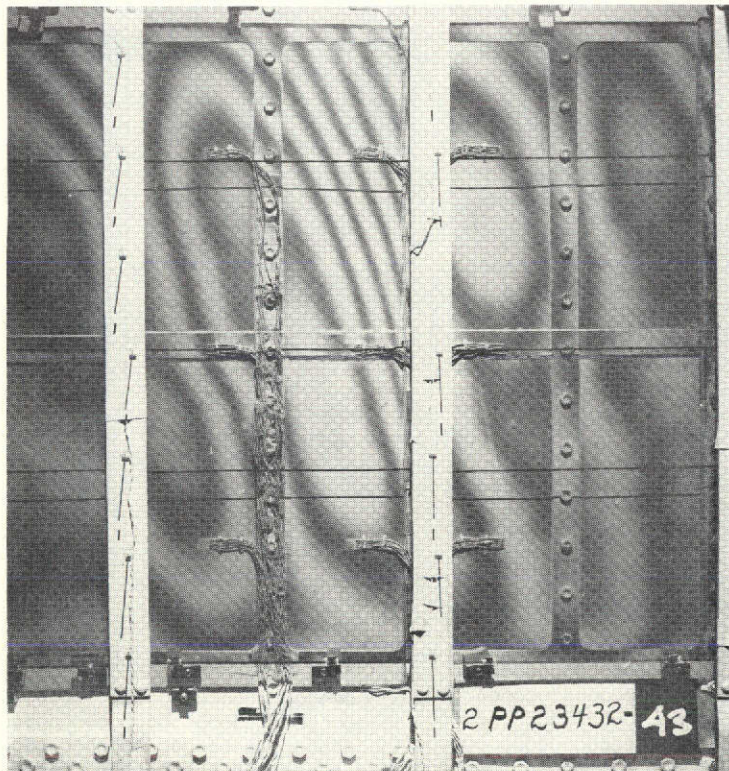
Figure B-16: TEST WEB 2 AT 300,000 LB (1.33 MN) IN 410TH LOADING
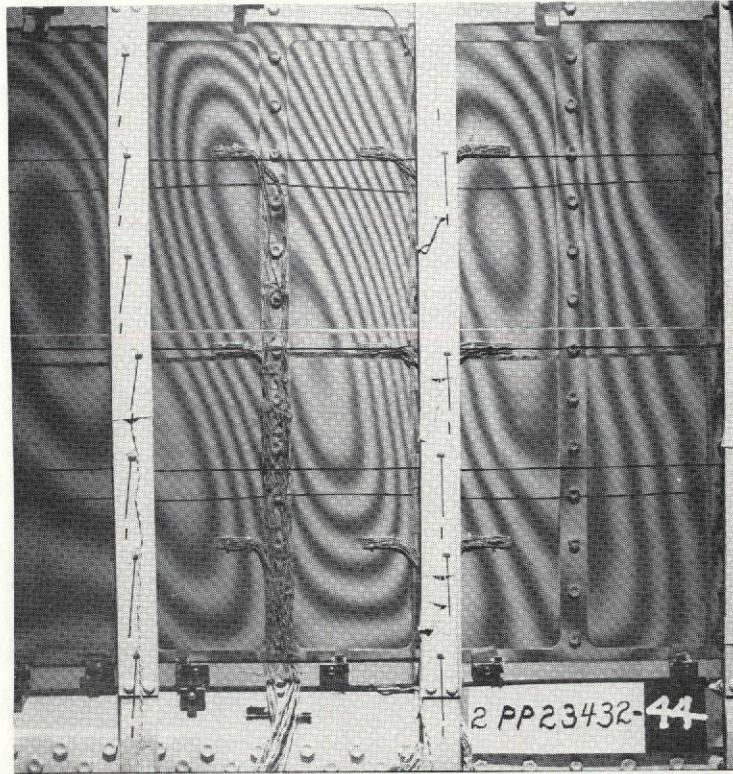
Figure B-17: TEST WEB 2 AT 400,000 LB (1.78 MN) IN 410TH LOADING
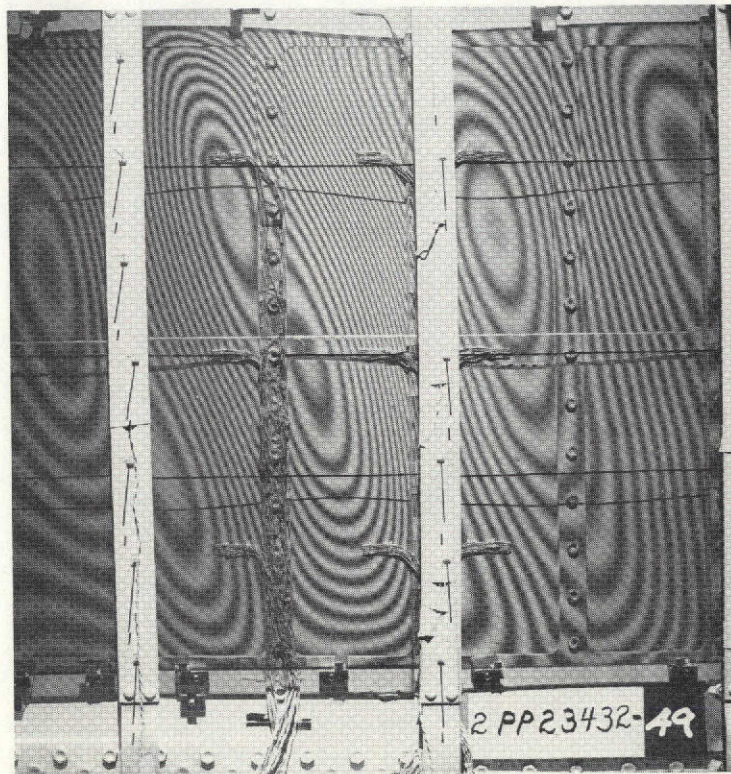
Figure B-18: TEST WEB 2 AT 500,000 LB (2.22 MN) IN 411TH (FINAL) LOADING
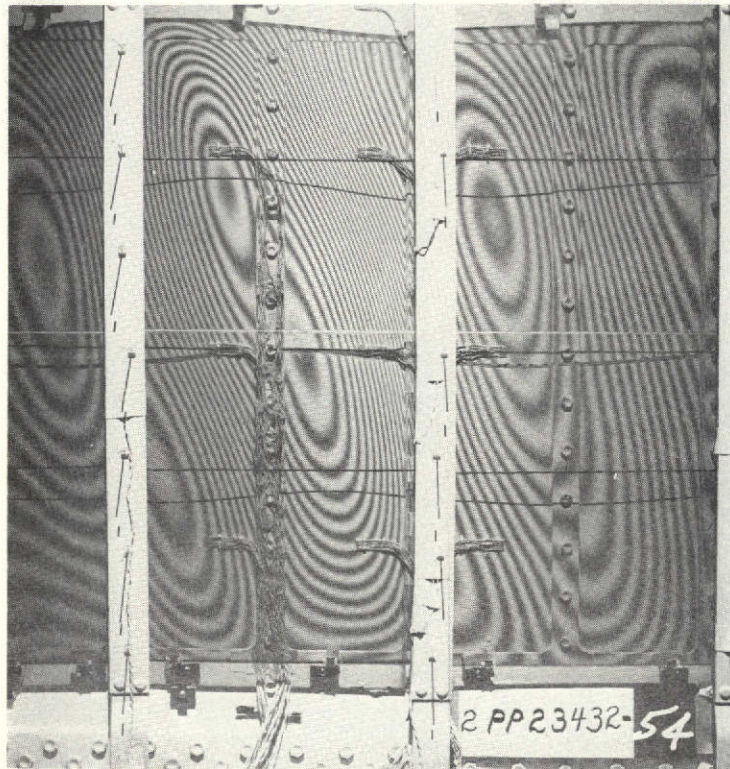
Figure B-19: TEST WEB 2 AT 525,000 LB (2.34 MN) IN 411th (FINAL) LOADING
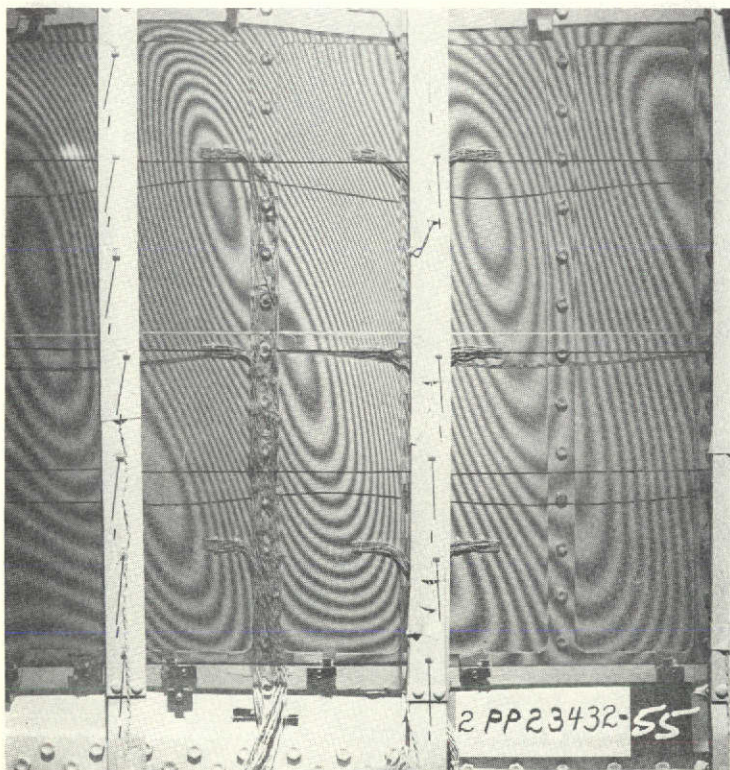
Figure B-20: TEST WEB 2 AT 530,000 LB (2.36 MN) MAXIMUM LOAD IN 411TH (FINAL) LOADING
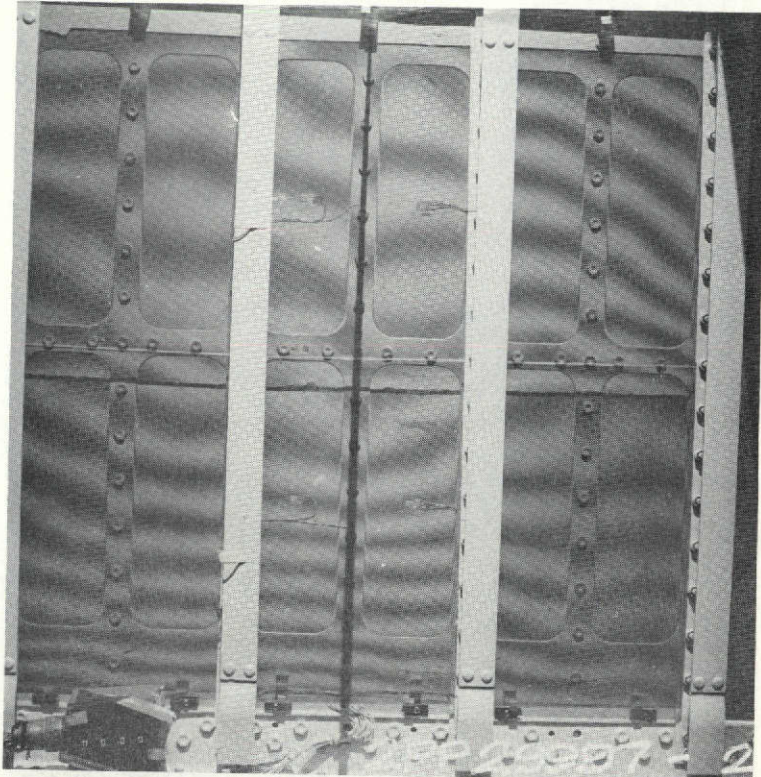
Figure B-21: TEST WEB 3 AT ZERO LOAD WITH BIASED GRID PANES
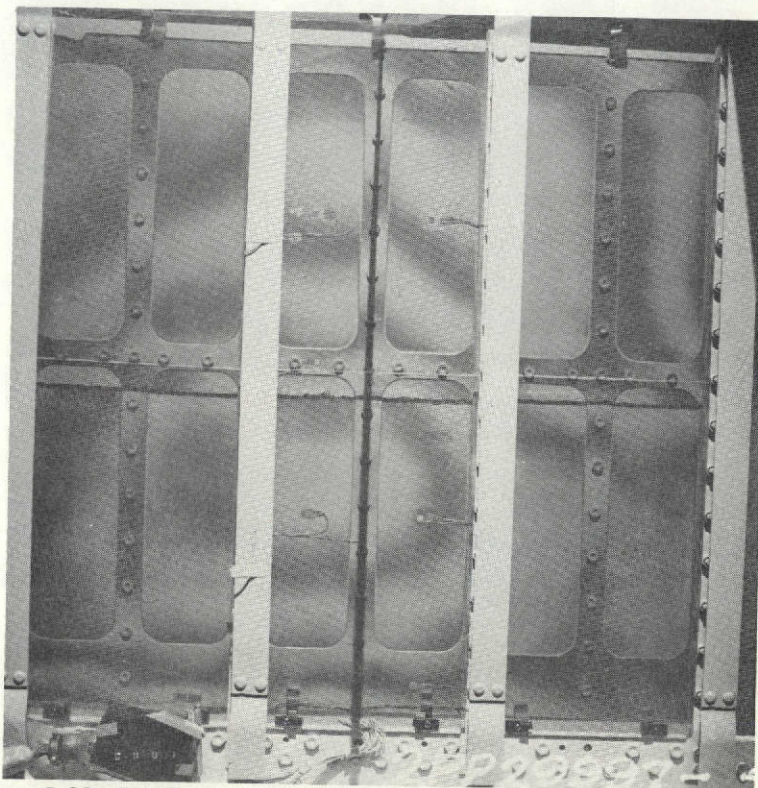
Figure B-22: TEST WEB 3 AT ZERO LOAD PRIOR TO FINAL LOADING
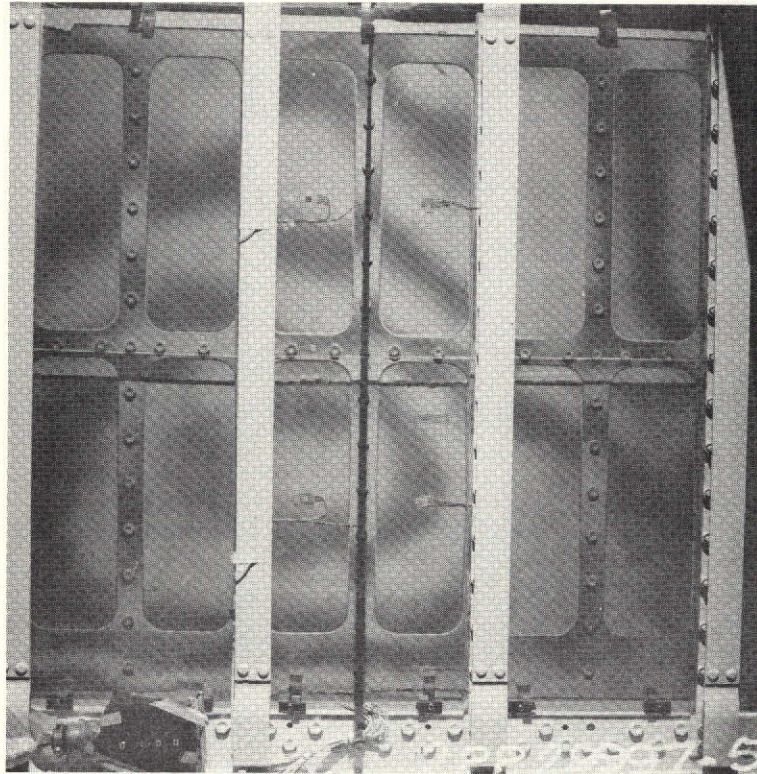
Figure B-23: TEST WEB 3 AT 100,000 LB (0.44 MN) IN FINAL LOADING
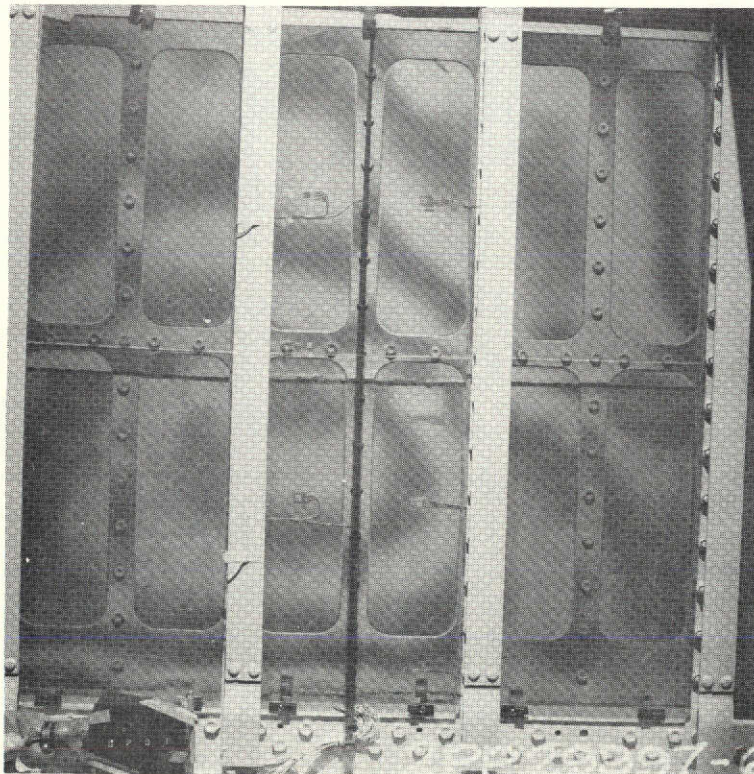
Figure B-24: TEST WEB 3 AT 201,000 LB (0.89 MN) IN FINAL LOADING
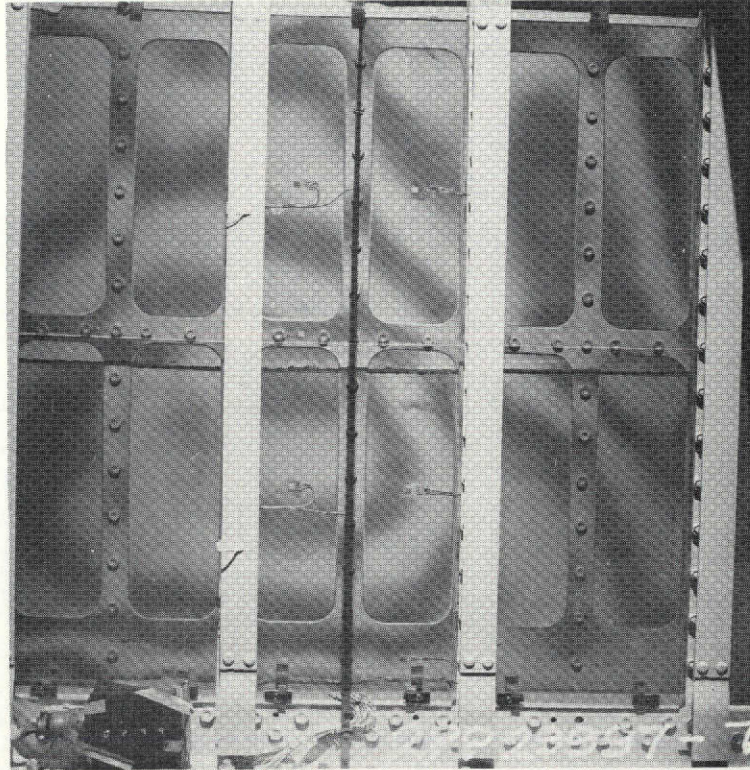
Figure B-25: TEST WEB 3 AT 299,000 LB (1.33 MN) IN FINAL LOADING
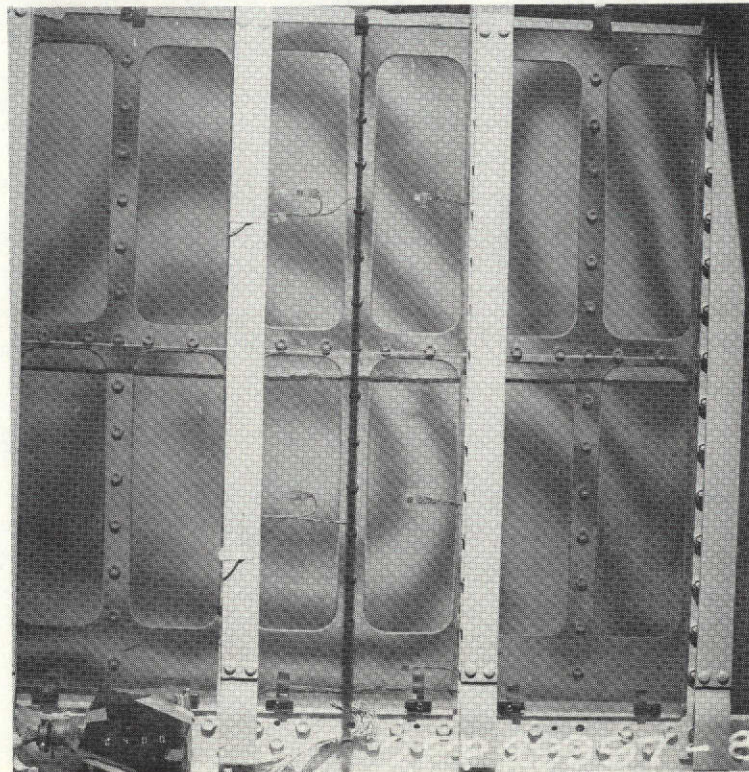
Figure B-26: TEST WEB 3 AT 400,000 LB (1.78 MN) IN FINAL LOADING
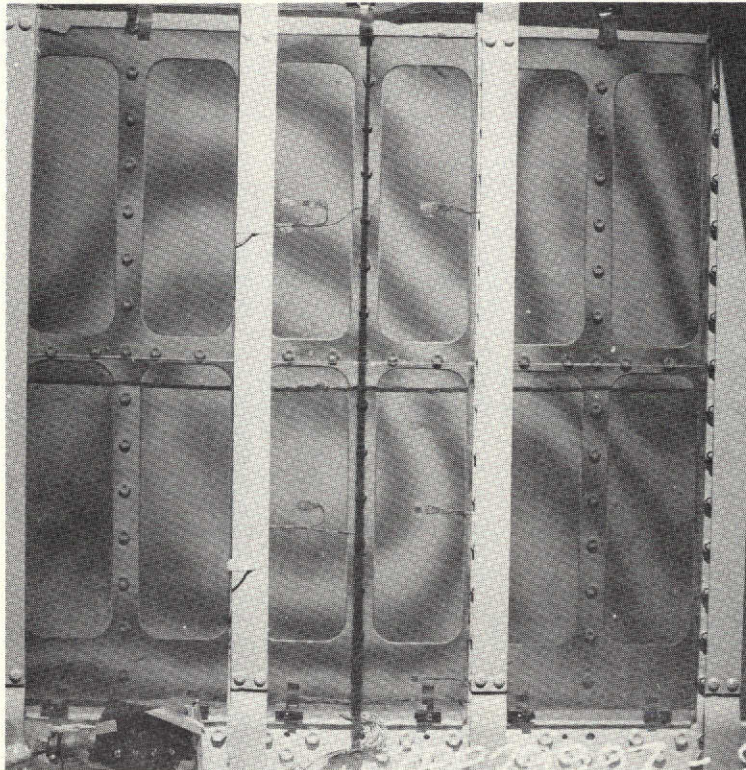
Figure B-27: TEST WEB 3 AT 426,000 LB (2.89 MN) IN FINAL LOADING
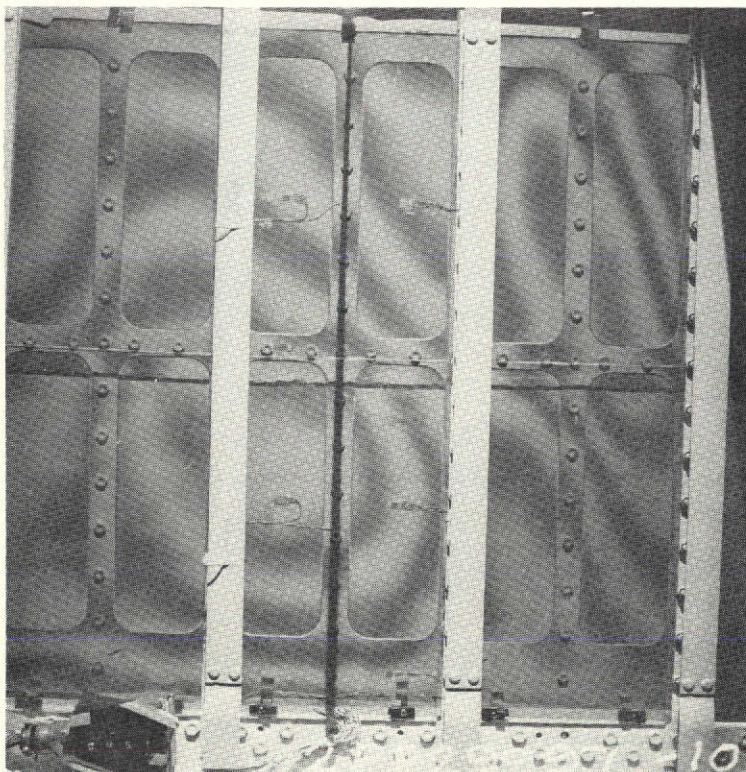
Figure B-28: TEST WEB 3 AT 451,000 LB (2.01 MN) IN FINAL LOADING
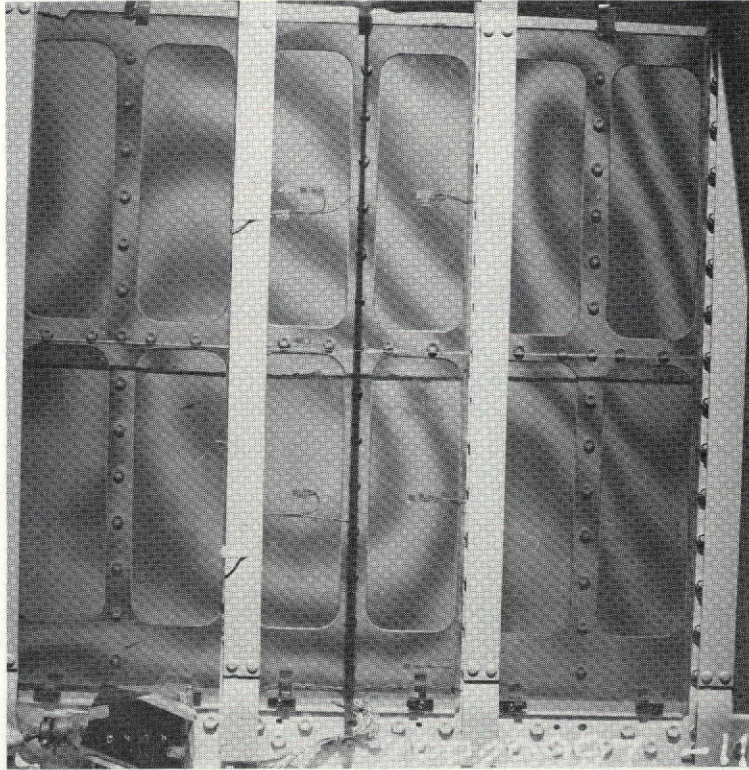
Figure B-29: *TEST WEB 3 AT 476,000 LB (2.12 MN) IN FINAL LOADING*
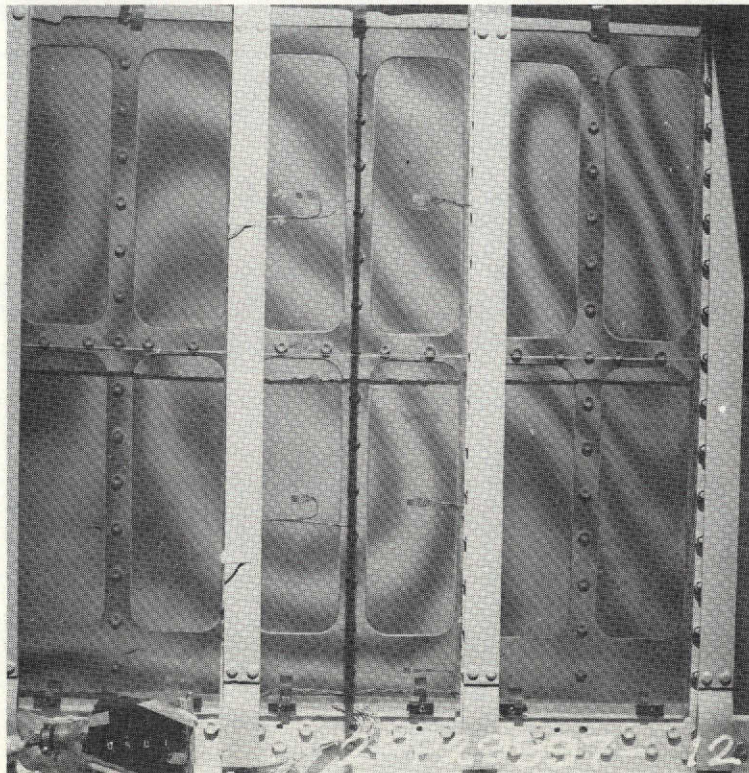
Figure B-30: *TEST WEB 3 AT 501,000 LB (2.23 MN) IN FINAL LOADING*
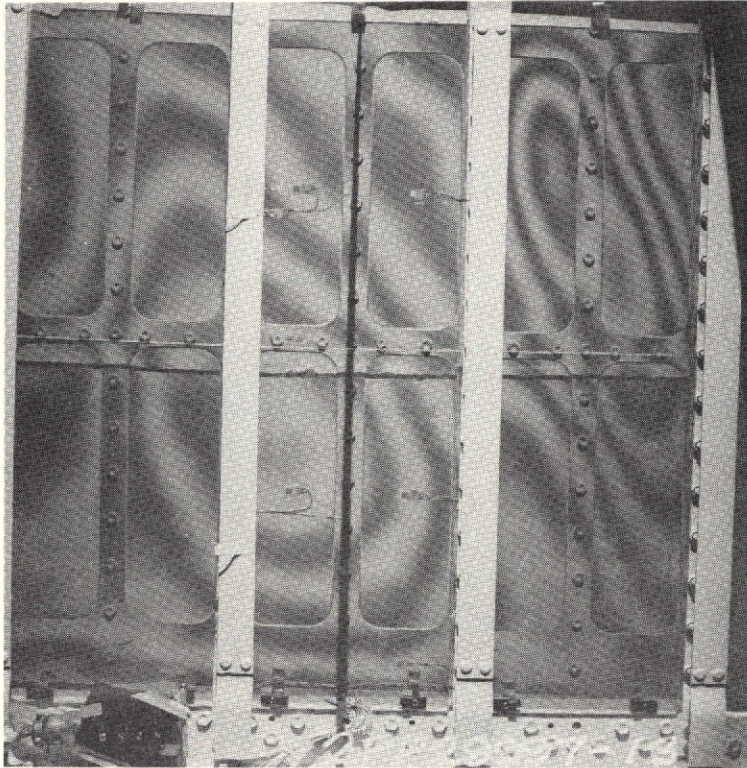
Figure B-31: TEST WEB 3 AT 526,000LB (2.34 MN) IN FINAL LOADING
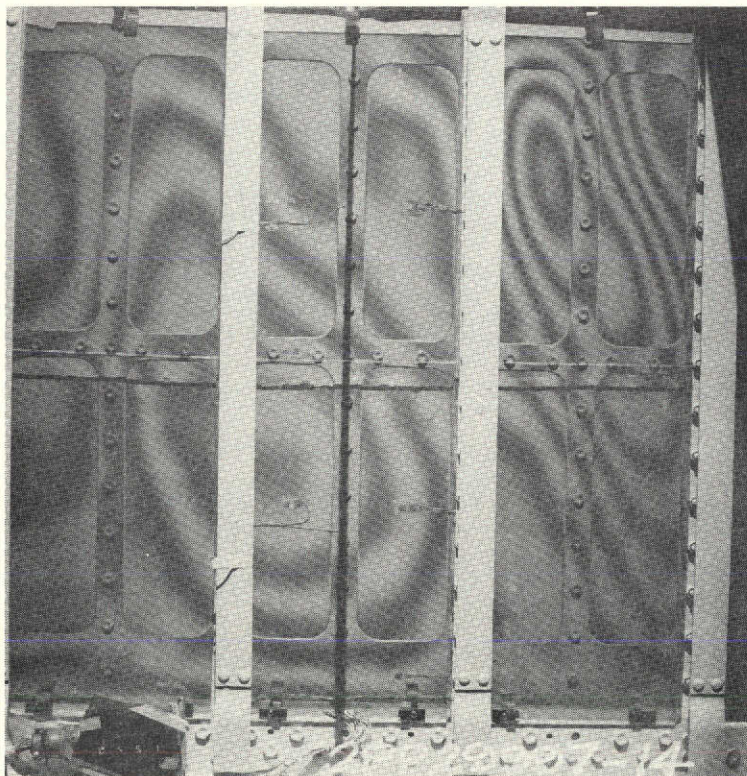
Figure B-32: TEST WEB 3 AT 551,000 LB (2.45 MN) IN FINAL LOADING

217
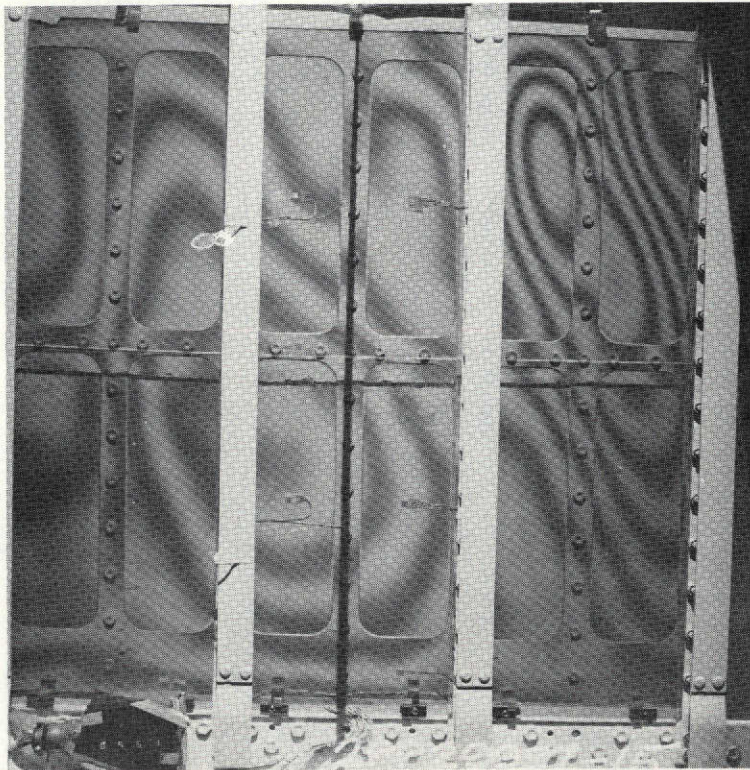
Figure B-33: TEST WEB 3 AT 551,000 LB (2.45 MN) AFTER 5 MINUTE LOAD HOLD PERIOD
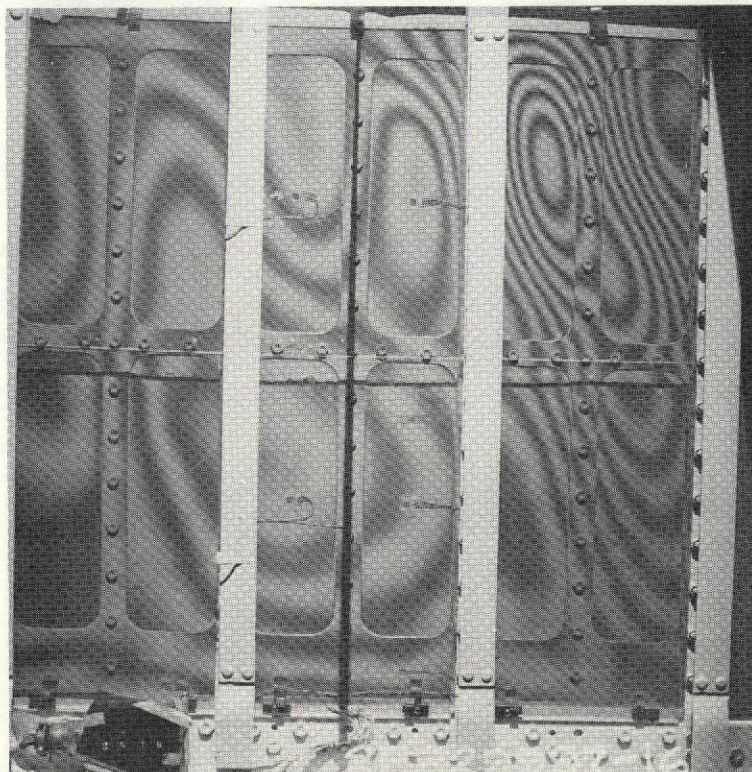
Figure B-34: TEST WEB 3 AT 576,000 LB (2.56 MN) FAILURE LOAD

APPENDIX C STRUCTURAL ANALYSIS EQUATIONS

This appendix presents the analysis equations that are coded in the
OPTRAN code for the "shear resistant" stiffened metal-clad composite
shear web design concept.

CONFIGURATION

Configuration details and variables are defined in Figures 83 to 88
of Section 10.1. The basic configuration parameters are:

Total web height H

Nominal laminate panel height H_p
    (effective web height)

Stiffener spacing S_s

The coordinate notation used in the analyses is:
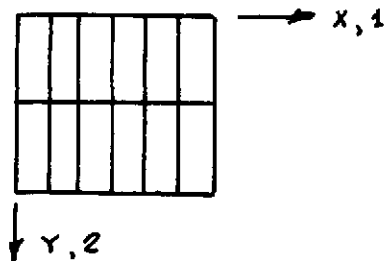
MATERIAL PROPERTIES

The room temperature material properties used in the structural analy-
ses are given in Table C-1.

	BORON/EPOXY UNIDIRECTIONAL PLIES (RIGIDITE 5505/4)	ADHESIVE (METLBOND 329)	TITANIUM 6AL-4V MILL ANNEALED	ALUMINUM 7075-T6
E_x 10^6 lb/in^2	30	0.5	16	10.3
E_y 10^6 lb/in^2	1.0	0.5	16	10.3
G_{xy} 10^6 lb/in^2	1.0	0.2	6.2	3.9
ν_{xy}	0.25	0.4	0.3	0.33
PLY THK. In.	0.0051	0.009	-	-
MIN. THK	-	-	0.019	0.019
VOLUME FRACTION %	50	-	-	-
UNIT. WT. lb/in^3	0.0725	0.0635	0.16	0.1012
ε_{ULT} 10^{-6} IN/IN	6000	-	-	-
F_{ty} lb/in^2	-	-	126000	67000

Table C1:

ROOM TEMPERATURE MATERIAL PROPERTIES USED IN STRUCTURAL ANALYSIS

220

ELASTIC STIFFNESSES

Web plate:

Membrane $\quad A_{ij}$

Bending $\quad D_{ij}$

$\left.\begin{array}{l} \\ \\ \\ \\ \end{array}\right\}\quad i,\ j = 1,\ 2,\ 3$

These stiffnesses are computed by classical laminate analysis for an orthotropic plate [8].

Transverse Stiffeners:

Bending stiffness $\quad EI_T$

$\qquad$ (about y-y neutral axis)

Longitudinal Stiffener:

Bending stiffness $\quad EI_L$

Stiffener stiffnesses are computed by conventional analyses. No web laminate parts are included in the stiffener stiffness analyses.

LOADS AND STRAINS

Applied uniform shear load

$$N_{xy} = N_3 = \frac{V}{H}$$

Web shear strain (membrane web strain)

$$\epsilon_{xy} = \epsilon_3 = \frac{N_{xy}}{A_{33}}$$

221

Applied chord strain due to beam bending: ε_C

Beam bending strain (membrane web strain) at the nominal laminate panel edge

$$\epsilon_{PX} = \frac{H_P}{H} \epsilon_C$$

Web load, at the panel edge

$$N_{PX} = A_{22} \epsilon_{PX}$$

The web is assumed to be in plane strain in the y direction to produce a conservative value for N_x.

Beam bending strain at the peak panel buckle area

$$\epsilon_{BPX} = \frac{2}{3} \epsilon_{PX}$$

Applied chord load due to beam bending: P_C

Web "crushing" load

$$N_Y = N_2 = \frac{P_C \epsilon_C}{H/2}$$

Web strain due to chord crushing

$$\epsilon_Y = \epsilon_2 = A_{22}^{-1} N_Y$$

where A_{ij}^{-1} is the inverse of A_{ij} , the web is assumed to be in plane stress in the X direction to produce a conservative value for ϵ_Y .

STRAIN TRANSFORMATION

The following transformation gives the composite strains in the ply coordinate systems.

$$\bar{\epsilon}_i = T_{ij}\epsilon_j = \frac{1}{2}\begin{bmatrix} 1 & 1 & -1 \\ 1 & 1 & 1 \\ -1 & 1 & 0 \end{bmatrix}\begin{bmatrix} \epsilon_j \end{bmatrix}$$
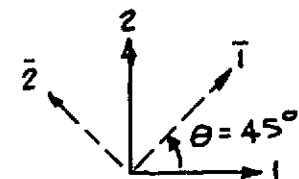
CLADDING STRESSES

$$\sigma_i = a_{ij}\epsilon_j \qquad i,j = 1,2,3$$

where a_{ij} are the cladding elastic modulus properties

$$a_{11} = a_{22} = E/(1-\nu^2) \qquad a_{33} = G$$

$$a_{12} = a_{21} = \nu a_{11} \qquad a_{13} = a_{31} = a_{23} = a_{32} = 0.$$

FAILURE MODES

CLADDING YIELDING

Von Mises yield condition [18]

$$F_e = \left[\sigma_1^2 + \sigma_2^2 - \sigma_1\sigma_2 + 3\sigma_3^2\right]^{1/2} = F_{TY}$$

COMPOSITE STRAIN

$|\bar{\epsilon}_1| = \epsilon$ Allowable (in the filament direction)

$|\bar{\epsilon}_2| = \epsilon$ Allowable

223

WEB SHEAR BUCKLING

A preliminary analysis method to treat shear instability was incorporated in the OPTRAN code. This analysis is based on Cook and Rockey [12] and Bleich [15]. The shear buckling coefficient data developed by Cook and Rockey was replotted and an expression was fitted that relates the shear coefficient for a longitudinally and transversely stiffened isotropic web (K_{SLT}) to the coefficient for a web with only transverse stiffening (K_{ST}), as a function of the ratio of the stiffening parameters and panel aspect ratio. Aspect ratios of 1, 2 and 5 were treated. The resulting equations are:

- Web Without Longitudinal Stiffening (Stein and Fralich [11] data fitted by Bleich)

$$K_{ST} = 5.34 + (5.5\alpha^2 - 0.6)\left[\frac{\gamma_T}{\gamma_{T_0}}\right]^{1/3} \qquad ; \quad \gamma_T < \gamma_{T_0}$$

$$\gamma_T = \frac{E I_T}{S_S D_{11}}$$

$$\gamma_{T_0} = 4(7\alpha^2 - 5)$$

$$\alpha = \frac{H_P}{S_S}$$

$$K_{ST} = 4.74 + 5.5\alpha^2 \qquad\qquad ; \quad \gamma_T \geq \gamma_{T_0}$$

- Web with Central Stiffener

$$K_{S_{LT}} = \eta \, K_{S_T}$$

where η is the K_s magnification factor which is applied to Bleich's K_{ST} to account for the central stiffener.

When $\qquad \gamma_L = \dfrac{E I_L}{H_P D_{11}} = 0 \qquad ; \quad \eta = 1.0$

When $\qquad \gamma_L > 0 \qquad\qquad\qquad ; \quad \eta = 1.84 \left[\dfrac{\gamma_L}{\gamma_T}\right]^{0.0747}$

If $\qquad \eta > \eta_{MAX} \qquad\qquad ; \quad \eta = \eta_{MAX}$

$$\eta_{MAX} = A \left[\dfrac{\gamma_L}{B}\right]^{-m} \qquad ; \quad \gamma_T < B$$

$$= A \qquad\qquad ; \quad \gamma_T \geq B$$

where $\qquad A = 2\, \alpha^{-0.357}$

$\qquad\qquad\qquad B = 21\, \alpha^{2.21}$

$\qquad\qquad\qquad m = 0.33\, \alpha^{-0.263}$

As shown in Figure 74 of Section 9.1, the equations may be unconservative in certain cases and therefore comparison of computed buckling coefficients with the original referenced data is necessary in all cases. Since the maximum panel aspect ratio

225

treated by Bleich and Cook and Rockey is 5.0, use of these fitted

equations for higher panel aspect ratios is not recommended.

The critical shear load is given by:

$$N_{XYCR} = \frac{K_{SLT} \, \pi^2 \, D_{11}}{H_P^2}$$

WEB BENDING BUCKLING

The critical web buckling load due to beam bending is analyzed by using

a form of the classical panel buckling analysis given by Bleich [15].

The critical compression load at the edge of the nominal laminate panel

on the compression side of the web is:

$$N_{PXCR} = \frac{K_B \, \pi^2 \, D_{11}}{S_J^2}$$

The buckling coefficient K_B is a function of the subpanel aspect ratio:

$$\zeta = \frac{S_S}{H_P/2}$$

Values for K_B were computed for a range of aspect ratios and are

shown in Figure 75 of Section 9.2. Fitted equations for the computed

values are:

$$K_B = 100 \left[\zeta / 0.1425 \right]^{-1.858} \qquad ; \quad 0.15 \leq \zeta \leq 0.25$$

$$K_B = 88.57 \left[\zeta / 0.1425 \right]^{-1.858} + 4.886 - 6.585 \zeta + 10.85 \zeta^2$$

$$- 3.568 \zeta^3 \qquad ; \quad 0.25 \leq \zeta \leq 1.5$$

226

Because of the dominant effect of shear load in buckling interaction, the stiffeners required to preclude shear instability are assumed to be adequate for development of the critical panel load for bending. Therefore a coupled plate/stiffener buckling analysis is not conducted with respect to beam bending loads. In both shear and bending buckling analyses, some conservatism is present due to the use of isotropic plate theory. The metal-clad web laminate is actually orthotropic and has excess twisting stiffness (D_{33}) compared to an isotropic plate with equivalent bending stiffnesses (D_{11}, D_{12}, D_{22}).

BUCKLING INTERACTION

The criterion for general instability failure is given by the classic relation:

$$R = R_S^2 + R_B^2 = 1.0$$

where

$$R_S = \frac{N_{XY}}{N_{XYCR}}$$

$$R_B = \frac{N_{PX}}{N_{PXCR}}$$

The buckling interaction parameter R is used in the prebuckling panel strain analysis. The effects of N_Y are omitted from the interaction analysis since this load is small relative to the shear load.

PRE-BUCKLING PANEL STRAIN ANALYSIS

The pre-buckling web panel deflection shape is assumed to develop from
an initial imperfection of the following form which is characteristic
of the buckled shape of long shear panels [13].

$$\omega = \omega_i \; \text{Sin} \; \frac{\pi Y}{L_Y} \; \text{Sin} \; \frac{\pi}{L_x} \left(x - \phi Y \right)$$

$$\phi = \text{Tan} \; \theta$$
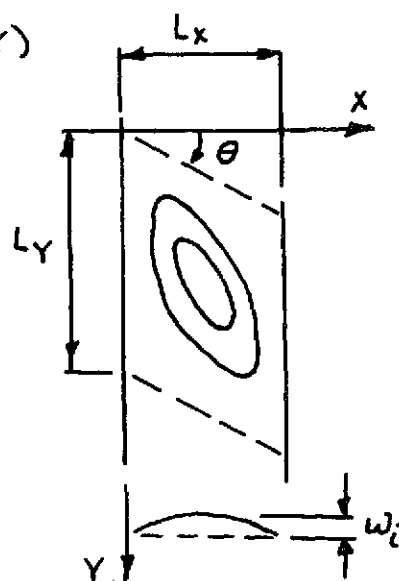
The characteristic modal parameters are initial peak imperfection
magnitude W_i, wave width L_x, wave length L_y, and skew angle θ.
The wave width is assumed equal to the transverse stiffener spacing
and wave length is assumed equal to the subpanel height:

$$L_x \approx S_s$$

$$L_y \approx {}^{H_P}\!/_2$$

228

The skew angle is assumed to be 60° for webs having the given configuration (Test Web 3):

$$\theta = 60°$$

At zero load, the panel curvatures κ_{i_o} are maximum at the peak buckle area:

$$K_{x_o} = K_{1_o} = -\omega_i \left[\frac{\pi}{L_x} \right]^2$$

$$K_{Y_o} = K_{2_o} = -\omega_i \left[\left(\frac{\pi}{L_Y} \right)^2 + \phi^2 \left(\frac{\pi}{L_x} \right)^2 \right]$$

$$K_{xY_o} = K_{3_o} = 0$$

The curvatures at a given load level defined by the buckling interaction parameter R are:

$$K_x = -\omega_i \left(\frac{\pi}{L_x} \right)^2 \left[\frac{1}{1 - R^{1/2}} - 1 \right]$$

$$K_Y = -\omega_i \left[\left(\frac{\pi}{L_Y} \right)^2 + \phi^2 \left(\frac{\pi}{L_x} \right)^2 \right] \left[\frac{1}{1 - R^{1/2}} - 1 \right]$$

The strains due to bending at a material point in the web laminate are given by:

$$\epsilon_{i_m}^B = K_i Z_m$$

where Z_m is the coordinate to the material point of interest from the neutral surface of the laminate.

229

The total strain at a point in the web laminate is:

$$\epsilon^T_{im} = \epsilon^M_i + \epsilon^B_{im}$$

where ϵ^M_i are the membrane web strains at the analysis location. For example, ϵ^M_i would be given by ϵ_{BP_i} which are the buckled panel membrane strains defined previously.

$$\epsilon^M_i = \epsilon_{BP_i} = \begin{bmatrix} \epsilon_{BPX} \\ \epsilon_Y \\ \epsilon_{XY} \end{bmatrix}$$

In the case of composite strain analysis the total strains are transformed to the ply coordinate system:

$$\bar{\epsilon}^M_i = T_{ij} \epsilon^M_i$$

The compression strain is the maximum absolute strain which is compared to the allowable composite strain in the filament direction in the computation of margin of safety for this failure mode.

FAILURE AT REINFORCED HOLES FOR STIFFENER FASTENERS

Allowable Strain:

$$\bar{\epsilon}_{RA} = 6000 - (6000 - 1400)\xi_R \quad (\mu\epsilon)$$

where ξ_R, is the net filamentary composite fraction in the reinforced laminate (less adhesive plies). The allowable strain function appears in Figure 19, Section 4.1, Reference [1].

230

Actual Diagonal Tension Strain:

$$\bar{\epsilon}_R \approx \frac{\bar{A}_{R_{11}}^{-1}}{\bar{A}_{11}^{-1}}$$

where $\bar{A}_{R_{11}}^{-1}$ and $\bar{A}_{11}^{-1}$ are terms from the inverted membrane stiffness matrices transformed to the $\Theta = 45°$ orientation for the reinforced and nominal laminates, respectively.

For an all-metal design case, the allowable $\bar{\epsilon}_R$ is arbitrarily selected to be 65% of the proportional limit tension strain to produce a pad-up in fastener hole areas.

The calculation of margin of safety for failure at reinforced holes is based on the comparison:

$$\bar{\epsilon}_R \leq \bar{\epsilon}_{RA}$$

CONSTRAINT ON STIFFENER GAGE

This relation is based on unpublished design data for shear resistant titanium webs [19] which requires that $T_S \geq 0.6 T_W$. The cladding reinforcement is assumed to act as effective stiffener attachment leg material. T_W is the web laminate structural thickness (less adhesive plies) and T_S is the stiffener gage.

WEIGHT ANALYSIS

. Nominal weights are computed and summed for the following items in

terms of weight per unit length of web.

    Nominal cladding skins

    Adhesive plies

    Filamentary composite plies

    Cladding reinforcement along stiffener fastener lines

    Nominal transverse stiffener section

    Transverse stiffener composite reinforcement

    Transverse stiffener metal flange cladding

    Longitudinal stiffener

A depth of H (full web depth) is assumed in the analyses. Weight

allowances for fasteners, radii, edge joints, reinforced cladding edge

areas, cutouts, stiffener end details and manufacturing tolerances are

not made in the OPTRAN weight analyses.

APPENDIX D   TEST WEB 3 DETAIL DESIGN DRAWINGS

| 7 | 6 | 4 | 3 | 2 | 1 |

SECTION A-A
ROTATED 90°
(NO SCALE)

TI CLAD SKIN
ADH I PLY
B/E I PLY
PRECURED LAMINATE SUBASSEMBLY -2
€ SYMMETRY
PRECURED LAMINATE SUBASSEMBLY -3
ADH I PLY
B/E I PLY
TI CLAD SKIN

PANEL TOP-CENTER INDEX

0.270 NOM. (2 PLACES)

PLY ORIENTATION
-45° 0° +45°

34.00

47.00

SK2-5085-118-1(-(-2)
(76 PLACES REF)
.25 (TYP)

-1 ASSEMBLY
(SCALE 1/2)

VIEW C-C
(SCALE 1/2)

PANEL TOP-CENTER INDEX

-8 (4 PLIES)
-7 (1 PLY)
-8 (4 PLIES)

STEP LAP FRAME BUTT JOINT
(4 PLACES)

-6 (2 PLACES)

-3 ASSY
STEP LAP FRAME-FAR SIDE
(SCALE 1/4)

DETAIL I
(SCALE 1/1)

.05 MAX GAP FROM STEP END TO NEXT STEP (TYP)

-8
-5-6

5.00
.054
.043
.032
.021
.010
.75 TYP ±.02
AS ETCHED RADIUS (TYP)

SECTION B-B
(NO SCALE)

42.00 TYP

STEP LAP FRAME BUTT JOINT (4 PLACES)

-8 (4 PLIES)
-7 (1 PLY)
-8 (4 PLIES)
-5 (2 PLACES)

-6 (2 PLACES)

31.00 TYP

-2 ASSY
STEP LAP FRAME-NEAR SIDE
(SCALE 1/4)

4.00
.054
.043
.032
.021
.010
.50 TYP ±.02

ALTERNATE
SECTION B-B
(NO SCALE)

NOTES

1. SPECIFICATIONS AND STANDARDS FOR THE CONTROL OF MANUFACTURING OPERATIONS (AS APPLICABLE)
   SURFACE ROUGHNESS SYMBOLS PER BAC0 5087   PART MARKING PER BAC 5307
   WELDING AND BRAZING SYMBOLS PER BAC0 2022   BOLT & NUT INSTALLATION PER BAC 5008
   FORM, STRAIGHTEN & FIT METAL PARTS PER BAC0 5300   FINISH CODES PER DOCUMENT D2-8000
   MATERIAL SUBSTITUTIONS & EQUIVALENTS PER BAC 5619   RIVET INSTALLATION & SYMBOLS PER BAC 5004

2. CHEMICAL MILL PER BAC 5842
3. CHEMICAL MILL PER BAC 5842. RADII AS ETCHED. DUE TO THICKNESS VARIATIONS ALONG THE STOCK SHEET, THE MILLED NOMINAL THICKNESS DIMENSIONS SHOWN MAY VARY ±.003 ALONG A STEP, BUT AT ANY CROSS SECTION THE STEP-TO-STEP THICKNESS VARIATION MUST NOT EXCEED .0055 ±.001 IN.
4. CLEAN TITANIUM DETAILS PER D6-23841TN SECTION 6.4.2.d.
5. BOND PER D6-23841TN SECTION 6.8.2.2
6. FABRICATE PER D6-23841TN SECTION 6.8.3.1
7. SURFACE SHALL BE FLAT WITHIN .001 IN/IN AND IN ANY CASE ONLY REQUIRE FINGER PRESSURE TO GIVE CONTINUOUS CONTACT OF THE MATING SURFACES.
8. TITANIUM 6AL-4V SHEET - MILL ANNEALED (.063×5.00×42.00)
9. TITANIUM 6AL-4V SHEET - MILL ANNEALED (.063×5.00×31.00)
10. TITANIUM 6AL-4V SHEET - MILL ANNEALED (.063×36.00×47.00)
11. NARMCO METLBOND 329 ADHESIVE
12. RIGIDITE 5505/4 B/E PREPREG TAPE - 116 PLIES TOTAL LAYUP IN -1 ASSY
13. STIFFENER LOCATED - DRILL STIFFENER ATTACHMENT HOLES TO MATCH

PARTS LIST
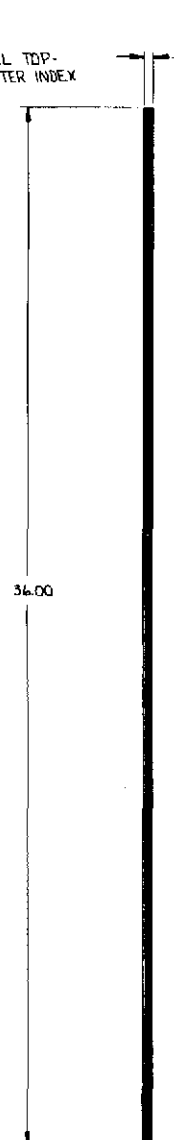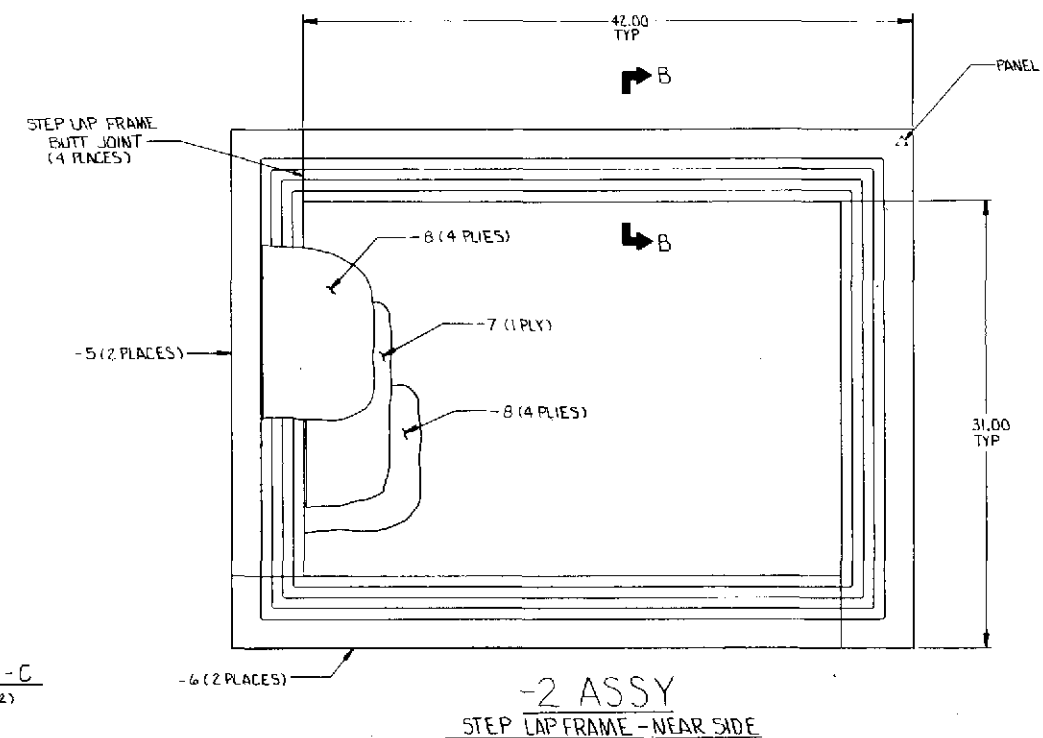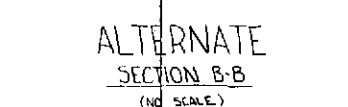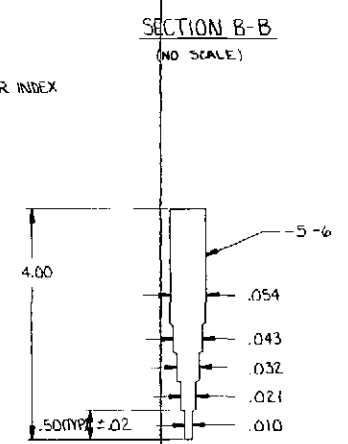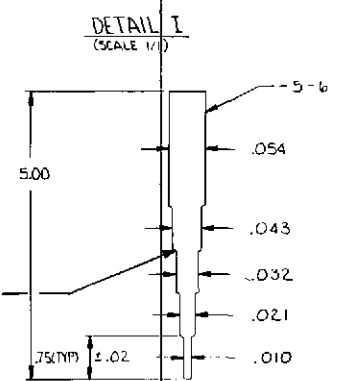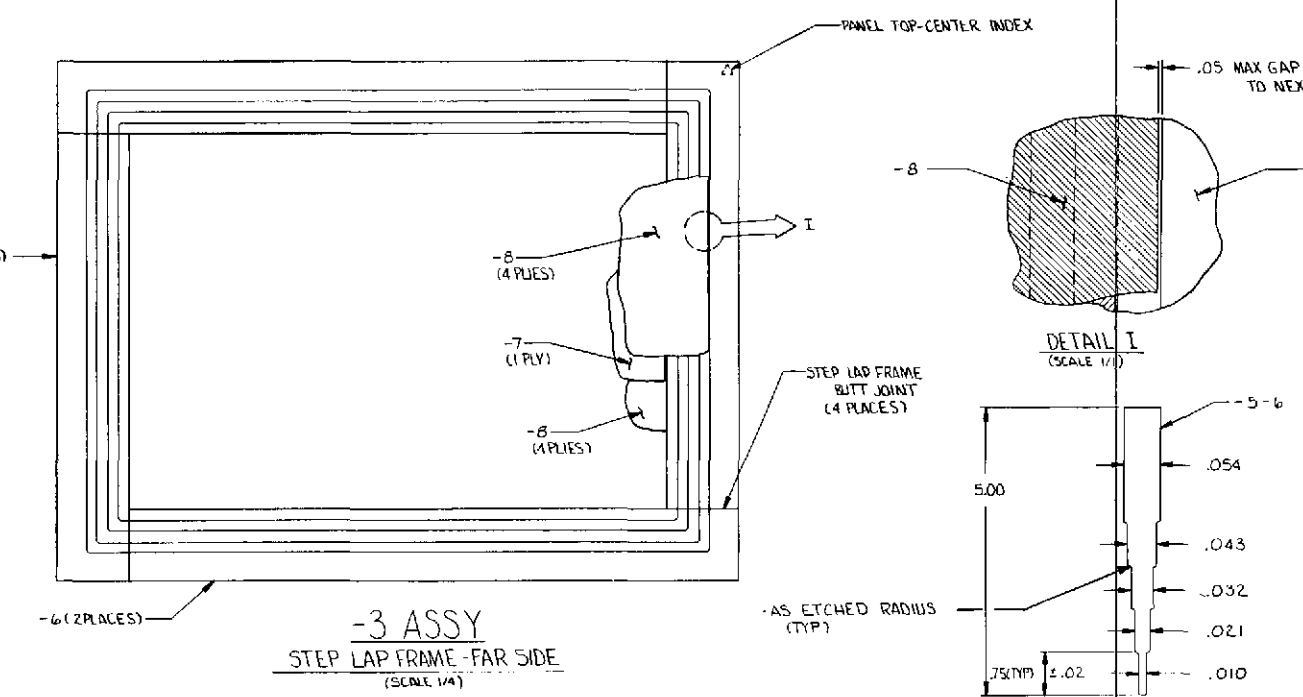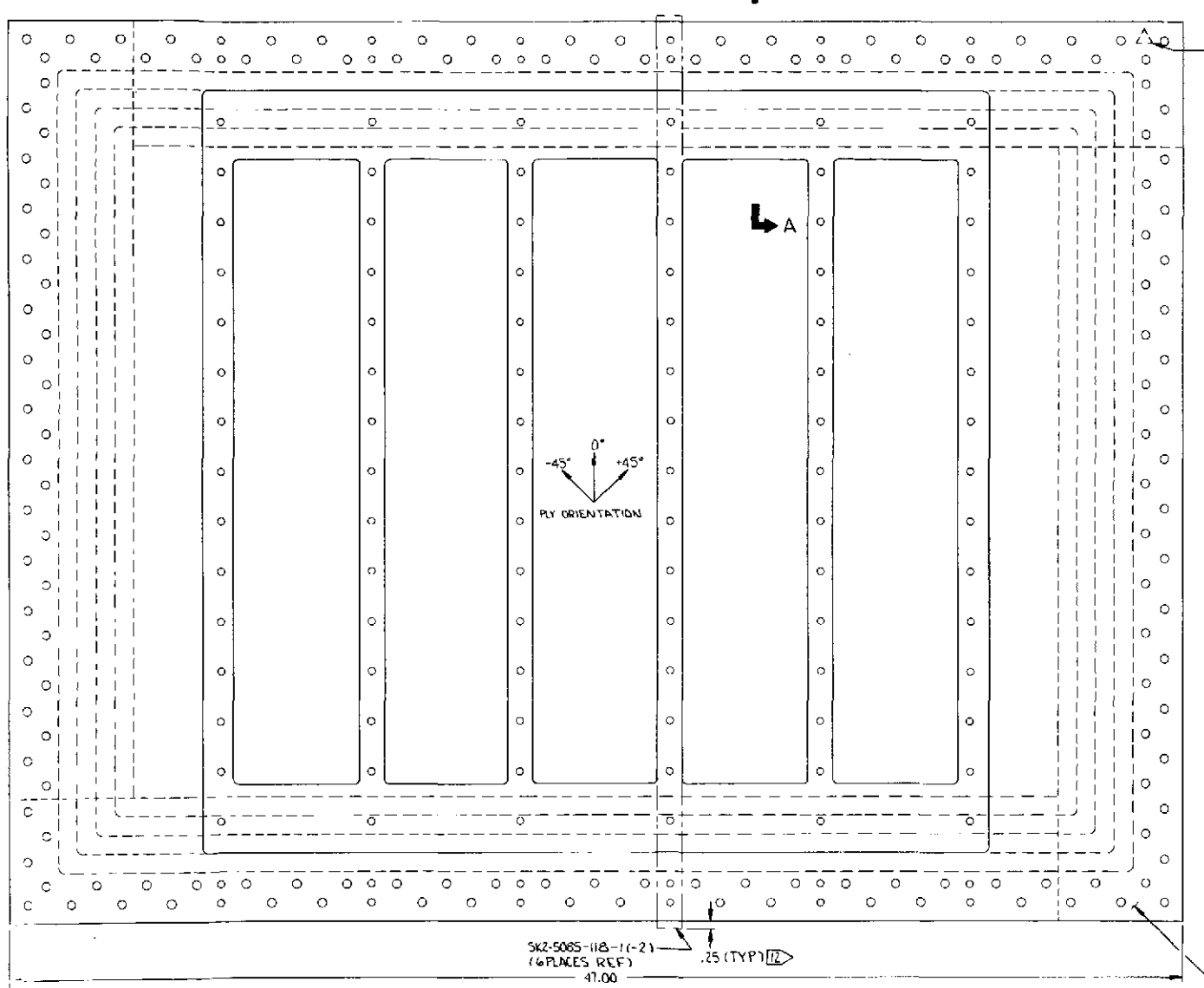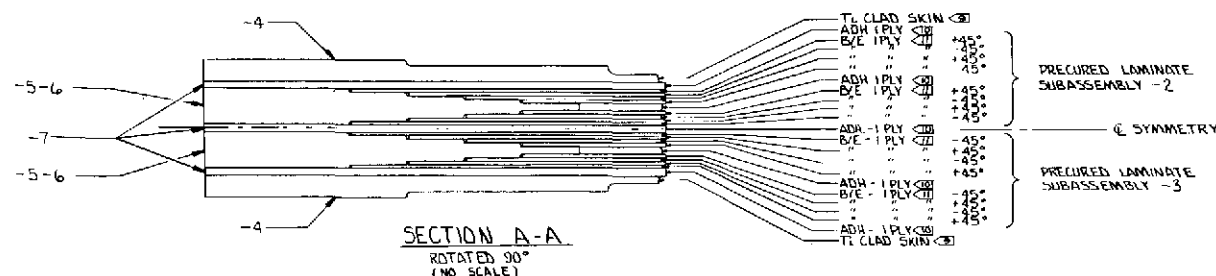
					PART OR IDENTIFYING NUMBER	NOMENCLATURE OR DESCRIPTION	ZONE	MATERIAL AND SPECIFICATION			
✓			2		-10	CLADDING SHEET					
-					-9	BOND ASSY					
✓	✓	✓	AR		-8	BORON/EPOXY					
✓	✓	✓	✓	AR	-7	ADHESIVE					
		✓	2		-6	STEP LAP DETAIL					
		✓	2		-5	STEP LAP DETAIL					
✓			2		-4	CLADDING SHEET					
✓	-		1		-3	FRAME ASSY - FAR					
✓	-		1		-2	FRAME ASSY - NEAR					
			1		-1	BOND ASSY					

CONTRACT NUMBER NAS1-10860
D.D. SMITH
D.D. SMITH
J.V. LAAKSO

THE BOEING COMPANY
CORPORATE OFFICES   SEATTLE, WASHINGTON 98124

TITANIUM CLAD BORON/EPOXY
SHEAR WEB TEST PANEL
-ASSEMBLY

SK2-5085-117

TEST ONLY

SK25085-117

.261 / .250 DIA HOLE (28 PLACES)

47.00

30.00
(6 EQUAL SPACES)

8.50

PANEL TOP
CENTER INDEX

5.50

2.75

5.00
(TYP)

A

A

6.25
(TYP)

1.875
(TYP)

1.875
(TYP)

1.55
(TYP)

28.00
(14 EQUAL SPACES
@ 2.00 TYPICAL)

31.00
(31 EQUAL SPACES
@ 1.00 STAGGERED
TYPICAL BOTH ENDS)

36.00

B

B

B

B

1.00 RAD
(TYP)

1.00 RAD.
(TYP)

.261 / .250 DIA HOLE
(17 PLACES)

.391 / .375 DIA. HOLE
(149 PLACES)

4.00

2.50

.75 (TYP)

.75 (TYP)

1.50 (TYP)

.75 (TYP)

1.50
(TYP)

2.50

42.00
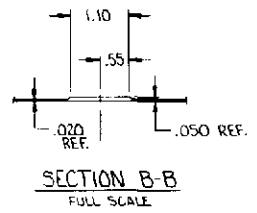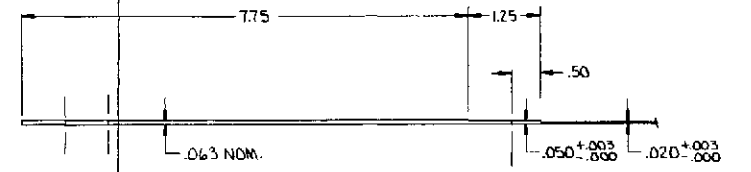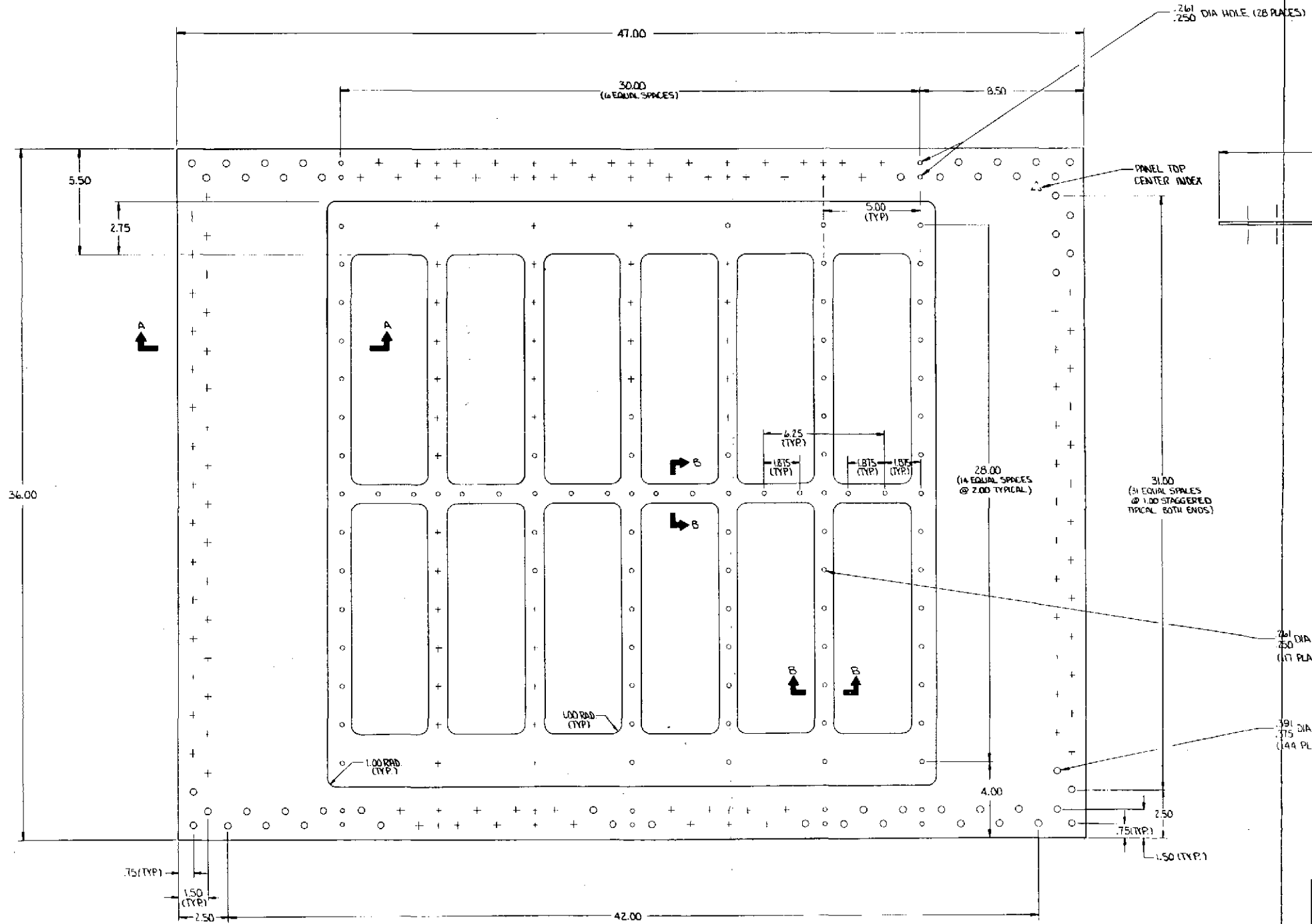
-10
TITANIUM CLADDING SHEET
SCALE: 1/2

7.75

1.25

.50

.063 NOM.

.050 +.003 / -.000

.020 +.003 / -.000

SECTION A-A
FULL SCALE

1.10

.55

.020
REF.

.050 REF.

SECTION B-B
FULL SCALE

SEE SHEET 1 FOR PARTS LIST AND NOTES

DATA REVIEW | CONTRACT NUMBER NAS1-10860

DRG QUAL

STRUCT

MATL & PRCS

ENGR D.D.SMITH

DRG J.H.LAAKSO

PROJECT APPROVAL

CHANGE/ITEM NUMBER

THE **BOEING** COMPANY
CORPORATE OFFICES   SEATTLE, WASHINGTON 98124

**TITANIUM CLAD B/E SHEAR
WEB TEST PANEL
NO. 3**

SIZE J | CODE IDENT NO | SK25085-117

SCALE NOTED | SH 3 of 3

DWG ORIG
BY IORGI

2KS-2082-117 3

SK25085-117 3

FOLDOUT FRAME 1

FOLDOUT FRAME 2

236

NOTES

REVISIONS

SECTION B7
(SCALE: 1/2)

40.00
30.75
20.75
3.50
10.75
15° (TYP)

SK2-5085-118-2 ASSY
SK2-5085-117-9 ASSY
SK2-5085-118-2 ASSY

SIDE VIEW
(SCALE: 1/2)

SK2-5085-118-2 ASSY
SK2-5085-117-9 ASSY

LONGITUDINAL STIFFENER CUTOUT DETAIL
SCALE: 1/1
(TYPICAL 3 PLACES)

SK2-5085-118-2 ASSY
.15 RAD (TYP)
10°
.150
SK2-5085-117-9 ASSY

.261 DIA HOLE
.250
LOCATE TO MATCH
SK2-5085-117-9 ASSY
(133 PLACES)
NAS1104-G
NAS679A4W
(38 PLACES)

-1 ASSEMBLY FRONT VIEW
(SCALE: 1/2)

B7 C7

.261 DIA HOLE
.250
LOCATE TO MATCH
SK2-5085-117-9 ASSY
(23 PLACES)
NAS1104-G
NAS679A4W
(19 PLACES)
NAS1104-8
NAS679A4W
(4 PLACES)

SK2-5085-118-2 ASSY
SK2-5085-117-9 ASSY
SK2-5085-118-2 ASSY (7 PLACES)

-1 ASSEMBLY REAR VIEW
(SCALE: 1/2)

.60
SK2-5085-117-9 ASSY
-3 (2 PLACES)
-4 (2 PLACES)

QTY						CODE	PART OR IDENTIFYING NUMBER	NOMENCLATURE OR DESCRIPTION	MATERIAL AND SPECIFICATION			
4							NAS1104-8	BOLT				
117							NAS1104-G	BOLT				
121							NAS679A4W	NUTS				
7							SK2-5085-118-2	STIFFENER ASSY				
1							SK2-5085-117-9	PANEL ASSY				
2							-4	SHIM	.012 ×1.25 ×8.75 2024-T6 AL SHEET			
2							-3	SHIM	.012 ×1.25 ×4.75 2024-T6 AL SHEET			
1							-2	STIFFENER	AND .0137 ×.606 U 40.0 LG 2024-T351 ALUM			
1							-1	TEST COMPONENT ASSEMBLY				

PARTS LIST

CONTRACT NUMBER NAS1-10860

THE BOEING COMPANY
CORPORATE OFFICES   SEATTLE, WASHINGTON 98124

TITANIUM CLAD BORON/EPOXY
SHEAR WEB TEST COMPONENT
ASSEMBLY (TEST WEB No.3)

SK2-5085-138